TU/e EINDHOVEN UNIVERSITY OF TECHNOLOGY

Hydrophilic Coatings Enabled by Wetting Agents and Phenolic Resins

Citation for published version (APA):
Moone, L. (2025). *Hydrophilic Coatings Enabled by Wetting Agents and Phenolic Resins*. [Phd Thesis 1 (Research TU/e / Graduation TU/e), Chemical Engineering and Chemistry]. Eindhoven University of Technology.

Document status and date:
Published: 07/05/2025

Document Version:
Publisher's PDF, also known as Version of Record (includes final page, issue and volume numbers)

Please check the document version of this publication:

• A submitted manuscript is the version of the article upon submission and before peer-review. There can be important differences between the submitted version and the official published version of record. People interested in the research are advised to contact the author for the final version of the publication, or visit the DOI to the publisher's website.
• The final author version and the galley proof are versions of the publication after peer review.
• The final published version features the final layout of the paper including the volume, issue and page numbers.

Link to publication

General rights
Copyright and moral rights for the publications made accessible in the public portal are retained by the authors and/or other copyright owners and it is a condition of accessing publications that users recognise and abide by the legal requirements associated with these rights.

• Users may download and print one copy of any publication from the public portal for the purpose of private study or research.
• You may not further distribute the material or use it for any profit-making activity or commercial gain
• You may freely distribute the URL identifying the publication in the public portal.

If the publication is distributed under the terms of Article 25fa of the Dutch Copyright Act, indicated by the "Taverne" license above, please follow below link for the End User Agreement:

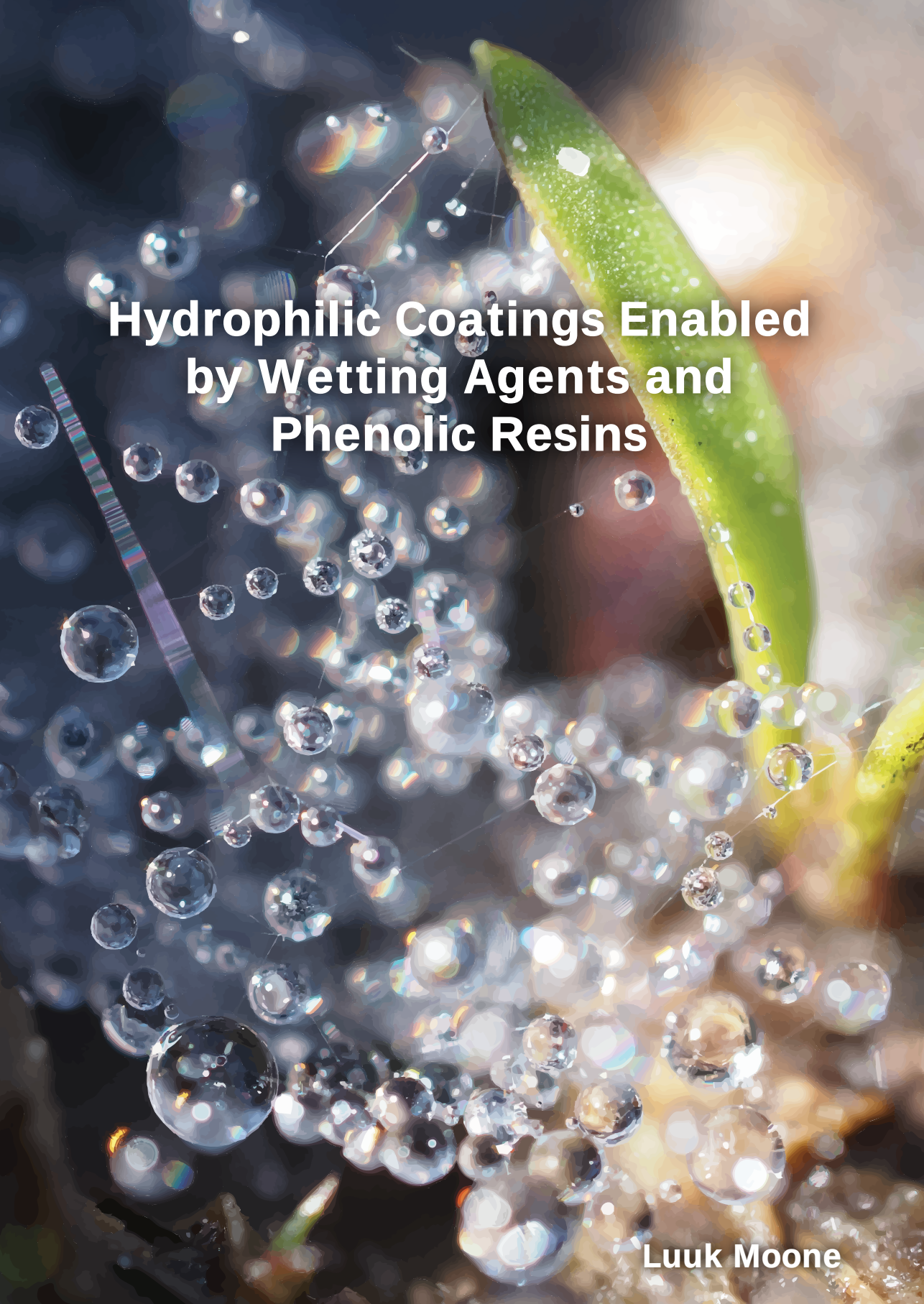
www.tue.nl/taverne

Take down policy
If you believe that this document breaches copyright please contact us at:

openaccess@tue.nl

providing details and we will investigate your claim.

Download date: 01. Apr. 2026



Hydrophilic Coatings Enabled by Wetting Agents and Phenolic Resins

Luuk Moone

Hydrophilic Coatings Enabled by Wetting Agents and Phenolic Resins

PROEFSCHRIFT

ter verkrijging van de graad van doctor aan de Technische Universiteit Eindhoven, op gezag van de rector magnificus prof.dr. S.K. Lenaerts, voor een commissie aangewezen door het College voor Promoties, in het openbaar te verdedigen op woensdag 7 mei 2025 om 16:00 uur

door

Luuk Moone

geboren te Eindhoven

Dit proefschrift is goedgekeurd door de promotoren en de samenstelling van de promotiecommissie is als volgt:

Voorzittter:	prof. dr. A.P.H.J. Schenning
Promotoren:	dr. A.C. de Carvalho Esteves
	prof. dr. R.A.T.M. van Benthem
Copromotor:	prof. dr. ir. R. Tuinier
Leden:	prof. dr. Ž. Tomović
	prof. dr. R.H.A. Ras (Aalto University)
	prof. dr. S. Kiil (Technical University of Denmark)
	dr. S.J. Garcia (Technische Universiteit Delft)

Het onderzoek dat in dit proefschrift wordt beschreven is uitgevoerd in overeenstemming met de TU/e Gedragscode Wetenschapsbeoefening.

Hydrophilic Coatings Enabled by Wetting Agents and Phenolic Resins

Luuk Moone

Eindhoven University of Technology, The Netherlands, 2025

The work in this thesis was supported by ROCKWOOL A/S, Hedehusene, Denmark and ROCKWOOL B.V. / Grodan, Roermond, The Netherlands, as part of the WETWOOL project.
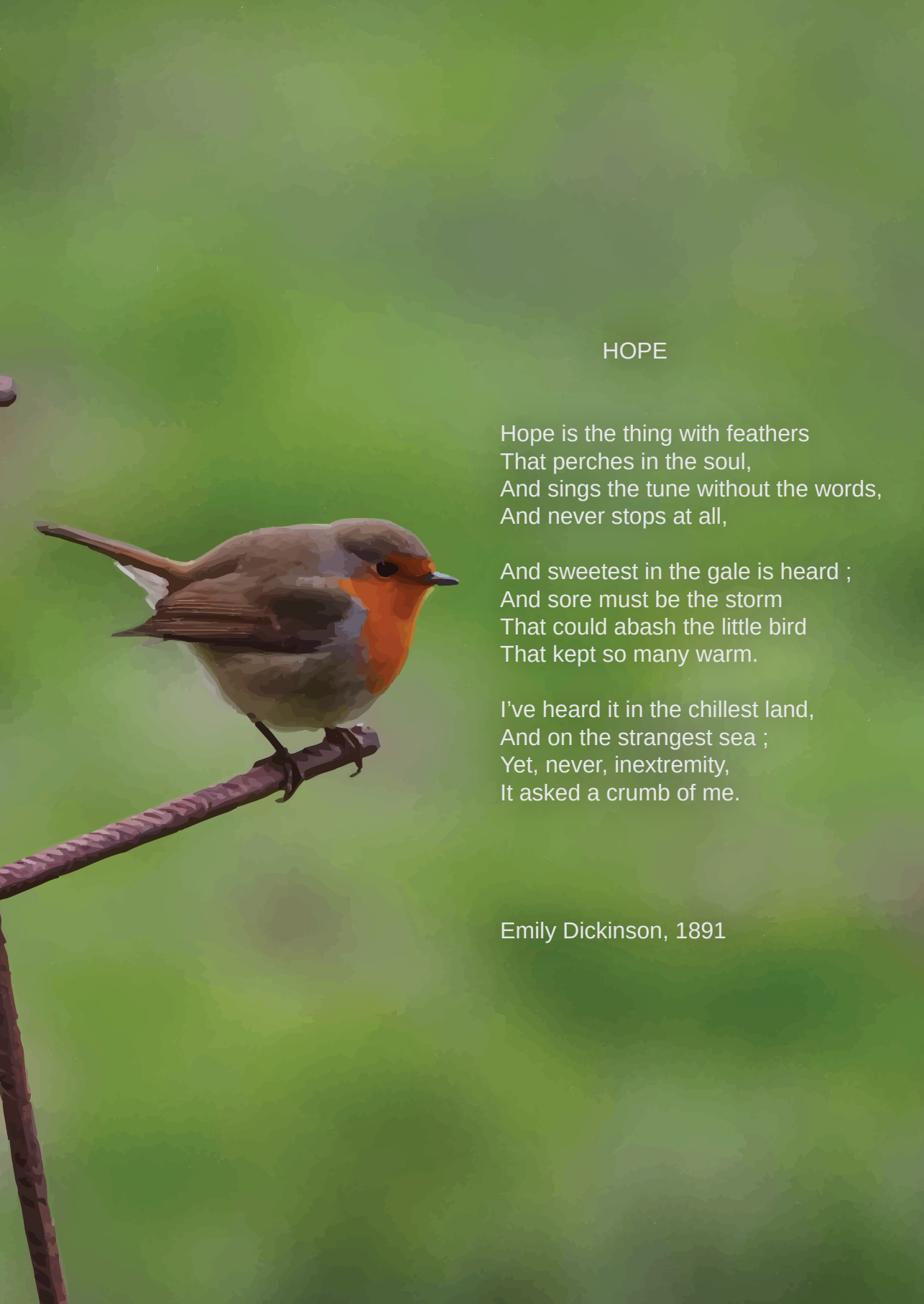
A catalogue record is available from the Eindhoven Technical University Library

ISBN: 978-90-386-6337-1

Copyright © Luuk Moone

Cover design and chapter title page design are photographs by Luuk Moone, converted to vector images using Adobe Illustrator.
Trigger warning: Arachnophobia, page 49

Printed by ProefschriftMaken – proefschriftmaken.nl



HOPE

Hope is the thing with feathers
That perches in the soul,
And sings the tune without the words,
And never stops at all,

And sweetest in the gale is heard ;
And sore must be the storm
That could abash the little bird
That kept so many warm.

I’ve heard it in the chillest land,
And on the strangest sea ;
Yet, never, inextremity,
It asked a crumb of me.

Emily Dickinson, 1891

Table of Contents

1. Introduction **1**
- 1.1. Hydrophilic Stone Wool 2
- 1.2. Phenolic Resins 3
- 1.3. Wetting Agents and Wettability 7
- 1.4. The Intersection of Phenolic Resins and Wetting Agents 10
- 1.5. Outline of Thesis 10
- References 11

2. Surface Characteristics of Phenolic Resin Coatings **19**
- 2.1. Introduction 20
- 2.2. Experimental Procedures 21
- 2.3. Results and Discussion 25
  - Resin Definition and Characterisation 25
  - Surface Morphology of Phenolic Resin Coatings 26
  - Influence of Surface Changes on Wettability 30
  - Influence of Curing Conditions on Surface Composition and Wettability 33
- 2.4. Conclusions 39
- References 40
- Appendices 42

3. Behaviour of Wetting Agents in Phenolic Resin Coatings **49**
- 3.1. Introduction 50
- 3.2. Experimental Procedures 51
- 3.3. Results and Discussion 55
  - Wetting Agent Characterisation 55
  - Wetting Agent – Binder Interactions through Contact Angle Measurements: Phenol-Urea-Formaldehyde Coatings 58
  - Wetting Agent – Binder Interactions through Contact Angle Measurements: Phenol-Formaldehyde Coatings 62
  - Effect of Inorganic Catalysts on Wetting Agent Distribution 66
  - Wetting Agent Mobility and Response to Relative Humidity 69
- 3.4. Conclusions 73
- References 74
- Appendices 77

4. Ageing Phenomena in Phenolic Resin Coatings **87**
- 4.1. Introduction 88
- 4.2. Experimental Procedures 91
- 4.3. Results and Discussion 97
  - Hygrothermal Stability of Wetting Agents 97
  - Hygrothermal Ageing of Phenolic Resin Coatings 100

Influence of Substrate on Ageing of Phenol-Urea-Formaldehyde Coatings 107
Investigating Inhibited Ageing of Phenol-Urea-Formaldehyde Coatings on Inert Substrates 116
4.4. Conclusions 119
References 120
Appendices 125

5. Stability of Phenolic Resin – Wetting Agent Mixtures upon Curing 141
5.1. Introduction 142
5.2. Experimental Procedures 143
5.3. Results and Discussion 145
Wetting Agents Selection and Characterisation 145
Effect of Alkyl and Ethylene Oxide Content of Wetting Agents on Miscibility with Phenolic Resins 147
Effect of the Ionic Headgroup of Wetting Agents on Miscibility with Phenolic Resins 152
5.4. Conclusions 154
References 155
Appendices 159

6. Epilogue 165
6.1. Conclusions 166
6.2. Outlook 167
References 170

Summary 173

Glossary 175

Curriculum Vitae 177

Publication List 179

Acknowledgements 181

1

Introduction



1.1. Hydrophilic Stone Wool

While the world population is ever-growing, predicted to be between 9–10 billion by 2050 [1–3], land, food, resources, and water availability is ever-dwindling [3,4]. Agriculture consumes approximately 70% of the world's fresh water [5], whilst typically also requiring plenty of space for the growth of crops [6]. At the same time, urbanisation is increasing, which potentially leads to conflicts as water demands in both cities and agricultural lands cannot be sufficiently met [7]. On many fronts, these societal problems require collaboration, dedication, and innovation in order to sustain life on Earth.

Horticulture can directly address the scarcities mentioned above, either through smart greenhouses or vertical farming setups [8,9]. An interesting example of an innovation in horticulture is hydroponics, which is a soilless method to grow vegetables and fruits, and allows for control and recycling of water usage [10,11]. This way, a reduction in land and water usage is attained compared to conventional agriculture [12–14], and additionally an increased yield of crops is obtained [12,13]. Media for hydroponic purposes can be only water, or more root-supporting materials such as peat, sand, polyurethane mats, and phenolic foams [10,15,16].

Another growth medium is stone wool, which is already widely used to germinate, propagate and cultivate fruits and vegetables (Figure 1.1a–b). It has numerous advantages as a growing medium: it is sterile, yields an increased quality and quantity of produce, and is versatile as it can, for instance, also be used to cultivate flowers [17–19]. Stone wool is produced from molten rocks (e.g., basalt, dolomite, and granite amongst others) and blast furnace slag, to which typically limestone and coke is added [10,17,20]. The melt is spun into fibres and subsequently sprayed with an aqueous phenolic resin (PR). The coated fibres are then pressed into mats and cured in an oven at elevated temperatures. The open, fibrous structure of the stone wool substrates ensures that the root system of growing crops always has access to water and nutrient solutions, while also providing sufficient aeration to prevent rot.

The applied PR coating has a twofold function. First, it acts as an adhesive, bonding stone wool fibres together, as shown in Figure 1.1c. It has been determined previously that approximately 40% of the fibre area is covered with micrometre-size binder droplets [21]. Besides droplets and larger patches of binder (Figure 1.1d), a nanometre-thick layer is also present over the length of the fibres [22–24]. Second, the PR coating applied to the fibres ensures a hydrophilic, e.g., 'water-loving', substrate. Desired water characteristics of the stone wool growth substrates are water retention and water uptake, facilitated by the hydrophilic coating. To ensure such characteristics wetting agents (WAs) are added to the resin formulation. Both phenolic resins and wetting agents are discussed in the next sections.

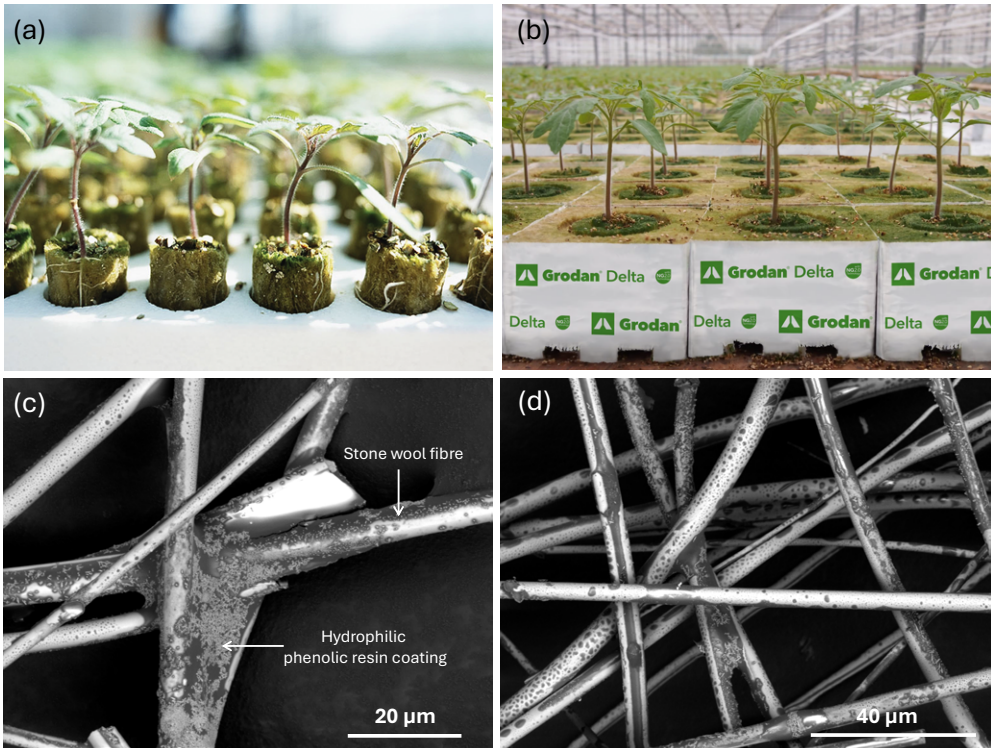


Figure 1.1. Stone wool substrates used in horticulture for (a) germination of seeds and (b) propagation of the young plants. Scanning electron micrographs of coated stone wool is shown in (c) and (d), where it can be seen that stone wool fibres are held together by a phenolic resin coating. The images in (a) and (b) were kindly provided by Grodan.

1.2. Phenolic Resins

The term 'phenolic resin' refers to a versatile class of polymers with an equally versatile range of applications. PRs are used for instance as adhesives and coatings for wood and metal substrates, and their varied applicability is due to a plethora of options for chemical modifications [20,25–27], outstanding mechanical and fire-retardant properties [28–30] after curing, and due to their favourable cost [25]. It is therefore no surprise that PRs are commonly used as wood adhesives, applied to for instance fibre- and particleboards or exterior-grade plywood [15,25,31–39]. Without any prior chemical modification, PRs already exhibit good chemical resistance and are known to enhance the adhesive strength of wood substrates [35,37,38]. Extensive research has also been carried out on the effect of chemical modification of PRs with for instance lignin, in order to increase mechanical and/or adhesive properties [40–44]. The use of PRs is not limited to just wood; they are also employed in ablative materials for air- and spacecraft [30,45,46], often in the form of composite materials [46,47], and as binders

for fibrous materials such as glass fibres and stone wool [20,48–50], as discussed in the previous section.

One of the simplest PRs are resoles, which are prepared by condensation of phenol (P) with formaldehyde (F) under basic conditions in water, typically with a molar ratio of F/P $\geq$ 1. The Lederer-Manasse reaction [51,52] between phenol and formaldehyde results in the addition of methylol groups at the *ortho* or *para* position of phenol, with the *para* position generally being the most favourable [53]. Upon exposure to heat, methylolated phenolic species condense and form a rigid thermoset network by formation of dimethylene ether (DMEb) and methylene (Mb) bridges between phenolic units (Figure 1.2a).

The properties of phenolic resins are strongly dependent on reaction parameters such as the F/P molar ratio, catalyst, pH, and reaction time and temperature. The impact of these synthesis variables on structural properties of the resin, for instance molar mass and gel time, and end-use properties like the mechanical strength of the cured resin, are generally well-investigated [16,20,37,53–57].

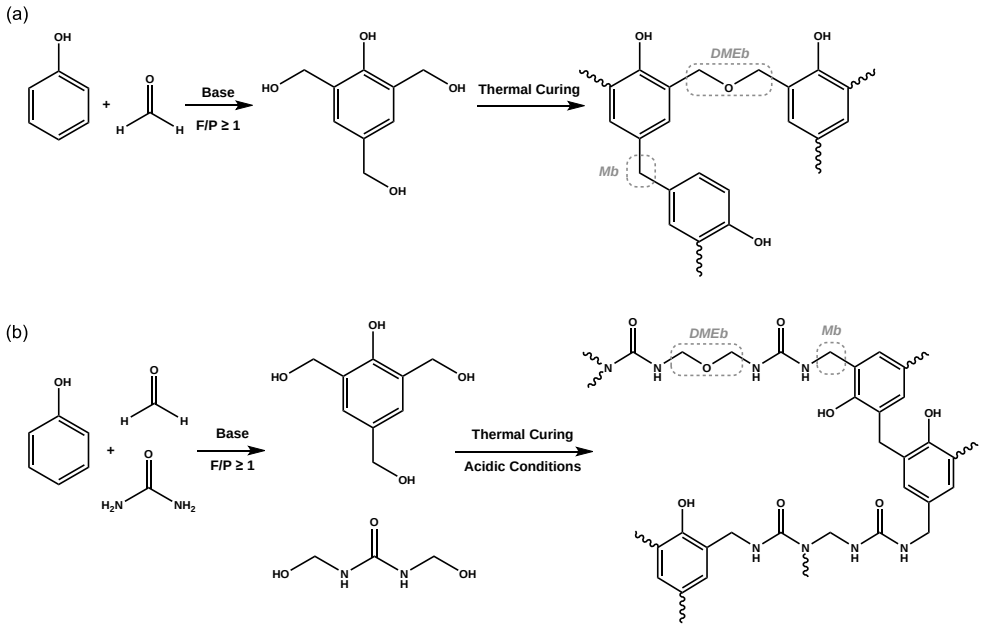


Figure 1.2. Synthesis and curing of (a) phenol-formaldehyde (PF) and (b) phenol-urea-formaldehyde (PUF) resin. Different linkages can be formed during curing: dimethylene ether (DMEb) or methylene bridges (Mb). It should be noted that the prepolymers shown (e.g., 2,4,6-trimethylolphenol and 1,2-dimethylolurea) are not the only species formed during the initial reaction between P, U and F, but the only species depicted for brevity.

The effect of the amount and type of catalyst on the reaction kinetics of forming phenolic prepolymers has also been studied in detail [54,58–62]. It is commonly found that organic catalysts, such as triethylamine (TEA), direct the addition reaction of formaldehyde to phenol to the *ortho* reactive sites, whereas for inorganic catalysts (e.g., NaOH, KOH, MgO, …) the *para* position is typically favoured [58,60,62]. Not only can the catalyst influence where formaldehyde reacts with phenol, the resulting linkages are also affected. TEA-catalysed phenolic prepolymers are linked mainly by dimethylene ether bridges. Conversely, NaOH-catalysed phenolic prepolymers contain predominantly methylene bridges [60]. As dimethylene ether linkages increase the oxygen content of the final cured resin, it is expected that a PF resin rich in these bridging groups exhibit a more polar character than PF-resins with predominantly methylene bridges. Furthermore, depending on the curing temperature and the F/P molar ratio, dimethylene ether bridges can be converted to methylene linkages, liberating formaldehyde [60].

Izumi *et al*. [63–67] studied the structure of cured novolac resins, which are PRs catalysed by an acid rather than a base. Inhomogeneous crosslinks in the cured resins were always observed, and affected by the F/P molar ratio, amount of crosslinker, and cure time and temperature. Regions with high and low crosslink density can therefore form in the final hardened resin [65,66]. It stands to reason that such inhomogeneities will affect material properties of the cured resin. De Boer [68] found an order of magnitude difference in the tensile strength of hardened PF resins which were determined experimentally compared to those determined theoretically, which Houwink [69] attributed to structural defects in the material as a result of crosslink inhomogeneities.

Resoles can easily be modified to form resins with improved properties for a vast range of applications [25–27,70–73]. As the free formaldehyde content increases with increasing F/P ratio for a given PF resin, it can become essential to adjust the resin to limit possible formaldehyde emissions whilst simultaneously enhancing resin properties. In general, this is achieved by addition of melamine, resorcinol or urea (U) to the mixture. For instance, urea acts as a formaldehyde scavenger, yielding methylolated urea species like mono-, di- and trimethylol urea [20]. Co-condensation of methylol phenol with methylol urea yields a phenol-urea-formaldehyde (PUF; Figure 1.2b) network with better mechanical and thermal characteristics compared to a PF network [20].

PUF resins can be synthesised either by co-condensing P, F and U in a single step, or by a multi-step procedure whereby PF fractions react with UF fractions [37,74–76]. As with PF resins, the molar ratio F/(P+U) has a pronounced influence on structural and thermal properties of PUF resins. Fan *et al*. [75] showed an increase in methylolated phenolic species upon increasing the formaldehyde content when using an MgO catalyst. Moreover, an increase in phenolic species bridged to urea by methylene linkages was also found.

To allow for effective condensation of methylolated urea species with methylolated phenolic species, acidic conditions are required. However, resoles themselves are not stable under acidic conditions, where polycondensates can be formed which can precipitate out of solution [20]. Therefore, latent acid hardeners such as $(NH_4)_2SO_4$ are usually employed, which at elevated temperatures neutralise the base. Additionally, through the reaction of ammonium sulphate with free and liberated formaldehyde, hexamethylenetetramine (HMTA) is formed, decreasing the pH [20]. HMTA can be formed following a series of subsequent reactions (Figure 1.3a) [20,77]. Ammonia can also be released during the curing process through reactions of urea with itself, forming biurets (Figure 1.3b). Such biurets can already form at temperatures above the melting point of urea (133 °C) [78,79]. Furthermore, hydrolysis of urea also leads to the production of ammonia [80,81]. Synthesis and reaction parameters will ultimately affect the amount of side products being formed.

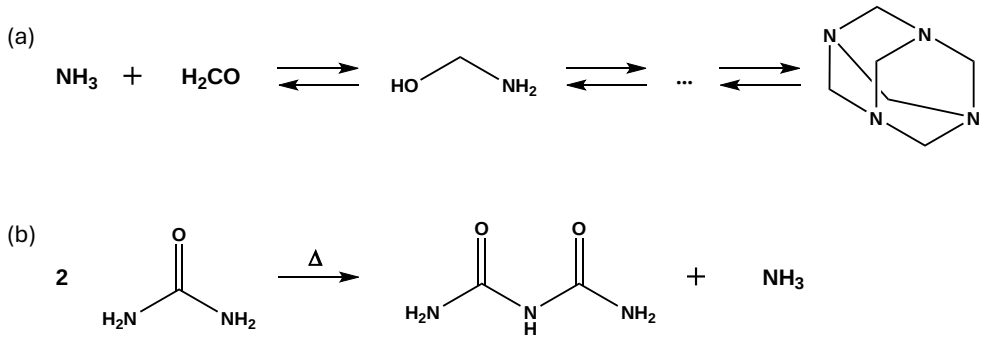


Figure 1.3. The formation of (a) hexamethylenetetramine (HMTA) upon reaction of ammonia with formaldehyde, and (b) biuret at elevated temperature, leading to the liberation of ammonia. Figure based on [20].

As mentioned before, different catalysts can be used for the synthesis and curing of phenolic resins. Alternatives for the use of inorganic catalysts to synthesise PUF resins are tertiary amines or tertiary alkanol amines [20,58,60,82]. Tertiary alkanol amines such as 2-dimethylamino-2-methyl-1-propanol ensure an initial high pH value of the resin. It is assumed that the incorporation of the catalyst in the thermoset network during curing results in acidification, ensuring proper co-condensation between UF- and PF-fractions [20,82]. Tertiary amines like triethylamine and dimethylethanolamine similarly allow for basic reaction conditions. During crosslinking of the resin at elevated temperatures, these catalysts evaporate and the resin is acidified by the methylolated phenolic species present in the system [20,82].

1.3. Wetting Agents and Wettability

Wetting agents (WAs) are a type of surfactant used to decrease the surface tension of solutions and facilitate their spreading on a surface. WAs are widely employed in various sectors, such as the coal industry [83–85], oil recovery [86], coating technology [87–89], agriculture, horticulture, and soil management [16,90–92]. For convenience, only water as a solvent will be considered below, although the concepts are valid for different solvents as well.

Molecules at an interface experience a smaller amount of intramolecular attractive forces compared to those in the bulk (Figure 1.4a). As a result of the increased energy of molecules at the interface, the interfacial area is minimised [88]. A typical WA consists of a polar part and a non-polar part, which gives the amphiphilic molecule its surface activity. In a solution, the non-polar part of the WA shuns interactions with the solvent whilst the polar part does not. For instance, the presence of hydrophobic groups in a hydrophilic solvent disrupts the solvent structure and increases the overall free energy of the system [93]. The work to then transport WAs to the interface is reduced, facilitating the replacement of higher-energy solvent molecules at the interface by the WAs [88,93]. As a result, the WAs spontaneously adsorb at the solvent–air interface, causing a net reduction of the surface tension (Figure 1.4b–c) [94].

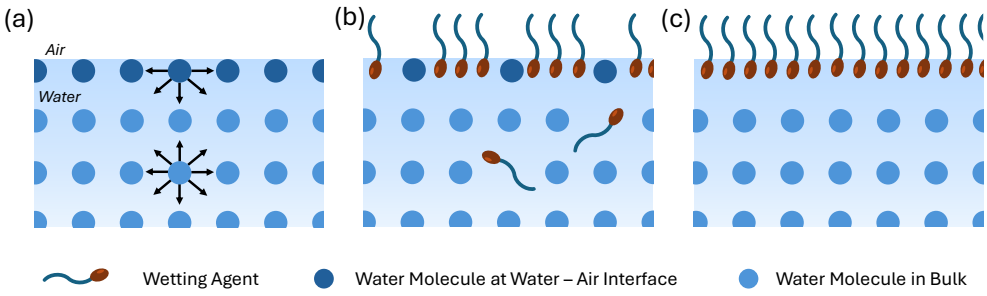


Figure 1.4. Schematic and simplified representation of (a) unequal intramolecular interactions between water molecules at the water–air interface, indicated with black arrows, and (b) the gradual enrichment of WAs at this interface with increasing concentration of WA until (c) the interface is saturated.

WAs can be classified as being nonionic or ionic (Figure 1.5), but both classes have the general structure of 'apolar–polar' in common. For ionic WAs, the polar part is commonly referred to as the headgroup, and dissociates into ions upon dissolution in water. Conversely, nonionic WAs are without such charge upon dissolution. Their solubility in water usually stems from the ethylene oxide (EO) part forming hydrogen bonds with water [95,96]. This hydration leads to the formation of solvation shells around the polar moiety, which is affected by, e.g., the polymer chain length and its conformation in water [95].

An important characteristic of WAs is the critical micelle concentration (CMC) in a given solvent. With increasing concentration of WA in water, the surface tension gradually decreases as more WAs are located at the water–air interface. Above the CMC, self-association in the bulk solution dominates and nearly all additional WAs self-assemble. The CMC usually coincides with saturation of the water–air interface. Self-assembled morphologies (e.g., micelles, vesicles, bilayers) form as in water the apolar tails of WAs will orient themselves towards one another, while the polar headgroups prefer to be in contact with water. Nonionic WAs typically have a lower CMC than ionic WAs, as the latter experience electrostatic repulsion which makes close packing of the headgroups unfavourable [88].

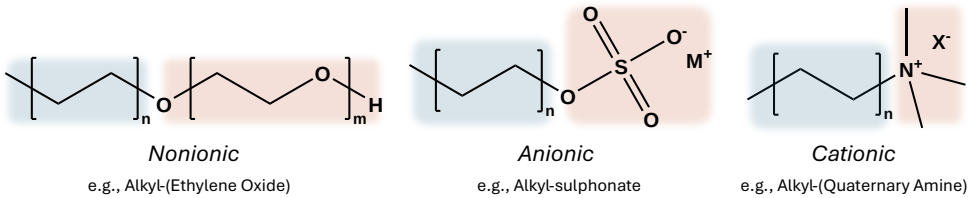


Figure 1.5. Examples of nonionic, anionic, and cationic WAs. Water-affine groups are shown in orange boxes, while the apolar tails are shown in the blue boxes.

Strategies to employ WAs in processes where increased wetting is required is to add them directly to water [83,84,97] or to spray them on the desired surface [16,98,99]. An alternative is to add WAs to a resin formulation [16,100–102], resulting in a more even distribution of the WA in the cured resin [16]. It should be noted that WAs are often added to formulations to improve for instant pigment wetting, as well as the wetting of a substrate by the resin [87,96]. However, WAs can also be used to functionalise a coating surface to make it more hydrophilic, as is already common practice for several growing media for hydroponic purposes [16,92,98–102]. In those cases, the coating–air interface is enriched by WAs upon curing the resin. If water then comes into contact with such a coating, the surface tension of the water droplet can still be decreased.

Surface wettability of coatings is most commonly assessed by means of contact angle goniometry (CAG), also called drop shape analysis (DSA), using water as a probe liquid. Thomas Young [103] correlated the interfacial tension between the solid–liquid phases (γ_{SL}), solid–vapour phases (γ_{SV}), and liquid–vapour phases (γ_{LV}) with the contact angle θ of a droplet on a solid surface (Figure 1.6). In case of a static water droplet, all forces acting on the droplet are balanced and hence there is equilibrium. Now commonly known as the Young–Dupré equation, the relation between these interfacial tension values is, for an inert and smooth surface,

$$\cos(\theta) = \frac{\gamma_{SV} - \gamma_{SL}}{\gamma_{LV}} , \tag{1.1}$$

with θ the water contact angle (WCA). For non-ideal (i.e., physically or chemically heterogeneous) surfaces the Wenzel [104] or Cassie–Baxter [105] models can be used.

Measuring interfacial tension values is not necessarily straightforward [106–108]. Although the surface tension of water (or any solvent or WA solution), γ_{LV}, can be readily determined from surface tension measurements (e.g., by using a pendant drop method [109], with a Wilhelmy plate [106,110], or by means of the capillary rise of the solution [111]), the determination of the other interfacial tension values requires more involved methods or approaches [108,112–115]. Nowadays, the experimentally observed apparent contact angle that is obtained from modern CAG (i.e., DSA) is based on digital fitting of a contour line around an optical image of a droplet with respect to the substrate[1] [116,117]. Physical or chemical heterogeneity is therefore indirectly taken into account, and heterogeneities are not expressed through an explicit parameter, unlike in, for instance, the Wenzel and Cassie-Baxter equations.

Nevertheless, the contact angle value which follows from Equation (1.1) or a static WCA measurement still yields information about the surface energy of the coating (albeit indirectly). It is generally accepted that surfaces are deemed to be hydrophobic when the WCA is larger than 90°, and hydrophilic if it is below 90°. When WAs are added to water, γ_{LV} will decrease and as a result the WCA value of a droplet of water with WA will decrease as well [118]. Hence, water-wettability of a surface is increased in presence of wetting agents.

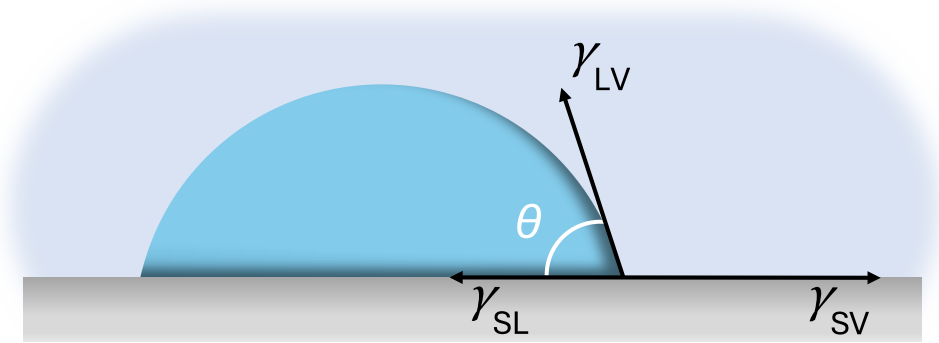


Figure 1.6. Schematic representation of a sessile drop on a solid surface. The contact angle θ results from a balance between the solid–liquid, solid–vapour, and liquid–vapour interfacial tension values.

[1] The surface energy of a coating can then also be determined by performing contact angle measurements with probe liquids which have different surface energy values. The Owens–Wendt–Rabel–Kaelble [113,114] or Van Oss–Good–Chaudhury [115] model can then be used to calculate γ_{SV} from the obtained data.

1.4. The Intersection of Phenolic Resins and Wetting Agents

The combination of WAs and PRs is not commonly investigated, although this type of formulation is industrially applied in, for instance, hydrophilic stone wool substrates [101,102,119]. A direct evaluation of the surface wettability of hydrophilic PR coatings, e.g., measured by CAG, has not been found in literature, despite the field of PRs being over 100 years old [25,120] and quite mature.

Studies involving a combination of surfactants and PRs commonly focus on mechanical or flame-retardant properties [121–123]. Patents on the use of WAs specifically in phenolic foams also exist, where WA effectiveness is gauged by the water absorption capacity and sinking time tests [98–100]. In a recent study, DSouza *et al*. [16] investigated the hydrophilicity of PF foams in presence of sodium dodecyl sulphate and sodium dodecylbenzene sulphonate. Whilst foams without WAs had a water absorption capacity of 190%, those with WAs showed an improved absorption of 1200%. Spraying WAs on the foam was also found to lead to a lower water uptake compared to addition of the WAs to the resin before the curing process, indicating that the distribution of the WAs strongly impacts the hydrophilicity of the foam [16].

Of note is also the research of Minu *et al*. [124], who studied the influence of dodecyl-based surfactants on the cure process of epoxy–novolac resins. It was found that the presence of surfactants decreases the ability of the resin to crosslink and plasticises the formed network. By extension, it stands to reason that WAs could have a similar effect on the network formation of phenolic resin coatings. Such research underscores the importance of understanding the interplay between both the PR and WA. Cultivating knowledge on how processing conditions of PRs, WA–PR interactions, and the behaviour of the PRs and WAs when exposed to water (vapour) affects surface characteristics of PR coatings provides valuable insights. These insights can be crucial for the optimisation and selection of the appropriate WAs for applications where phenolic resin coatings with hydrophilic surfaces are required. An example is hydrophilic stone wool substrates to which the work in this thesis is related.

1.5. Outline of Thesis

This thesis aims to provide more understanding of the surface properties of hydrophilic phenolic resin coatings for applications such as stone wool growing substrates for hydroponic purposes. First, the influence of the resin composition and curing conditions on surface characteristics such as morphology, chemistry and wettability is studied in **Chapter 2.** This is done by using various resin compositions (PF and PUF) and different catalysts for their synthesis and curing (organic and inorganic catalysts).

Chapter 3 focuses on surface wettability of phenolic resin coatings which contain wetting agents. The interaction between three chemically distinct WAs and PUF and PF

resin was studied by successive advancing contact angle measurements, assessing not only the WA persistence in the surface layers but also the transient response of the PR coating to the presence of water.

Since possible ageing in e.g. stone wool substrates may lead to changes in water characteristics, the stability of WAs and PR coatings is explored in **Chapter 4**. The role of different glassy substrates on the surface wettability of PR coatings after exposure of the surfaces to elevated temperature and relative humidity for a prolonged period is also considered.

The influence of the chemical composition of WAs on their compatibility with PUF and PF resins is also studied by systematically changing the length of the alkyl block or ethylene oxide block of nonionic and anionic WAs. As such, **Chapter 5** details the relationship between phenolic resin chemistry and wetting agent chemistry.

Finally, **Chapter 6** highlights the most important findings, and provides an outlook for future studies.

References

[1] R. Taagepera and M. Nemčok, "World population growth over millennia: Ancient and present phases with a temporary halt in-between," *Anthr. Rev.*, vol. 11, no. 1, pp. 163–183, 2024, doi: 10.1177/20530196231172423.

[2] H. C. J. Godfray, J. R. Beddington, I. R. Crute, L. Haddad, D. Lawrence, J. F. Muir, J. Pretty, S. Robinson, S. M. Thomas, and C. Toulmin, "Food Security: The Challenge of Feeding 9 Billion People," *Science*, vol. 327, no. 5967, pp. 812–818, 2010, doi: 10.1126/science.1185383.

[3] V. Smil, "How Many People Can the Earth Feed?," *Popul. Dev. Rev.*, vol. 20, no. 2, pp. 255–292, 1994, doi: 10.2307/2137520.

[4] P. Smith, "Delivering food security without increasing pressure on land," *Glob. Food Secur.*, vol. 2, no. 1, pp. 18–23, 2013, doi: 10.1016/j.gfs.2012.11.008.

[5] H. Kashiwase and T. Fusj, "Strains on freshwater resources," in *Atlas of Sustainable Development Goals 2023*, A. F. Pirlea, U. Serajuddin, A. Thudt, D. Wadhwa, and M. Welch, Eds., Washington, DC, 2023.

[6] H. Ritchie and M. Roser, "Land Use," *Our World Data*, 2024, Accessed: 2024. [Online]. Available: https://ourworldindata.org/land-use

[7] M. Flörke, C. Schneider, and R. I. McDonald, "Water competition between cities and agriculture driven by climate change and urban growth," *Nat. Sustain.*, vol. 1, no. 1, pp. 51–58, 2018, doi: 10.1038/s41893-017-0006-8.

[8] M. Brandon, T. Kozai, N. Lu, T. Yamaguchi, M. Takagaki, T. Maruo, and W. Yamori, *Next revolution of Agriculture: A review of innovations in plant factories*. 2016. doi: 10.13140/RG.2.1.3170.6000.

[9] X. Jiang, W. Zhang, A. R. Fernie, and W. Wen, "Combining novel technologies with interdisciplinary basic research to enhance horticultural crops," *Plant J.*, vol. 109, no. 1, pp. 35–46, 2022, doi: 10.1111/tpj.15553.

[10] C. M. Olympios, "Soilless media under protected cultivation rockwool, peat, perlite and other substrates," *Acta Hortic.*, no. 323, pp. 215–234, 1993, doi: 10.17660/ActaHortic.1993.323.20.

[11] H. S. Grewal, B. Maheshwari, and S. E. Parks, "Water and nutrient use efficiency of a low-cost hydroponic greenhouse for a cucumber crop: An Australian case study," *Agric. Water Manag.*, vol. 98, no. 5, pp. 841–846, 2011, doi: 10.1016/j.agwat.2010.12.010.

[12] D. I. Pomoni, M. K. Koukou, M. G. Vrachopoulos, and L. Vasiliadis, "A Review of Hydroponics and Conventional Agriculture Based on Energy and Water Consumption, Environmental Impact, and Land Use," *Energies*, vol. 16, no. 4, Art. no. 4, 2023, doi: 10.3390/en16041690.

[13] G. L. Barbosa, F. D. A. Gadelha, N. Kublik, A. Proctor, L. Reichelm, E. Weissinger, G. M. Wohlleb, and R. U. Halden, "Comparison of Land, Water, and Energy Requirements of Lettuce Grown Using Hydroponic vs. Conventional Agricultural Methods," *Int. J. Environ. Res. Public. Health*, vol. 12, no. 6, Art. no. 6, 2015, doi: 10.3390/ijerph120606879.

[14] P. Bradley and C. Marulanda, "Simplified hydroponics to reduce global hunger," *Acta Hortic.*, no. 554, pp. 289–296, 2001, doi: 10.17660/ActaHortic.2001.554.31.

[15] A. Gardziella, L. A. Pilato, and A. Knop, "Economic Significance, Survey of Applications, and Six Bonding Functions," in *Phenolic Resins: Chemistry, Applications, Standardization, Safety and Ecology*, A. Gardziella, L. A. Pilato, and A. Knop, Eds., Berlin, Heidelberg: Springer, 2000, pp. 122–487. doi: 10.1007/978-3-662-04101-7_6.

[16] G. C. DSouza, H. Li, Z. Yuan, C. C. Xu, M. B. Ray, and A. Prakash, "Investigating the hydrophilicity of phenol formaldehyde foams: Effects of synthesis parameters," *J. Appl. Polym. Sci.*, vol. 141, no. 5, p. e54877, 2024, doi: 10.1002/app.54877.

[17] F. L. Verwer and J. C. Welleman, "Irrigation and growing on Grodan rockwool," *Acta Hortic.*, no. 119, Art. no. 119, 1981, doi: 10.17660/ActaHortic.1981.119.16.

[18] J. C. C. Welleman and P. M. J. A. Smulders, "Latest developments in soilless growing on Grodan rockwool in Holland," *Acta Hortic.*, no. 221, Art. no. 221, 1988, doi: 10.17660/ActaHortic.1988.221.38.

[19] W. T. Bussell and S. Mckennie, "Rockwool in horticulture, and its importance and sustainable use in New Zealand," *N. Z. J. Crop Hortic. Sci.*, vol. 32, no. 1, Art. no. 1, 2004, doi: 10.1080/01140671.2004.9514277.

[20] S. Kowatsch, "Mineral Wool Insulation Binders," in *Phenolic Resins: A Century of Progress*, L. Pilato, Ed., Berlin, Heidelberg: Springer, 2010, pp. 209–242. doi: 10.1007/978-3-642-04714-5_10.

[21] M. Nooijens, "A study on the influence of wetting agents on binder distribution and water characteristics of Grodan substrates," Eindhoven University of Technology & Grodan, Eindhoven & Roermond, Confidential Internship Report, 2022.

[22] S. H. Q. Barly, D. V. Okhrimenko, M. Solvang, Y. Yue, and S. L. S. Stipp, "Dissolution of Stone Wool Fibers with Phenol-urea-formaldehyde Binder in a Synthetic Lung Fluid," *Chem. Res. Toxicol.*, vol. 32, no. 12, Art. no. 12, 2019, doi: 10.1021/acs.chemrestox.9b00179.

[23] D. V. Okhrimenko, M. Ceccato, S. Tougaard, M. Foss, E. Pezennec, and M. Solvang, "Comment on 'Which fraction of stone wool fibre surface remains uncoated by binder? A detailed analysis by time-of-flight secondary ion mass spectrometry and X-ray photoelectron spectroscopy' by Hirth et al. , 2021, RSC Adv. , 11 , 39545, DOI: 10.1039/d1ra06251d," *RSC Adv.*, vol. 13, no. 24, pp. 16688–16692, 2023, doi: 10.1039/D2RA07959C.

[24] M. Solvang, D. V. Okhrimenko, and C. Koch, "Investigation of the occurrence of binder material on airborne respirable mineral wool fibers," *J. Occup. Environ. Hyg.*, vol. 20, no. 5–6, pp. 240–253, 2023, doi: 10.1080/15459624.2023.2205470.

[25] L. Pilato, "Phenolic resins: 100 Years and still going strong," *React. Funct. Polym.*, vol. 73, no. 2, Art. no. 2, 2013, doi: 10.1016/j.reactfunctpolym.2012.07.008.

[26] C. P. R. Nair, "Advances in addition-cure phenolic resins," *Prog. Polym. Sci.*, vol. 29, no. 5, pp. 401–498, 2004, doi: 10.1016/j.progpolymsci.2004.01.004.

[27] K. Tang, A. Zhang, T. Ge, X. Liu, X. Tang, and Y. Li, "Research progress on modification of phenolic resin," *Mater. Today Commun.*, vol. 26, p. 101879, 2021, doi: 10.1016/j.mtcomm.2020.101879.

[28] C. Morterra and M. J. D. Low, "I.R. studies of carbons—VII. The pyrolysis of a phenol-formaldehyde resin," *Carbon*, vol. 23, no. 5, pp. 525–530, 1985, doi: 10.1016/0008-6223(85)90088-0.

[29] B. K. Kandola, A. R. Horrocks, P. Myler, D. Blair, G. L. Nelson (Ed.), and C. A. Wilkie (Ed.), "Thermal Characterization of Thermoset Matrix Resins," in *Fire and Polymers*, vol. 797, in ACS Symposium Series, vol. 797. , Washington, DC, 2001, pp. 344–360.

[30] R. J. Zaldivar, G. L. Ferrelli, V. Arredondo, and H. I. Kim, "Effect of cure temperature on the thermal degradation, mechanical, microstructural and moisture absorption behavior of vacuum-only, carbon-fiber reinforced phenolic composites," *J. Appl. Polym. Sci.*, vol. 139, no. 34, p. e52819, 2022, doi: 10.1002/app.52819.

[31] A. Trosa and A. Pizzi, "Industrial hardboard and other panels binder from waste lignocellulosic liquors/phenol-formaldehyde resins," *Eur. J. Wood Wood Prod.*, vol. 56, no. 4, pp. 229–233, 1998, doi: 10.1007/s001070050307.

[32] A. Pizzi, A. N. Papadopoulos, and F. Policardi, "Wood Composites and Their Polymer Binders," *Polymers*, vol. 12, no. 5, Art. no. 5, 2020, doi: 10.3390/polym12051115.

[33] J. L. Paris, F. A. Kamke, R. Mbachu, and S. K. Gibson, “Phenol formaldehyde adhesives formulated for advanced X-ray imaging in wood-composite bondlines,” *J. Mater. Sci.*, vol. 49, no. 2, pp. 580–591, 2014, doi: 10.1007/s10853-013-7738-2.

[34] D.-B. Fan, J.-M. Chang, J.-Z. Li, B.-H. Xia, and Z.-T. Sang, “Cure properties and adhesive performances of cure-accelerated phenol-urea-formaldehyde resins,” *Eur. J. Wood Wood Prod.*, vol. 69, no. 2, pp. 213–220, 2011, doi: 10.1007/s00107-010-0414-1.

[35] H. Kajita and Y. Imamura, “Improvement of physical and biological properties of particleboards by impregnation with phenolic resin,” *Wood Sci. Technol.*, vol. 26, no. 1, pp. 63–70, 1991, doi: 10.1007/BF00225692.

[36] M. Dunky and A. Pizzi, “Chapter 23 - Wood adhesives,” in *Adhesion Science and Engineering*, D. A. Dillard, A. V. Pocius, and M. Chaudhury, Eds., Amsterdam: Elsevier Science B.V., 2002, pp. 1039–1103. doi: 10.1016/B978-044451140-9/50023-8.

[37] B. Tomita and C.-Y. Hse, “Phenol–urea–formaldehyde (PUF) co-condensed wood adhesives,” *Int. J. Adhes. Adhes.*, vol. 18, no. 2, pp. 69–79, 1998, doi: 10.1016/S0143-7496(97)00047-X.

[38] W. N. Ahamad, S. Salim, S. H. Lee, M. A. Abdul Ghani, R. A. Mohd Ali, P. Md Tahir, W. Fatriasari, P. Antov, and M. A. R. Lubis, “Effects of Compression Ratio and Phenolic Resin Concentration on the Properties of Laminated Compreg Inner Oil Palm and Sesenduk Wood Composites,” *Forests*, vol. 14, no. 1, Art. no. 1, 2023, doi: 10.3390/f14010083.

[39] Z. Yang, G. Xian, and H. Li, “Effects of alternating temperatures and humidity on the moisture absorption and mechanical properties of ramie fiber reinforced phenolic plates,” *Polym. Compos.*, vol. 36, no. 9, pp. 1590–1596, 2015, doi: 10.1002/pc.23067.

[40] H. Younesi-Kordkheili and A. Pizzi, “A Comparison among Lignin Modification Methods on the Properties of Lignin–Phenol–Formaldehyde Resin as Wood Adhesive,” *Polymers*, vol. 13, no. 20, Art. no. 20, 2021, doi: 10.3390/polym13203502.

[41] S. Yang, Y. Zhang, T.-Q. Yuan, and R.-C. Sun, “Lignin–phenol–formaldehyde resin adhesives prepared with biorefinery technical lignins,” *J. Appl. Polym. Sci.*, vol. 132, no. 36, 2015, doi: 10.1002/app.42493.

[42] W. Yang, M. Rallini, M. Natali, J. Kenny, P. Ma, W. Dong, L. Torre, and D. Puglia, “Preparation and properties of adhesives based on phenolic resin containing lignin micro and nanoparticles: A comparative study,” *Mater. Des.*, vol. 161, pp. 55–63, 2019, doi: 10.1016/j.matdes.2018.11.032.

[43] N. S. Çetin and N. Özmen, “Use of organosolv lignin in phenol-formaldehyde resins for particleboard production: II. Particleboard production and properties,” *Int. J. Adhes. Adhes.*, vol. 22, no. 6, pp. 481–486, 2002, doi: 10.1016/S0143-7496(02)00059-3.

[44] S. Sarkar and B. Adhikari, “Lignin-modified phenolic resin: synthesis optimization, adhesive strength, and thermal stability,” *J. Adhes. Sci. Technol.*, vol. 14, no. 9, pp. 1179–1193, 2000, doi: 10.1163/156856100743167.

[45] H. Kollek, H. Brockmann, and H. Muller von der Haegen, “Chemistry of curing and adhesion properties of phenolic resins,” *Int. J. Adhes. Adhes.*, vol. 6, no. 1, pp. 37–41, 1986, doi: 10.1016/0143-7496(86)90070-9.

[46] X. Xing, Y. Zhao, X. Zhang, J. Wang, T. Hong, Y. Li, S. Wang, C. Zhang, and X. Jing, “Healable ablative composites from synergistically crosslinked phenolic resin,” *Chem. Eng. J.*, vol. 447, p. 137571, 2022, doi: 10.1016/j.cej.2022.137571.

[47] J. Si, J. Li, S. Wang, Y. Li, and X. Jing, “Enhanced thermal resistance of phenolic resin composites at low loading of graphene oxide,” *Compos. Part Appl. Sci. Manuf.*, vol. 54, pp. 166–172, 2013, doi: 10.1016/j.compositesa.2013.07.019.

[48] A. Pizzi, Ed., “Phenolic Resin Adhesives,” in *Handbook of Adhesive Technology*, 3rd ed., CRC Press, 2017.

[49] A. Zafar, J. Schjødt-Thomsen, R. Sodhi, R. Goacher, and D. de Kubber, “Investigation of the ageing effects on phenol-urea-formaldehyde binder and alkanol amine-acid anhydride binder coated mineral fibres,” *Polym. Degrad. Stab.*, vol. 98, no. 1, pp. 339–347, 2013, doi: 10.1016/j.polymdegradstab.2012.09.007.

[50] D. V. Okhrimenko, A. B. Thomsen, M. Ceccato, D. B. Johansson, D. Lybye, K. Bechgaard, S. Tougaard, and S. L. S. Stipp, “Impact of curing time on ageing and degradation of phenol-urea-formaldehyde binder,” *Polym. Degrad. Stab.*, vol. 152, pp. 86–94, 2018, doi: 10.1016/j.polymdegradstab.2018.04.001.

[51] H. E. Faith, “Aldehyde—Phenol Reaction Products and Derivatives,” *J. Am. Chem. Soc.*, vol. 72, no. 2, pp. 837–839, 1950, doi: 10.1021/ja01158a049.

[52] M. V. Alonso, J. J. Rodríguez, M. Oliet, F. Rodríguez, J. García, and M. A. Gilarranz, "Characterization and structural modification of ammonic lignosulfonate by methylolation," *J. Appl. Polym. Sci.*, vol. 82, no. 11, pp. 2661–2668, 2001, doi: 10.1002/app.2119.

[53] M.-F. Grenier-Loustalot, S. Larroque, P. Grenier, J.-P. Leca, and D. Bedel, "Phenolic resins: 1. Mechanisms and kinetics of phenol and of the first polycondensates towards formaldehyde in solution," *Polymer*, vol. 35, no. 14, pp. 3046–3054, 1994, doi: 10.1016/0032-3861(94)90418-9.

[54] M.-F. Grenier-Loustalot, S. Larroque, D. Grande, P. Grenier, and D. Bedel, "Phenolic resins: 2. Influence of catalyst type on reaction mechanisms and kinetics," *Polymer*, vol. 37, no. 8, pp. 1363–1369, 1996, doi: 10.1016/0032-3861(96)81133-5.

[55] M.-F. Grenier-Loustalot, S. Larroque, and P. Grenier, "Phenolic resins: 5. Solid-state physicochemical study of resoles with variable FP ratios," *Polymer*, vol. 37, no. 4, pp. 639–650, 1996, doi: 10.1016/0032-3861(96)83151-X.

[56] L. Gollob and A. (Ed.) Pizzi, "The Correlation Between Preparation and Properties in Phenolic Resins," in *Wood Adhesives. Chemistry and Technology*, 1st ed., vol. 2, Boca Raton: CRC Press, 1989, pp. 121–153. doi: 10.1201/9780203733721-5.

[57] G. He and B. Riedl, "Phenol-urea-formaldehyde cocondensed resol resins: Their synthesis, curing kinetics, and network properties," *J. Polym. Sci. Part B Polym. Phys.*, vol. 41, no. 16, pp. 1929–1938, 2003, doi: 10.1002/polb.10558.

[58] G. Astarloa-Aierbe, J. M. Echeverría, A. Vázquez, and I. Mondragon, "Influence of the amount of catalyst and initial pH on the phenolic resol resin formation," *Polymer*, vol. 41, no. 9, pp. 3311–3315, 2000, doi: 10.1016/S0032-3861(99)00519-4.

[59] J. Bouajila, G. Raffin, H. Waton, C. Sanglar, J. O. Païsse, and M. F. Grenier-Loustalot, "Phenolic Resins – Characterizations and Kinetic Studies of Different Resols Prepared with Different Catalysts and Formaldehyde/Phenol Ratios (I)," *Polym. Polym. Compos.*, vol. 10, no. 5, pp. 341–360, 2002, doi: 10.1177/096739110201000502.

[60] N. Gabilondo, M. Larrañaga, C. Peña, M. A. Corcuera, J. M. Echeverría, and I. Mondragon, "Polymerization of resole resins with several formaldehyde/phenol molar ratios: Amine catalysts against sodium hydroxide catalysts," *J. Appl. Polym. Sci.*, vol. 102, no. 3, pp. 2623–2631, 2006, doi: 10.1002/app.24017.

[61] D. Fan, F. Chu, T. Qin, and J. Li, "Effect of Synthesis Conditions on the Structure and Curing Characteristics of High-Urea Content PUF Resin," *J. Adhes.*, vol. 87, no. 12, pp. 1191–1203, 2011, doi: 10.1080/00218464.2011.628871.

[62] B. Kałędkowski and J. Hetper, "Synthesis of phenol–formaldehyde resole resins in the presence of tetraalkylammonium hydroxides as catalysts," *Polymer*, vol. 41, no. 5, pp. 1679–1684, 2000, doi: 10.1016/S0032-3861(99)00345-6.

[63] A. Izumi, Y. Shudo, T. Nakao, and M. Shibayama, "Cross-link inhomogeneity in phenolic resins at the initial stage of curing studied by 1H-pulse NMR spectroscopy and complementary SAXS/WAXS and SANS/WANS with a solvent-swelling technique," *Polymer*, vol. 103, pp. 152–162, 2016, doi: 10.1016/j.polymer.2016.09.067.

[64] A. Izumi, T. Nakao, H. Iwase, and M. Shibayama, "Structural analysis of cured phenolic resins using complementary small-angle neutron and X-ray scattering and scanning electron microscopy," *Soft Matter*, vol. 8, no. 32, pp. 8438–8445, 2012, doi: 10.1039/C2SM26072G.

[65] A. Izumi, T. Nakao, and M. Shibayama, "Gelation and cross-link inhomogeneity of phenolic resins studied by 13C-NMR spectroscopy and small-angle X-ray scattering," *Soft Matter*, vol. 9, no. 16, pp. 4188–4197, 2013, doi: 10.1039/C3SM27438A.

[66] A. Izumi, Y. Shudo, and M. Shibayama, "Network structure evolution of a hexamethylenetetramine-cured phenolic resin," *Polym. J.*, vol. 51, no. 2, pp. 155–160, 2019, doi: 10.1038/s41428-018-0133-8.

[67] A. Izumi, Y. Shudo, M. Shibayama, N. Miyata, T. Miyazaki, and H. Aoki, "In Situ Neutron Reflectometry Analysis of Interfacial Structure Formation between Phenolic Resin and Silica during Curing," *Langmuir*, vol. 37, no. 47, pp. 13867–13872, 2021, doi: 10.1021/acs.langmuir.1c02313.

[68] J. H. de Boer, "The influence of van der Waals' forces and primary bonds on binding energy, strength and orientation, with special reference to some artificial resins," *Trans. Faraday Soc.*, vol. 32, no. 0, pp. 10–37, 1936, doi: 10.1039/TF9363200010.

[69] R. Houwink, "The strength and modulus of elasticity of some amorphous materials, related to their internal structure," *Trans. Faraday Soc.*, vol. 32, no. 0, pp. 122–131, 1936, doi: 10.1039/TF9363200122.

[70] J. Grinins, M. Iesalnieks, V. Biziks, I. Gritane, and G. Sosins, “Birch Wood Surface Characterization after Treatment with Modified Phenol-Formaldehyde Oligomers,” *Polymers*, vol. 14, no. 4, Art. no. 4, 2022, doi: 10.3390/polym14040671.

[71] Y. Li, H. Wei, L. Li, J. Wang, X. Qian, L. He, X. Wang, Q. Ouyang, Y. Chen, Y. Zhang, *et al.*, “High-efficiency surfactant prepared from phenolic resin for multi-walled carbon nanotube aqueous suspension,” *J. Nanoparticle Res.*, vol. 20, no. 6, p. 162, 2018, doi: 10.1007/s11051-018-4264-9.

[72] D. Wang, J. Ding, B. Wang, Y. Zhuang, and Z. Huang, “Synthesis and Thermal Degradation Study of Polyhedral Oligomeric Silsesquioxane (POSS) Modified Phenolic Resin,” *Polymers*, vol. 13, no. 8, Art. no. 8, 2021, doi: 10.3390/polym13081182.

[73] G. Vázquez, F. López-Suevos, A. Villar-Garea, J. González-Alvarez, and G. Antorrena, “13C-NMR analysis of phenol-urea-formaldehyde prepolymers and phenol-urea-formaldehyde-tannin adhesives,” *J. Adhes. Sci. Technol.*, vol. 18, no. 13, pp. 1529–1543, 2004, doi: 10.1163/1568561042411231.

[74] B. Tomita and C.-Y. Hse, “Cocondensation of urea with methylolphenols in acidic conditions,” *J. Polym. Sci. Part Polym. Chem.*, vol. 30, no. 8, pp. 1615–1624, 1992, doi: 10.1002/pola.1992.080300814.

[75] D.-B. Fan, G.-Y. Li, T.-F. Qin, and F.-X. Chu, “Synthesis and Structure Characterization of Phenol-Urea-Formaldehyde Resins in the Presence of Magnesium Oxide as Catalyst,” *Polymers*, vol. 6, no. 8, Art. no. 8, 2014, doi: 10.3390/polym6082221.

[76] B. Pang, M.-K. Li, S. Yang, T.-Q. Yuan, G.-B. Du, and R.-C. Sun, “Eco-Friendly Phenol–Urea–Formaldehyde Co-condensed Resin Adhesives Accelerated by Resorcinol for Plywood Manufacturing,” *ACS Omega*, vol. 3, no. 8, pp. 8521–8528, 2018, doi: 10.1021/acsomega.8b01286.

[77] M. T. Feldmann, S. L. Widicus, G. A. Blake, D. R. Kent IV, and W. A. Goddard III, “Aminomethanol water elimination: Theoretical examination,” *J. Chem. Phys.*, vol. 123, no. 3, p. 034304, 2005, doi: 10.1063/1.1935510.

[78] C. E. Redemann, F. C. Riesenfeld, and F. S. La. Viola, “Formation of Biuret from Urea,” *Ind. Eng. Chem.*, vol. 50, no. 4, pp. 633–636, 1958, doi: 10.1021/ie50580a035.

[79] A. Kawasaki and Y. Ogata, “Kinetics of the formation of biuret from urea in 2-methoxyethanol,” *Tetrahedron*, vol. 21, no. 10, pp. 2893–2898, 1965, doi: 10.1016/S0040-4020(01)98374-7.

[80] O. Steinhof, É. J. Kibrik, G. Scherr, and H. Hasse, “Quantitative and qualitative 1H, 13C, and 15N NMR spectroscopic investigation of the urea–formaldehyde resin synthesis,” *Magn. Reson. Chem.*, vol. 52, no. 4, pp. 138–162, 2014, doi: 10.1002/mrc.4044.

[81] R. C. Warner, “The kinetics of the hydrolysis of urea and of arginine,” *J. Biol. Chem.*, vol. 142, no. 2, pp. 705–723, 1942, doi: 10.1016/S0021-9258(18)45072-7.

[82] G. Wu, “Strongly basic tertiary amino alcohols as catalyst,” WO1997000900A1, 1997 Accessed: 2022. [Online]. Available: https://patents.google.com/patent/WO1997000900A1/en?oq=WO+1997%2f000900

[83] Z. Chao, W. Xinglong, L. Shugang, J. Bingyou, Z. Cheng, Z. Chuanjie, and N. Guanhua, “Development and application of a new compound wetting agent for coal seam water infusion,” *Fuel*, vol. 314, p. 122767, 2022, doi: 10.1016/j.fuel.2021.122767.

[84] J. Li, F. Zhou, and H. Liu, “The Selection and Application of a Compound Wetting Agent to the Coal Seam Water Infusion for Dust Control,” *Int. J. Coal Prep. Util.*, vol. 36, no. 4, pp. 192–206, 2016, doi: 10.1080/19392699.2015.1088529.

[85] K. Wang, C. Ding, S. Jiang, W. Zhengyan, H. Shao, and W. Zhang, “Application of the addition of ionic liquids using a complex wetting agent to enhance dust control efficiency during coal mining,” *Process Saf. Environ. Prot.*, vol. 122, pp. 13–22, 2019, doi: 10.1016/j.psep.2018.11.011.

[86] Z. Bi, W. Liao, and L. Qi, “Synthesis and wetting properties of a novel wetting agent by molecular design process,” *Colloids Surf. Physicochem. Eng. Asp.*, vol. 256, no. 2, pp. 117–121, 2005, doi: 10.1016/j.colsurfa.2004.12.046.

[87] S. Swarup and C. K. Schoff, “A survey of surfactants in coatings technology,” *Prog. Org. Coat.*, vol. 23, no. 1, pp. 1–22, 1993, doi: 10.1016/0033-0655(93)80002-R.

[88] D. Myers, *Surfactant Science and Technology*. John Wiley & Sons, 2005.

[89] F. Cazaux and X. Coqueret, “Polydimethylsiloxanes with vinyl ether end-groups—I. Synthesis and properties as polymerizable wetting agents,” *Eur. Polym. J.*, vol. 31, no. 6, pp. 521–525, 1995, doi: 10.1016/0014-3057(94)00211-8.

[90] B. Chang, B. Wherley, J. Aitkenhead-Peterson, N. Ojeda, C. Fontanier, and P. Dwyer, “Effect of Wetting Agent on Nutrient and Water Retention and Runoff from Simulated Urban Lawns,” 2020, doi: 10.21273/HORTSCI14982-20.

[91] S. Laha, B. Tansel, and A. Ussawarujikulchai, “Surfactant–soil interactions during surfactant-amended remediation of contaminated soils by hydrophobic organic compounds: A review,” *J. Environ. Manage.*, vol. 90, no. 1, pp. 95–100, 2009, doi: 10.1016/j.jenvman.2008.08.006.

[92] M. C. Basso, A. Pizzi, F. Al-Marzouki, and S. Abdalla, “Horticultural/hydroponics and floral natural foams from tannins,” *Ind. Crops Prod.*, vol. 87, pp. 177–181, 2016, doi: 10.1016/j.indcrop.2016.04.033.

[93] T. Cosgrove, *Colloid science: principles, methods and applications*, 2nd ed. Chichester, United Kingdom: Wiley, 2010.

[94] F. E. Bartell, “Wetting Agents,” *Ind. Eng. Chem.*, vol. 33, no. 6, pp. 737–740, 1941, doi: 10.1021/ie50378a012.

[95] A. M. Rozza, D. E. P. Vanpoucke, E.-M. Krammer, J. Bouckaert, R. Blossey, M. F. Lensink, M. J. Ondrechen, I. Bakó, J. Oláh, and G. Roos, “Hydration sphere structure of architectural molecules: Polyethylene glycol and polyoxymethylene oligomers,” *J. Mol. Liq.*, vol. 384, p. 122172, 2023, doi: 10.1016/j.molliq.2023.122172.

[96] J. Bieleman, *Additives for coatings*. Weinheim: Wiley-VCH, 2000.

[97] F. M. Fowkes, “Role of Surface Active Agents in Wetting,” *J. Phys. Chem.*, vol. 57, no. 1, pp. 98–103, 1953, doi: 10.1021/j150502a021.

[98] V. L. Smithers, “Absorbent material for floral arrangements,” US2753277A, 1956 Accessed: 2024. [Online]. Available: https://patents.google.com/patent/US2753277A/en

[99] F. Weissenfels and W. Engels, “Method for the preparation of highly absorbent phenolic resin foams,” US4426462A, 1984 Accessed: 2024. [Online]. Available: https://patents.google.com/patent/US4426462A/en

[100] L. A. Pilato, “Floral foam product and method of producing the same which incorporates a flower preservative and a bacteriocide,” US4225679A, 1980 Accessed: 2024. [Online]. Available: https://patents.google.com/patent/US4225679A/en

[101] J. M. W. Cuypers, D. D. Kubber, and P. Bouwens, “Growth substrates, their production and their use,” US8181390B2, 2012 Accessed: 2024. [Online]. Available: https://patents.google.com/patent/US8181390B2/en?assignee=rockwool+international+a.s.&oq=rockwool+international+a.s.

[102] J. Cuypers, K. D. De, and P. Bouwens, “Method of Growing Plants,” EP2048935B1, 2016

[103] T. Young, “An essay on the cohesion of fluids,” *Philos. Trans. R. Soc. Lond.*, vol. 95, pp. 65–87, 1805, doi: 10.1098/rstl.1805.0005.

[104] R. N. Wenzel, “Resistance of solid surfaces to wetting by water,” *Ind. Eng. Chem.*, vol. 28, no. 8, pp. 988–994, 1936, doi: 10.1021/ie50320a024.

[105] A. B. D. Cassie and S. Baxter, “Wettability of porous surfaces,” *Trans. Faraday Soc.*, vol. 40, no. 0, pp. 546–551, 1944, doi: 10.1039/TF9444000546.

[106] B. M. Oosterlaken and G. de With, “How Reliable Are Surface Tension Data?,” *Acc. Mater. Res.*, vol. 3, no. 9, pp. 894–899, 2022, doi: 10.1021/accountsmr.2c00129.

[107] K. Grundke, T. Bogumil, T. Gietzelt, H.-J. Jacobasch, D. Y. Kwok, and A. W. Neumann, “Wetting measurements on smooth, rough and porous solid surfaces,” in *Interfaces, Surfactants and Colloids in Engineering*, H.-J. Jacobasch, Ed., Darmstadt: Steinkopff, 1996, pp. 58–68. doi: 10.1007/BFb0114445.

[108] D. Li and A. W. Neumann, “Equation of state for interfacial tensions of solid-liquid systems,” *Adv. Colloid Interface Sci.*, vol. 39, pp. 299–345, 1992, doi: 10.1016/0001-8686(92)80064-5.

[109] J. D. Berry, M. J. Neeson, R. R. Dagastine, D. Y. C. Chan, and R. F. Tabor, “Measurement of surface and interfacial tension using pendant drop tensiometry,” *J. Colloid Interface Sci.*, vol. 454, pp. 226–237, 2015, doi: 10.1016/j.jcis.2015.05.012.

[110] B. M. Oosterlaken, A. van den Bruinhorst, and G. de With, “On the Use of Probe Liquids for Surface Energy Measurements,” *Langmuir*, vol. 39, no. 47, pp. 16701–16711, 2023, doi: 10.1021/acs.langmuir.3c00910.

[111] J. Drelich, C. Fang, and C. L. White, “Measurement of interfacial tension in fluid-fluid systems,” in *Encyclopedia of Surface and Colloid Science*, Marcel Dekker Inc., 2002, pp. 3152–3166.

[112] S. Mohammadi-Jam and K. E. Waters, “Inverse gas chromatography applications: A review,” *Adv. Colloid Interface Sci.*, vol. 212, pp. 21–44, 2014, doi: 10.1016/j.cis.2014.07.002.

[113] D. K. Owens and R. C. Wendt, “Estimation of the surface free energy of polymers,” *J. Appl. Polym. Sci.*, vol. 13, no. 8, pp. 1741–1747, 1969, doi: 10.1002/app.1969.070130815.
[114] D. H. Kaelble, “Dispersion-Polar Surface Tension Properties of Organic Solids,” *J. Adhes.*, vol. 2, no. 2, pp. 66–81, 1970, doi: 10.1080/0021846708544582.
[115] C. J. Van Oss, R. J. Good, and M. K. Chaudhury, “Additive and nonadditive surface tension components and the interpretation of contact angles,” *Langmuir*, vol. 4, no. 4, pp. 884–891, 1988, doi: 10.1021/la00082a018.
[116] P. Cheng, D. Li, L. Boruvka, Y. Rotenberg, and A. W. Neumann, “Automation of axisymmetric drop shape analysis for measurements of interfacial tensions and contact angles,” *Colloids Surf.*, vol. 43, no. 2, pp. 151–167, 1990, doi: 10.1016/0166-6622(90)80286-D.
[117] D. Y. Kwok and A. W. Neumann, “Contact angle measurement and contact angle interpretation,” *Adv. Colloid Interface Sci.*, vol. 81, no. 3, pp. 167–249, 1999, doi: 10.1016/S0001-8686(98)00087-6.
[118] L. K. Koopal, “Wetting of Solid Surfaces: Fundamentals and Charge effects,” *Adv. Colloid Interface Sci.*, vol. 179–182, pp. 29–42, 2012, doi: 10.1016/j.cis.2012.06.009.
[119] A. Blaakmeer, “Plant growth substrates,” WO2001082683A1, 2001 Accessed: 2024. [Online]. Available: https://patents.google.com/patent/WO2001082683A1/en?oq=WO+01%2f82683+
[120] L. H. Baekeland, “Method of making insoluble products of phenol and formaldehyde,” US942699A, 1909 Accessed: 2022. [Online]. Available: https://patents.google.com/patent/US942699A/en
[121] K. R. Denslow and G. K. Rickle, “Surfactant Effects in Phenolic Foam Resins,” *J. Cell. Plast.*, vol. 25, no. 1, pp. 31–42, 1989, doi: 10.1177/0021955X8902500102.
[122] X. Hu, W. Cheng, C. Li, G. Wang, X. Lin, and Z. Liu, “Effects of surfactants on the mechanical properties, microstructure, and flame resistance of phenol–urea–formaldehyde foam,” *Polym. Bull.*, vol. 73, no. 1, pp. 1–20, 2016, doi: 10.1007/s00289-015-1470-9.
[123] I. Muylaert, A. Verberckmoes, J. De Decker, and P. Van Der Voort, “Ordered mesoporous phenolic resins: Highly versatile and ultra stable support materials,” *Adv. Colloid Interface Sci.*, vol. 175, pp. 39–51, 2012, doi: 10.1016/j.cis.2012.03.007.
[124] S. Minu, R. Ramani, R. Indu Shekar, T. Math Kotresh, and N. Vijay Padaki, “Influence of dodecyl surfactants on the cross-linking, plasticization and damping behavior of epoxy novolac resins,” *Soft Matter*, vol. 18, no. 38, pp. 7380–7393, 2022, doi: 10.1039/D2SM01126C.

2

Surface Characteristics of Phenolic Resin Coatings



Abstract

Phenolic resins are commonly used as polymer binders for metal, paper and mineral wool substrates. For these applications, mechanical, adhesive and thermal properties are considered most important, and the effect of synthesis and structural parameters on such end-use characteristics are well-documented. However, surface characteristics of cured phenolic resins can be equally relevant and are often overlooked. To gain more insight into surface characteristics such as morphology, chemical composition and wettability of cured phenol-urea-formaldehyde (PUF) and phenol-formaldehyde (PF) resins, different binder formulations were applied on glass substrates and subsequently characterised by Scanning Electron Microscopy (SEM), Contact Angle Goniometry (CAG) and X-Ray Photoelectron Spectroscopy (XPS). The effect of catalyst, chemical composition and curing conditions on surface characteristics of various PUF and PF coatings was investigated. The curing temperature was found to have a strong influence on surface properties: curing at 200 °C yields a surface with varying degrees of oxidation, differences in linkages between phenolic and urea species, and a lower overall nitrogen content for the urea-containing coatings, resulting in stronger fluctuations in water-wettability compared to surfaces hardened at lower temperatures.

This chapter is based on L. Moone, M.P.J. Donners, K. van Durme, D.V. Okhrimenko, R.A.T.M. van Benthem, R. Tuinier, and A.C.C. Esteves, Surface characteristics of phenolic resins, *Surfaces and Interfaces*, **2024**, vol. 45, 103840.

2.1. Introduction

Phenolic resins (PRs) are widely known and used as adhesives and coatings for wood and metal substrates, and their varied applicability is due to their favourable cost, a plethora of options for chemical modifications [1–4], and good mechanical and fire-retardant properties [5–7] after curing. As such, the impact of reaction parameters like the formaldehyde/phenol (F/P) molar ratio, catalyst, pH, and reaction time and temperature on the structural and mechanical properties of (cured) resoles are well-investigated [2, 8–13]. Conversely, surface properties of cured PRs, like water-wettability, roughness, and surface morphology, are typically not researched. These characteristics are of considerable importance when a hardened resole is used in applications where it is in direct and near-continuous contact with water. This is for instance the case in coated hydrophilic stone wool used in horti- and floriculture. Here, the wettability of the stone wool substrates with coated fibres is vital to provide water and nutrients to plants at the right amount and rate during different stages of crop growth and development.

One of the few studies which are devoted to characterising the surface energy and water-wetting of cured phenolic resins is that of Matsushita *et al*. [14], where phenol-formaldehyde resins were prepared, cured and subsequently analysed with contact angle goniometry (CAG) and inverse gas chromatography (iGC). Phenol-formaldehyde resins with an F/P molar ratio of 2.2 were synthesised using NaOH as catalyst. Coatings prepared thereof yielded water contact angle values of 59.9° ± 1.6° after 50 measurements, indicating excellent reproducibility of the water wetting characteristics.

Lee *et al*. [15] investigated curing parameters of phenol-formaldehyde (PF) resins by monitoring the curing behaviour of resins synthesised with F/P of 1.3, 1.9 and 2.5 and an NaOH catalyst. Moreover, surface energy of the resulting PF networks was assessed using CAG on coatings cured at 140 °C, 150 °C, 160 °C for times up to 60 minutes. It was observed that the water contact angle on PF surfaces increases steadily with increasing curing time. Expectedly, the surface energy of these coatings decreased with increasing curing time, mainly because of a decline in the polar component of the surface energy. The authors postulate that these results indicate a surface which is more deprived of polar hydroxyl groups for longer curing times but note that a surface re-orientation effect of certain groups is still likely to occur. Unfortunately, dynamic contact angle measurements were not performed to test if this was indeed the case.

In this Chapter, surface characteristics and water-wettability properties of PF and phenol-urea-formaldehyde (PUF) coatings are investigated. As is evident from the overview given in the Chapter 1, there is already ample knowledge on the structural, mechanical and adhesive properties of phenolic resins and coatings prepared thereof, but the relation between surface properties and wettability remains non-investigated so far.

Starting from PF coatings, the chemical complexity was increased by including coatings made from PUF resins in the scope of this research. Hereby, the influence of catalyst type, organic or inorganic (triethylamine (TEA) versus potassium hydroxide (KOH)), was considered, allowing for a complete comparison of: 1) the chemistry (PF versus PUF), 2) the surface roughness and morphology, and 3) the effect of curing conditions (temperature, time, atmosphere) of the various phenolic resin coatings. The water-wettability of the different coatings was determined with contact angle goniometry (CAG) and the effect of water on the surface morphology was investigated by scanning electron microscopy (SEM) studies. Additionally, the response of the different coatings to repeated wetting and dewetting of the surface was studied through successive dynamic contact angle measurements. The influence of curing conditions on static water contact angle (WCA) measurements was investigated by determining the surface chemistry using X-ray photoelectron spectroscopy (XPS) and correlating the composition to wettability. In this way, a greater understanding of the impact of catalyst, chemistry and curing conditions on surface properties of phenolic resin coatings is obtained.

2.2. Experimental Procedures

Materials

Commercial PUF resin (PUF-KOH) was kindly provided by ROCKWOOL A/S (Hedehusene, Denmark). Ammonium sulphate (≥ 99%), triethylamine (> 99.5%), urea (U; ≥ 99%), and phenol (> 99%) were obtained from Sigma-Aldrich. Ammonia 25 wt% in water and K_2SO_4 (≥ 99%) were obtained from Merck. Formaldehyde 37 wt% solution in water (including 10-15% methanol stabiliser) was purchased from ThermoScientific. Before use phenol was stored at room temperature under P_2O_5 in a desiccator and commercial PUF resin was stored in a freezer at -19 °C; all other chemicals were used as received.

Syntheses

Salt-free PUF resin (PUF-TEA; F/P = 3.5) was synthesised as follows: phenol (20 g; 0.21 mol), formaldehyde (60 g; 54 mL; 0.74 mol) and triethylamine (5.8 mL; 0.04 mol) were charged into a three-neck flask equipped with a stirring bar, reflux condenser and thermometer. Next, the methylolation and oligomerisation of the phenolic species was carried out at 70 °C whilst stirring at 180 RPM. After 4 hours a solution of urea (18.99 g, 0.32 mol) in water (30 g) was added to the flask and the reaction was continued for 2 h at 55 °C. Thereafter, the reaction was quenched by placing the reactor in an ice bath and the resin was stored in a fridge at 5 °C until further use.

Salt-free PF resin (PF-TEA; F/P = 2.6–3.4) was synthesised as follows: phenol (e.g., 20 g; 0.21 mol), formaldehyde (e.g., 44 g; 39 mL; 0.54 mol) and triethylamine (e.g., 5 mL; 0.04 mol) were charged into a three-neck flask equipped with a stirring bar, reflux condenser and thermometer. The reaction between phenol and formaldehyde was carried out for 1 hour at 85 °C whilst stirring at 180 RPM. Thereafter, the reaction was quenched by placing the reactor in an ice bath and the resin was stored in a fridge at 5 °C until further use.

Binder and Coating Preparation

The commercial PUF binder (PUF-KOH; F/P = 3.3, P/U = 1.3, urea content approximately 45% based on solids; solids content approximately 50%) was prepared by addition of ammonia (0.03 g / g PUF-KOH resin) and ammonium sulphate (0.09 g / g PUF-KOH resin) to the commercial PUF resin and stirred for at least 1 hour with a magnetic stirring bar before application on glass substrates.

The phenolic resin coatings were applied by means of dip coating using a Biolin Scientific KSV NIMA LayerBuilder with an immersion and withdrawal speed of 100 mm/min, using the three different binder types. Soda lime glass microscopy slides were used as substrates, which were cleaned by sonication for at least 30 minutes in acetone and in isopropyl alcohol, consecutively, after which they were wiped dry with lint-free paper and further blown dry with air. The applied binder layers were subsequently cured in either an oven for 10 or 20 minutes at 200 °C under air atmosphere, or in a semi-closed chamber with a heating plate at 150 °C under an N_2 or air flow of approximately 150 L/h at 1 bar. Curing time for PUF-TEA and PUF-KOH inside the semi-closed chamber was 20 minutes and for PF-TEA coatings 15 minutes. The resulting coating thicknesses were between 4–12 µm (estimated with SEM or contact profilometry).

^{13}C-Nuclear Magnetic Resonance Measurements

Liquid resins were characterised by qualitative ^{13}C-nuclear magnetic resonance (NMR) spectroscopy on a Bruker Advance III HD 400 MHz spectrometer using DMSO-d6 as solvent. Spectra are the average of 160 spectra recorded with a recycle delay of 4 s.

Water Contact Angle Measurements

Static and advancing water contact angle measurements were conducted on a Dataphysics OCA30 goniometer, using MilliQ water (resistivity of 18.2 MΩ·cm) as probe liquid. For static water contact angle (WCA) measurements, droplet volumes were 2 µL and measurements were performed on at least three different spots per coating, recording the contact angle for at least 30 s using the OCA20 software. Values reported are the average of all individual left and right contact angle values after 30 s measurement time. Dynamic contact angle measurements were carried out by first

placing a droplet of 2 µL on the coating surface. From there, the droplet volume was increased and decreased by 25 µL respectively at a rate of 0.25 µL/s. The advancing contact angle (ACA) was determined following the procedure of Korhonen *et al.* [16], where the advancing contact angle is taken from the data points where the contact angle remains more or less stable, but the droplet volume and base diameter are still changing (Figure 2.1).

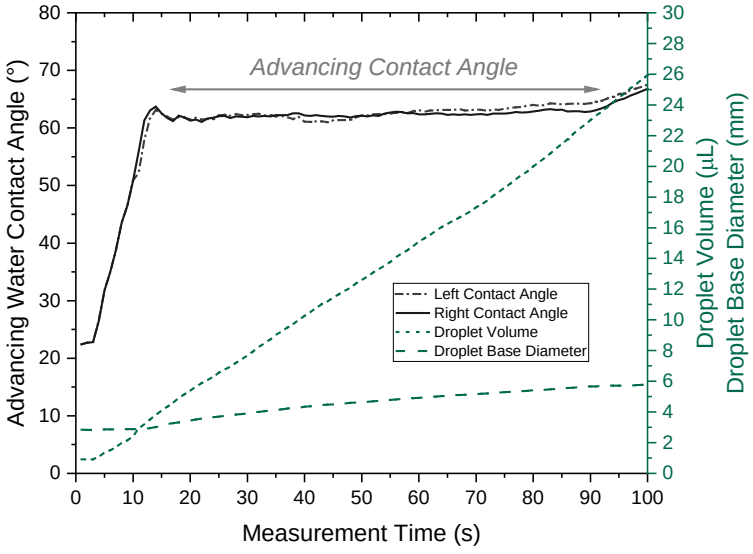


Figure 2.1. Example of an ACA measurement on a PUF-TEA surface.

Water–Air Interfacial Tension Measurements

The interfacial tension (IFT) of the water-air interface of water which had been in contact with a coating surface was measured on a Dataphysics OCA30 goniometer, using the pendant drop method preceded by dynamic contact angle measurements as shown schematically in Figure 2.2. First, a droplet of MilliQ water of approximately 2 µL was deposited on the coating surface using a needle of 0.52 mm diameter. From there, the droplet volume was increased by 30 µL at a rate of 0.25 µL/s. Then, an empty needle of 1.65 mm in diameter was injected into the droplet after which 28 µL of the droplet was repeatedly withdrawn into and dispensed from the needle at least 2 times at a rate of 0.25 µL/s. Finally, the droplet was suspended in air from the needle to determine the interfacial tension using the OCA20 software. The IFT was recorded for at least 60 s at a frequency of 1 datapoint per second. Reported values are from the average of one IFT measurement on two different coatings. For measurements on water which contained cured PUF-TEA powder (size range 180–450 µm), the water was passed through a 0.45 µm cellulose filter before the measurement. All measurements were carried out at room temperature.

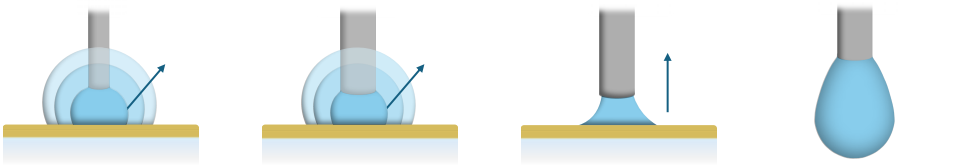


Figure 2.2. Method for combining multiple dynamic contact angle measurements with measuring the water–air interfacial tension of the water droplet used for probing the coating surface.

Scanning Electron Microscopy

Coating surfaces were characterized using scanning electron microscopy (SEM; ThermoFisher Scientific Phenom Pro X and ThermoFisher Scientific Quanta 200 3D-FEG) and energy-dispersive X-ray spectroscopy (EDX; ThermoFisher Scientific Phenom Pro X). All surfaces were coated with a thin gold layer (approximately 5 nm) using a Quorum Technologies Q150TS sputter coater to minimise charging effects.

Attenuated Total Reflection Infra-Red Spectroscopy

Bulk chemistry of coatings of PUF-TEA and PF-TEA was characterised with attenuated total reflection infra-red spectroscopy (ATR-FTIR) on a ThermoFisher Nicolet iS20 with diamond ATR crystal, scanning from 450–4000 cm^{-1} and averaging 8 scans per measurement.

X-ray Photoelectron Spectroscopy

Chemical composition of coating surfaces (approximately up to the first 10 nm) was obtained by means of X-ray photoelectron spectroscopy (XPS), using a ThermoFisher Scientific K-Alpha instrument with an aluminium anode (monochromated Al Kα radiation of 1486.6 eV) and a flood gun for charge compensation. Binding energy spectra of C 1s ($E_b^{C,1s}$ = 284.8 eV), N 1s ($E_b^{N,1s}$ = 399 eV) and O 1s ($E_b^{O,1s}$ = 532 eV) electrons were recorded using ThermoFisher Scientific Avantage software, using 30 scans, a pass energy of 50 eV and a step size of 0.1 eV. Data was processed using CasaXPS software, where the binding energy spectra were used to obtain atomic concentrations for each coating. A Shirley background and relative sensitivity factors for each element ($RSF_{C,1s}$ = 1, $RSF_{O,1s}$ = 2.881, $RSF_{N,1s}$ = 1.676) were used. The C 1s spectrum was charge corrected so that C-C bonds corresponded to a binding energy of 284.8 eV.

The C 1s binding energy spectrum was deconvoluted into C-C/C-H/C=C (284.8 eV), C-O/C-N (286.4 ± 0.2 eV), C=O/N-C=O (287.4 ± 0.3 eV) and NCON (289 ± 0.2 eV) [17, 18] to ascertain the relative amount of different bonds or functionalities at the surface.

Besides this, a CO/CC ratio was determined, defined as the fraction of oxygen-carbon to carbon-carbon bonds [19]:

$$\frac{CO}{CC} = \frac{C_{286.4} + C_{287.4} + C_{289}}{C_{284.8}} = \frac{(C\text{-}O) + (C{=}O) + (NCON)}{C\text{-}C}, \quad (2.1)$$

where $C_{284.8}$, $C_{286.4}$, $C_{287.4}$ and C_{289} refer to the atomic percentage of C-C/C-H/C=C, C-O/C-N, C=O/N-C=O and NCON contributions, respectively.

2.3. Results and Discussion

Resin Definition and Characterisation

Henceforth, coatings prepared from commercial PUF binder are referred to as PUF-KOH, those prepared from salt-free, own-synthesised PUF binder will be referred to as PUF-TEA and coatings made from salt-free, own-synthesised PF binder are termed PF-TEA.

Figure 2.3 shows the qualitative ^{13}C-NMR spectra of PUF-KOH, PUF-TEA, and PF-TEA resins. For all resins, characteristic signals of substituted phenoxy and aromatic carbon atoms (151–158 ppm and 127–135 ppm respectively), as well as those of the methylol carbon bound to phenol (65 ppm and 61 ppm respectively), indicate that the methylolation of phenol was successful [8, 20]. Moreover, oligomer formation was confirmed by the presence of peaks corresponding to methylene bridges at 36.1 ppm and 41.5 ppm. A multitude of signals can be observed in the phenoxy carbon and aromatic carbon region. This is due to the large variation in both the type of group (e.g., -H, -COH, -COC-, ...) and degree of substitution of the phenyl ring. The most significant differences between the spectra are the peaks from 158–163 ppm. These peaks correspond the presence of free and methylolated urea. An additional contribution of the methylol urea group is seen at 65 ppm, which mostly coincides with the phenolic methylol group [20]. This indicates that the PUF resins are blends of UF and PF, with prior to curing still some degree of free urea. The ^{13}C-NMR spectrum of PF-TEA shows a stronger presence of reactive formaldehyde adducts (80–100 ppm) compared to PUF-TEA because of a shorter reaction time. Moreover, the shorter reaction time also means that the free phenolic content is larger than for the other resins, based on the intensity of the peak at 158 ppm which corresponds to the phenoxy carbon of unsubstituted phenol. Last, for the PF-TEA resin, there is a larger content of unsubstituted *para* phenolic species, indicated by the peak at 121 ppm.

Additional ^{13}C-NMR and ^{1}H-NMR spectra of different PUF-TEA batches are shown in Figure A2.1. Batch-to-batch, the own-synthesised PF-TEA and PUF-TEA resins showed only minute variations in their ^{1}H-NMR and ^{13}C-NMR spectra and solids content (typically, approximately 38–39% for PF-TEA and 33–34% for PUF-TEA), indicating that

the synthesis procedure allowed for obtaining adequately reproducible resins that could be used for further studies.

Comparing the different resins with each other, main structural differences can be found in the formed species, with the PUF resins naturally containing methylolated urea. The PF resins overall tended to be less further reacted as seen by the free and unsubstituted phenol.

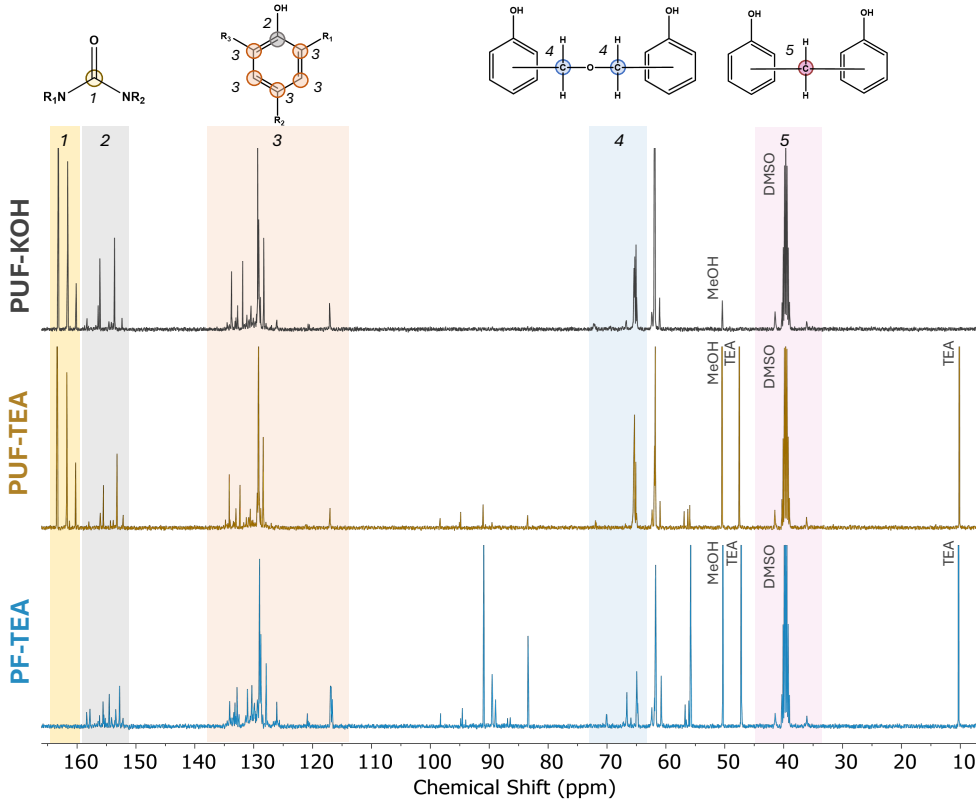


Figure 2.3. ^{13}C-NMR spectra of PUF-KOH, PUF-TEA and PF-TEA resin measured in DMSO-d6, which was used as internal reference at a chemical shift of 39.5 ppm. The presence of methanol in the spectra is from the formaldehyde solution, which contains methanol as stabiliser. Some characteristic areas and corresponding structures are indicated. R_1, R_2, and R_3 refer to either a methylol group, hydrogen atom, dimethylene ether or methylene bridge.

Surface Morphology of Phenolic Coatings

PUF-KOH, PUF-TEA and PF-TEA resins were applied on glass substrates by dip-coating, and subsequently cured at elevated temperatures inside an oven or a semi-closed chamber equipped with a hot plate.

It is well-known that wetting of surfaces by water is governed not only by chemical, but also by physical (in)homogeneity. Therefore, surface characterization for the phenolic resin coatings before and after wetting with water was conducted by SEM. For PF-TEA and PUF-TEA surfaces, a scratch was made on the coating to allow for proper focussing on the surface. Both pristine PF-TEA and PUF-TEA surfaces are largely devoid of features, indicating that there is no initial surface roughness influencing water wettability (Figure 2.4a–b). Deposits of particles could be seen near the edges of PUF-TEA and PUF-KOH coatings cured in the oven, possibly from unreacted urea or UF which precipitated out of solution during curing and drying of the coating (Figure A2.2). Lowering the curing temperature or increasing the coating thickness by increasing the withdrawal speed during dip coating was found to minimise the formation of these deposits near the film edges. This could be attributed to a lower difference between evaporation rates of the solvent at the edges versus the middle of the coatings, thereby preventing urea or UF fractions to precipitate out of solution.

A vastly different surface morphology was observed for PUF-KOH coatings, where crystals and surface irregularities were visible (Figure 2.4c–e[1]). Based on EDX analyses, these crystals were determined to be K_2SO_4 (Figure A2.3), the origin of which could be traced back to the catalysts used during the synthesis (KOH) and curing ($(NH_4)_2SO_4$) of the PUF-KOH resin. It was found that the K_2SO_4 crystals induce a significant surface roughness (average roughness R_a = 2.6 ± 0.3 µm; estimated with a laser scanning confocal microscopy measuring the top layer), with crystals also seen throughout the cross-section of the film. Conversely, cross-sections of PUF-TEA and PF-TEA films were devoid of such features (Figure A2.3).

Surface roughness is able to affect the apparent contact angle, as described through wettability models such as those proposed by Wenzel [22], Cassie and Baxter [23], and Marmur [24]. However, in this specific case the surface roughness is bound to vary during the measurement, on account of dissolution of the salt crystals into the water droplet, as well as after the measurement due to the redeposition of crystals on the surface. This leads to a complex and dynamic influence of crystal-induced roughness on the wetting of PUF-KOH surfaces by water. This could be discerned from the individual wetting profiles of measurements carried out on PUF-KOH coatings, which were in general fluctuating more over measurement time than for instance wetting profiles for PUF-TEA coatings. This also has implications for applications where additives such as surfactants are included in the binder formulation, as interactions between crystals and additives are to be expected. For example, additives in the form of ions, small- or macromolecules influence nucleation, growth, aggregation, dissolution and growth habit of crystals [25–29]. As a result, the distribution of additives throughout the coating can also be affected, and hence surface properties such as water-wettability can vary.

Modifying PF resins to PUF is expected to increase the hydrophilicity of coatings on account of a larger content of hydrophilic moieties. Somewhat surprisingly, the static

[1] Incidentally, the micrograph in Figure 2.4e was the winner of the 2022 NEMI photo competition [21].

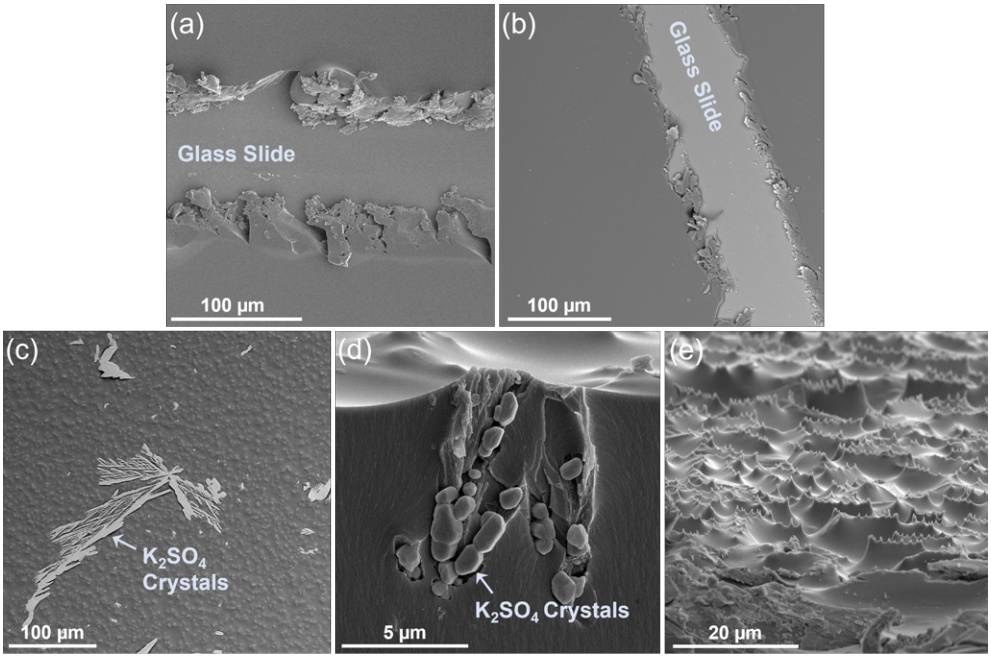


Figure 2.4. Scanning electron micrographs of surfaces of (a) PF-TEA, (b) PUF-TEA and (c) PUF-KOH coatings. A cross-section of a PUF-KOH coating is shown in (d), where K_2SO_4 crystals are visible throughout the thickness of the coating. The surface of a PUF-KOH coating under a tilt angle is shown in (e), visualising the roughness induced by the crystals.

WCA values of the coatings prepared from the phenolic resins are quite similar (Figure 2.5a). The tested F/P molar ratios were found to not have an influence on the average WCA value. For the probed coatings, within the first 10 to 15 seconds of measuring, there is typically a non-linear decrease in the water contact angle value which is a result of spreading of the droplet on the surface, irrespective of the phenolic resin type. Spreading can be seen as an increase in the base diameter of the droplet in the first stages of the measurement (Figure A2.5). The subsequent, often linear, decrease is due to water penetration into the surface layers and (water droplet) evaporation [30, 31]. In case the contact line of the water droplet is pinned, the radius or base diameter remains constant during evaporation, but the volume and contact angle decrease [32]. It is important to note that in case of surface effects such as rearrangements due to a change in interface (*i.e.*, from coating–air to coating–water), after a few tens of seconds it can be assumed that this response has occurred and its influence on the contact angle value is exerted [33]. For fair comparison and to account for possible surface responses of the coatings to water, henceforth water contact angles measured after 30 seconds are used for comparison.

Interestingly, for some of the phenolic coating surfaces a macroscopically visible drying mark could be discerned after water contact angle measurements at the

position where water droplets had previously been deposited. For PUF-KOH, SEM imaging of these spots show a significant change in the amount of K_2SO_4 crystals on the surface, which initially dissolved from the surface layers into the water droplet and were then redeposited upon droplet evaporation (Figure 2.5b). For PF-TEA and PUF-TEA, wetting and allowing the droplet to evaporate from the surface typically yielded wrinkles and cracks, likely a result of stress release and dissolution of unreacted moieties (Figure 2.5c–d). On top of that, the surface of PUF coatings contained new deposits after wetting and drying the surface. No matter the phenolic resin coating, contact with water results in changes in the surface morphology. In all cases mentioned above, subsequent wetting of these surfaces is expected to be affected by these changes on the surface on account of introduction of chemical and physical heterogeneity.

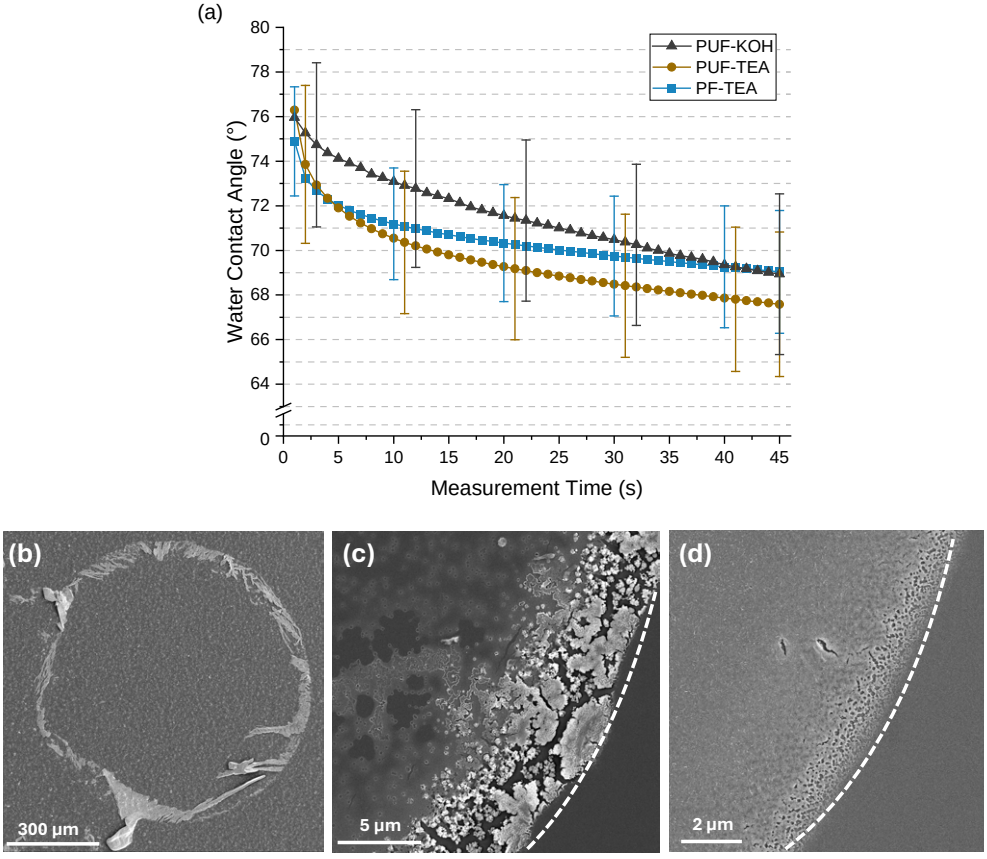


Figure 2.5. (a) Average WCA as function of measurement time on PUF-KOH, PUF-TEA, and PF-TEA coatings. PUF-KOH was cured in an oven at 200 °C for 10 minutes, PUF-TEA in a semi-closed chamber at 150 °C for 20 minutes and PF-TEA in a semi-closed chamber at 150 °C for 15 minutes. Scanning electron micrographs of (b) PUF-KOH, (c) PUF-TEA and (d) PF-TEA coating surfaces after locally wetting with water and drying in air, allowing the water droplet to evaporate from the coating surface. Dotted lines were added to the micrographs (c) and (d) to indicate the boundary between pristine and wetted parts of the coatings.

Influence of Surface Changes on Wettability

It is clear that for PUF-KOH, PUF-TEA, and PF-TEA the coating surface is affected by water, especially if water is allowed to evaporate from the surface. Besides surface roughness, also chemical heterogeneity is introduced. To investigate the effect of leachables (such as K_2SO_4 and urea) on the water wettability, coatings were subjected to repeated dynamic water contact angle measurements, after which the interfacial tension of the water droplet in air was determined. Combined with scanning electron microscopy characterisation of the measured spots, this allows to elucidate possible factors affecting the water contact angle measurements.

Figure 2.6 shows the advancing water contact angle (ACA) when repeatedly measuring on a PUF-KOH, PUF-TEA, and PF-TEA surface. The first measurement for these experiments always occurs on a pristine coating surface. For all probed coatings, it was observed that the first determined ACA is higher than the subsequently measured advancing contact angle values, although for PF-TEA this effect appeared to be less strong. While the actual values of the advancing contact angles with successive measurements were found to vary between coatings made from the same resin, as well as for coatings of the various phenolic resins, the trend of an initial change and the subsequent slower increase in wettability of the surfaces was seen for all the phenolic resin coatings measured this way. In principle, these changes in wettability can be the result of four different effects: 1) leaching of surface-active species into the water used for measurements, 2) plasticisation of surface layers, 3) introduction of surface roughness due to and during the measurement and 4) reorientation of surface groups either into the bulk or towards the coating-air interface in between measurements, or the coating-water interface during measurements.

To account for the possible influence of surface-active leachables from the coating surface into the water droplet during contact angle measurements, the water–air interfacial tension of the probe liquid was determined after repeated dynamic contact angle measurements. Interestingly, the interfacial tension of water droplets used for the successive dynamic water contact angle measurements on PUF-KOH, PUF-TEA, and PF-TEA surfaces show similar values, which is approximately that of pure water (72.1 ± 0.4 mN/m; see Table 2.1). Additionally, refreshing the water in between successive dynamic contact angle measurements was found to have little influence on the obtained ACA value (Figure A2.6). This implies either that there is no leaching of surface-active components into the water droplet, or that the concentration of such species is too low to have an impact on the interfacial tension and therefore cannot influence the results. Similar results were obtained for cured PUF-TEA and PUF-KOH resin powders (sieved for a particle size range of 180–425 µm) which were in contact with water for an extended period (Table 2.1). After filtrating the powders, the water–air interfacial tension of the used water was evaluated, and again yielded values close to that of pure water.

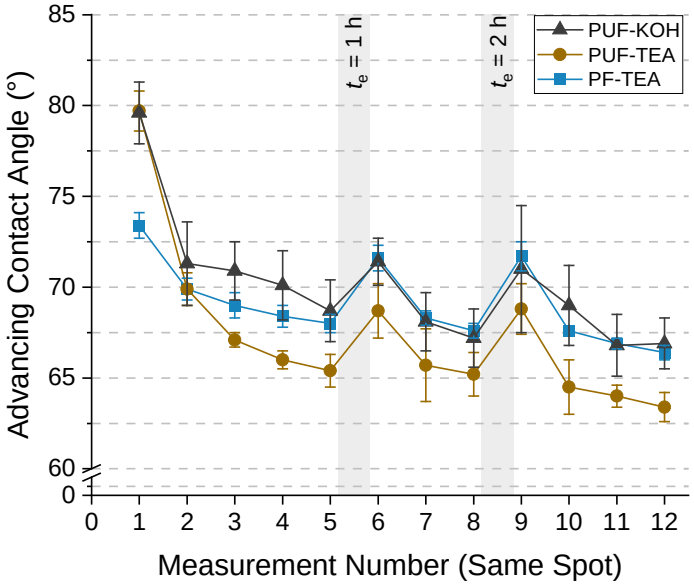


Figure 2.6. Successive advancing contact angle measurements on a PUF-KOH, PUF-TEA, and PF-TEA coating surface. In between measurement 5–6 and 8–9, coatings were dried in air under room conditions for t_e = 1 h and t_e = 2 h, respectively, before continuing.

To investigate the possible effects of plasticization and reorientation, drying times of 1 h and 2 h under room conditions were included in between some of the measurements, as shown in Figure 2.6. For the three different coatings, a slight increase in the advancing water contact angle value is seen where the obtained values approximate that of the second measurement upon drying the surface in air. This indicates a possible reversal of surface plasticisation or the occurrence of a reorientation of surface groups, which for polymers are known to occur as a result of a change in interface conditions (e.g., due to a change in the interface from coating–water to coating–air) [34–37].

Table 2.1. Water-air interfacial tension (IFT) values for water used for repeated dynamic water contact angle measurements on and immersion of PUF-KOH, PUF-TEA, and PF-TEA coatings, respectively. Measurements were performed at 20 °C.

Sample	$IFT_{coating}$ [a] (mN/m)	IFT_{powder} [b] (mN/m)
PUF-KOH	72.3 ± 0.3	72.3 ± 0.2
PUF-TEA	72.1 ± 0.2	71.9 ± 0.2
PF-TEA	72.2 ± 0.2	-

[a] IFT measurement of water used for at least 3 successive dynamic contact angle measurements.

[b] IFT measurement of water which contained cured, powdered resin for 1 day (0.5 g resin in 15 mL water).

It is also noticeable that the initial water ACA measurements in Figure 2.6 appear to permanently alter the surface. After this initial surface change, drying the surface yields

a reproducible increase to approximately the ACA value of measurement 2. To some degree, the reason that the ACA value does not increase to above this value is likely due to too short drying times but might also be attributed to a change in surface morphology and roughness. However, typically only significant morphology changes were observed upon evaporating water directly from the coating surface, as shown in Figure 2.7. These SEM micrographs show that the surface contains cracks and (urea) deposits, which was not observed as a direct result of the dynamic measurements, but rather as a result of water evaporation from the surface. Additionally, even if roughness was induced by the successive dynamic contact angle measurements, the increase in surface wettability upon drying would imply that roughness changes cannot solely explain the observed behaviours of the phenolic resin coating surfaces.

Presumably, the presence of water can induce plasticisation and/or surface rearrangement effects. This is supported by the work of Zhao *et al*. [38] who studied the effects of moisture on the relaxation mechanisms of cross-linked PF-resins and found that water acts as a plasticiser by breaking hydrogen bonds between the hydroxyl groups of the network. Additionally, Zaldivar *et al*. [7] observed a decrease in glass transition temperature (T_g) for carbon fibre–phenolic resin composites with increasing moisture content, where the magnitude of the decrease was influenced by the state of cure.

While the T_g at varying relative humidity has not been determined within this research, it was found that free-standing thin PUF-TEA films (approximately 40–80 µm) exhibit a dimensional change at elevated relative humidity, indicating the possibility of such a cured system to swell (Figure A2.7). Moreover, to some extent the cracks in the surface of the PUF-TEA coating shown in Figure 2.7 can be a result of swelling and tension forces due to water uptake and evaporation, respectively. Thus, continued plasticisation of the surface during successive contact angle measurements can be expected and would allow for the observed reversibility of the advancing contact angle values upon drying, as shown in Figure 2.6.

The possibility of surface rearrangements has not been explicitly investigated in this research. However, reorganisation at the surface as a result of a change in environment can occur even for glassy polymers, as such restructuring typically readily occurs over a distance of only 1–2 nm [39]. Furthermore, Lu *et al*. [34] have shown in their research that for a bisphenol type phenolic resin the orientation of surface phenyl groups depends on the relative humidity of the environment, and that changes in the surface structure are reversible. Because this could imply that measurement conditions will strongly affect the obtained results, coatings of PUF-TEA were stored at elevated relative humidity (approximately 92% RH) for up to 23 days and their wettability was probed at various intervals (Figure A2.8). No discernible changes in water contact angle values were found. It should be noted that this does not exclude the possibility of rearrangements or reorientations on the surface. However, for the coatings investigated in this work, effects of humidity on the wettability appeared to be minimal.

It should be noted that the effect of relative humidity on the dynamic contact angle values was not assessed but given the unaffected static contact angle values this influence is believed to be minimal as well.

Overall, the observed effects of repeated wetting on the phenolic coatings indicate that first wetting of the surface greatly alters its surface characteristics. An interplay between locally induced morphology changes, compositional drift, and plasticisation effects are suspected to be at the basis of these surface changes.

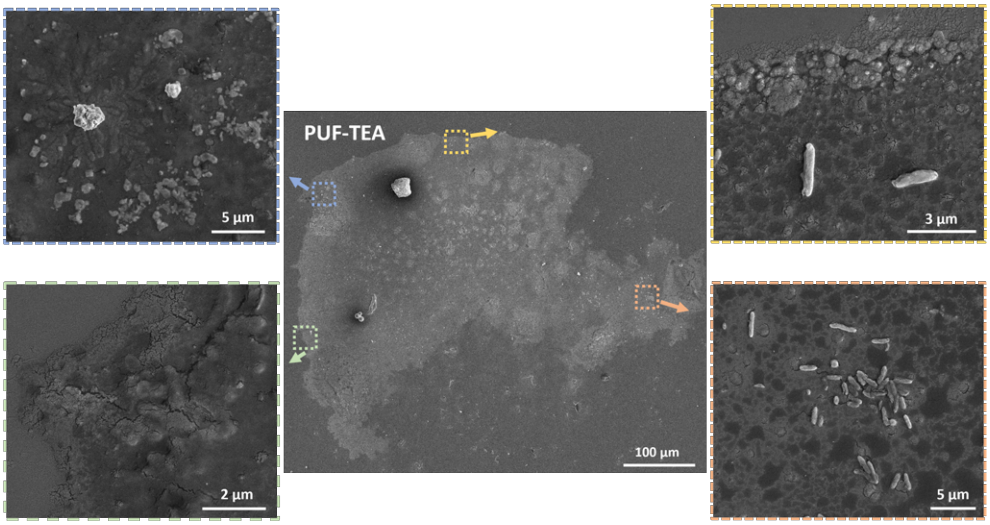


Figure 2.7. Scanning electron micrographs of a PUF-TEA coating surface after repeated dynamic contact angle measurements on the same spot, after allowing water to evaporate from the surface after the very last measurement. The identified regions show different effects and features on the surface such as crystallisation and deposition of urea-species, and cracks in and dissolution of surface layers.

Influence of Curing Conditions on Surface Composition and Wettability

For the different phenolic coatings, special attention was paid to the coating surface composition, determined by X-ray photoelectron spectroscopy, whilst varying curing parameters such as temperature and time (Table 2.2). As it was found that for PUF-KOH surfaces the S:C ratio was typically smaller than 0.002, it is assumed that the contribution from K_2SO_4 crystals to the total oxygen content is minimal and can therefore be neglected.

The main influence on chemical composition was found to be the curing temperature rather than the curing time, as coatings cured in an air convection oven at 200 °C have a similar surface composition after 10 and 20 minutes of hardening time (Table 2.2). It is likely that processes that influence and define the final surface composition and state of cure occur relatively rapidly, and do not vary significantly within the studied

variations of curing time. Additionally, for PUF-TEA the amount of nitrogen in the surface layers is consistently lower when curing at 200 °C, showing to be considerably decreased compared to 150 °C.

The results for PUF-KOH cured at 200 °C match well with those of PUF-TEA cured at the same temperature. In these cases, thermal degradation of UF species could have occurred at the elevated hardening temperature, leading to a surface which is less enriched by UF fractions.

Table 2.2. Overview of chemical composition, estimated with XPS, of phenolic resin coatings cured in an air convection oven varying the curing temperature and time.

Sample		Curing Conditions	O:C	N:C	CO/CC
PUF-KOH	Oven	200 °C 10 min	0.29 ± 0.02	0.15 ± 0.01	0.70 ± 0.03
PUF-TEA	Oven	200 °C 10 min	0.29 ± 0.01	0.14 ± 0.01	0.64 ± 0.05
		200 °C 20 min	0.28 ± 0.02	0.15 ± 0.01	0.62 ± 0.03
		150 °C 20 min	0.31 ± 0	0.22 ± 0.01	0.83 ± 0.02
PF-TEA	Oven	200 °C 10 min	0.29 ± 0.01	-	0.39 ± 0.01
		200 °C 20 min	0.31 ± 0.01	-	0.37 ± 0.01
		150 °C 20 min	0.28 ± 0.01	-	0.49 ± 0.03

The CO/CC ratio as determined with XPS can be used a measure of the polarity of the surface, as it relates to the state of cure of the phenolic resin and for PUF-TEA and PUF-KOH takes into account the urea carbonyl content. Overall, there appear to be two causes for the decrease in CO/CC ratio with increasing curing temperature. First, in line with the corresponding N:C ratios, the curing conditions dictate the actual urea content at the surface of PUF-KOH and PUF-TEA coatings, which then affects the polarity of the surface. Next, oxidation can occur, which is offset by the selective evaporation of formaldehyde from dimethylene ether bridges, converting these into methylene linkages between PF and UF species.

Both processes were observed from the C 1s and O 1s binding energy spectra of the coatings (representative XPS spectra are shown in Figure 2.8 and Figure A2.9). For PF-TEA, coatings hardened at elevated temperatures exhibited a small shoulder around 287.5 eV, which could be attributed to the presence of newly formed C=O bonds.

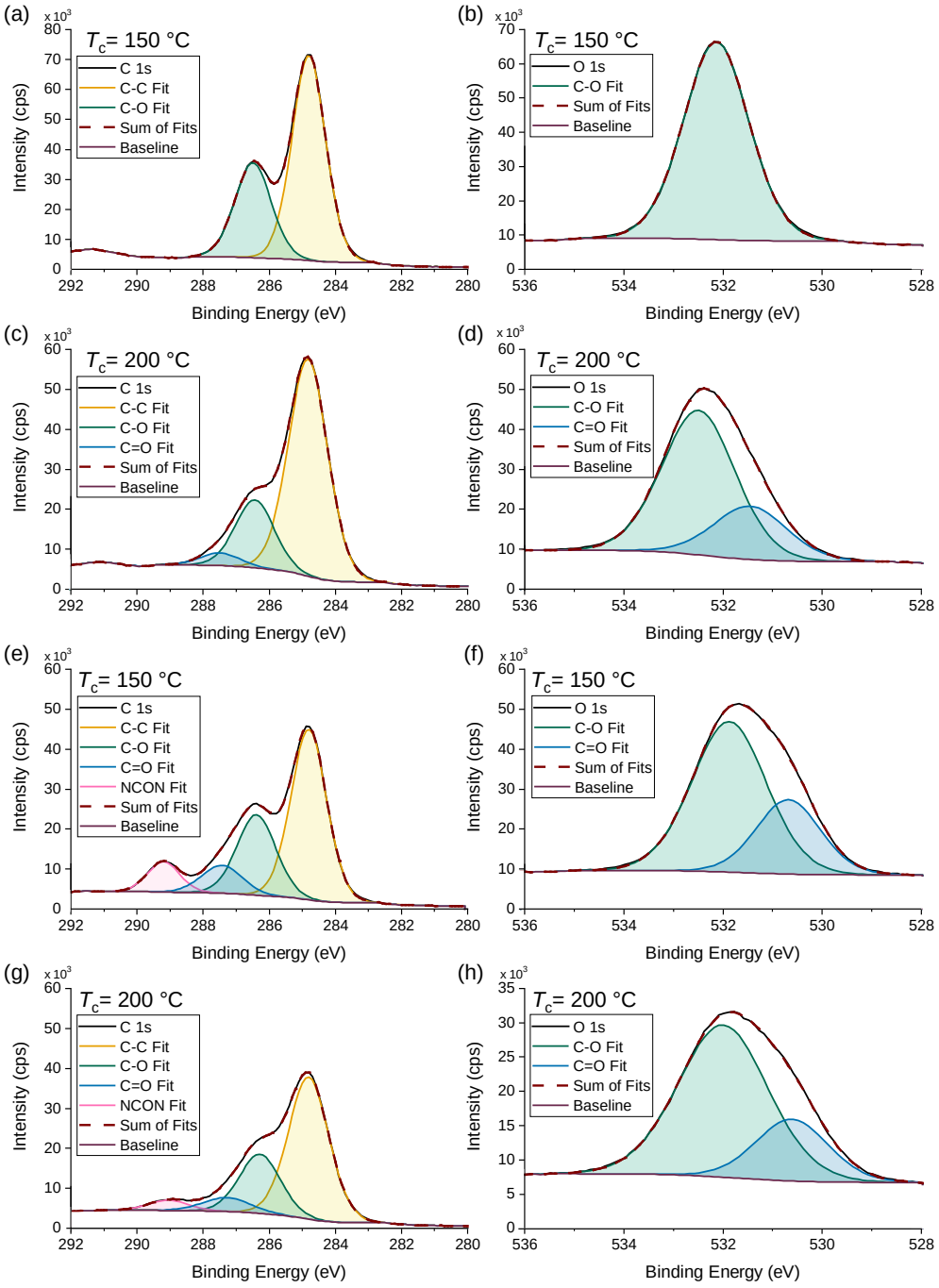


Figure 2.8. C 1s and O 1s binding energy spectra of PF-TEA (a–d) and PUF-TEA (e–h) coatings cured at either T_c = 150 °C or T_c = 200 °C.

For PUF-TEA surfaces, the NCON and C=O contributions decreased with increasing curing temperature, indicating either rearrangement or decomposition of urea moieties. Thermal degradation of urea-formaldehyde resins is known to start at 200 °C [40, 41], and pure urea is even less thermally stable and starts to decompose at temperatures of 180 °C [42].

Examination of the deconvoluted O 1s spectra of the different phenolic resin coatings showed an increase in the full width at half maximum (FWHM) when curing at 200 °C, with the peak broadening towards lower binding energies. This could correspond to the presence of additional C=O bonds, seen from the binding energy spectra (shown for PF-TEA and PUF-TEA in Figure 2.8, and for PUF-KOH in Figure A2.9) [18]. Peak broadening was best seen for PF-TEA coatings, due to the initial absence of C=O bonds, where the FWHM of the O 1s spectra increased on average from 1.6 eV to 2.0 eV.

Besides XPS data showing oxidation in the first few surface layers, ATR-FTIR analyses also indicate that bulk chemistry of the cured resins is affected by curing temperature (Figure 2.9). For instance, for PUF-TEA hardened at 200 °C the presence of carboxylic acid or aldehyde groups was observed (C=O stretch at 1720 cm^{-1} and C=O overtone at 3620 cm^{-1}). The FTIR spectra of PF-TEA coatings cured at 200 °C are also markedly different from the spectra of PF-TEA hardened at 150 °C, with an increased signal at 1680 cm^{-1} and 1650 cm^{-1} which could indicate a larger number of C=O moieties [43]. Conley and Bieron [43] similarly observed chemical changes for phenolic resins when heated, albeit only after heating cured resins in air for several hours. Their observed changes included decreases in the number of methylene bridges between phenolic species, and an increase in for instance the -COOH and C=O content.

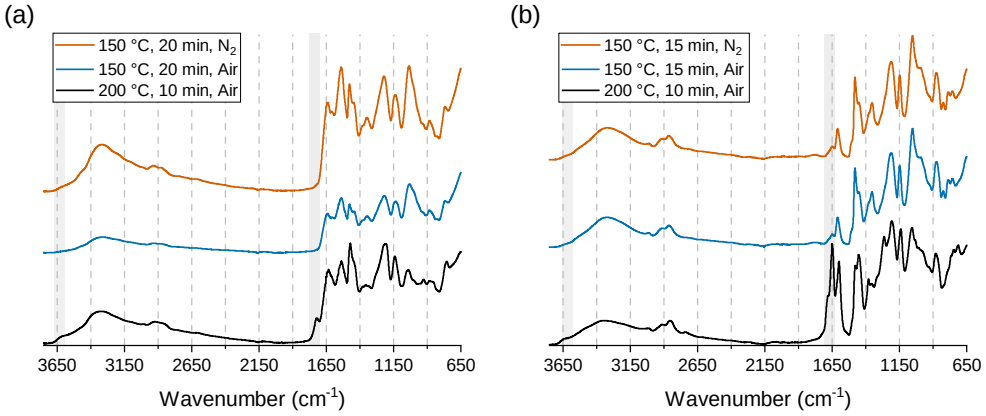


Figure 2.9. ATR FT-IR spectra of (a) PUF-TEA and (b) PF-TEA coatings cured at various conditions. Grey boxes are added to guide the eye to some of the most important differences between the spectra as a result of oxidation.

The effect of curing atmosphere was also investigated by curing the different phenolic resins inside a semi-closed chamber under controlled nitrogen or air conditions. The curing temperature was held at 150 °C, which was the upper limit of the heating element inside the semi-closed chamber. The elemental composition of surfaces obtained this way is shown in Table 2.3. As discussed above, the curing time has little impact on the surface composition. Hence, it can reasonably be assumed that the composition of PF-TEA cured for 15 minutes is similar to that after curing for 20 minutes.

In general, there appears to be no direct influence of atmosphere on the chemical composition of the different coatings. Still, it should be noted that only for PUF-TEA coatings cured in an air-rich atmosphere the spread in CO/CC ratio was found to be larger than all other coatings. From the ATR-FTIR data follows that the bulk structure, however, shows no signs of oxidation at 150 °C of the PUF-TEA and PF-TEA coatings (Figure 2.9). Most likely, the absence of chemical changes with curing atmosphere is the result of the relatively low curing temperature, which limits both oxidation and selective evaporation of formaldehyde from dimethylene ether bridges. This is in line with results previously reported by Hu *et al.* [44], where only for resoles cured at temperatures above 160 °C the formation of carbonyl groups and breaking down of ether bridges was observed.

Table 2.3. Overview of chemical composition, estimated with XPS, of phenolic resin coatings cured inside a semi-closed chamber under an air or nitrogen flow.

Sample	Curing Atmosphere	O:C	N:C	CO/CC
PUF-KOH 150 °C 20 min	Air	0.33 ± 0.01	0.21 ± 0.01	0.80 ± 0.06
	N_2	0.33 ± 0.02	0.19 ± 0.01	0.76 ± 0.03
PUF-TEA 150 °C 20 min	Air	0.33 ± 0.01	0.21 ± 0.02	0.72 ± 0.12
	N_2	0.34 ± 0.01	0.22 ± 0.01	0.80 ± 0.04
PF-TEA 150 °C 15 min	Air	0.28 ± 0	-	0.48 ± 0.01
	N_2	0.28 ± 0.01	-	0.48 ± 0.02

These results can now be connected with the results of the water-wettability study of, for instance, PUF-TEA coatings in which unstable results were observed, demonstrated by a significant spread in water contact angle values (Figure A2.10). Disparities in water contact angle values were predominantly observed for coatings cured inside the oven,

where variations where seen: 1) between coatings made from the same batch of PUF-TEA resin, 2) between coatings made from different batches of PUF-TEA resin, and 3) even within a PUF-TEA coating itself. These variations between batches of the same type occurred even though chemically the liquid resins showed only minute differences in their composition (based on ^{13}C-NMR analyses, Figure 2.3). Although it is hypothesised that there is little control over the co-condensation between PF and UF fractions during curing when using TEA as catalyst (resulting in surfaces which are then either PF- or UF-rich; see also CO/CC ratio of PUF-TEA cured in air in Table 2.3), the variation in wettability between PUF-TEA coatings cured inside the semi-closed chamber was typically found to be small. This is in stark contrast with coatings hardened in the oven. For instance, comparing water-wettability of different PUF-TEA coatings, the average water contact angle for a set of 9 coatings produced from one batch, cured in the oven, was 69.8° ± 12.5°, whilst that of 18 coatings cured in the semi-closed chamber was 68.1° ± 3.2°.

The aforementioned observation was, to varying degrees, valid for all studied coatings. Table 2.4 shows an overview of the wettability and CO/CC ratio of some of the samples (an overview of all samples is given in Table A2.1). For PUF-KOH surfaces, variations in the water contact angle values appear to be less strongly fluctuating compared to PUF-TEA and PF-TEA. Typically, the largest differences in surface wettability of the studied coatings were always found for PUF-TEA. The major difference between the PF-TEA and PUF-TEA, and the PUF-KOH resin is the catalysts used for synthesis and hardening, and as a result the pH during curing can vary. For instance, compared with PUF-TEA, for PUF-KOH a lower pH during curing can be attained due to the use of the latent acid hardener $(NH_4)_2SO_4$, which then facilitates a better co-condensation between UF and PF fractions. Thus, the fluctuations in chemical composition due to variations in curing parameters are weaker, which in turn yields a more chemically homogeneous surface, regardless of hardening conditions.

Table 2.4. Influence of curing conditions of phenolic resin coatings on their water-wettability.

Conditions	Sample	CO/CC	FWHM O 1s (eV)	WCA (°)
Oven 200 °C Air	PUF-KOH[a]	0.70 ± 0.03	2.56 ± 0.06	70.5 ± 3.6
	PUF-TEA[b]	0.62 ± 0.03	2.65 ± 0.10	73.8 ± 5.6
	PF-TEA[b]	0.37 ± 0.01	2.06 ± 0.03	76.4 ± 7.7
Semi-closed Chamber 150 °C N_2	PUF-KOH[b]	0.76 ± 0.03	2.39 ± 0.08	70.0 ± 1.5
	PUF-TEA[b]	0.80 ± 0.04	2.38 ± 0.05	70.8 ± 2.5
	PF-TEA[c]	0.48 ± 0.02	1.62 ± 0.04	69.7 ± 2.7

[a] Curing time 10 minutes. [b] Curing time 20 minutes. [c] Curing time 15 minutes.

Although statistically the wettability of most coating surfaces presented in Table 2.4 can be considered similar, it is evident that the spread in water contact angle values is affected by the curing temperature, which influences the degree of oxidation as well as the state of cure. As shown, curing TEA-containing phenolic resins appears to lead to coating surfaces with a larger spread in wettability compared to KOH-containing coatings and phenolic resin coatings cured at lower temperatures. The curing atmosphere was found to not have an apparent influence on either the absolute value or the standard deviation. Still, it is important to take the curing conditions into account when a reliable wettability of phenolic resin coatings is required.

2.4. Conclusions

Several factors that influence the surface properties of phenolic resin coatings were investigated. Coatings were prepared from three different resin formulations, where both the chemistry (PUF or PF) and catalyst (KOH or TEA) were varied. It was found that the surface wettability of the prepared coatings was similar, despite coatings exhibiting both chemical and morphological differences. The use of inorganic catalysts for curing and hardening the PUF-KOH resin leads to coating surfaces containing water-soluble K_2SO_4 crystals, which create a rough surface before wetting, and which readily dissolve in water during wetting. Although this yields a dynamic surface, such coatings were found to exhibit similar behaviour as PUF-TEA and PF-TEA surfaces upon repeated wetting. Contact with water affects every coating surface by changing the surface morphology, predominantly when the water is allowed to evaporate from the coating surface. Changes occur either through dissolution and redistribution of components or by tensile forces exerted due to the evaporation of water from the surface. However, no influence of leachables on the interfacial tension of the water in contact with the surfaces was found. Water also has a plasticising effect on all the coating surfaces, as successive dynamic contact angle measurements show a gradual, reversible decrease in wettability after a first wetting.

Surface chemistry of the phenolic resin coatings cured at various conditions largely followed the same trend. For a temperature of 200 °C, the state of cure for all coatings was markedly different compared to lower curing temperatures, which was reflected in the amount of dimethylene ether bridges being lower than for coatings cured at 150 °C, as seen by a change in CO/CC ratio. For urea-containing coatings, the nitrogen content exhibited the same behaviour, indicating that surface chemistry and polarity is largely governed by the distribution of UF fractions in the coating matrix and potential degradation of urea. Yet, oxidation at elevated temperatures was also found to occur. Major contributions to the surface chemistry and wettability variations of PUF-KOH and PUF-TEA stem from the distribution and co-condensation of urea species within and with the PF species. For applications in which a reliable wettability of phenolic resin coatings is required, a careful consideration of the curing conditions is advised.

References

[1] L. Pilato, "Phenolic resins: 100 Years and still going strong," *React. Funct. Polym.*, vol. 73, no. 2, Art. no. 2, 2013, doi: 10.1016/j.reactfunctpolym.2012.07.008.

[2] S. Kowatsch, "Mineral Wool Insulation Binders," in *Phenolic Resins: A Century of Progress*, L. Pilato, Ed., Berlin, Heidelberg: Springer, 2010, pp. 209–242. doi: 10.1007/978-3-642-04714-5_10.

[3] C. P. R. Nair, "Advances in addition-cure phenolic resins," *Prog. Polym. Sci.*, vol. 29, no. 5, pp. 401–498, 2004, doi: 10.1016/j.progpolymsci.2004.01.004.

[4] K. Tang, A. Zhang, T. Ge, X. Liu, X. Tang, and Y. Li, "Research progress on modification of phenolic resin," *Mater. Today Commun.*, vol. 26, p. 101879, 2021, doi: 10.1016/j.mtcomm.2020.101879.

[5] C. Morterra and M. J. D. Low, "I.R. studies of carbons—VII. The pyrolysis of a phenol-formaldehyde resin," *Carbon*, vol. 23, no. 5, pp. 525–530, 1985, doi: 10.1016/0008-6223(85)90088-0.

[6] B. K. Kandola, A. R. Horrocks, P. Myler, D. Blair, G. L. Nelson (Ed.), and C. A. Wilkie (Ed.), "Thermal Characterization of Thermoset Matrix Resins," in *Fire and Polymers*, vol. 797, in ACS Symposium Series, vol. 797. , Washington, DC, 2001, pp. 344–360.

[7] R. J. Zaldivar, G. L. Ferrelli, V. Arredondo, and H. I. Kim, "Effect of cure temperature on the thermal degradation, mechanical, microstructural and moisture absorption behavior of vacuum-only, carbon-fiber reinforced phenolic composites," *J. Appl. Polym. Sci.*, vol. 139, no. 34, p. e52819, 2022, doi: 10.1002/app.52819.

[8] B. Tomita and C.-Y. Hse, "Phenol–urea–formaldehyde (PUF) co-condensed wood adhesives," *Int. J. Adhes. Adhes.*, vol. 18, no. 2, pp. 69–79, 1998, doi: 10.1016/S0143-7496(97)00047-X.

[9] M.-F. Grenier-Loustalot, S. Larroque, P. Grenier, J.-P. Leca, and D. Bedel, "Phenolic resins: 1. Mechanisms and kinetics of phenol and of the first polycondensates towards formaldehyde in solution," *Polymer*, vol. 35, no. 14, pp. 3046–3054, 1994, doi: 10.1016/0032-3861(94)90418-9.

[10] M.-F. Grenier-Loustalot, S. Larroque, D. Grande, P. Grenier, and D. Bedel, "Phenolic resins: 2. Influence of catalyst type on reaction mechanisms and kinetics," *Polymer*, vol. 37, no. 8, pp. 1363–1369, 1996, doi: 10.1016/0032-3861(96)81133-5.

[11] M.-F. Grenier-Loustalot, S. Larroque, and P. Grenier, "Phenolic resins: 5. Solid-state physicochemical study of resoles with variable FP ratios," *Polymer*, vol. 37, no. 4, pp. 639–650, 1996, doi: 10.1016/0032-3861(96)83151-X.

[12] L. Gollob and A. (Ed.) Pizzi, "The Correlation Between Preparation and Properties in Phenolic Resins," in *Wood Adhesives. Chemistry and Technology*, 1st ed., vol. 2, Boca Raton: CRC Press, 1989, pp. 121–153. doi: 10.1201/9780203733721-5.

[13] G. He and B. Riedl, "Phenol-urea-formaldehyde cocondensed resol resins: Their synthesis, curing kinetics, and network properties," *J. Polym. Sci. Part B Polym. Phys.*, vol. 41, no. 16, pp. 1929–1938, 2003, doi: 10.1002/polb.10558.

[14] Y. Matsushita, S. Wada, K. Fukushima, and S. Yasuda, "Surface characteristics of phenol–formaldehyde–lignin resin determined by contact angle measurement and inverse gas chromatography," *Ind. Crops Prod.*, vol. 23, no. 2, pp. 115–121, 2006, doi: 10.1016/j.indcrop.2005.04.004.

[15] Y.-K. Lee, H.-J. Kim, M. Rafailovich, and J. Sokolov, "Curing monitoring of phenolic resol resins via atomic force microscope and contact angle," *Int. J. Adhes. Adhes.*, vol. 22, no. 5, pp. 375–384, 2002, doi: 10.1016/S0143-7496(02)00017-9.

[16] J. T. Korhonen, T. Huhtamäki, O. Ikkala, and R. H. A. Ras, "Reliable Measurement of the Receding Contact Angle," *Langmuir*, vol. 29, no. 12, pp. 3858–3863, 2013, doi: 10.1021/la400009m.

[17] A. Zafar, J. Schjødt-Thomsen, R. Sodhi, R. Goacher, and D. de Kubber, "Investigation of the ageing effects on phenol-urea-formaldehyde binder and alkanol amine-acid anhydride binder coated mineral fibres," *Polym. Degrad. Stab.*, vol. 98, no. 1, pp. 339–347, 2013, doi: 10.1016/j.polymdegradstab.2012.09.007.

[18] L. Liang *et al.*, "Surfactant-Induced Reconfiguration of Urea-Formaldehyde Resins Enables Improved Surface Properties and Gluability of Bamboo," *Polymers*, vol. 13, no. 20, Art. no. 20, 2021, doi: 10.3390/polym13203542.

[19] L. M. Matuana and D. P. Kamdem, "Accelerated ultraviolet weathering of PVC/wood-flour composites," *Polym. Eng. Sci.*, vol. 42, no. 8, pp. 1657–1666, 2002, doi: 10.1002/pen.11060.

[20] G. Vázquez, F. López-Suevos, A. Villar-Garea, J. González-Alvarez, and G. Antorrena, "13C-NMR analysis of phenol-urea-formaldehyde prepolymers and phenol-urea-formaldehyde-tannin

adhesives," *J. Adhes. Sci. Technol.*, vol. 18, no. 13, pp. 1529–1543, 2004, doi: 10.1163/1568561042411231.

[21] "2022 NEMI Photo Competition winners! – Nemi." Accessed: Aug. 02, 2024. [Online]. Available: https://nemi.microscopie.nl/news/2022-nemi-photo-competition-winners/

[22] R. N. Wenzel, "Resistance of solid surfaces to wetting by water," *Ind. Eng. Chem.*, vol. 28, no. 8, pp. 988–994, 1936, doi: 10.1021/ie50320a024.

[23] A. B. D. Cassie and S. Baxter, "Wettability of porous surfaces," *Trans. Faraday Soc.*, vol. 40, no. 0, pp. 546–551, 1944, doi: 10.1039/TF9444000546.

[24] A. Marmur, "Wetting on Hydrophobic Rough Surfaces: To Be Heterogeneous or Not To Be?," *Langmuir*, vol. 19, no. 20, pp. 8343–8348, 2003, doi: 10.1021/la0344682.

[25] F. Kuschel, An. König, and S. Herold, "Crystallization of potassium sulfate from pure aqueous solution and in presence of surfactants," *Cryst. Res. Technol.*, vol. 18, no. 4, pp. 427–434, 1983, doi: 10.1002/crat.2170180402.

[26] J. P. Canselier, "The Effects of Surfactants on Crystallization Phenomena," *J. Dispers. Sci. Technol.*, vol. 14, no. 6, pp. 625–644, 1993, doi: 10.1080/01932699308943435.

[27] H. Füredi-Milhofer and S. Sarig, "Interactions between polyelectrolytes and sparingly soluble salts," *Prog. Cryst. Growth Charact. Mater.*, vol. 32, no. 1, pp. 45–74, 1996, doi: 10.1016/0960-8974(96)00006-X.

[28] M. Bujan, M. Sikirić, N. Filipović-Vinceković, N. Vdović, N. Garti, and H. Füredi-Milhofer, "Effect of Anionic Surfactants on Crystal Growth of Calcium Hydrogen Phosphate Dihydrate," *Langmuir*, vol. 17, no. 21, pp. 6461–6470, 2001, doi: 10.1021/la0107190.

[29] H. Füredi-Milhofer, D. Škrtić, M. Marković, and Lj. Komunjer, "Kinetic analysis of the influence of additives on spontaneous precipitation from electrolytic solutions," *Dispersed Syst.*, pp. 195–200, 1988, doi: 10.1007/BFb0116783.

[30] C. Bourges-Monnier and M. E. R. Shanahan, "Influence of Evaporation on Contact Angle," *Langmuir*, vol. 11, no. 7, pp. 2820–2829, 1995, doi: 10.1021/la00007a076.

[31] A. K. Panwar, S. K. Barthwal, and S. Ray, "Effect of evaporation on the contact angle of a sessile drop on solid substrates," *J. Adhes. Sci. Technol.*, vol. 17, no. 10, pp. 1321–1329, 2003, doi: 10.1163/156856103769172760.

[32] A. J. D. Shaikeea, S. Basu, A. Tyagi, S. Sharma, R. Hans, and L. Bansal, "Universal representations of evaporation modes in sessile droplets," *PLOS ONE*, vol. 12, no. 9, p. e0184997, 2017, doi: 10.1371/journal.pone.0184997.

[33] D. Y. Kwok and A. W. Neumann, "Contact angle measurement and contact angle interpretation," *Adv. Colloid Interface Sci.*, vol. 81, no. 3, pp. 167–249, 1999, doi: 10.1016/S0001-8686(98)00087-6.

[34] X. Lu *et al.*, "Phenolic resin surface restructuring upon exposure to humid air: a sum frequency generation vibrational spectroscopic study," *J. Phys. Chem. B*, vol. 113, no. 39, pp. 12944–12951, 2009, doi: 10.1021/jp9058092.

[35] K. B. Lewis and B. D. Ratner, "Observation of Surface Rearrangement of Polymers Using ESCA," *J. Colloid Interface Sci.*, vol. 159, no. 1, pp. 77–85, 1993, doi: 10.1006/jcis.1993.1299.

[36] J. K. Pike, T. Ho, and K. J. Wynne, "Water-Induced Surface Rearrangements of Poly(dimethylsiloxane−urea−urethane) Segmented Block Copolymers," *Chem. Mater.*, vol. 8, no. 4, pp. 856–860, 1996, doi: 10.1021/cm9504596.

[37] A. C. C. Esteves, I. D. Günbas, J. M. van Riel, B. A. J. Noordover, G. de With, and R. A. T. M. van Benthem, "Time-resolved surface rearrangements of polymer films monitored by dynamic recovery contact angle (DRCA)," *RSC Adv.*, vol. 4, no. 39, pp. 20094–20101, 2014, doi: 10.1039/C4RA01329H.

[38] W. Zhao, S. L. Hsu, S. Ravichandran, and A. M. Bonner, "Moisture Effects on the Physical Properties of Cross-linked Phenolic Resins," *Macromolecules*, vol. 52, no. 9, pp. 3367–3375, 2019, doi: 10.1021/acs.macromol.9b00385.

[39] J. T. Koberstein, "Molecular design of functional polymer surfaces," *J. Polym. Sci. Part B Polym. Phys.*, vol. 42, no. 16, pp. 2942–2956, 2004, doi: 10.1002/polb.20157.

[40] G. Camino, L. Operti, and L. Trossarelli, "Mechanism of thermal degradation of urea-formaldehyde polycondensates," *Polym. Degrad. Stab.*, vol. 5, no. 3, pp. 161–172, 1983, doi: 10.1016/0141-3910(83)90007-1.

[41] K. Siimer, T. Kaljuvee, and P. Christjanson, "Thermal behaviour of urea-formaldehyde resins during curing," *J. Therm. Anal. Calorim.*, vol. 72, no. 2, pp. 607–617, 2003, doi: 10.1023/A:1024590019244.

[42] N. Zhu, F. Qian, X. Xu, M. Wang, and Q. Teng, "Thermogravimetric Experiment of Urea at Constant Temperatures," *Materials*, vol. 14, no. 20, p. 6190, 2021, doi: 10.3390/ma14206190.

[43] R. T. Conley and J. F. Bieron, “A study of the oxidative degradation of phenol-formaldehyde polycondensates using infrared spectroscopy,” *J. Appl. Polym. Sci.*, vol. 7, no. 1, pp. 103–117, 1963, doi: 10.1002/app.1963.070070110.

[44] H. Hu *et al.*, “Curing mechanism of resole phenolic resin based on variable temperature FTIR spectra and thermogravimetry-mass spectrometry,” *Polym. Polym. Compos.*, vol. 30, p. 09673911221102114, 2022, doi: 10.1177/09673911221102114.

Appendices

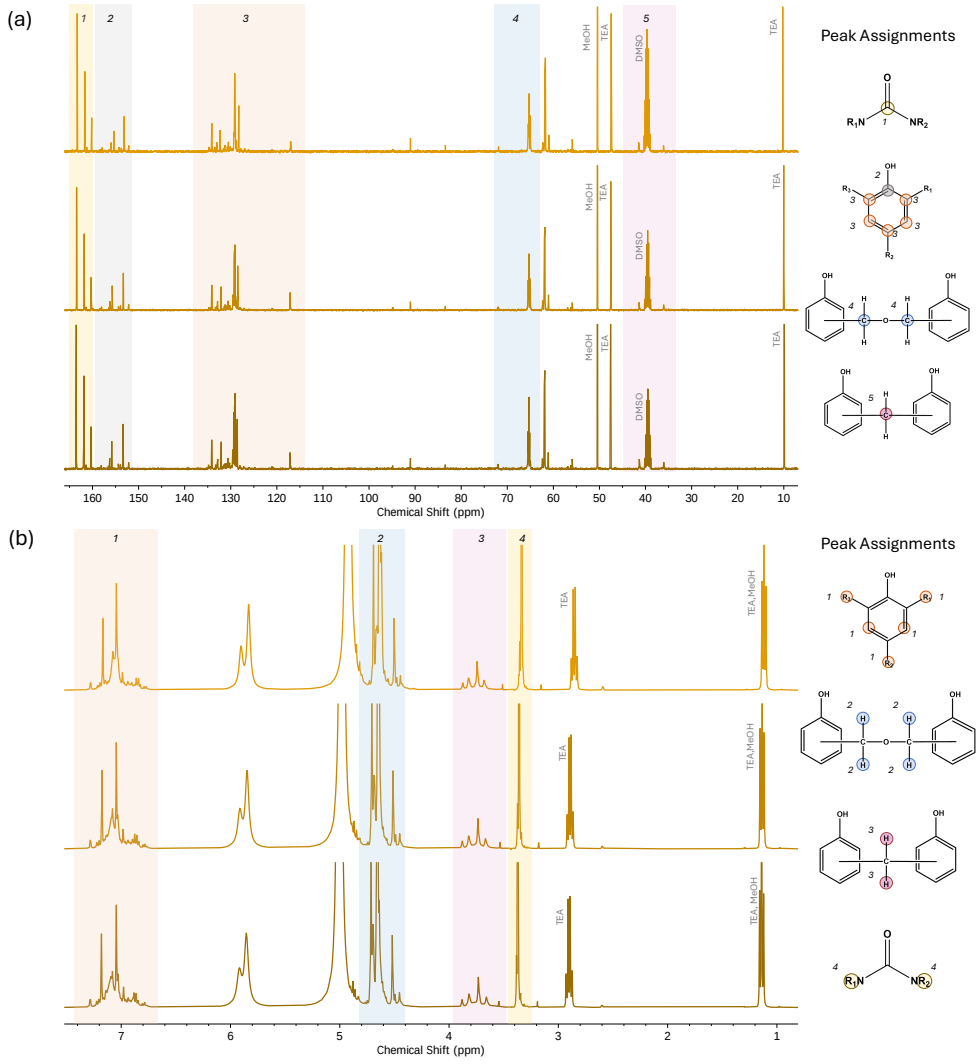


Figure A2.1. (a) ^{13}C-NMR and (b) ^{1}H-NMR spectra of three different batches of PUF-TEA, showing consistent peak position and intensity. Peak assignments for the ^{1}H-NMR spectra were based on heteronuclear single quantum coherence measurements.

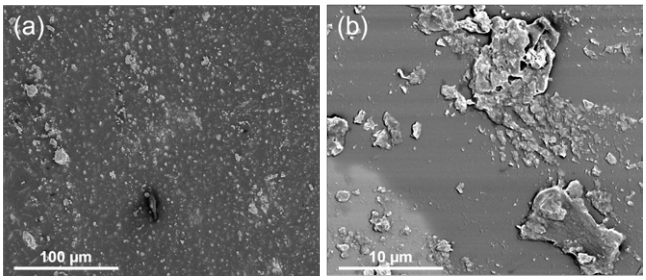


Figure A2.2. Scanning electron micrographs of irregularities at the edges of (a) PUF-KOH and (b) PUF-TEA coating surface.

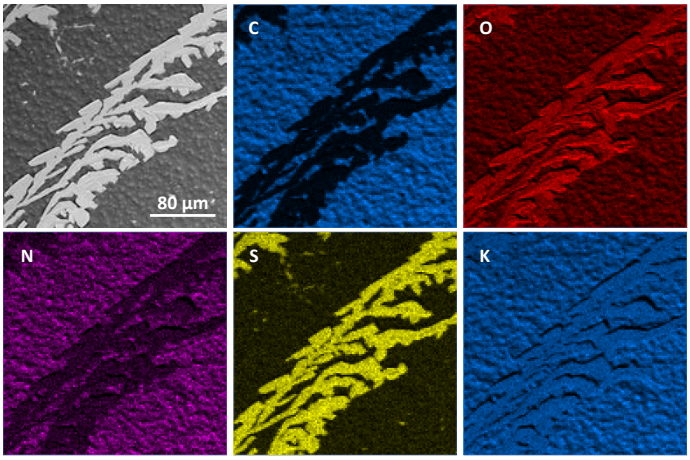


Figure A2.3. Elemental map scans as determined with EDX of crystals on a PUF-KOH coating surface. Crystals on top of the coating surface are devoid of carbon, and rich in sulphur, oxygen and potassium.

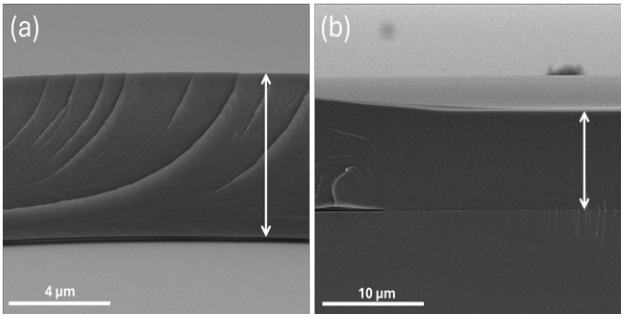


Figure A2.4. SEM micrographs of cross-sections of (a) PUF-TEA and (b) PF-TEA.

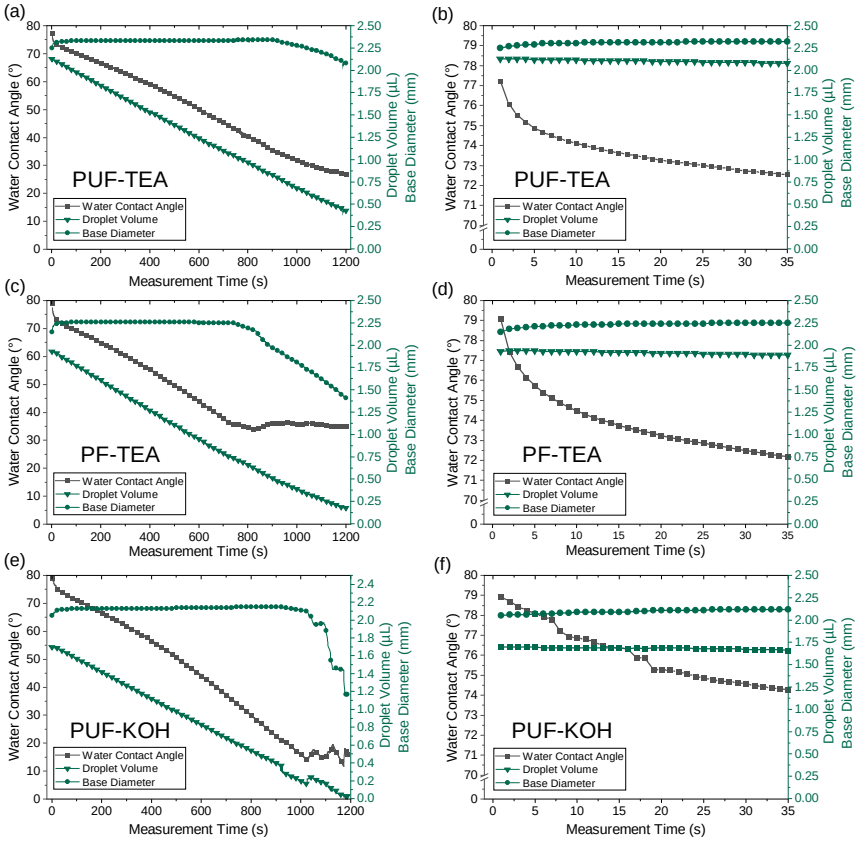


Figure A2.5. Droplet volume, base diameter and water contact angle of a water droplet on (a–b) PUF-TEA, (c–d) PF-TEA and (e–f) PUF-KOH surface as function of time.

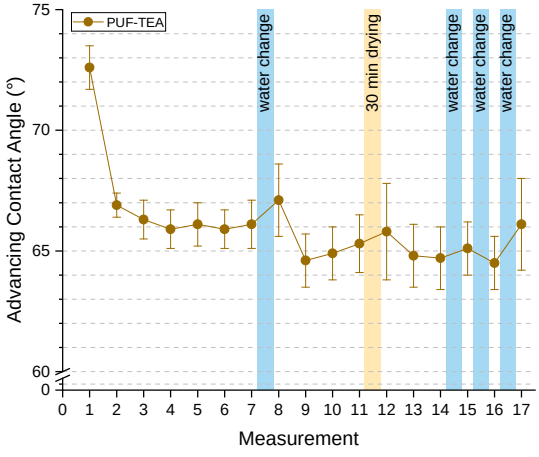


Figure A2.6. S-ACA values on a PUF-TEA coating surface. In between indicated measurements, water in the syringe was refreshed with new water to test for a possible influence of leachables on the ACA value.

Dynamic Vapour Sorption measurements

Dynamic vapour sorption (DVS) measurements were performed using a Surface Measurement Systems DVS Resolution, with water as the probe vapour. A thin layer of PUF-TEA resin was cast on an aluminium panel and subsequently cured at 150 °C for 20 minutes. By bending the substrate, PUF-TEA flakes were obtained and approximately 1–2 mg was added to a quartz sample pan. Changes in sample mass were recorded while the sample was exposed to 0, 75 and 90% relative humidity for 1200 minutes. Images of the sample where recorded every 15 minutes in order to monitor possible changes in sample dimension, of which an extreme example is shown in Figure A2.7. Other samples measured this way showed similar behaviour, although the clarity of swelling and deswelling was found to be dependent on the size of the flake and its orientation relative to the camera.

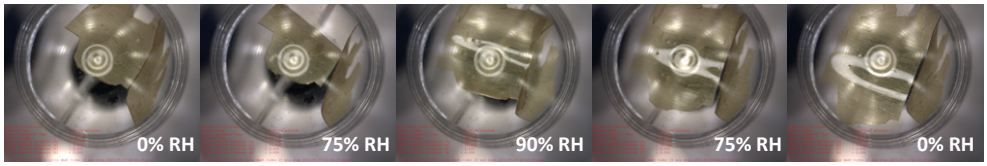


Figure A2.7. Swelling and deswelling of a PUF-TEA flake upon exposure to elevated and lower relative humidity, respectively, seen as a change in volume.

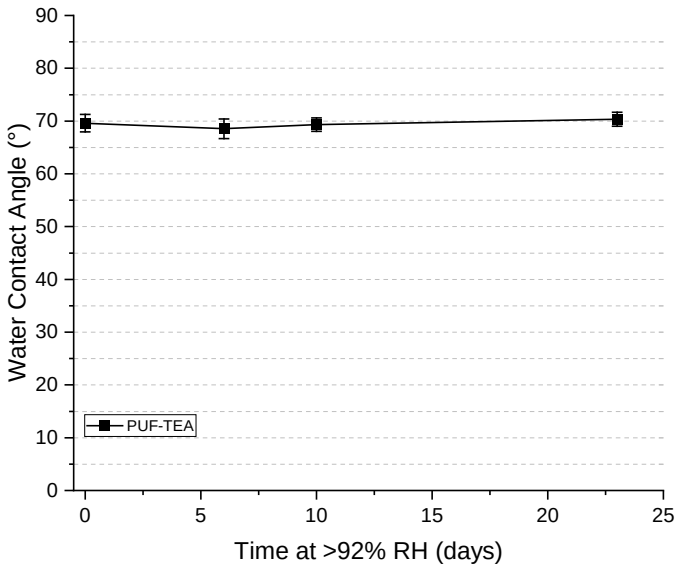


Figure A2.8. WCA value of PUF-TEA coatings stored at elevated RH for up to 23 days.

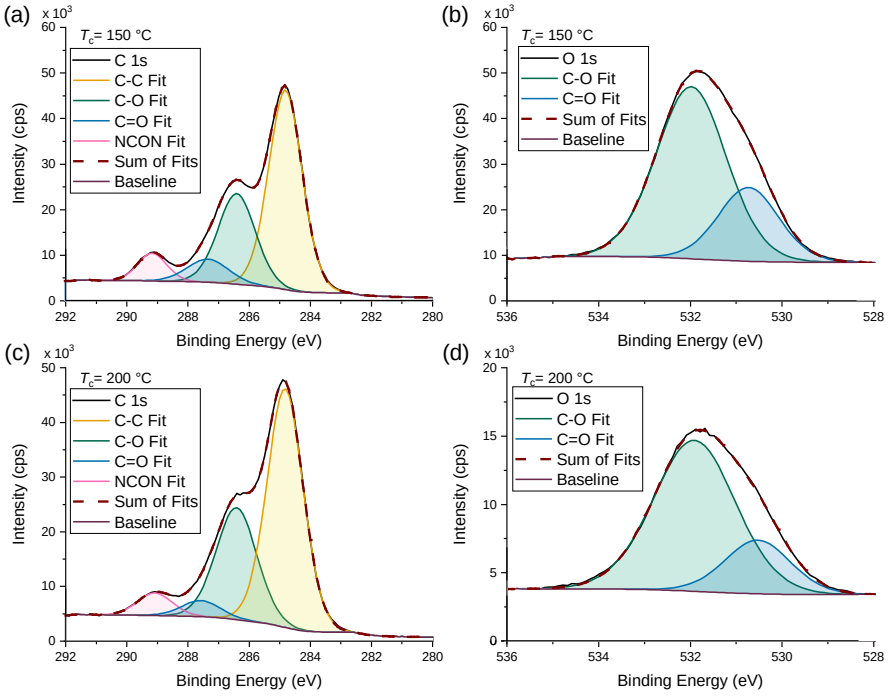


Figure A2.9. Representative deconvoluted C 1s and O 1s binding energy spectra of PUF-KOH cured at T_c = 150 °C (a–b) or at 200 °C (c–d).

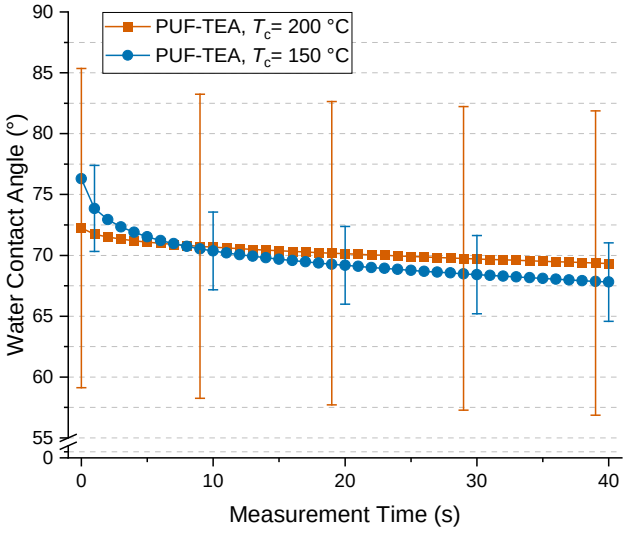


Figure A2.10. Average water contact angle over time for PUF-TEA coatings cured either in air in convection oven at T_c = 200 °C for 10 minutes (9 coatings from 1 batch) or in N_2 in a semi-closed chamber at T_c = 150 °C for 20 minutes (18 samples from 3 different batches).

Table A2.1. Overview of the chemical composition and water contact angle (WCA) for various phenolic resin coatings cured under various conditions. Unless otherwise specified, curing atmosphere was air.

Coating		Conditions	O:C	N:C	CO/CC	FWHM (eV)	WCA (°)
PUF-KOH	Oven	200 °C 10 min	0.29 ± 0.02	0.15 ± 0.01	0.70 ± 0.03	2.56 ± 0.06	70.5 ± 3.6
	Semi-closed Chamber	150 °C 20 min	0.33 ± 0.01	0.21 ± 0.01	0.80 ± 0.06	2.41 ± 0.09	67.7 ± 2.1
		150 °C 20 min N_2	0.33 ± 0.02	0.19 ± 0.01	0.76 ± 0.03	2.39 ± 0.08	70.0 ± 1.5
PUF-TEA	Oven	200 °C 10 min	0.29 ± 0.01	0.14 ± 0.01	0.64 ± 0.05	2.51 ± 0.08	70.8 ± 6.0
		200 °C 20 min	0.28 ± 0.02	0.15 ± 0.01	0.62 ± 0.03	2.65 ± 0.10	73.8 ± 5.6
		150 °C 20 min	0.31 ± 0	0.22 ± 0.01	0.83 ± 0.02	2.45 ± 0.03	66.1 ± 3.2
	Semi-closed Chamber	150 °C 20 min	0.33 ± 0.01	0.21 ± 0.02	0.72 ± 0.12	2.38 ± 0.05	75.3 ± 4.6
		150 °C 20 min N_2	0.34 ± 0.01	0.22 ± 0.01	0.80 ± 0.04	2.32 ± 0.08	70.8 ± 2.5
PF-TEA	Oven	200 °C 10 min	0.29 ± 0.01	-	0.39 ± 0.01	1.96 ± 0.03	74.8 ± 5.1
		200 °C 20 min	0.31 ± 0.01	-	0.37 ± 0.01	2.0 ± 0.06	76.4 ± 7.7
		150 °C 20 min	0.28 ± 0.01	-	0.49 ± 0.03	1.62 ± 0.04	70.6 ± 3.7
	Semi-closed Chamber	150 °C 15 min	0.28 ± 0	-	0.49 ± 0.02	1.59 ± 0.02	71.2 ± 3.0
		150 °C 15 min N_2	0.28 ± 0.01	-	0.48 ± 0.02	1.62 ± 0.04	69.7 ± 2.7



3

Behaviour of Wetting Agents in Phenolic Resin Coatings

Abstract

The behaviour of three hydrophilic wetting agents of different chemical nature in phenol-formaldehyde (PF) and phenol-urea-formaldehyde (PUF) coatings was investigated using contact angle goniometry. Nonionic ethoxylated fatty acid (EFA) was seen to phase separate during curing regardless of the resin used, leading to a wetting agent (WA) rich surface layer which could easily be removed by mechanically wiping with a wet tissue. The anionic WAs, a branched alkylbenzene sulphonate (BAS) and an alkyl ethoxylated sulphate (AES), were found to phase-separate only in PF coatings. Thus, a compatibilising effect of the presence of urea in PUF coatings was observed, resulting in a less strong surface enrichment of anionic WAs in PUF coatings. Successive wetting of coatings was seen to yield a plasticising effect on PUF and PF surfaces, which was found to be partially reversible when exposing the surfaces to air under ambient room conditions. This matrix plasticisation effect was typically also observed in the presence of WAs. Understanding both the polymer–WA interaction, and the behaviour of the polymer matrix and WAs when exposed to water or water vapour, gives crucial insights for the optimisation and selection of the appropriate WA for applications where hydrophilic surfaces are required.

This chapter is based on L. Moone, I.A.C. van de Ven, M.P.J. Donners, K. van Durme, D.V. Okhrimenko, R.A.T.M. van Benthem, R. Tuinier, and A.C.C. Esteves, Tunable wettability of phenolic resin coatings, *Progress in Organic Coatings*, **2025**, vol. 198, 108883

3.1. Introduction

One example of the use of phenolic resins is as an adhesive in stone wool, of which applications include thermal and acoustic insulation, or as a growing medium in horti- and floriculture [1,2], also known as a hydroponic use. It is common procedure to include additives in the phenolic resin to impart specific properties to the final cured product, such as de-dusting oils, urea, or coupling agents [2]. In case of hydrophilic stone wool products for hydroponic purposes, wetting agents (WAs) are added into the resin to increase the water uptake and retention of the stone wool substrate made of coated fibres [3–5]. For an optimal substrate hydrophilicity, it is desirable that the WAs are well-distributed through the applied coating.

In general, the distribution of additives within a coating is dependent on several factors such as compatibility and interactions between additive and matrix, surface activity of the additive, kinetics of diffusion versus that of the film formation, and interactions between additive and substrate [6–11]. This implies that the substrate type (i.e., its polarity), and the matrix and additive characteristics (i.e., structure, functionality, and molar mass) all contribute to the final distribution. For instance, Thorstenson *et al.* [8] found that the addition of silicone–poly(ether) block copolymers in an acrylic–melamine system leads to a less strong enrichment at the coating–air interface compared to the same additive in an acrylic–isocyanate system. This difference was attributed to less compatibility between the block copolymer and the acrylic-isocyanate system, leading to a stronger segregation towards the coating–air interface. Similar observations regarding compatibility between additives and matrices have been made for surfactant distributions in latexes [6,7,12,13] and in poly(vinyl alcohol) [9,14], and for block copolymers in various polymer matrices [10,15–18].

The distribution of additives in a coating will inherently affect the coating performance. For instance, strong surface segregation or phase separation of additives results in most, if not all, of the additive at the coating–air interface. This makes the surface highly susceptible to loss of its functionality due to damage, wear or leaching. Moreover, it is important to note that the distribution of additives can change over time due to diffusion to the coating–air interface [12], or as a result of aggregation [19] or additive degradation [13].

Several strategies to elucidate the distribution of additives in a coating include X-ray photo-electron spectroscopy [10,20,21] and quantitative attenuated total reflectance Fourier transform infrared spectroscopy [6,8]. Another approach is to probe surface properties such as wettability, which in the case of wetting agents additionally provides direct information about their wetting performance.

In this Chapter, the influence of wetting agents on the surface wettability is investigated to gauge the performance and distribution of the surfactant within coatings prepared from PUF and PF resins. Three different wetting agents were used (Figure 3.1): a

nonionic ethoxylated fatty acid (EFA), an anionic alkyl ethoxylated sulphate (AES), and an anionic branched alkylbenzene sulphonate (BAS). These WAs are representative of commercially used additives and are all different in chemical structure. To detect initial performance differences, static water contact angle (WCA) measurements were made on PUF and PF coatings with a normalised amount of wetting agent. The response of the coating matrix with and without wetting agents towards direct contact with water was evaluated by successive advancing contact angle measurements.

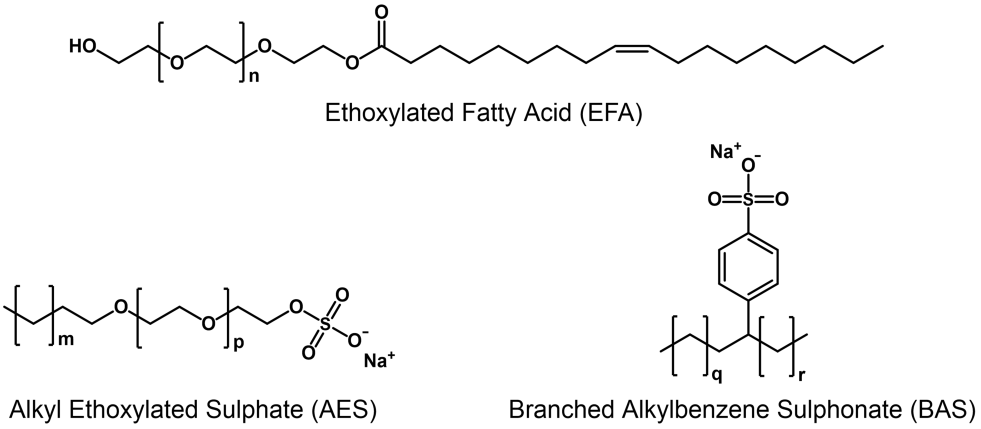


Figure 3.1. Chemical structures of the wetting agents used in this study.

By using both PUF and PF resins, differences in WA distribution and behaviour were determined in matrices which are comparable, to a certain extent, but simultaneously exhibit a significant chemical difference. Furthermore, the response of wetting agents to changes in relative humidity was investigated by subjecting coatings to high or low relative humidity environments, and subsequently determining the water wettability of the surfaces. Last, the mobility of the wetting agents within these coatings was assessed by introducing a barrier to the coatings in the form of an overcoating membrane. In this way, some insights into the wetting agent–phenolic resin matrix interactions were obtained which could help selecting future additives for hydrophilic phenol resin applications.

3.2. Experimental Procedures

Materials

Triethylamine (TEA; > 99.5%), urea (≥ 99%), and phenol (> 99%) were obtained from Sigma-Aldrich. Formaldehyde 37 wt% solution in water (including 10–15% methanol

stabiliser) was purchased from ThermoScientific. Ethoxylated fatty acid (EFA), branched alkylbenzenesulphonate (BAS; active substance (a.s.) 25 wt% in water), and alkyl ethoxylated sulphate (AES; active substance 27 wt% in water) were kindly supplied by ROCKWOOL A/S. Linear vinyl-terminated poly(dimethylsiloxane) (PDMS; 17200 g/mol) was obtained from Gelest. Tetrakis(dimethylsiloxy)silane (97%) was purchased from ABCR GmbH & Co. Karstedt's catalyst (Platinum(0)-1,3-divinyl-1,1,3,3-tetramethyldisiloxane complex solution; 2% Pt in xylene) was received from Aldrich. Before use phenol was stored at room temperature under Ar atmosphere and with P_2O_5 in a desiccator. Tetrakis(dimethylsiloxy)silane was stored in a desiccator with drying agent. All other chemicals were used as received.

Syntheses

The synthesis of PUF-TEA and PF-TEA resin is described in Chapter 2, including the chemicals used.

Resin Formulation Preparation

The solids content (S.C.) of the resins was determined by the difference in resin mass before (m_i) and after (m_f) curing approximately 0.8–2 g of resin at 200 °C for 1 h:

$$S.C. = \frac{m_f}{m_i} \cdot 100\% \tag{3.1}$$

PUF resin formulations with wetting agents were prepared by addition of either AES (43 mg / g resin), BAS (47 mg / g resin) or EFA (12 mg / g resin) to PUF resin (S.C. approximately 34–35%) and magnetic stirring for at least 1 h. The amount of wetting agent added to the resin was chosen such that the active substance (weight fraction of wetting agent) was the same for each compound (i.e., 0.012 g WA / g resin for PUF resin with solids content of approximately 34–35%). Formulations of PF-WA (S.C. approximately 38–39%) with wetting agents were prepared by converting the relative amounts of wetting agent as used in PUF-WA formulations based on the solids content. Before the formulations were used for coating application, stirring was stopped for at least 20 minutes.

Coating Preparation

The procedure for applying coatings to the glass substrates is described in Chapter 2. All phenolic resin coatings in this Chapter were cured in a semi-closed chamber with a heating plate at 150 °C under an N_2 flow of approximately 150 L/h at 1 bar, with a curing time of 20 minutes.

Membrane and Overcoat Preparation

PDMS membranes were prepared following the procedure described by Esteves *et al*. [22]. A solution of 2.4 mg/mL of Karstedt's catalyst in toluene was prepared. The ratio between Si-H groups of the crosslinker and vinyl groups of the PDMS was set to 2.7 : 1. Membranes were prepared by adding the crosslinker (29.1 µL) to 1 g of PDMS. After stirring by hand for approximately 1 minute, 20 µL of the catalyst solution was added and the mixture was mixed further by hand. The mixtures were cast onto poly(tetrafluoroethylene) (PTFE) substrates onto which a square mould was made with 0.98 mm thick heat-resistant tape. The PDMS membranes were cured under vacuum at 80 °C for approximately 24 hours. Membranes were peeled from the PTFE substrate and had an average thickness of 415 ± 39 µm, as measured with a calliper.

Wetting agent-free layers of PUF were applied on existing PUF-WA coatings by dip coating (100 mm/min immersion and withdrawal speed) in a PUF dispersion and subsequently curing at 150 °C for 20 minutes in the semi-closed chamber under a nitrogen flow.

Water Contact Angle Measurements

The procedure for static WCA measurements is described in Chapter 2.

For some measurements, coatings were placed in an environmental chamber connected to a humidity generator (Dataphysics TPC 100 and Dataphysics HGC 30). Relative humidity inside the chamber was both set and monitored with the generator, operated with an N_2 flow at 1 L/min.

Successive advancing contact angle (S-ACA) measurements were performed by first placing a droplet of 2 µL on the coating surface. Unless otherwise specified, the droplet volume was then increased and decreased by 25 µL respectively at a rate of 0.25 µL/s, in succession. For experiments where coating surfaces were exposed to air under room conditions in between measurements, the droplet was fully withdrawn from the surface. For PUF, PUF-BAS and PUF-AES, the reported averages are from three of such series of measurements on three different coatings, where the standard deviation of the average ACA at each measurement *i*, termed σ_{X_i}, was taken as a pooled standard deviation:

$$\sigma_{X_i} = \sqrt{\frac{\sigma_{1_i}^2 + \sigma_{2_i}^2 + \sigma_{3_i}^2}{3}}, \tag{3.2}$$

where σ_{1_i}, σ_{2_i} and σ_{3_i} refer to the standard deviation of the advancing contact angle for measurement *i* on three different coatings.

For PF, PF-AES, and PF-BAS, the reported averages are from two measurement series on two different coatings, appropriately adjusting Equation 3.2 for the standard

deviation. The average ACA and standard deviation of a single measurement was determined in the range where the left and right contact angles were more or less constant, while the droplet volume and droplet base diameter were still increasing. Any deviations in the ACA plateau due to chemical or physical heterogeneity is reflected in the corresponding standard deviation. Although the number of datapoints per ACA plateau was different per measurement and per coating, the weight of every measurement was considered to be the same. Hence, no correction for number of datapoints was included in the pooled standard deviation as given in Equation 3.2.

Water Gel Content Measurement

Resin was cured in an oven at 150 °C for 20 minutes after which it was crushed to a powder (particle size range between 180–425 µm). Powders were then stored under vacuum for 4 days to remove residual moisture. Gel content of PUF and PF resin was determined by immersing approximately 0.38 g of cured and powdered resin in approximately 3.2 mL Milli-Q water. To allow for easy separation of powder and water, the powder was kept in a dialysis tube when immersed in water. The mass of all individual dialysis bags and resin samples was recorded before immersion. Immersed samples were placed on a shaking table at 250 RPM for 24 h, after which the bags with powder were dried briefly in an oven for 30 minutes at 70 °C and subsequently stored in a desiccator with P_2O_5 for 24 h. Before gel content determination, samples were kept under vacuum for 4 days. Reported results are the average of two samples per resin, taking into account the average mass loss observed from blank measurements with only a dialysis bag in water.

Water–Air Interfacial Tension Measurements

The procedure for water–air interfacial tension measurements on water which had been in contact with a coating surface, and water which contained cured PUF-WA powder, is described in Chapter 2.

Surface Tension Measurements

The surface tension (SFT) of the wetting agents in water was measured with a Dataphysics DCAT 21 tensiometer, using a Pt-Ir Wilhelmy plate of 10 x 1.9 x 0.2 mm (l x w x t). Before the first measurement, the Wilhelmy plate was rinsed in MilliQ water and heated in an open flame until red hot. The measurement of the SFT was stopped when the difference in recorded surface tension was approximately 0.2 mN/m over 20 s. To determine the critical micelle concentration (CMC) of the WAs, the surface tension at various surfactant concentrations was measured by adding a volume of WA and stirring the solution. The critical CMC was determined to be at the concentration where the slope in the SFT versus the logarithm of WA concentration changed. Measurements over the concentration range were performed separately at least two times.

^{1}H-Nuclear Magnetic Resonance Measurements

WAs were characterised by ^{1}H-NMR on a Bruker Advance III HD 400 MHz spectrometer. Either acetone-d6 (ACE) or $CDCl_3$ was used as solvent, with tetramethylsilane (TMS) used as reference. 32 spectra were recorded and averaged with a recycle delay of 2 s.

3.3. Results and Discussion

Wetting Agent Characterisation

The structure of the wetting agents used in this study and their ^{1}H-NMR spectra are shown in Figure 3.2. Two different types of WA were used; EFA (ethoxylated fatty acid) is a nonionic surfactant, whilst BAS (branched alkylbenzene sulphonate) and AES (alkyl ethoxylated sulphate) are anionic wetting agents. ^{1}H-NMR spectra were used to determine the average molar mass ($\bar{M}_n$) of the wetting agents (Table 3.1).

From the ^{1}H-NMR spectra of AES it was observed that the wetting agent solution not only contained sodium lauryl ether sulphate (SLES), but also sodium lauryl sulphate (SLS), similar to previously reported spectra [23]. Approximately 63% of the wetting agent in the mixture was determined to be SLES, i.e., ethoxylated, with the remainder being SLS. For EFA, several signals around 5.5–6.5 ppm are discernible. These match with protons from a conjugated alkyl tail, as for instance found in conjugated linoleic acid, which is likely one of the main sources for the production of EFA. Considering the signals at 5.5–6.5 ppm, at least 1 in 4 EFA molecules are conjugated in the apolar alkyl chain.

Table 3.1. Overview of wetting agent number average molar mass from ^{1}H-NMR and critical micelle concentration in water at 20 °C (given as mg active substance (a.s.)/L and mmol/L), and the surface pressure at the CMC, from surface tension measurements.

WA	$\bar{M}_n^{NMR}$ (g/mol)[a]	CMC (mg a.s. /L)	CMC (mmol/L)	CMC Literature (mmol/L)[b]	π_{CMC} (mN/m)
EFA	580	1.1	$1.9 \cdot 10^{-3}$	-	35.3
BAS	341	634	1.9	1.9 [24]	37.6
AES	371	332	0.9	0.8 [25]	47.5

[a]Average determined from at least 2 spectra.

[b]CMC values from literature are provided for comparison, even though for BAS and AES a direct comparison is not possible on account of differences in alkyl chain distribution for BAS or presence of both SLES and SLS in AES. No suitable reference was found for EFA.

The difference in surface activity of the wetting agents was determined by measuring the surface tension at the air–WA solution interface as a function of WA concentration (Figure 3.3). The critical micelle concentration (CMC; reported in Table 3.1) was obtained from the point at which the absolute value of the slope changes.

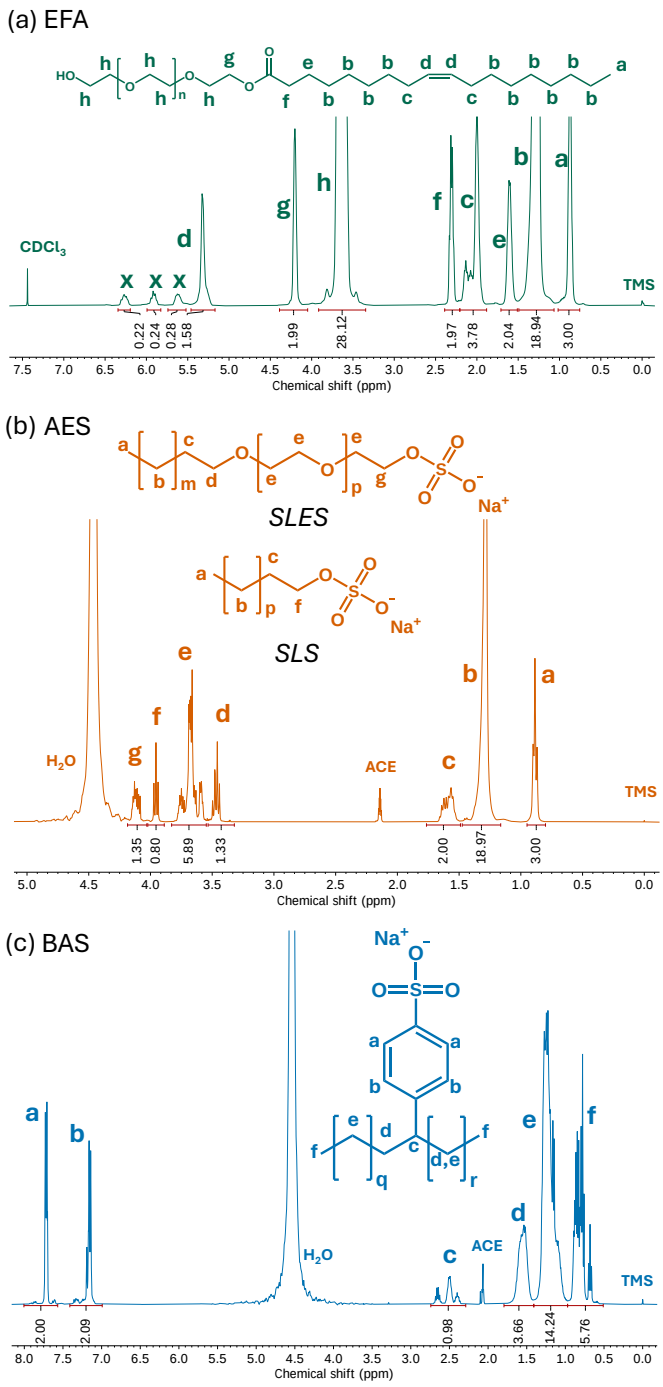


Figure 3.2. Chemical structures and ^{1}H-NMR spectra of the wetting agents used in this study. (a) EFA in $CDCl_3$, (b) AES and (c) BAS in acetone-d6 (ACE), with TMS as a reference. In the spectrum of EFA, the label x refers to protons from EFA with a conjugated alkyl tail.

Due to the absence of repulsive electrostatic interactions, the nonionic surfactant has a CMC which is significantly lower than the CMC of the anionic wetting agents. The results of the surface tension measurements in Figure 3.2 corroborate the fact that AES is not pure, evidenced by an increase in surface tension above the CMC which points towards the presence of a hydrophobic component. For BAS, it is known that length of the respective branches strongly affects the CMC [26,27]. The BAS used in this study is a mixture of different branch lengths, seen from the spread and splitting of signals c–f in the ^{1}H-NMR spectrum in Figure 3.1c, with on average an alkyl chain length of 11.5. The obtained CMC value is not unreasonable and falls in between values determined by García *et al.* [27] for BAS homologues with an alkyl chain length of 11 and 12.

Wetting agent performance can be described by efficiency and effectiveness [28,29]. Efficiency relates to the bulk concentration required to reduce the surface tension of the solvent significantly, whereas effectiveness relates to the maximum reduction in surface tension of the solvent that is possible [28,29]. It can be seen that EFA and BAS have a similar effectiveness, which can be expressed by the surface pressure

$$\pi_{CMC} = \gamma_{H_2O} - \gamma_{CMC} \,, \tag{3.3}$$

where γ_{H_2O} is the surface tension of pure water (72.7 mN/m at 293 K) and γ_{CMC} the surface tension of the WA solution at the critical micelle concentration.

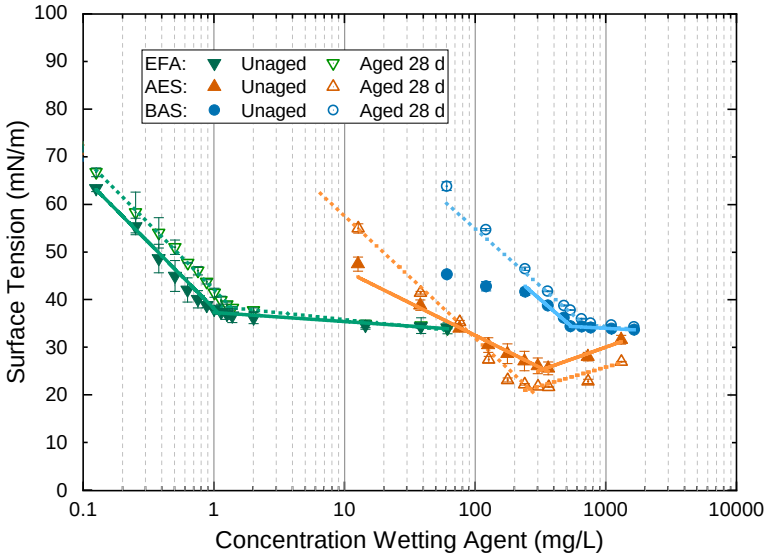


Figure 3.3. Surface tension as function of WA concentration for the nonionic EFA, anionic BAS and anionic AES in water. Results are the average of two separate measurements.

AES showed the strongest decrease in surface tension at the CMC, which can be attributed to the presence of lauryl alcohol or the presence of SLS which can be

regarded as a homologue of different molar mass [30–34]. Lauryl alcohol is known to be more hydrophobic than SLS and SLES, leading to a saturated water–air interface even at small fractions of lauryl alcohol in the solution [33,35]. With increasing WA concentration, the lauryl alcohol is eventually absorbed in the micelles formed by the SLES and SLS, leading to the characteristic increase in surface tension.

Wetting Agent–Binder Interactions Through Contact Angle Measurements: Phenol-Urea-Formaldehyde Coatings

Henceforth, coatings are referred to by the resin type (PF or PUF) and the presence of wetting agent in general, or the specific wetting agent (e.g., PUF-WA or PUF-EFA).

Although inclusion of wetting agents in the coating formulations could lead to an improved wetting of the glass substrates by the resins, the main difference was found in the wettability of the cured coatings. PUF-WA coatings all show a different absolute water-wettability, where the average water contact angle value is decreased compared to PUF coatings (Figure 3.4a). For the same amount of active substance, PUF-BAS coatings are slightly less hydrophilic than PUF-AES surfaces. This could indicate a slightly better compatibility of BAS with the polymer matrix due to its aromatic content. Characteristic for all surfaces of PUF, PUF-BAS and PUF-EFA, is a decrease in contact angle value in the first few seconds of the measurement. Evaluation of the droplet base diameter and volume shows that the decrease in contact angle value is predominantly due to spreading of the droplet on the coating surface (Figure A3.1). It should be noted that evaporation and possible imbibition will also affect the measurement. For PUF-AES, this spreading effect was present the least as seen by the more relatively stable wetting profile in Figure 3.4.

Interestingly, the incorporation of EFA in the resin formulation resulted in demixing of the wetting agent upon curing, yielding a slightly hazy coating with an EFA-rich top layer. This top layer could easily be disturbed by wiping the surface (Figure A3.2). As a consequence of both the demixing and the effectiveness of the nonionic wetting agent in reducing the surface energy of the water droplet at the surface, PUF-EFA coatings exhibited the lowest WCA value: around 10° within just 30 seconds. Due to these observations PUF-EFA was in some cases disregarded for further studies.

Successive advancing contact angle measurements were performed on PUF coatings with and without BAS and AES (Figure 3.5a). In between the indicated ACA measurements, coating surfaces were exposed to environmental conditions (air) for a given exposure time t_e before continuing the experiment. As referred to above, these measurements could not be performed on coatings containing EFA due to the virtually immediate wetting of the surface, whereupon the droplet spread beyond the field of view of the camera and could not be fully withdrawn from the surface anymore.

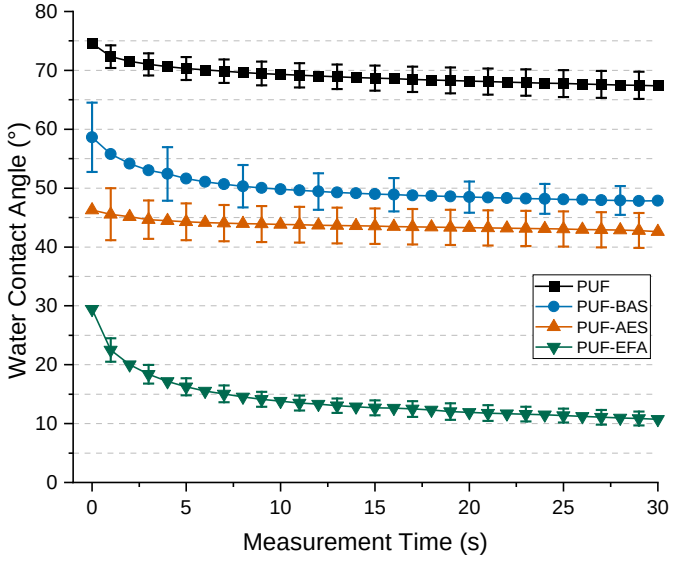


Figure 3.4. Static WCA values of PUF coatings with and without wetting agents.

Wetting, dewetting and exposing the surface to air appear to have a characteristic effect on all coating surfaces. In general, the absolute ACA value is determined by the absence or presence of wetting agent, but the response to air exposure after wetting and dewetting the surface appears to mainly stem from the polymer matrix. This is demonstrated by the continuous ACA measurement on PUF (Figure 3.5a, open squares), where the ACA value steadily decreases and potentially reaches a plateau for long(er) measurement times. Probing the surfaces successively with water appears to influence the measured property. Interestingly, the effect of air exposure is only temporary, as each second measurement after air exposure resulted in a rapid decrease to lower advancing contact angle values. For two different PUF coatings, it was found that probing the surface with water without explicit air exposure times results in a gradual decrease in the rate at which the ACA value decreases, indicating that eventually the WCA becomes stable (Figure 3.5a, open squares, and Figure A3.4).

For PUF the effect of air exposure was the most pronounced, although even a relatively long air exposure time of 16 hours did not yield an increase in ACA value above that of the second measurement. A measurement series was also performed on a PUF(-WA) surface with a prolonged drying time of 64 hours, where a larger increase to above the value of the second measurement was observed (Figure 3.5b). However, the initial ACA value was still not attained. This can be due to a difference in kinetics of a plasticisation process relative to the drying effects, or a permanently induced surface change by the presence of water. The observed hysteresis was also seen from dynamic vapour sorption measurements on cured PUF flakes (Figure A3.5). Here, the mass gain as a

result of exposing the sample to a relative humidity (RH) of 90% was not lost within the same time when the sample was subsequently held at 0% RH.

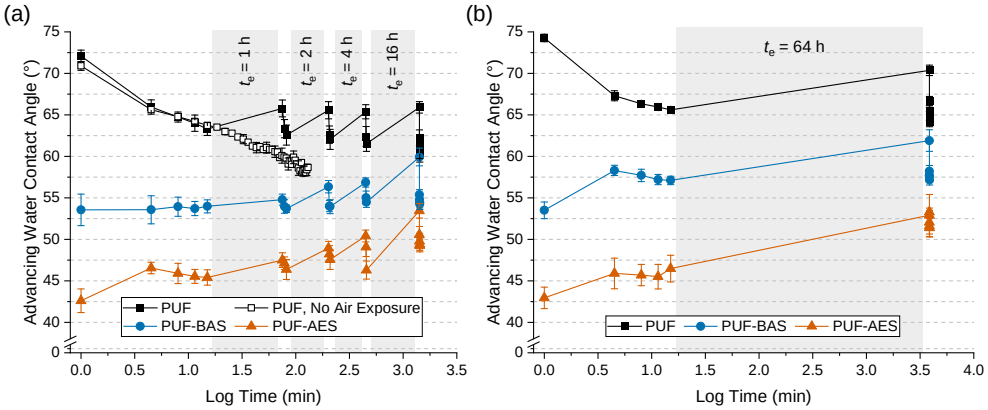


Figure 3.5. S-ACA values of PUF coatings with and without wetting agents. Between indicated measurements the surfaces were exposed to air under environmental lab conditions, for the shown amount of time (solid symbols). Datapoints indicated with the open squares are from one PUF coating which was continuously probed with water, without interrupting the measurement. The first measurement was set to a log time of 0, with each subsequent measurement taking approximately 3.5 minutes. (For a different representation of the same data, the reader is referred to Figure A3.3).

To investigate the possibility of the measurements permanently inducing surface changes, the gel content of cured, powdered PUF resin (particle size 180–425 µm) in water after 1 day was determined and found to be approximately 95%. It could therefore be the case that the direct contact with water during the first measurement was already enough to extract some of the 'leaching' material which thereby changes the surface characteristics of the coating.

Coatings of PUF-BAS and PUF-AES also exhibited other interesting behaviours. For instance, the plasticisation effect which was observed for PUF was typically found to be smaller for the coatings with WAs for shorter air exposure times. In general, it appeared that the trend in the ACA values was still dictated by the matrix (plasticisation), but the absolute ACA value was affected by the presence of WA, at times masking the matrix effect. Additionally, PUF-AES coatings appeared to increase slightly in ACA value with additional measurements. Furthermore, the first ACA measurement on previously unwetted PUF-AES coatings (i.e., data points at log time of 0 min in Figure 3.5a) showed a characteristic stick-and-slip behaviour (see Figure A3.6a). Subsequent ACA measurements, even after air exposure, did not show indications of such behaviour. This implies that the initial measurement affects the wetting agent distribution on the surface.

The increase in ACA value of PUF-AES coatings could imply changes in distribution of AES in the coating surface layers, but also a continuous leaching of AES into the water during the successive measurements. To evaluate if the latter is the case, the water–air interfacial tension (IFT) of water droplets which had been in contact with the coating surfaces was determined with the pendant drop method (Table 3.2). For this, first a droplet of approximately 28 µL (at a rate of 0.25 µL/s) was deposited on the coating surface, which was then withdrawn with another, thicker needle connected to an empty syringe. Two additional dynamic measurements were then performed with this setup on the coating surface, after which the water–air interfacial tension was determined with a pendant drop method. For comparison, coatings of PUF-EFA were also used for these experiments. However, for PUF-EFA, a single drop of approximately 30 µL was deposited on the surface at a rate of 0.25 µL/s and then withdrawn with an empty, wide needle before determining the water–air IFT, as dynamic measurements on these surfaces were not feasible.

Leaching of anionic WAs or surface-active components from the PUF matrix as a result of S-ACA measurements was not observed, as the water–air IFT value of a water droplet used for these measurements was similar to that of pure water (Table 3.2). However, a significant change in IFT was detected when immersing cured PUF-WA powders in water for 1 day and subsequently measuring, indicating that WAs do in fact leach out from cured PUF-WA powders. It is likely that for the PUF-WA coatings, the concentration of potential WA leachables might be too low to significantly decrease the water–air interfacial tension (and hence not affecting the S-ACA measurements this way). However, this would also imply that the PUF surface itself barely changes in terms of surface energy, which would not explain the observed behaviour shown in Figure 3.5a–b. Thus, it is therefore thought that the observed effects are a result of reorientation or clustering of WAs when in contact with water, decreasing their effectiveness.

Table 3.2. Water–air interfacial tension at 298 K of a droplet which either had been in contact with a coating surface, or from water in which cured and powdered resin (size of 180–425 µm) was dispersed for 1 day.

	$IFT^{a}_{S\text{-}ACA}$ (mN/m)	IFT^{b}_{powder} (mN/m)
Milli-Q Water (Reference)	72.3 ± 0.3	71.2 ± 0.4
PUF	72.1 ± 0.2	71.9 ± 0.2
PUF-BAS	72.2 ± 0.2	41.2 ± 0.5
PUF-AES	71.7 ± 0.3	41.1 ± 0.7
PUF-EFA	36.0 ± 0.3	38.6 ± 1.0

[a]: average of two measurements total, each performed on a different coating surface.
[b]: average of four measurements total for two different samples. For PUF, the reported average is of three measurements total for two different samples.

Wetting Agent–Binder Interactions Through Contact Angle Measurements: Phenol-Formaldehyde Coatings

In a similar approach as described in the previous section for PUF, coatings of PF were prepared with and without WAs to study the contribution of the polar urea moieties on the interactions between wetting agents and matrix. This interaction was again assessed by both static and dynamic wetting measurements.

Due to differences in reaction time and the omission of adding a solution of urea in water, PF resins were found to have a slightly higher solids content compared with PUF resins. This was considered when preparing the initial resin formulations. When using the same amount of wetting agent in PUF (active substance concentration of approximately 0.34 mg / (g · S.C.), or a concentration of approximately 13 mg a.s./g PF resin), PF-WA coatings were found to become hazy during curing, indicating that the WA had demixed. Furthermore, the WCA values were low compared to PUF-WA, with complete wetting for coatings with anionic WAs transpiring within 10 seconds (Figure 3.6a–b).

The presence of demixed anionic WAs in PF coatings indicates an incompatibility between the WAs and the coating matrix. This incompatibility was not readily observed for the anionic WAs in PUF-matrices, signifying that urea moieties function as a compatibilizer. For the nonionic EFA, similar results were obtained for PF-EFA and PUF-EFA, meaning that urea does not necessarily influence the compatibility between EFA and the resin.

Concentration series of PF-WA were made to try to achieve similar wettability as the PUF-WA coatings, as shown in Figure 3.6a–b (more concentrations are included in Figure A3.7). For the nonionic wetting agent in PUF and PF coatings, it was expected that at all tested concentrations induced demixing of the WA would lead to similar hydrophilicity. However, it appears that there exists a certain concentration regime below which compatibility and miscibility of the WA with the resin increases and as a result the surface wettability decreases. For a high enough concentration of EFA, demixing from the resin always occurs, leading to more or less similar WCA values and wetting profiles (see also Figure A3.7 for a concentration of EFA in PUF of 0.68 mg a.s./ (g S.C.)).

Reducing the concentration of anionic WA in PUF leads to a less strong decrease in hydrophilicity compared to PF-WA coatings. Additionally, PF-WA surfaces typically showed a larger variation in the surface wettability. For the lowest concentration, such variations are likely due to an inherently heterogeneous coating–air interface on account of the low amount of WA present in the coating system. It was found that, for the resin formulations used, a concentration of 0.08 mg a.s. / (g S.C.) in PF resin yielded similar contact angle values for BAS and AES relative to their PUF-WA counterparts (Figure A3.7). This reduction in amount of wetting agent needed can be regarded as a

double-edged sword for applications: on one hand, similar surface properties can be achieved with much less wetting agent, but on the other hand changes on the surface are more noticeable because there is less wetting agent overall in the system.

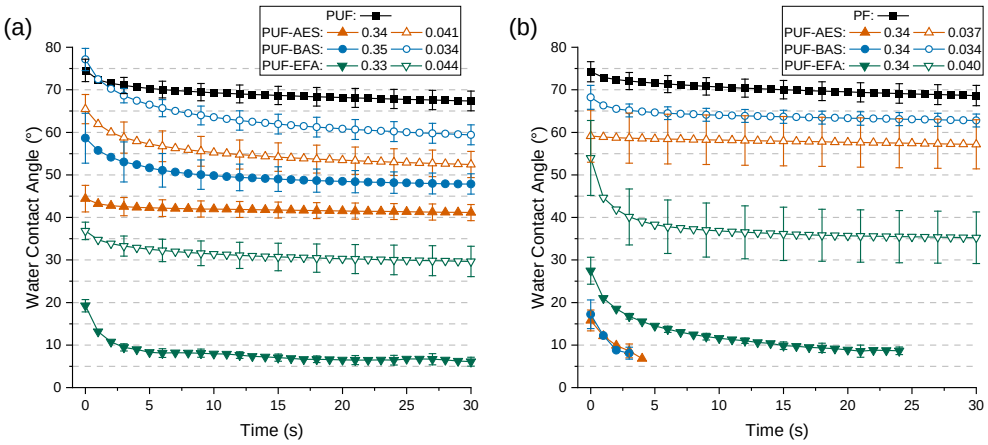


Figure 3.6. WCA values for (a) PUF- and (b) PF-WA coatings with varying concentration of WA. Concentrations are given as mg a.s. / (g S.C.). For the S-ACA measurements in (b), a concentration of 0.08 mg a.s. / (g S.C.) AES and BAS in PF was used which yielded surfaces with similar hydrophilicity as their PUF counterparts. Results at intermediate concentrations are implemented in Figure A3.7.

It should also be noted that it appears that the relation between BAS and AES as found in PUF coatings still holds true for PF coatings: for the same concentration below 0.34 mg a.s. / (g S.C.), BAS appears to lower the WCA less than AES. This could again be due to a slightly better compatibility with the PF matrix. However, contrary to PUF-WA formulations, the addition of wetting agents to PF resin did not yield consistent outcomes in terms of coating quality and absolute values of the coating wettability, in part also reflected in the standard deviation of the results. For different batches of PF resin, similar concentrations of AES for instance yielded different CA values (Figure A3.8). The reason for this observation can be twofold. First, the wetting agent concentration is in most cases relatively low, so small deviations as a result of variations in mixing or weighing likely have a large impact. Second, the distribution of this relatively low amount of wetting agent is likely greatly affected by the demixing during curing, which in itself most probably cannot be considered consistent in terms of its kinetics (a result of local thermal and concentration differences during curing). Still, decreasing the wetting agent concentration decreases the hydrophilicity, and in general a lower amount of WA is required in PF coatings to achieve a similar wettability to PUF-WA coatings.

Repeated wetting of PF coatings, like PUF coatings, shows a partially reversible increase in hydrophilicity (Figure 3.7). Compared to PUF and to results as shown in

Chapter 2, the decrease in S-ACA was found to not be as drastic. This might be due to an increase in curing time relative to previous research, and additionally the lack of polar urea moieties. The gel content of PF was determined to be approximately 92.1%, slightly lower than that of PUF. Interestingly, despite a lower gel content, the decrease in CA with successive measurements is still less strong. This indicates that the more dominant factor affecting the change in contact angle value for coatings without wetting agents is plasticisation rather than possible leaching of material. It is reasonable that for identical curing conditions the observed plasticisation effects are stronger for PUF on account of the presence of more hydrophilic urea moieties.

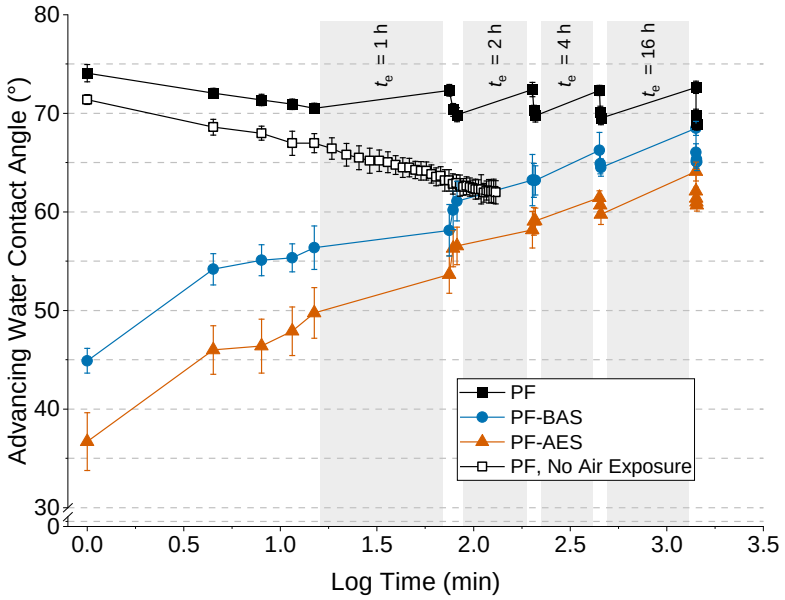


Figure 3.7. S-ACA measurements on PF surfaces with and without WA. WA concentration was 0.08 mg a.s. / (g S.C.), yielding surfaces with similar initial wettability as PUF-WA coatings shown in Figure 3.4.

The S-ACA measurements on PF-AES and PF-BAS show a significantly larger decrease in surface wettability compared to their PUF counterparts. A slight plasticisation effect was only seen for later measurements (typically after 4 hours of air exposure time). Water droplets during the first measurement on a surface of PF-BAS now also exhibited stick-and-slip behaviour, which was previously only seen for AES-containing coatings (Figure A3.6b). Kwok and Neumann [36] describe that such behaviour is the result of an energy barrier which the droplet has to overcome before its three-phase contact line can move over the surface. The exact origin of this energy barrier can vary depending on the studied surface and the degree of non-inertness of the surface [37,38]. Still, it is believed that in this case the stick-and-slip behaviour of PF-BAS is indicative of a more heterogeneous surface compared to PUF-BAS.

It is assumed that, as with PUF-WA coatings, the WAs are removed from and/or redistributed on the surface with each measurement, which seems to be more significant as the CA values for PF coatings with BAS and AES approach that of PF without WA. Because the concentration of WA is relatively low in PF, such a surface change impacts the resulting wettability more prominently. Still, water–air interfacial tension measurements on droplets which have been in contact with a PF-AES surface show no significant decrease in interfacial tension, which was determined to be 71.2 ± 0.6 mN/m as an average from two measurements.

Wetting agent distribution and persistence in the surface layers was also studied by consecutively wiping the surface of PUF- and PF-WA coatings once with a wet and dry tissue paper whilst exerting a force of 10 N. Wettability of the coatings was probed before and after the wiping procedure. After wiping, EFA-containing coatings return to a contact angle value which is similar to that of PUF or PF surfaces (Figure 3.8). As indicated above, and shown in Figure A3.2, the top layer of PUF-EFA could be readily disturbed by wiping with a dry cotton swab. Wiping in presence of water, however, resulted in virtually complete removal of the WA from the surface. Hence, for both PF-EFA and PUF-EFA it can be ascertained that nearly all of the WA is at the coating–air interface. Replenishment of the initial hydrophilicity was therefore also not observed for coatings stored at 55 °C and 87% RH for 7 days, as there was either no or too little WA left in the bulk to migrate to the coating–air interface.

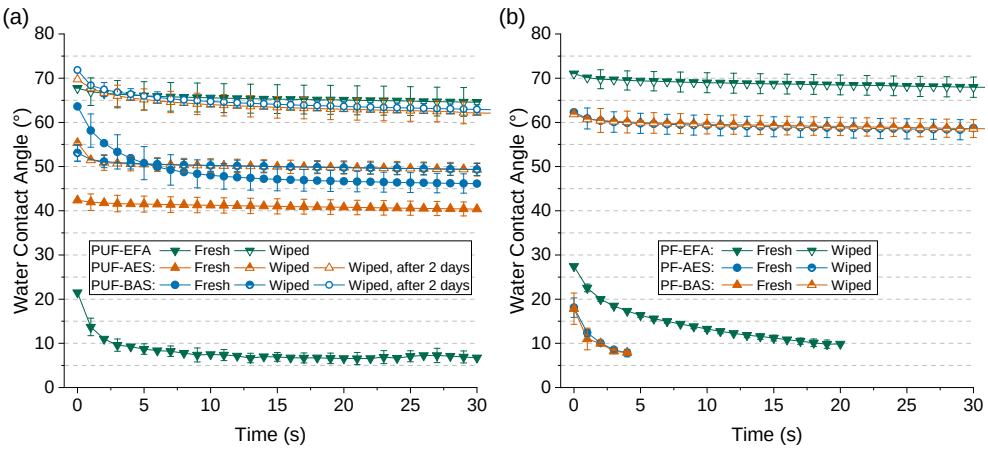


Figure 3.8. WCA values for (a) PUF- and (b) PF-WA coatings directly before and after wiping with a wet and dry tissue, respectively. Results are the average of three measurements per coating, on two coatings per formulation. In (a), WCA values of PUF-AES and PUF-BAS surfaces after wiping and storing at ambient conditions are also shown.

Typically, PUF-AES coatings also showed an increase in WCA directly after the wiping procedure, although the resulting CA is still indicative of WA being present in the

surface layers. PUF-BAS on the other hand appeared to be relatively unaffected by the wiping. Further proof of demixing of the anionic WA in PF coatings was also found when wiping PF-AES and PF-BAS surfaces: all coatings show a significant increase in WCA after the procedure. Although the original WCA value of a pure PF surface was only seen when wiping a PF-EFA coating, the strong decrease in wettability for the PF coatings with the anionic WAs indicates a loss of WA at the surface. This is in line with the increasing S-ACA values observed in Figure 3.7.

Interestingly, the WCA continued to increase for PUF-AES and PUF-BAS coatings after the wiping procedure (Figure 3.8a). As the wiping of the surfaces clearly does not remove all of the WA, this implies that there is a continuous response to the wetting and drying of the surface. To some degree, this response is reminiscent of what happens during the S-ACA measurements (Figure 3.5b–c and Figure 3.7), in that wetting and subsequent exposure to air under ambient room conditions leads to an increase in WCA. For PUF coatings without WAs, the wiping procedure also leads to results similar to those of the S-ACA measurements in that directly after wiping a decrease in WCA value is observed (Figure A3.9). This value is close to what was found for S-ACA measurement on PUF without explicit intermittent air exposure (Figure 3.5a).

The effect of wiping and subsequent changes in hydrophilicity was sometimes seen to vary in strength between coatings. This is likely in part an effect of the wiping being done manually, and hence the speed not being controlled, as well as some inherent variations in WA concentration in surface layers between coatings.

Effect of Inorganic Catalysts on Wetting Agent Distribution

It should be noted that the catalyst type also affects the distribution of WAs. For instance, as established in Chapter 2, the use of inorganic and latent catalysts such as in PUF-KOH results in crystal formation in the binder during the curing process.

Crystallisation phenomena are strongly influenced by additives such as ions, small- or macromolecules [39,40]. The presence of surfactants for instance can influence not only nucleation, but also the crystal growth, dissolution rate, and crystal habit [39–44]. Kuschel *et al*. [45] studied the growth and dissolution rates of K_2SO_4 single crystal faces in pure and supersaturated solution, and in supersaturated solutions of potassium sulphate with either sodium dodecyl sulphonate or potassium dodecanoate. They found that depending on the surfactant concentration and type, both dissolution and growth of the single crystal can be inhibited. This indicates that the adsorption of a surfactant can differ for each crystal face, as different faces have a different surface energy [46,47]. This difference in interaction was directly observed for coatings of PUF-KOH with and without WAs. As already presented in Chapter 2, after wetting and drying PUF-KOH coatings, K_2SO_4 crystals could be observed on the coating surface. The morphology and number density of the crystals was strongly dependent on the concentration and type of WA used (Figure 3.9). Typically, in presence of EFA, the

crystals were scattered more and blocky, whereas for AES and BAS the crystals were in general larger and agglomerated.

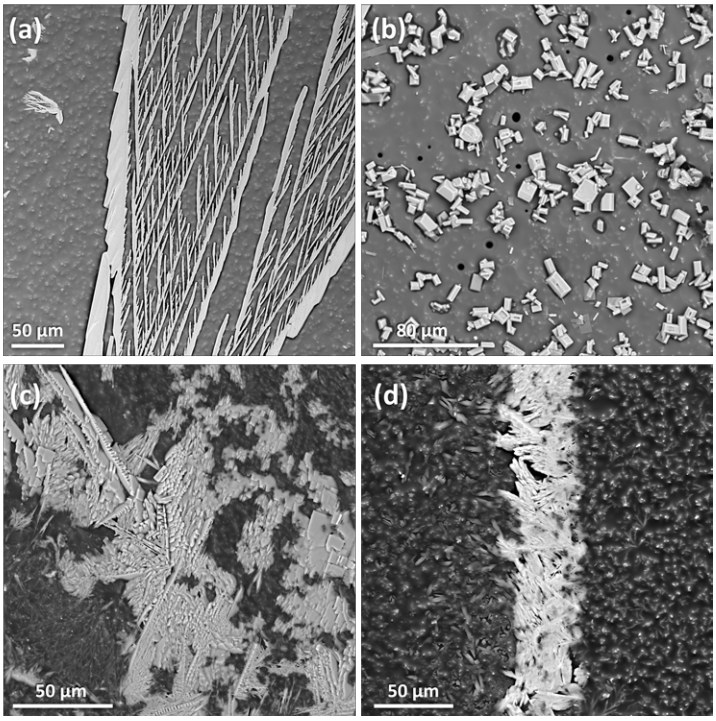


Figure 3.9. Scanning electron micrographs of coating surfaces of PUF-KOH (a) without WA, (b) with EFA, (c) with AES and (d) with BAS. Surfaces were wetted with water and dried before analysis.

Differences in resulting crystal morphology and number density after wetting and drying are presumed to be a result of both the WA effectiveness and their adsorption to different crystal faces. Due to this adsorption, the distribution of WA and crystals are to some degree inherently linked. This might also explain the wettability of PUF-KOH-WA coatings compared to the PUF-TEA-WA counterparts (Figure 3.10). Although in general there was no significant difference between the WA-free coatings, in presence of crystals it was seen that the WAs increase the hydrophilicity to a lesser degree. It is expected that this variation in performance will differ strongly between batches on account of the unpredictable nature of the crystal formation itself. Additionally, EFA was seen to yield inconsistent hydrophilic surfaces. The reason for this is that the final WA distribution is dependent on multiple aspects, not all of which can be completely tuned: the compatibility with the resin and forming network, the kinetics of segregation to the surface, and the interaction with the forming crystals all affect the lateral and transversal concentration gradient of the WA within the coating.

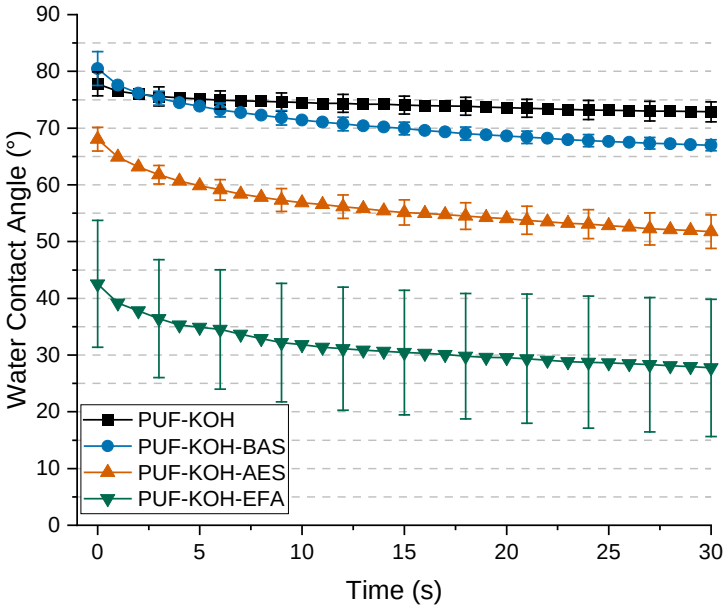


Figure 3.10. WCA values for PUF-KOH coatings with and without WA. Results are the average of five measurements per coating, on two different coatings per formulation. WA concentration was mass-normalised to AES.

Interestingly, when measuring the IFT of a water droplet which had been in contact with a PUF-KOH-WA coating surface, a relatively large decrease in water–air IFT was obtained (Table 3.3). Due to the dissolution of K_2SO_4 crystals over the course of the successive dynamic wetting, WAs also leach more easily into the water droplet compared to similar procedures performed on crystal-free surfaces (as shown in Table 3.2).

Table 3.3. Water–air interfacial tension values at 298 K of a droplet of water which had been in contact with a PUF-KOH(-WA) surface. Coatings used for these experiments contained different amounts of WA (not mass-normalised to AES).

Sample	$IFT_{S\text{-}ACA}$ (mN/m)
Milli-Q Water (Reference)	72.3 ± 0.3
PUF-KOH	72.4 ± 0.3
PUF-KOH-AES	51.1 ± 1.8
PUF-KOH-BAS	48.8 ± 0.7

Wetting Agent Mobility and Response to Relative Humidity

It has been shown in the previous sections that direct contact with water can affect the surface wettability of PF and PUF coatings. Additionally, for PUF-WA, plasticisation in combination with what is assumed to be wetting agent redistribution at the surface was observed by means of the S-ACA measurements. The ability of WAs to rearrange or migrate was further studied by exposure of coatings to varying levels of relative humidity.

Storage of PUF coatings with and without anionic WAs at elevated relative humidity shows that only the AES-containing coatings exhibit a peculiar behaviour under these conditions (Figure 3.11a). A drastic decrease in the WCA value within 1 hour was observed for these coatings when exposed to 90% RH, which was not seen for the other PUF surfaces on these timescales. Interestingly, the increase in hydrophilicity for PUF-AES is reversible. This behaviour of the wetting agent is not affected by the polymer matrix, which is supported by a similar change in surface wettability for PF-AES under the same conditions.

It should be noted that the measurements at 10% RH in Figure 3.11a either show a slight decrease in contact angle value (for PUF and PUF-BAS), or for PUF-AES a reversibility in surface wettability. The initial reference WCA values could not be attained at low relative humidity due to the increased evaporation rate of the water droplet from the coating surface compared to ambient conditions (see Figure A3.10 for an example of this effect). Enhanced evaporation is not only the result of the low relative humidity, but also of the continuous, relatively warm nitrogen flow (typically 24–27 °C) entering the environmental chamber to control the RH level. Despite this, it is evident that there appears to be a strong reversibility towards higher WCA values upon decreasing the relative humidity for PUF-AES coating surfaces.

The drastic increase in wettability of PUF-AES coatings when stored at elevated relative humidity values could imply a transversal or lateral rearrangement of the WA at the surface. Björklund and Kocherbitov [48] investigated how film hydration evolved when various surfactant films were exposed to varying degrees of humidity, using a humidity scanning quartz crystal microbalance with dissipation monitoring. When a sodium dodecyl sulphate (SDS) film was subjected to a water activity of 0.98, a phase transition from the solid state to a two-phase region in between the micellar and solid phase was observed [48]. It is also known that above a critical relative humidity, a liquid surfactant placed on top of a substrate can begin to spread due to the adsorption of water from air to the front of the three-phase contact line, facilitating subsequent wetting [49,50]. Although there is a difference between the threshold relative humidity at which SDS and AES respond, at the very least there are indications that reversible, humidity-induced structural changes or rearrangements for SDS-like surfactants can occur depending on environmental conditions.

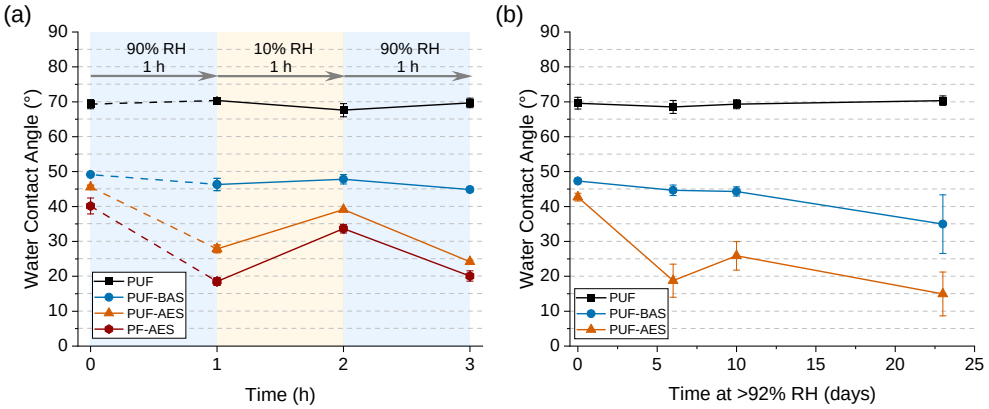


Figure 3.11. Effect of relative humidity on the WCA of PUF coatings with and without anionic WAs. (a): WCA values of PUF-WA coatings (0.34 mg a.s./ (g · S.C.)) after equilibration for 1 h in a semi-closed chamber at 90% or 10% relative humidity. The first datapoints correspond to values of the coatings determined outside of the chamber, under ambient conditions and relative room humidity. Reported values are the average of six measurements total, each time on a different spot, on two different coatings. Also included is the response of PF-AES coatings (0.08 mg a.s./ (g S.C.)) to changes in relative humidity. (b): WCA values of PUF-WA coatings after storage in a desiccator with an aluminium cup filled with water for longer exposure times. Reported values are the average of three measurements on three coatings.

Interestingly, the response towards high relative humidity was not readily observed for PUF-BAS coatings. Even when the exposure time of coatings was increased to 10 days, only a minor decrease in WCA value of PUF-BAS surfaces was measured (Figure 3.11b). The measured values were sometimes also obtained for similar coatings kept at ambient conditions, and hence fall within the expected range of possible WCA values. For longer exposure times of 23 days, coatings of PUF-BAS and PUF-AES both exhibited a larger variation in their wettability. Prior to WCA measurements, macroscopically visible spots could be seen on most of the coating surfaces. It is thought that exposure to high RH has led to clustering of WA at the surface, resulting in hydrophilic spots. As exemplified by the standard deviation for PUF-BAS, the distribution of these spots was rather irregular, leading to a heterogeneous surface. Furthermore, the exact critical relative humidity was not investigated. Coatings of PUF-WA stored at 82% RH for 34 days showed only for AES-containing coatings a larger variation in average WCA, but not as strong as shown in Figure 3.11 (see also Figure A3.11).

Driven by the behaviour of AES in the PUF matrix, the mobility and possibility of diffusion of wetting agents was tested by adding a membrane on coatings to create a new coating–air interface initially devoid of wetting agents (Figure 3.12). WA-free coating–air interfaces were created either by placing a PDMS membrane on the surface, or by applying a PUF overcoat and subsequently measuring the water contact angle value of these new surfaces over time. PDMS was chosen on account of its generally high permeance to water vapour [51], whilst at the same time providing a low solubility for liquid water. To cover the existing coating surfaces with a PUF overcoat,

wet films were applied by means of dip coating. As a control, several coatings were also 'dip coated' with water in order to verify that the method of applying the additional PUF layer does not in itself affect the WAs on the surface significantly (e.g., by dissolution of WAs into the resin formulation; Table A3.1). Overcoat thickness was found to be approximately 4–6 µm (determined with contact profilometry; Table A3.2).

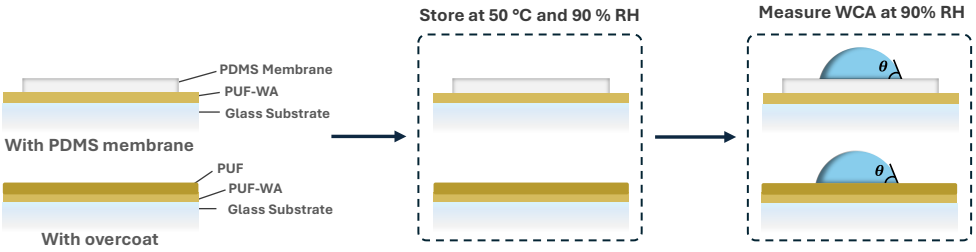


Figure 3.12. Method to study possible diffusion of WAs through a membrane. First, either a hydrophobic PDMS membrane or a WA-free PUF coating was applied on a surface of PUF-WA. Surfaces where then stored at elevated temperature and relative humidity for varying times, after which the WCA was measured on the top surface in an environmental chamber at 90% RH.

Placing a PDMS membrane on top of a droplet of wetting agent and subsequently measuring the WCA in a humidity chamber at 90% RH showed that the only wetting agent capable of fast diffusion through the membrane was the nonionic EFA (Figure 3.13). Quite rapidly, a water droplet placed on top of the membrane showed an appreciable decrease in contact angle value as it began to spread on the surface. Even for longer measurement times, the anionic surfactants did not exhibit such a behaviour. It should be noted, however, that EFA is an oily substance whereas BAS and AES are solutions in water. This means that EFA is mobile by itself, whereas effective diffusion on the same timescale for BAS and AES would have to be mediated by absorbed water. At the end of the measurements the spot where droplets of anionic wetting agent were placed had dried out, thereby limiting the potential of these wetting agents to diffuse on this timescale.

Subsequent experiments with PDMS membranes on top of coatings were carried out by storing the samples in an oven at 50 °C and 90% RH, to accelerate possible diffusion processes. The high humidity environment was used to facilitate migration of anionic species towards the new membrane–air interface. Although the membranes were relatively thick compared to research of Camós Noguer *et al.* [52] in which surfactant diffusion was studied, a long exposure time of 13 days was still not enough to detect any anionic WA on the surface of the PDMS membrane (Figure 3.13b; note that the decrease in WCA value within the first 10 seconds for all samples is due to rearrangements of the PDMS at the surface). Again, only the nonionic WA was able to diffuse towards the new interface, which was verified by monitoring the evolution of the

droplet base diameter and volume over time (Figure A3.12). The diffusion of EFA through the PDMS membrane was also already observed after intermittingly probing the surface with water after 6 days.

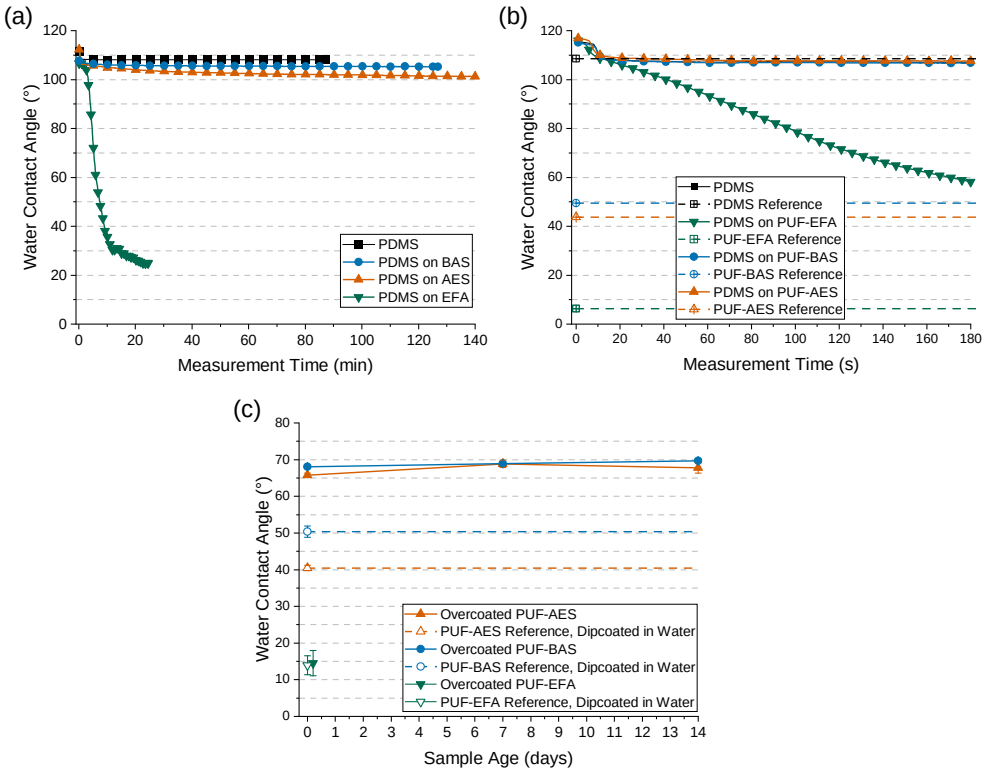


Figure 3.13. WCA values of PDMS membranes (thickness approximately 415 µm) on top of (a) liquid wetting agent or (b) a PUF-WA coating, and (c) WCA values of PUF coatings (thickness approximately 4–5 µm) on top of PUF-WA coatings (two coatings per formulation). Measurements in (a) where performed in a humidity chamber set to 90% RH. Prior to the measurements as shown in (b), the coatings were stored at approximately 50 °C and 90% RH for 13 days. Prior to the measurements as shown in (c), the coatings were stored at approximately 50 °C and 90% RH.

Finally, a thinner barrier in the form of a layer of PUF free of wetting agent showed that still there was no tendency for the anionic wetting agents to migrate to a new coating–air interface, at least on the timescale of 14 days exposure to 50 °C and 90% RH (Figure 3.13c). Samples monitored for 34 days likewise showed no indication of wetting agent at the surface (Figure A3.13). By contrast, a newly applied layer of PUF on top of a PUF-EFA coating showed immediate signs of wetting agent being present in the new surface layers. As the nonionic wetting agent is known to be present as a virtually continuous layer on the coating surface, it is expected that it can easily migrate to the new interface

upon application of a water-rich resin layer. Additionally, the subsequent thermal curing likely helps accelerate this diffusion.

3.4. Conclusions

The behaviour of three wetting agents of different chemical nature in two different phenolic resin coatings, for which the key difference was the presence or absence of urea, was investigated. The nonionic WA was found to induce demixing in both PUF and PF coatings, leading to an oily top layer which could be easily removed from the surface by wiping with a wet tissue paper. Anionic wetting agents were found to be more compatible with the urea-containing PUF resin, while in PF coatings demixing of anionic wetting agents could be observed for a concentration above approximately 0.34 mg a.s./ (g S.C.). In general, the concentration of WA required in PF coatings to achieve similar wettability as in PUF coatings was typically found to be significantly smaller, as a result of lower matrix compatibility and hence higher surface enrichment, yet at the expense of higher surface heterogeneity.

The employed S-ACA measurement method affected the measured wettability, as seen by the water plasticisation effects of PUF and PF surfaces. Nevertheless, this method still provides insights regarding the persistence of WAs in the surface layers and how the matrix itself is affected by the presence of water on the surface. The plasticisation when in contact with water was seen to be partly reversible. A hysteresis effect was discernible, as this plasticisation process was faster than the drying effect. It is believed that this is partly due to the affinity of the coatings towards moisture, which makes it difficult for the surfaces to completely and properly dry in air at ambient room conditions. As the drying starts from the top of the coating surface, leading to vitrification of these surface layers, the subsequent drying of lower layers is slowed down. Additionally, the plasticisation is typically stronger for PUF surfaces, likely due to the presence of the more hydrophilic urea moieties.

The surface plasticisation by water and drying effects of the PUF matrix was still seen when the anionic WAs were present. Overall, it can be stated that the presence or absence of wetting agent determines the absolute value of the ACA, but for PUF coatings the polymer matrix influences the trend. For PF-WA coatings, although plasticisation was still observed, water on the coating surface appeared to mainly remove or redistribute the WAs. This is likely a result of having a low concentration of surfactant near the surface as it has less interactions with the matrix than in the case of PUF. Any changes on the surface as a result of removal or redistribution are then more strongly noticeable.

Interestingly, both anionic WAs do not appear to diffuse through PUF coatings for the probed timescales, despite AES showing a striking response to high relative humidity which lowers the WCA by approximately 20°. Only the nonionic EFA was seen to be able to diffuse through a PDMS membrane and a WA-free PUF overcoat, with the anionic wetting agents appearing to be more fixed within the coating.

In short, several facile methods to test the distribution, performance and persistence of WAs in two types of phenolic resin coatings have been used. Understanding the behaviour of both the polymer matrix as well as the WAs when exposed to water or water vapour allows for the optimisation and selection of the appropriate WA for applications where phenolic resin coatings with hydrophilic surfaces are required.

References

[1] M. Jiřičková and R. Černý, "Effect of hydrophilic admixtures on moisture and heat transport and storage parameters of mineral wool," *Constr. Build. Mater.*, vol. 20, no. 6, pp. 425–434, 2006, doi: 10.1016/j.conbuildmat.2005.01.055.

[2] S. Kowatsch, "Mineral Wool Insulation Binders," in *Phenolic Resins: A Century of Progress*, L. Pilato, Ed., Berlin, Heidelberg: Springer, 2010, pp. 209–242. doi: 10.1007/978-3-642-04714-5_10.

[3] J. Cuypers, K. D. De, and P. Bouwens, "Use of a Linear Alkyl Benzene Sulphonate Anionic Surfactant to Improve the Water Distribution Over the Height of a Mineral Wool Substrate," EP2048938B1, 2019

[4] J. Cuypers, K. D. De, and P. Bouwens, "Method of Growing Plants," EP2048935B1, 2016

[5] A. Blaakmeer, "Plant growth substrates," WO2001082683A1, 2001 Accessed: 2024. [Online]. Available: https://patents.google.com/patent/WO2001082683A1/en?oq=WO+01%2f82683+

[6] T. A. Thorstenson and M. W. Urban, "Surface and interfacial FTIR spectroscopic studies of latexes. IV. The effect of surfactant structure on the copolymer–surfactant interactions," *J. Appl. Polym. Sci.*, vol. 47, no. 8, pp. 1381–1386, 1993, doi: 10.1002/app.1993.070470808.

[7] K. W. Evanson and M. W. Urban, "Surface and interfacial FTIR spectroscopic studies of latexes. III. The effects of substrate surface tension and elongation on exudation of surfactants," *J. Appl. Polym. Sci.*, vol. 42, no. 8, pp. 2309–2320, 1991, doi: 10.1002/app.1991.070420822.

[8] T. A. Thorstenson, J. B. Huang, M. W. Urban, and K. Haubennestel, "Mobility and distribution of silicone additives in coatings; a spectroscopic study," *Prog. Org. Coat.*, vol. 24, no. 1, pp. 341–358, 1994, doi: 10.1016/0033-0655(94)85024-0.

[9] A. Briddick, P. Li, A. Hughes, F. Courchay, A. Martinez, and R. L. Thompson, "Surfactant and Plasticizer Segregation in Thin Poly(vinyl alcohol) Films," *Langmuir*, vol. 32, no. 3, pp. 864–872, 2016, doi: 10.1021/acs.langmuir.5b03758.

[10] S. P. W. Govers, N. Alexander, M. Al-Masri, J. Omeis, L. G. J. van der Ven, G. de With, and A. C. C. Esteves, "Surface segregation of polydimethylsiloxane-polyether block copolymers in coatings driven by molecular architecture," *Prog. Org. Coat.*, vol. 150, p. 105991, 2021, doi: 10.1016/j.porgcoat.2020.105991.

[11] W. Ming, M. Tian, R. D. van de Grampel, F. Melis, X. Jia, J. Loos, and R. van der Linde, "Low Surface Energy Polymeric Films from Solventless Liquid Oligoesters and Partially Fluorinated Isocyanates," *Macromolecules*, vol. 35, no. 18, pp. 6920–6929, 2002, doi: 10.1021/ma020650i.

[12] J. L. Keddie and A. F. Routh, "Surfactant Distribution in Latex Films," in *Fundamentals of Latex Film Formation: Processes and Properties*, J. L. Keddie and A. F. Routh, Eds., Dordrecht: Springer Netherlands, 2010, pp. 185–212. doi: 10.1007/978-90-481-2845-7_6.

[13] D. Scalarone, M. Lazzari, V. Castelvetro, and O. Chiantore, "Surface Monitoring of Surfactant Phase Separation and Stability in Waterborne Acrylic Coatings," *Chem. Mater.*, vol. 19, no. 25, pp. 6107–6113, 2007, doi: 10.1021/cm0714077.

[14] R. J. Fong, O. Squillace, C. D. Reynolds, J. F. K. Cooper, R. M. Dalgliesh, J. Tellam, F. Courchay, and R. L. Thompson, "Segregation of Amine Oxide Surfactants in PVA Films," *Langmuir*, vol. 36, no. 17, pp. 4795–4807, 2020, doi: 10.1021/acs.langmuir.0c00084.

[15] D. R. Iyengar, S. M. Perutz, C.-A. Dai, C. K. Ober, and E. J. Kramer, "Surface Segregation Studies of Fluorine-Containing Diblock Copolymers," *Macromolecules*, vol. 29, no. 4, pp. 1229–1234, 1996, doi: 10.1021/ma950544z.

[16] H. Lee and L. A. Archer, "Functionalizing Polymer Surfaces by Field-Induced Migration of Copolymer Additives. 1. Role of Surface Energy Gradients," *Macromolecules*, vol. 34, no. 13, pp. 4572–4579, 2001, doi: 10.1021/ma001278e.

[17] H. Lee and L. A. Archer, "Functionalizing polymer surfaces by surface migration of copolymer additives: role of additive molecular weight," *Polymer*, vol. 43, no. 9, pp. 2721–2728, 2002, doi: 10.1016/S0032-3861(02)00041-1.

[18] J. Wang, A. Reyna-Valencia, and B. D. Favis, “Surface Migration of Conductive PEBA in Ternary Polymer Blend Films with Different Wetting Morphologies,” *Macromolecules*, vol. 54, no. 12, pp. 5607–5617, 2021, doi: 10.1021/acs.macromol.1c00696.

[19] A.-C. Hellgren, P. Weissenborn, and K. Holmberg, “Surfactants in water-borne paints,” *Prog. Org. Coat.*, vol. 35, no. 1, pp. 79–87, 1999, doi: 10.1016/S0300-9440(99)00013-2.

[20] C. L. Zhao, F. Dobler, T. Pith, Y. Holl, and M. Lambla, “Surface composition of coalesced acrylic latex films studied by XPS and SIMS,” *J. Colloid Interface Sci.*, vol. 128, no. 2, pp. 437–449, 1989, doi: 10.1016/0021-9797(89)90359-7.

[21] C. Arnold, G. Klein, M. Maaloum, M. Ernstsson, A. Larsson, P. Marie, and Y. Holl, “Surfactant distribution in waterborne acrylic films: 2. Surface investigation,” *Colloids Surf. Physicochem. Eng. Asp.*, vol. 374, no. 1, pp. 58–68, 2011, doi: 10.1016/j.colsurfa.2010.11.008.

[22] A. C. C. Esteves, J. Brokken-Zijp, J. Laven, H. P. Huinink, N. J. W. Reuvers, M. P. Van, and G. de With, “Influence of cross-linker concentration on the cross-linking of PDMS and the network structures formed,” *Polymer*, vol. 50, no. 16, pp. 3955–3966, 2009, doi: 10.1016/j.polymer.2009.06.022.

[23] S. H. Im and J. J. Ryoo, “Characterization of sodium laureth sulfate by reversed-phase liquid chromatography with evaporative light scattering detection and 1H nuclear magnetic resonance spectroscopy,” *J. Chromatogr. A*, vol. 1216, no. 12, pp. 2339–2344, 2009, doi: 10.1016/j.chroma.2009.01.005.

[24] G. A. Smith, A. Huggett, C. Jones, and G. Ortego, “Surface Activity and Performance Properties of Gemini Salts of Linear Alkylbenzene Sulfonate in Aqueous Solution,” *J. Surfactants Deterg.*, vol. 24, no. 4, pp. 563–574, 2021, doi: 10.1002/jsde.12496.

[25] M. Aoudia, T. Al-Maamari, and F. Al-Salmi, “Intramolecular and intermolecular ion–dipole interactions in sodium lauryl ether sulfates (SLES) self-aggregation and mixed micellization with Triton X-100,” *Colloids Surf. Physicochem. Eng. Asp.*, vol. 335, no. 1, pp. 55–61, 2009, doi: 10.1016/j.colsurfa.2008.10.026.

[26] Y.-P. Zhu, M. J. Rosen, S. W. Morrall, and J. Tolls, “Surface properties of linear alkyl benzene sulfonates in hard river water,” *J. Surfactants Deterg.*, vol. 1, no. 2, pp. 187–193, 1998, doi: 10.1007/s11743-998-0018-2.

[27] M. T. García, E. Campos, M. Dalmau, I. Ribosa, and J. Sánchez-Leal, “Structure–activity relationships for association of linear alkylbenzene sulfonates with activated sludge,” *Chemosphere*, vol. 49, no. 3, pp. 279–286, 2002, doi: 10.1016/S0045-6535(02)00182-0.

[28] M. J. Rosen, “The relationship of structure to properties in surfactants. IV. Effectiveness in surface or interfacial tension reduction,” *J. Colloid Interface Sci.*, vol. 56, no. 2, pp. 320–327, 1976, doi: 10.1016/0021-9797(76)90257-5.

[29] M. J. Rosen, “Relationship of structure to properties in surfactants: II. Efficiency in surface or interfacial tension reduction,” *J. Am. Oil Chem. Soc.*, vol. 51, no. 10, pp. 461–465, 1974, doi: 10.1007/BF02635155.

[30] E. L. Correia, N. Brown, A. Ervin, D. V. Papavassiliou, and S. Razavi, “Contamination in Sodium Dodecyl Sulfate Solutions: Insights from the Measurements of Surface Tension and Surface Rheology,” *Langmuir*, vol. 38, no. 23, pp. 7179–7189, 2022, doi: 10.1021/acs.langmuir.2c00460.

[31] V. B. Fainerman, S. V. Lylyk, E. V. Aksenenko, J. T. Petkov, J. Yorke, and R. Miller, “Surface tension isotherms, adsorption dynamics and dilational visco-elasticity of sodium dodecyl sulphate solutions,” *Colloids Surf. Physicochem. Eng. Asp.*, vol. 354, no. 1, pp. 8–15, 2010, doi: 10.1016/j.colsurfa.2009.02.022.

[32] G. D. Miles and L. Shedlovsky, “Minima in Surface Tension–Concentration Curves of Solutions of Sodium Alcohol Sulfates.,” *J. Phys. Chem.*, vol. 48, no. 1, pp. 57–62, 1944, doi: 10.1021/j150433a007.

[33] D. Vollhardt and G. Czichocki, “Influence of small quantities of isomeric alcohols on the surface tension behavior of aqueous sodium alkyl sulfate solutions,” *Colloids Surf.*, vol. 11, no. 3, pp. 209–217, 1984, doi: 10.1016/0166-6622(84)80280-2.

[34] L.-J. Chen, S.-Y. Lin, C.-S. Chern, and S.-C. Wu, “Critical micelle concentration of mixed surfactant SDS/NP(EO)40 and its role in emulsion polymerization,” *Colloids Surf. Physicochem. Eng. Asp.*, vol. 122, no. 1, pp. 161–168, 1997, doi: 10.1016/S0927-7757(96)03851-4.

[35] P. A. Kralchevsky, K. D. Danov, V. L. Kolev, G. Broze, and A. Mehreteab, “Effect of Nonionic Admixtures on the Adsorption of Ionic Surfactants at Fluid Interfaces. 1. Sodium Dodecyl Sulfate and Dodecanol,” *Langmuir*, vol. 19, no. 12, pp. 5004–5018, 2003, doi: 10.1021/la0268496.

[36] D. Y. Kwok and A. W. Neumann, “Contact angle measurement and contact angle interpretation,” *Adv. Colloid Interface Sci.*, vol. 81, no. 3, pp. 167–249, 1999, doi: 10.1016/S0001-8686(98)00087-6.

[37] H. Tavana, G. Yang, C. M. Yip, D. Appelhans, S. Zschoche, K. Grundke, M. L. Hair, and A. W. Neumann, "Stick–Slip of the Three-Phase Line in Measurements of Dynamic Contact Angles," *Langmuir*, vol. 22, no. 2, pp. 628–636, 2006, doi: 10.1021/la051715o.

[38] B. Zuo, F. F. Zheng, Y. R. Zhao, T. Chen, Z. H. Yan, H. Ni, and X. Wang, "Stick–Slip Phenomenon in Measurements of Dynamic Contact Angles and Surface Viscoelasticity of Poly(styrene-b-isoprene-b-styrene) Triblock Copolymers," *Langmuir*, vol. 28, no. 9, pp. 4283–4292, 2012, doi: 10.1021/la300119n.

[39] J. P. Canselier, "The Effects of Surfactants on Crystallization Phenomena," *J. Dispers. Sci. Technol.*, vol. 14, no. 6, pp. 625–644, 1993, doi: 10.1080/01932699308943435.

[40] H. Füredi-Milhofer and S. Sarig, "Interactions between polyelectrolytes and sparingly soluble salts," *Prog. Cryst. Growth Charact. Mater.*, vol. 32, no. 1, pp. 45–74, 1996, doi: 10.1016/0960-8974(96)00006-X.

[41] A. S. Michaels and F. W. Tausch, "Modification and growth rate and habit of adipic acid crystals with surfactants," *J. Phys. Chem.*, vol. 65, no. 10, pp. 1730–1737, 1961, doi: 10.1021/j100827a014.

[42] N. Singh, R. Yeri, and J. Chakraborty, "Effect of Ionic Surfactants and Alcohols on the Morphology of CuSO4·5H2O Crystals: Combined Use of Factors and Significance of Threshold Surfactant Concentration," *Ind. Eng. Chem. Res.*, vol. 52, no. 43, pp. 15041–15048, 2013, doi: 10.1021/ie4024403.

[43] H. Wei, Q. Shen, Y. Zhao, D. Wang, and D. Xu, "Crystallization habit of calcium carbonate in the presence of sodium dodecyl sulfate and/or polypyrrolidone," *J. Cryst. Growth*, vol. 260, no. 3, pp. 511–516, 2004, doi: 10.1016/j.jcrysgro.2003.08.047.

[44] X. Wei, J. Yang, Z. Li, Y. Su, and D. Wang, "Comparison investigation of the effects of ionic surfactants on the crystallization behavior of calcium oxalate: From cationic to anionic surfactant," *Colloids Surf. Physicochem. Eng. Asp.*, vol. 401, pp. 107–115, 2012, doi: 10.1016/j.colsurfa.2012.03.034.

[45] F. Kuschel, An. König, and S. Herold, "Crystallization of potassium sulfate from pure aqueous solution and in presence of surfactants," *Cryst. Res. Technol.*, vol. 18, no. 4, pp. 427–434, 1983, doi: 10.1002/crat.2170180402.

[46] R. Ho, D. A. Wilson, and J. Y. Y. Heng, "Crystal Habits and the Variation in Surface Energy Heterogeneity," *Cryst. Growth Des.*, vol. 9, no. 11, pp. 4907–4911, 2009, doi: 10.1021/cg900696f.

[47] U. V. Shah, D. Olusanmi, A. S. Narang, M. A. Hussain, J. F. Gamble, M. J. Tobyn, and J. Y. Y. Heng, "Effect of crystal habits on the surface energy and cohesion of crystalline powders," *Int. J. Pharm.*, vol. 472, no. 1, pp. 140–147, 2014, doi: 10.1016/j.ijpharm.2014.06.014.

[48] S. Björklund and V. Kocherbitov, "Hydration-Induced Phase Transitions in Surfactant and Lipid Films," *Langmuir*, vol. 32, no. 21, pp. 5223–5232, 2016, doi: 10.1021/acs.langmuir.6b00452.

[49] N. A. Ivanova, N. S. Kubochkin, and V. M. Starov, "Wetting of hydrophobic substrates by pure surfactants at continuously increasing humidity," *Colloids Surf. Physicochem. Eng. Asp.*, vol. 519, pp. 71–77, 2017, doi: 10.1016/j.colsurfa.2016.07.096.

[50] S. Zhu, W. G. Miller, L. E. Scriven, and H. T. Davis, "Superspreading of water—silicone surfactant on hydrophobic surfaces," *Colloids Surf. Physicochem. Eng. Asp.*, vol. 90, no. 1, pp. 63–78, 1994, doi: 10.1016/0927-7757(94)02904-0.

[51] J. A. Barrie and B. Platt, "The diffusion and clustering of water vapour in polymers," *Polymer*, vol. 4, pp. 303–313, 1963, doi: 10.1016/0032-3861(63)90038-7.

[52] A. C. Noguer, S. M. Olsen, S. Hvilsted, and S. Kiil, "Diffusion of surface-active amphiphiles in silicone-based fouling-release coatings," *Prog. Org. Coat.*, vol. 106, pp. 77–86, 2017, doi: 10.1016/j.porgcoat.2017.02.014.

Appendices

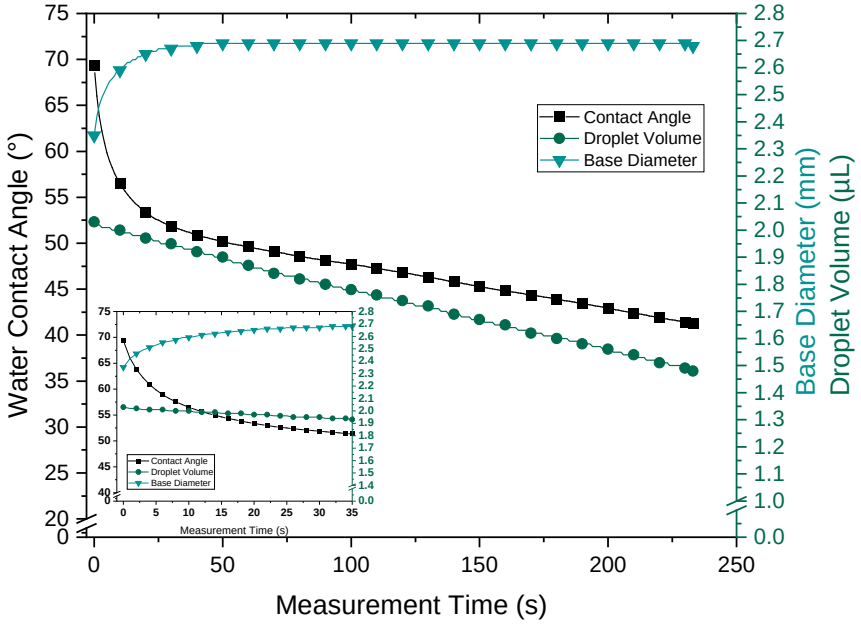


Figure A3.1. Evolution of the WCA, droplet volume and droplet base diameter on a PUF-BAS surface. For clarity, every 10th datapoint is shown. The inset shows the same properties from 0–35 s, where every 2nd datapoint is shown.

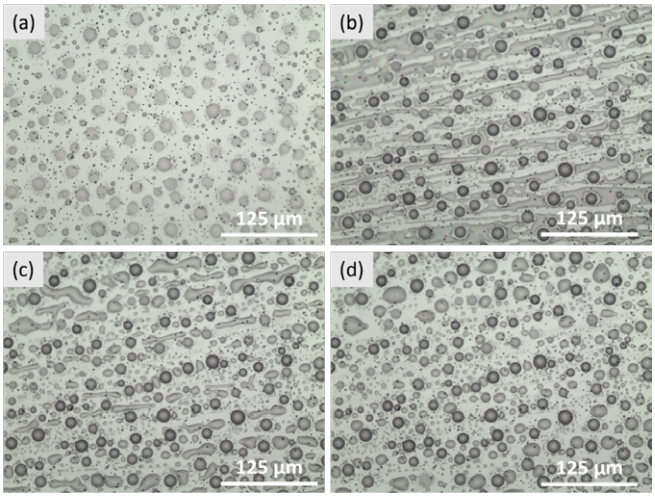


Figure A3.2. Optical micrographs of a PUF-EFA surface (a) before and (b)-(d) after wiping with a cotton swab. The dark, circular features are resin-covered air bubbles in the coating. After wiping the surface, it can be seen that residual EFA starts to form droplets on the coating surface.

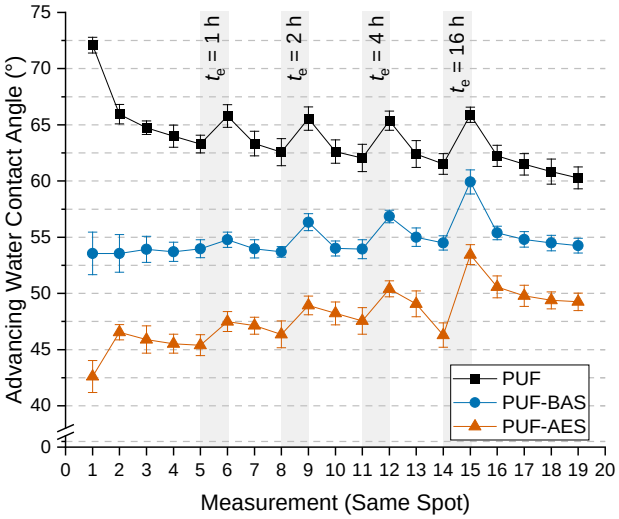


Figure A3.3. S-ACA results as a function of the number of measurements. Drying times (t_e), where the coatings were exposed to air under ambient room conditions in between measurements, are indicated in the graph.

Fitting Through ACA Data

A two-component exponential decay was used to fit the data ($R^2 > 0.99$) in order to estimate when the contact angle would become more or less become constant. The simulated curves in Figure A3.4 do not take into account any fit parameter errors, which are given below.

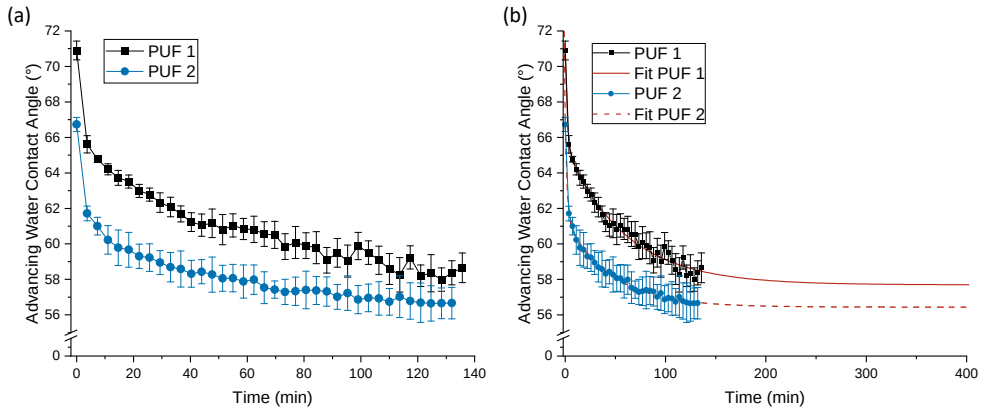


Figure A3.4. S-ACA values for two different PUF coatings (a) up to approximately 135 min without interrupting the measurements and (b) including a fit through the measured values to show the levelling off of the data. For the dataset given with the circles, the continuous measurements were performed after a series of measurements as described in the main text, which is the reason the starting point is lower compared to the other curve (squares).

For PUF 1, the best fit was found with:

$$y(x) = A_1 \cdot \exp\left(-\left(\frac{x-x_0}{t_1}\right)\right) + A_2 \cdot \exp\left(-\left(\frac{x-x_0}{t_2}\right)\right) + y_0\,, \tag{A3.1}$$

with A_1 = 5.82 °, t_1=1.74 ± 0.37 min, A_2 = 7.89 °, t_2 = 58.41 ± 5.68 min, x_0 = -0.15 min and y_0=57.69 ± 0.30 °. Adjusted R^2 was 0.991.

For PUF 2, the best fit was found with:

$$y(x) = A_1 \cdot \exp\left(-\frac{x}{t_1}\right) + A_2 \cdot \exp\left(-\frac{x}{t_2}\right) + y_0\,, \tag{A3.2}$$

with A_1 = 5.32 ± 0.16 °, t_1 = 1.86 ± 0.17 min, A_2 = 4.97 ± 0.11 °, t_2 = 44.89 ± 3.3 min and y_0 = 56.44 ± 0.11 °. Adjusted R^2 was 0.998.

A slightly different function was required for fitting the data of PUF 1 and PUF 2 due to the difference in starting point for the successive measurements. Furthermore, the fits are given for demonstration purposes only. Still, the plasticisation is expected to level off eventually, which the results seem to indicate.

Hysteresis as seen with Dynamic Vapour Sorption

Mass changes of cured PUF flakes exposed to varying relative humidity were monitored by dynamic vapour measurements (DVS) on a Surface Measurement System DVS Resolution. Approximately 2.7 mg of sample was subjected to a cycle of 0% RH → 90% RH → 0% RH, recording the mass changes over time. A d*m*/d*t* method was used, where the relative humidity was only changed either when the mass change was < 0.001 %/min for 30 minutes, or when the time the sample was exposed to the set RH exceeded 2400 minutes.

From the first cycle can be seen that moisture uptake is fast, with the strongest mass change occurring in the first 300 minutes. A stable mass reading was found after exposing the sample to 90% RH for approximately 900 minutes. The absorbed water was not fully lost within a similar time when the sample was at 0% RH, indicating that there is a hysteresis. For subsequent exposures to 90% RH, the total mass change was found to be both increasing and faster. Still, the reverse process was always slower.

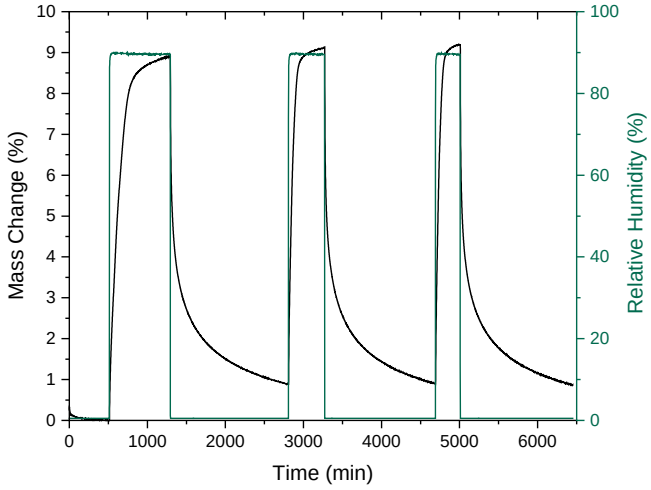


Figure A3.5. Mass change (in %) of cured PUF as a result of exposure to 0 or 90% relative humidity, as determined with DVS.

Spreading of Water Droplets on Coating Surfaces

Coatings of PUF-AES, PF-AES and PF-BAS exhibited a stick-and-slip behaviour during the first advancing contact angle measurement, as shown in Figure A3.6. After the first measurement, the stick and slip behaviour was not readily observed any more, even after exposing the surface to air and then continuing the successive dynamic contact angle measurements. This implies a change in lateral distribution of the wetting agent in the surface layers.

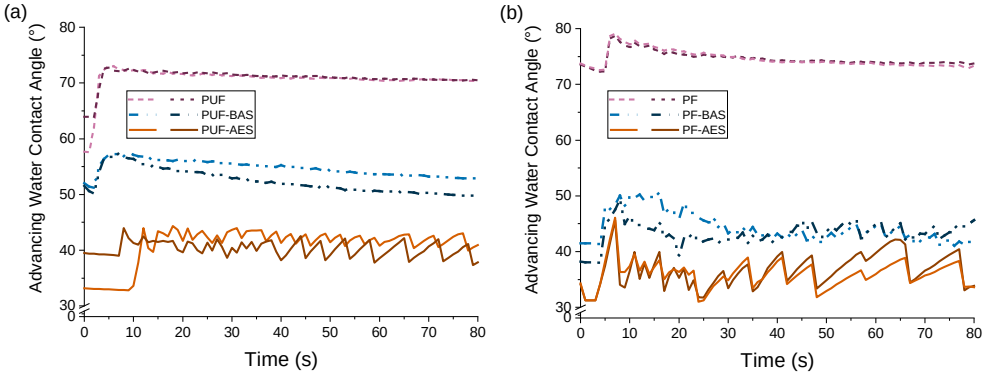


Figure A3.6. First ACA measurements on (a) PUF(-WA) and (b) PF(-WA) coating surfaces. Individual (i.e., either left of right) CA values are shown.

Additionally, PUF-BAS surfaces typically showed a decrease in ACA value over the course of the first dynamic wetting. This decrease varied in severity but was found to disappear with successive measurements. After exposing PUF-BAS coatings to air, this behaviour was seen again. This likely means that a slight reorientation of the branched alkylbenzene sulphonate occurred due to changes in the environment.

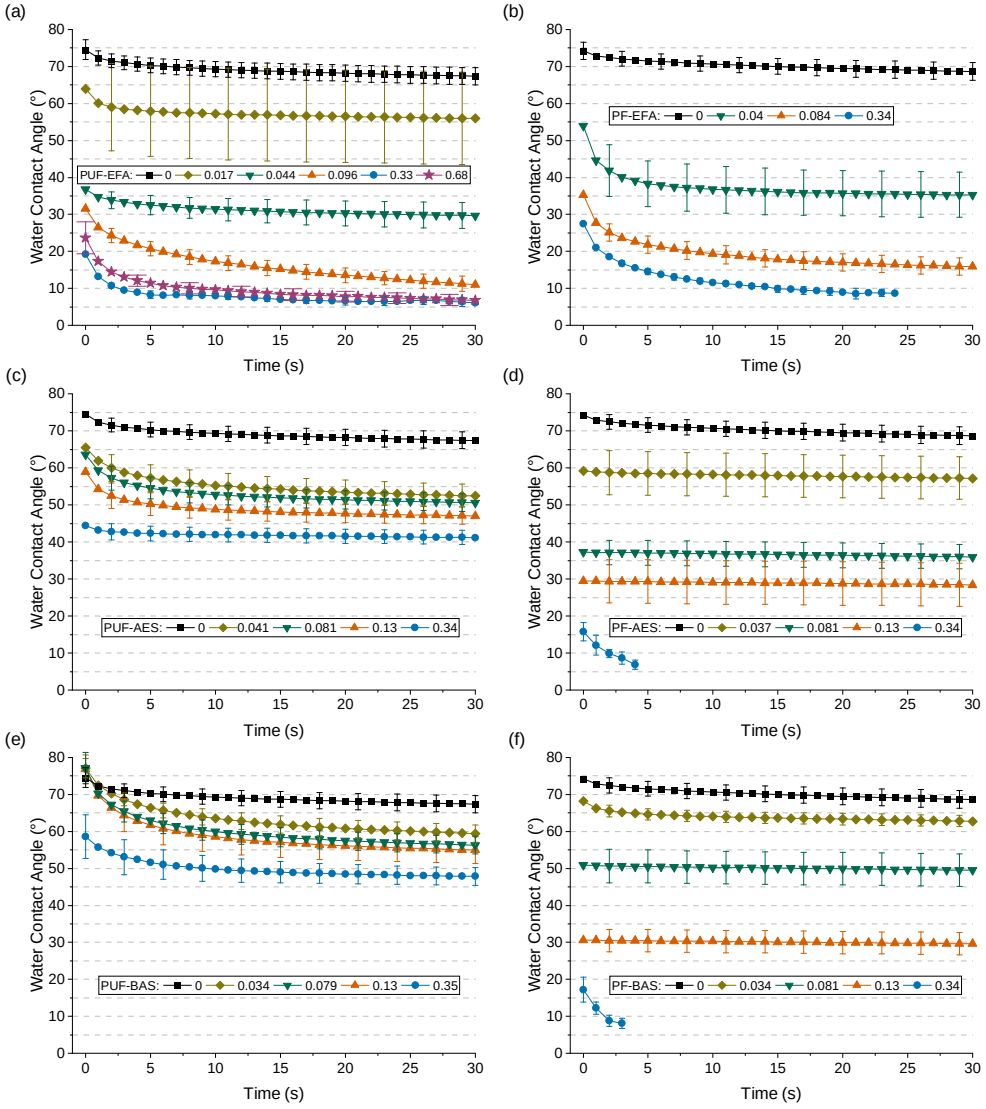


Figure A3.7. Average WCA values of coatings of (a) PUF-EFA, (b) PF-EFA, (c) PUF-AES, (d) PF-AES, (e) PUF-BAS, and (f) PF-BAS, using varying concentrations of WA. Concentrations of WA used are given as mg a.s. / (g S.C.).

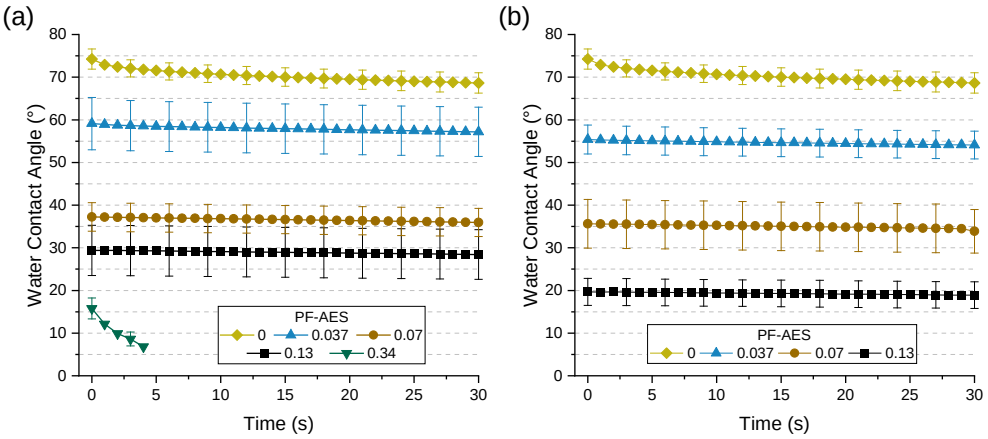


Figure A3.8. Average water contact angle values on PF-AES coatings. Concentration series were made using 2 different PF-AES batches, indicated by (a) and (b). Concentrations are given as mg a.s. / (g S.C.).

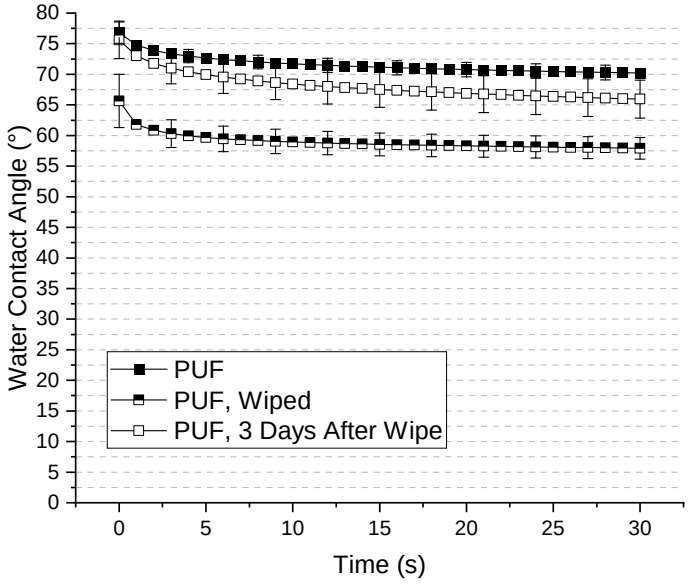


Figure A3.9. Average WCA values for PUF coatings directly before and after wiping with a wet and dry tissue, respectively.

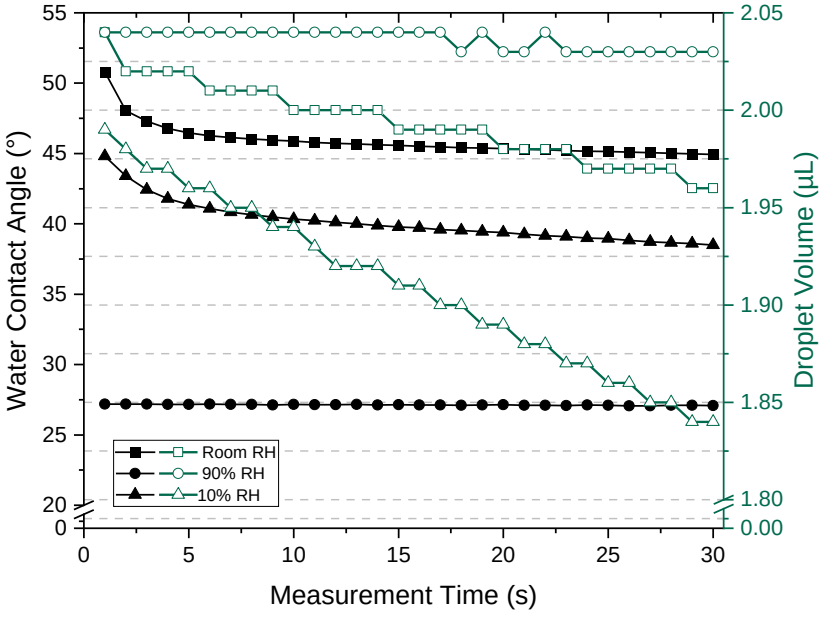


Figure A3.10. Example of the evolution of the water contact angle (closed symbols) and droplet volume (open symbols) on a PUF-AES surface, measuring at ambient conditions (Room RH; for the sample shown approximately 30% RH), or under controlled relative humidity of 90% or 10%.

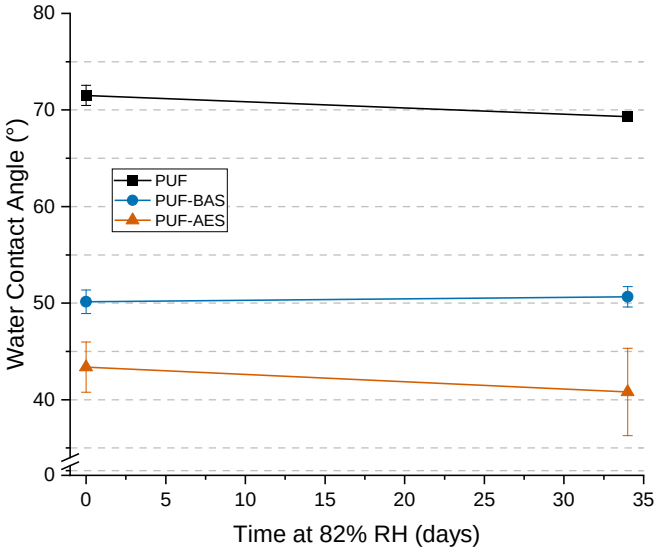


Figure A3.11. Average water contact angle values of PUF(-WA) coatings before and after storage at 82% RH for 34 days.

Spreading of Water Droplets on PDMS in Contact with PUF-WA Surfaces

As proposed by Shaikeea *et al*. [A1], by presenting the water contact angle value and the base diameter of the water droplet in a polar plot, information regarding the evaporation mode of a water droplet can be obtained. However, additionally, this also allows to easily verify whether a decrease in water contact angle value is due to evaporation or because of spreading.

In case of evaporation, either the water contact angle value remains constant whilst the base diameter decreases, or the base diameter remains constant whilst the water contact angle value becomes smaller [A1]. Data then follows either a circular arc or an arrested angle in the polar plot [A1]. In case of spreading, however, a simultaneous increase in base diameter and decrease in water contact angle value can be observed. A possible disadvantage of this representation of data is the lack of a time axis and hence the loss of information about the kinetics of the processes represented in the polar plot.

As shown in Figure A3.12, initially all droplets show some spreading behaviour. However, this corresponds to the first 10 seconds of the measurement and is therefore related to the rearrangements of PDMS at the surface. After this, only the water droplet on PDMS on the PUF-EFA coating shows signs of spreading, as for both the reference and PDMS on the PUF-BAS coating the datapoints only show a minor change at a constant base diameter.

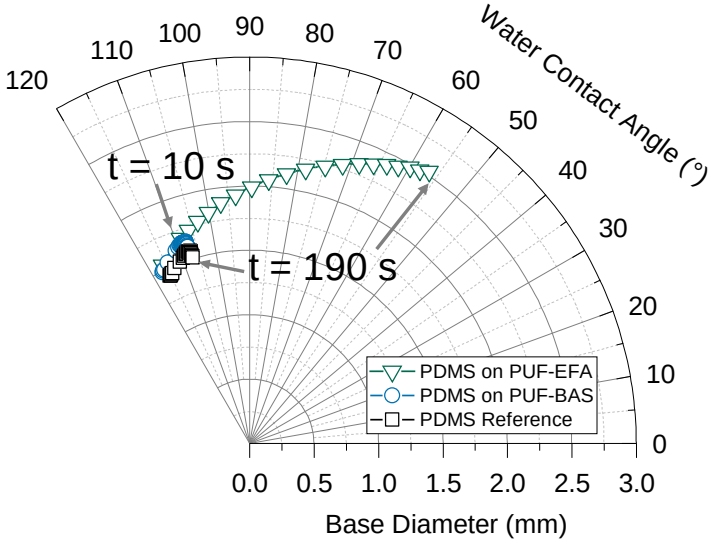


Figure A3.12. Changes in water contact angle value and droplet base diameter of a water droplet on a PDMS membrane in contact with a PUF-EFA or PUF-BAS coating.

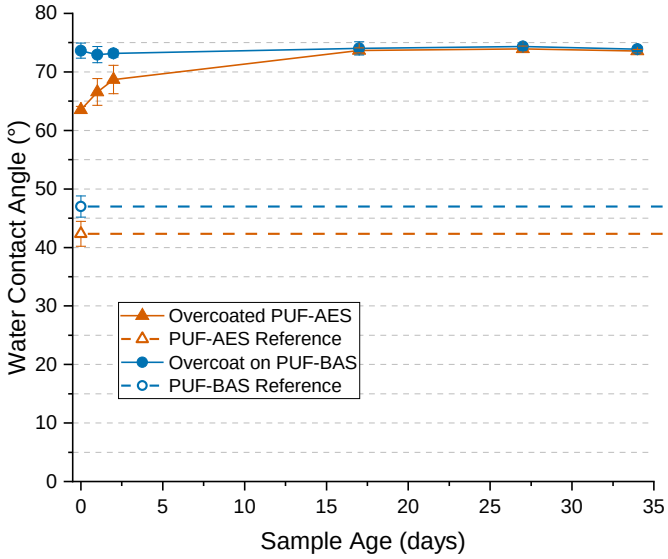


Figure A3.13. Average water contact angle values of an overcoated PUF-AES and an overcoated PUF-BAS surface over time. Coatings were stored at ambient conditions.

Table A3.1. Water contact angle values before and after dip coating PUF-WA coatings in water.

Sample	WCA Before Dip Coating in H_2O (°)	WCA After Dip Coating in H_2O (°)
PUF-AES	40.4° ± 0.6°	40.5° ± 0.7°
PUF-BAS	49.2° ± 0.1°	50.4° ± 1.5°
PUF-EFA	13.9° ± 2.6°	14.5° ± 3.4°

Table A3.2. Average coating thickness of PUF(-WA) coatings with and without a PUF overcoat as determined with contact profilometry (Bruker Dektak XT). Results are the average of 6 measurements, 2 of which were done at the upper half of the coating, 2 at approximately the middle, and 2 at the lower half.

Sample	Coating Thickness (µm)	
	Without Overcoat	With Overcoat
PUF	4.9 ± 1.5	8.8 ± 0.7
PUF-AES	4.2 ± 0.2	9.8 ± 0.6
PUF-BAS	4.1 ± 0.2	9.0 ± 1.7

References

[A1] A. J. D. Shaikeea, S. Basu, A. Tyagi, S. Sharma, R. Hans, and L. Bansal, “Universal representations of evaporation modes in sessile droplets,” PLOS ONE, vol. 12, no. 9, p. e0184997, 2017, doi: 10.1371/journal.pone.0184997.

4

Ageing Phenomena in Phenolic Resin Coatings

Abstract

Effects of physical and chemical ageing on the surface wettability of hydrophilic phenol-urea-formaldehyde (PUF) coatings were studied. All individual wetting agents (WAs) were thermally stable when exposed to common cure conditions and when subjected to accelerated ageing conditions of 70 °C and 75% RH. Ageing PUF coatings at 70 °C and 75% RH has shown that the surfaces undergo post-cure reactions, seen from both a change in surface chemistry and water contact angle value. PUF coatings containing anionic WAs which were stored at elevated temperatures showed a moderate increase in average water contact angle value. This change was attributed to chemical and physical changes in the PUF surface layers rather than degradation of the WAs. The substrate on which the coatings were applied was found to influence the degree of ageing at 70 °C and 75% RH of the surface wettability. When PUF-WA coatings were applied on soda lime glass, only a limited decrease in hydrophilicity was observed due to leaching of sodium hydroxide from the glass substrate. The presence of mobile sodium ions ensures mobility of the WAs upon ageing, allowing them to remain at the coating-air interface despite the surface rearrangements of PUF. However, ageing coatings at a lower relative humidity of 20% at the same temperature of 70 °C cannot prevent the loss of hydrophilicity, regardless of the substrate that is used. Addition of sodium methanesulphonate to the resin formulation reduces ageing even of coatings on glass substrates which are not prone to leaching of sodium hydroxide. These insights provide a basis to develop tools to extend the life and service time of hydrophilic phenolic resin coatings.

This chapter is based on L. Moone, I.A.C. van de Ven, M. Robben M.P.J. Donners, K. van Durme, D.V. Okhrimenko, R.A.T.M. van Benthem, R. Tuinier, and A.C.C. Esteves, Ageing phenomena in hydrophilic phenolic resin coatings, *in preparation*

4.1. Introduction

In an ideal world, a given coating lasts infinitely long without the loss of its properties. The gift and curse of reality is, however, that ideal cases are more often than not rarely true. Thus, functional coatings have a finite life and service time. A change in surface functionality is broadly referred to as ageing, and can be due to weathering from thermal, UV, moisture or chemical exposure, or because of wear and physical damage. Naturally, the effect of the exposure of a material to e.g. elevated temperatures depends on the chemistry of the material. Nevertheless, detailed studies have been done to try and establish descriptions on how weathering affects physical and chemical properties of coatings [1–5].

Physical ageing describes changes in material properties due to relaxation processes of a polymer or organic coating in its glassy state, in absence of a phase change or chemical reaction [6]. Such changes are reversible, as opposed to those due to chemical ageing [7–9]. Physical ageing phenomena in both thermoplastics and thermosets have been studied extensively over the years, with an increasing focus on organic coatings [7,10–18]. External factors like temperature and relative humidity (RH) are known to affect physical ageing processes [8,19]. For instance, epoxy coatings held at 0% RH developed tensile stresses over time, whereas coatings stored at 52% and 97% RH showed compressive stresses building up [19]. For a carboxylic acid functional polyester–triglycidyl isocyanurate powder coating, Perera [8] found that the higher the RH, the higher the rate of initial physical ageing is, but the smaller the final effect is. This was attributed to water plasticisation effects for polymeric materials, resulting in a decrease in the glass transition temperature. Physical ageing as a consequence of relaxation of polymers has been observed for phenol-formaldehyde novolac cured epoxy resins, where the relaxation behaviour is dependent on the crosslink density [20]. As these cured resins were found to increasingly absorb water with increasing crosslink density, it can be argued that humidity will therefore also affect the relaxation times of these resins.

Chemical ageing relates to irreversible changes as a result of, for instance, post-cure reactions, accelerated by elevated thermal conditions, UV radiation, or exposure to water [18]. As a result, chain scission or further crosslinking can occur, inevitably affecting the chemistry of the coating and its surface [12,17,21,22]. The occurrence of multiple phenomena at the same time can make ageing complex to understand on account of all the ongoing processes and the multitude of factors that contribute to them. As an example, for thermosets chemical ageing can lead to physical ageing, i.e., post-curing reactions can induce stress inside a coating [23].

The thermal stability and ageing of phenolic resin coatings and foams has been studied previously [24–29]. Even at moderate conditions (20 °C and ambient relative humidity of 40%), phenolic resin coatings age slightly [27]. Most notably, there is evidence of post-cure reactions occurring, even in the glassy state [27,28], and as a result the total

surface energy of these coatings decreases [27], which would make the surface more hydrophobic. Okhrimenko *et al*. [29] studied the hydrothermal (liquid water) and hygrothermal (water vapour) stability of cured PUF binders by accelerated ageing of stone wool fibres coated with PUF in a water bath at 80 °C for 3 h, or in a climate-controlled chamber at 70 °C and 91% RH for 7 days. A strong influence of curing time on the hydrolytic stability of the linkages between formaldehyde and methylolated urea species was found. Furthermore, a decrease in the urea content was observed, indicating limited thermal stability relative to the phenolic moieties in the polymer network [29]. In case of hydrophilic phenolic resin coatings, there is an additional consideration *a priori* ageing, namely the relative thermal stability of the wetting agents (WAs) in the resin formulation. Common industrial curing procedures for phenolic resins are at temperatures above 180 °C [30]. Therefore, WAs have to be thermally stable so that they can withstand curing conditions [31] and enable hydrophilic surfaces.

Most of the ageing phenomena of coatings as described above do not explicitly consider the substrate on which the coating is applied. Even before ageing, substrates can strongly influence the distribution of additives in a coating (see also the introduction of Chapter 3) [32,33]. Evanson and Urban [33] studied the influence of the surface energy of substrates on the mobility of surfactants in synthetic acrylic latex copolymers. For this, poly(tetrafluoroethylene) (PTFE) and glass-like substrates were used. It was found that the low surface energy of the PTFE substrates brought forth an enrichment of surfactants at the substrate–coating interface, while on the glass-like material almost no enrichment was observed at this interface. The authors postulate that the resin does not readily wet the PTFE substrate due to the low surface energy of the substrate, and hence surfactants are required to decrease the interfacial tension between the resin and PTFE [33]. Continued migration of surfactants in latexes over time is also known to occur, where the nature of the substrate also influences the degree of enrichment at the coating–substrate interface [34].

In most cases, the substrate is regarded as passive or inert: it has a certain surface energy which only affects the initial additive distribution during film formation. Yet, some substrates can be regarded as ‘active’ over time. When a coating is applied on a complex glass such as soda lime (SL), aluminosilicate, or borosilicate glass, leachables from the glass network can end up in the coating. This contrasts with fused quartz glass (QZ). The major difference between complex silicates and fused quartz is the presence of network modifiers in case of the former, and the absence of such cations in case of the latter (Figure 4.1).

When a complex silicate is in contact with aqueous solutions, three processes can occur [35]: hydration, hydrolysis, and ion exchange and migration. Hydration refers to the case where water penetrates the glass as an intact species [35]. Hydrolysis, facilitated by hydration of the glass, occurs when water reacts with Si-O-Si bonds,

thereby yielding silanol groups. For ion exchange, cations present in the glassy network leach into the solution upon substitution for protons from the solvent (e.g., hydroxonium ions) [36–38], leading to what is also known as glass corrosion. Hydrolysis and ion exchange are both dependent on the composition of the glass and pH of the solution with which the glass is in contact. While corrosion of glass is commonly studied at acidic conditions (e.g., using hydrochloric or nitric acid) [39–41], in general glass corrosion through dissolution of the silicate network is more significant below a pH above 9, whilst alkali leaching occurs mostly below pH 9 [35,42,43].

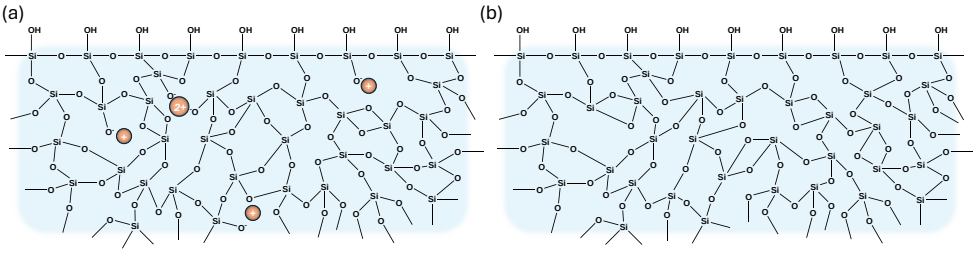


Figure 4.1. Schematic representation of the surface of (a) a complex silicate and (b) fused quartz glass. Mono- and divalent cations (orange spheres) are present at interstitial sites where there are non-bridging oxygen atoms.

Corrosion of glass is also strongly dependent on other factors besides acidity, such as the glass composition, temperature, and relative humidity of the environment [44–50]. Abrajano *et al.* [44,45] studied how humidity affects the corrosion of silicates. Boro- and aluminosilicates were aged under severe conditions: 202 °C and 95–100% RH. Still, it was found that there exists a critical relative humidity above which hydration and subsequent dealkalinisation of the surface effectively occurs. Comparing the hydration layer thickness of glasses of the same composition in contact with either saturated water vapour (relative humidity 100%) or liquid water showed that the hydration layer of the latter was almost 4 times higher than that of the former. Similar glasses exposed to 47 and 58% RH did not show any appreciable difference in hydration rate or hydration layer [44]. Laso *et al.* [50] showed a clear difference in both the species and amount that leaches when glasses of different composition (soda lime, potash, or mixed alkali silicate glass) were exposed to 30, 70, or 100% RH. In all cases, glass corrosion was more pronounced with increasing RH [50].

The actual rate-limiting step and corresponding mechanism for leaching of cations as a result of ion exchange reactions has been a point of debate for some time [36,51,52]. Leaching due to ion exchange between sodium ions and hydroxonium ions has been proposed to proceed according to:



(1)

On the other hand, it has also been observed that when water molecules react with non-bridging oxygen atoms, sodium ions are no longer bound to the glassy network and leach to form an alkali depletion layer [35,36,44,53,54] according to:



(2)

The leaching of sodium ions in this case is accompanied by the release of hydroxide ions. This has also been shown with relatively recent reactive molecular dynamics simulations [55,56], where contact of a simulated glass with water results in a decrease in the concentration of non-bridging oxygen content and an increase in hydroxyl ion concentration within the surface layers of the substrate.

The ion exchange and subsequent migration as discussed above is only valid for complex silicates on account of the presence of network modifiers. In case of fused quartz glass, no ion exchange can occur because of a lack of alkali-ions. Hence, even when in contact with water for prolonged times at elevated temperatures, no leaching of sodium ions from fused quartz glass will be observed [57].

Although the fundamental question of the exact rate-limiting step of glass corrosion remains discussable, it is important to note that, whichever true, both scenarios lead to the loss of sodium ions from the glass. For applications such as hydrophilic stone wool for hydroponic purposes, this is an important consideration as here the phenolic resin coats fibres made from natural rocks such as volcanic basalt glass [58]. From a product performance point of view, it is crucial to understand the potential impact of leached ions on the wettability of the coating.

The ageing phenomena that might occur in hydrophilic phenolic resin coatings are studied in this Chapter. Both cure conditions and long hygrothermal exposure are used to gauge if significant changes occur to WAs and phenolic resin coatings. Additionally, the ageing study explicitly involves different glass substrates to determine the influence of leachables from the substrate on the possible ageing phenomena.

4.2. Experimental Procedures

Materials

Methyl red (MR; ACS grade), triethylamine (TEA; > 99.5%), urea (U; ≥ 99%), and phenol (P; > 99%) were obtained from Sigma-Aldrich. Formaldehyde (F) 37 wt% solution in water (including 10-15% methanol stabiliser) and sodium methanesulphonate (NaMeS; ≥ 98%) were purchased from ThermoScientific. Ethoxylated fatty acid (EFA), branched alkylbenzenesulphonate (BAS; active substance (a.s.) 25 wt% in water), and alkyl ethoxylated sulphate (AES; active substance 27 wt% in water) were kindly

supplied by ROCKWOOL A/S. Before use phenol was stored at room temperature under Ar atmosphere and with P_2O_5 in a desiccator. All other chemicals were used as received.

Silicon wafers (Si-W) were single sided polished and purchased from Siegert Wafers. Soda lime glass (SL) microscopy slides were obtained from Merck (Epredia™ Superfrost™) and the fused quartz (QZ) substrates were purchased from ThermoScientific. Stone melt wafers (SMW) were kindly supplied by ROCKWOOL A/S, and mechanically polished and cut into 1 x 1 cm substrates.

Resin Synthesis and Binder Preparation

PUF-TEA and PF-TEA were synthesised as described in Chapter 2, and will henceforth be called PUF and PF. Commercial PUF-KOH resin was used to prepare coatings with and without wetting agents.

PUF resin with dye (PUF-MR) was prepared by addition of methyl red (MR; 16 mg / 25 g resin) and using a vortex mixer until the dye was dissolved. PUF-MR coatings were applied on both soda lime glass and fused quartz glass. Coatings of PUF, PUF-AES, and PUF-BAS were applied on soda lime glass, fused quartz glass, Si wafers, and stone melt wafers. EFA was not considered for these experiments, on account of its demixing upon curing.

PUF-WA-NaMeS coatings were prepared by addition of a molar excess of NaMeS relative to AES and BAS ($n_{NaMeS} = 5 \cdot n_{WA}$). For PUF-AES, this amounted to 0.0176 g NaMeS / g PUF and for PUF-BAS, this amounted to 0.0191 g NaMeS / g PUF.

Silicon wafers were cut to a similar size as the soda lime glass microscopy slides. Prior to coating application, the fused quartz and silicon wafers were stored in isopropyl alcohol at room temperature for at least 1 day. Substrates were cleaned by wiping with lint-free paper and subsequently blowing the surface with air. To enable facile dip coating of the stone melt wafers, they were first adhered to piece of Si wafer using PUF resin which was subsequently cured for 20 minutes. Then, the surface of the stone melt wafers were cleaned with acetone and ethanol, consecutively, before dip coating.

After dip coating using a withdrawal speed of 100 mm/min, all coatings were cured in a semi-closed chamber at 150 °C for 20 minutes under an N_2 flow of approximately 150 L/h at 1 bar.

Thermal Studies of Wetting Agents

Hygrothermal ageing of wetting agents was performed by placing vials with approximately 4 g of WA in a desiccator with a saturated NaCl solution in an oven at 70 °C. Samples were aged for up to 28 days, after which they were dried in a desiccator with P_2O_5 for 3 days. The WA structure after ageing was studied with attenuated total reflection infra-red (ATR-FTIR) and ^{1}H-nuclear magnetic resonance (NMR)

spectroscopy. To determine the critical micelle concentration (CMC) of the aged wetting agents, after drying, they were redissolved in MilliQ water to restore the original active substance.

For experiments where WAs were exposed to temperatures commonly used for curing phenolic resins, 8 mL of WA was added to a 200 mL flask. Samples were then placed in an oven at 200 °C for 10 and 30 minutes. Finally, wetting agent structure and performance was studied with ATR-FTIR and ^{1}H-NMR, and surface tension (SFT) measurements, respectively. In case of BAS and AES, some samples were frozen in liquid nitrogen and subsequently dried using a Christ Alpha 1-4 LDplus freeze-drier at approximately -50 °C and 0.15 mbar for at least 48 hours.

The procedure for the ATR-FTIR, ^{1}H-NMR, and SFT measurements is described in Chapters 2 and 3.

Hygrothermal Ageing of PUF Coatings

For all ageing procedures, coatings were stored in a desiccator containing a saturated NaCl or LiCl solution, providing an environment with a theoretical relative humidity of approximately 75% and 11% RH, respectively [59]. Relative humidity and temperature of samples was recorded over the course of the experiment with an Ebro EBI 20-TH1 logger (see Figure A4.1). The accuracy of the loggers was ± 0.8 °C and ± 3% RH.

Before the start of the hygrothermal ageing experiments of PUF coatings, the average WCA value of coatings without WAs was determined from two measurements on two different spots per coating. For PUF-BAS and PUF-AES coatings, 1 measurement per coating was performed. The average of all measurements was used as the average WCA value before ageing, i.e., day 0. After performing the reference WCA measurements, coatings were aged at 75% RH and room temperature or 70 °C. Coatings were taken out of the desiccator after a set amount of time, and subsequently 7–9 WCA measurements were performed to determine the average WCA value and standard deviation after ageing. The measurements performed on individual coatings were used to determine the change in hydrophilicity (ΔWCA) of each specific coating as a result of the ageing (i.e., on individual basis):

$$\Delta WCA = WCA_n^{t=i} - WCA_n^{t=0} \quad , \tag{4.1}$$

where $WCA_n^{t=0}$ indicates the WCA value of coating n before ageing ($t=0$), and $WCA_n^{t=i}$ the WCA value of that same coating n after ageing for i days ($t=i$).

For the ageing of PUF-MR coatings two desiccators were used, with a saturated NaCl solution to keep the inside at 75% RH. One of these desiccators was placed in an oven at 70 °C whilst the other was kept at 20 °C ± 0.5 °C (room temperature). For ageing of

PUF(-WA) coatings on different glass substrates, only ageing at 70 °C was done, either exposing samples to 75% RH or 20% RH.

Salt-Doped Coating Preparation

Salt-doped PUF(-WA) coatings were prepared by addition of 0.0248 g K_2SO_4 / g PUF resin and stirring the solutions until the salt was completely dissolved. The resin was applied by means of dipcoating on glass substrate and cured in either an oven or semi-closed chambers as described in Chapter 2.

For each coating, several droplets of water (each approximately 2 µL) were placed on the surface and evaporated in air under ambient conditions. This way, both the crystals that dissolved and were redistributed by the presence and evaporation of water, as well as the crystals in surface layers, could be monitored over the course of the experiment.

Thermogravimetric Analyses

Thermogravimetric analyses (TGA) were performed on a TA Instruments Discovery TGA 550. PUF resins were measured under N_2, and WAs were measured under both N_2 and air. In case of BAS and AES, samples were first held at 120 °C for 60 minutes to evaporate water. The first mass recorded after this isotherm was set to 100% of the sample weight. Subsequently, sample mass changes were recorded when heating at a rate of 10 °C/min to 700 °C.

UV-Vis Spectrophotometry

UV-Vis measurements on liquid samples were performed on a Shimadzu UV 2700 spectrophotometer. For the PUF-MR coatings, UV-Vis measurements were done on a Perkin Elmer Lambda 750 UV/Vis/NIR spectrophotometer. Depending on the coating substrate, either soda lime or quartz glass was used as the baseline.

Water Contact Angle Measurements

Water contact angle (WCA) measurements were performed as described in Chapter 2. The reported results are, in general, the average of at least three measurements per coating, on at least two coatings per formulation, including the standard deviation. Due to the small size, typically only two measurements per coating on the stone melt wafers was performed.

X-Ray Photoelectron Spectroscopy

Coating and substrate composition was determined with X-ray photoelectron spectroscopy (XPS), for which the measurements were largely performed as described in Chapter 2. For measurements on uncoated soda lime glass, quartz glass and stone

melt wafers, the number of detailed scans was set to 50, and a pass energy of 50 eV and a step size of 0.1 eV was used, measuring the C 1s ($E_b^{C,1s}$ = 284.8 eV), Na 1s ($E_b^{Na,1s}$ = 471.4 eV), O 1s ($E_b^{O,1s}$ = 532 eV), Si 2p ($E_b^{Si,2p}$ = 100.0 eV), Al 2p ($E_b^{Al,2p}$ = 72.9 eV), Ca 2p ($E_b^{Ca,2p}$ = 345.9 eV), Fe 2p ($E_b^{Fe,2p}$ = 706.9 eV), Mg 1s ($E_b^{Mg,1s}$ = 1303.1 eV) and K 2p ($E_b^{K,2p}$ = 293 eV) binding energy spectra. For measurements on coatings, 30 scans with a pass energy of 50 eV and a step size of 0.1 eV were made to record the binding energy spectrum of C 1s, N 1s ($E_b^{N,1s}$ = 399 eV), O 1s, and Na 1s. All binding energy spectra were recorded with the ThermoFisher Scientific Avantage software and subsequently analysed with CasaXPS. A Shirley background and relative sensitivity factors (RSF) for each element ($RSF_{C,1s}$ = 1, $RSF_{O,1s}$ = 2.881, $RSF_{N,1s}$ = 1.676, $RSF_{Al,2p}$ = 0.56, $RSF_{Ca,2p}$= 5.970, $RSF_{Mg,1s}$ = 14.941, $RSF_{Na,1s}$= 10.588, $RSF_{Si,2p}$ = 0.9, $RSF_{K,2p}$ = 4.671, $RSF_{Fe,2p}$ = 14.35) were used to obtain relative atomic percentages. Reported values are the average of at least two measurements, each performed on a different location of the sample. Reported errors are the corresponding standard deviation based on at least two measurements.

Dynamic Vapour Sorption

Mass changes of PUF and PF powders exposed to different relative humidity values at 25 °C were measured on a Surface Measurement Systems DVS Revolution II. Prior to each measurement, samples were stored in a desiccator with P_2O_5. Measurements consisted of a drying step at 0% RH for at least 60 minutes, after which the RH was increased to 75%. Measurements were stopped when the change in mass was more or less negligible (i.e., when mass changes were smaller than 0.001%).

Free standing PF films were prepared by adding a small quantity of resin to an aluminium cup, and subsequently curing the resin in the semi-closed chamber at 150 °C for 20 minutes under N_2. The hardened resin was then separated from the cup, and was cut to size (approximately 5 mm diameter). Free standing PUF films were prepared by smearing a thin layer of PUF resin on an aluminium Q-panel and curing under similar conditions as described above. Flakes of PUF were obtained by bending the coated plate after curing. The resulting films were then used for the determination of the water diffusion coefficient by clamping them in a Payne cell.

Crank and Park [60] derived, for a plane sheet, that the ratio of sorption for a single side at time *t* to sorption at equilibrium is[1]

$$\frac{M_t}{M_\infty} = 2\sqrt{\frac{Dt}{\pi d^2}} \quad , \tag{4.2}$$

[1]In the book 'Diffusion in Polymers' [60], 'π' has been misplaced in the printed equation in Chapter 5: *The Glassy State and Slow Process Anomalies*. The correct equation is given in Chapter 1: *Methods of Measurement* as Equation 36, as well as in [61].

where M_t is the amount of vapour adsorbed at time t, M_∞ the amount of vapour adsorbed at equilibrium, D the diffusion coefficient, d the film thickness and t the time.

Using Equation 4.2, the diffusion coefficient can be determined when considering the slope of the plot of $\frac{M_t}{M_\infty}$ versus $\frac{\sqrt{t}}{d}$, taking into account that for the Payne cell setup a humidity gradient was used (meaning that the experiment was single-sided, e.g., only sorption from one face of the film):

$$D = \left(\frac{\Delta\left(\frac{M_t}{M_\infty}\right)}{\Delta\left(\frac{\sqrt{t}}{d}\right)} \right)^2 \cdot \frac{\pi}{4} \quad . \tag{4.3}$$

Typically, the fit for the slope is only considered valid for the first stage of diffusion, up to $\frac{M_t}{M_\infty} = 0.5$ [61]. Reported results were obtained over the range $0.1 \leq \frac{M_t}{M_\infty} \leq 0.4$, with $R^2 = 0.990$.

The flux of vapour J through a film can be defined with Fick's law of diffusion [62]

$$J = \frac{1}{A} \cdot \frac{\mathrm{d}m}{\mathrm{d}t} \quad , \tag{4.4}$$

where A is the area of the film and $\frac{\mathrm{d}m}{\mathrm{d}t}$ the mass change over time, which can be determined from sorption data as measured with DVS.

The flux through a film can also be defined when there is a pressure difference Δp across the film [60], which in turn is related to the relative humidity:

$$J = \frac{P\Delta p}{d} = \frac{P\,(p_0 RH_{75} - p_0 RH_0)}{d \cdot 100} = \frac{P \cdot p_0 RH_{75}}{d \cdot 100} \, , \tag{4.5}$$

with P the permeability, p_0 the pressure at 100 % RH, RH_{75} the relative humidity of 75% and d the film thickness.

Hence, relating Equations 4.5 and 4.6, the permeability can be calculated by

$$P = \frac{d \cdot 100}{p_0 RH_{75}} \cdot \frac{1}{A} \cdot \frac{\mathrm{d}m}{\mathrm{d}t} \quad . \tag{4.6}$$

Last, the permeability and the diffusion coefficient are linked via the solubility S by the relation [60]:

$$S = \frac{P}{D} \, . \tag{4.7}$$

Surface Tension Measurements

Surface tension (SFT) measurements were performed according to the method in Chapter 3, and results supplemented by the calculation of the adsorbed amount:

$$\Gamma_{max} = -\frac{1}{RT} \cdot \frac{d\gamma}{d\ln(c)}, \tag{4.8}$$

where R is the gas constant, T the temperature of the solution, γ the surface tension and c the concentration of WA.

4.3. Results and Discussion

Hygrothermal Stability of Wetting Agents

Thermal stability of WAs was evaluated by TGA in both air and N_2, and additional experiments were done by keeping samples of WA at temperatures similar to common curing temperatures of phenolic resins (200 °C). A detailed description of the results can be found in the Appendix of this Chapter, but the most important observation was that there was no convincing indication of degradation occurring for WAs exposed to temperatures below 200 °C.

To study long-term stability of WAs, samples were hygrothermally aged by exposing them to 70 °C and 75% relative humidity for up to 28 days. For this, WAs were used as received, i.e., AES and BAS were solutions in water. Physical changes occurred to some of the WAs over the course of the ageing procedure (Figure 4.2). Most notably, AES and BAS became more solid-like upon ageing due to the loss of water. After 1 day of ageing, AES in fact had already become a gel, after which it turned into a white paste. Eventually, after 28 days a gel had once again formed. The morphology of AES with varying degrees of ethoxylation is known to undergo several changes depending on the relative amount of water [63–65]. Similar observations have been made for BAS, of which the phase behaviour is affected by both the counterion and amount of water [66].

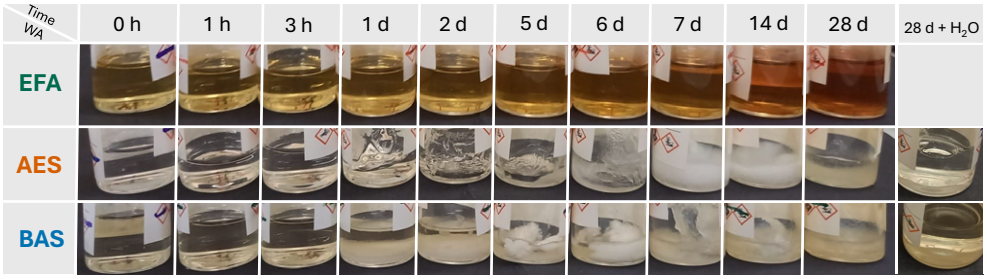


Figure 4.2. Visible physical changes of WAs after exposure to 70 °C and 75% RH. After 28 days of ageing, addition of water to BAS and AES resulted in a physical state similar to that of unaged WA.

Examination of the ATR-FTIR and ^{1}H-NMR spectra of the WAs shows no significant discernible differences (Figure 4.3). However, intermittent analyses indicated variations in samples of AES aged for 14 and 28 days (Figure A4.6). Since no chemical changes were seen in the corresponding ^{1}H-NMR spectra, these differences are likely a result of the variations in the structural ordering of AES [67,68].

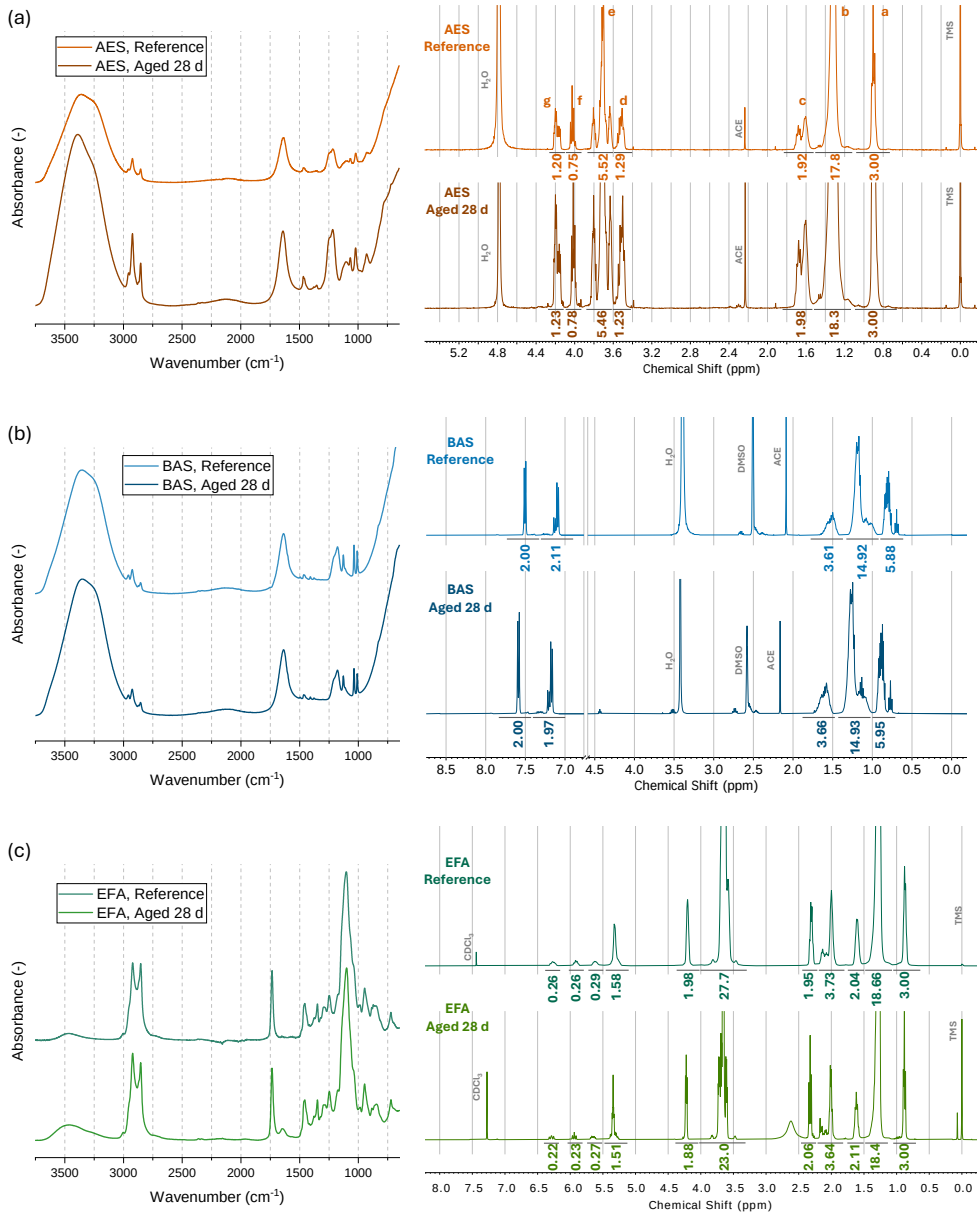


Figure 4.3. ATR-FTIR and ^{1}H-NMR spectra of (a) AES, (b) BAS, and (c) EFA before and after ageing at 75% RH and 70 °C for 28 days.

EFA, comprised of ethoxylated linoleic acid, turned to a darker orange colour upon ageing. It has been reported previously that heating oleic acid will result in the darkening of the oleic acid [69–72]. This is a result of oxidation which is enhanced by the presence of minor constituents (e.g., $C_{46}H_{76}O_{13}$ and $C_{24}H_{41}O_7$) [71].

Depending on the type of minor constituent, the colour stability of oleic acid is already severely affected for concentrations of as low as < 1.0% [70]. The ATR-FTIR spectra of EFA in Figure 4.3c show the emergence of a peak 1648 cm^{-1} upon ageing. On one hand, this could correspond to the C=C stretch of conjugated double bonds, which would make sense given the colour change and oxidation of EFA. On the other hand, an increase in the signal at 3462 cm^{-1} is observed, which together with the increase at 1648 cm^{-1} suggests the presence of water. Drying aged EFA samples in a desiccator with P_2O_5 shows that the removal of water results in a decrease in both signals. The reverse was also observed; an increase in sample mass was detected only for EFA upon ageing, implying the uptake of moisture (Figure A4.7). Conversely, a mass loss for BAS and AES was measured due to the evaporation of water from their solutions. Last, it should be noted that the ^{1}H-NMR spectra of aged EFA also shows the presence of water through the broad signal observed at 2.6 ppm. Overall, although physical changes of EFA were noticeable, the chemical changes were minor.

Despite there being differences between the CMC of the unaged and aged WAs, and hence some variation in their efficiency, the effectiveness as evaluated by the surface pressure was more or less the same (Figure 4.4 and Table 4.1). The strongest change for the anionic WAs was for their maximum adsorbed amount at the water–air interface, where typically an increase was seen. Despite this, the WAs used in this study are quite stable at the chosen accelerated ageing conditions.

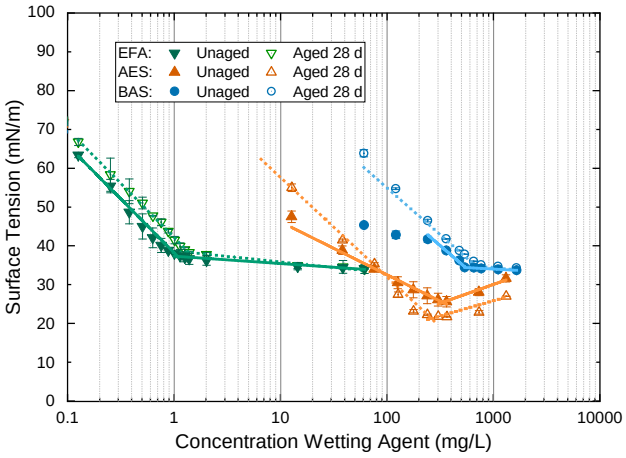


Figure 4.4. Surface tension values of WAs in water at 20 °C as a function of the WA concentration before (filled symbols) and after (open symbols) ageing at 70 °C and 75% RH for 28 days. Lines represent linear fits which were used to determine the critical micelle concentration.

Table 4.1. Overview of the CMC, surface pressure at the CMC, and the adsorbed amount of wetting agents at 20 °C before and after ageing the wetting agents at 70 °C and 75% RH.

Wetting Agent	Time (days)	CMC (mg/L)	π_{CMC} (mN/m)	$\Gamma_{max} \cdot 10^{10}$ (mol/cm^2)
EFA	0	1.1	35.3	5.1
	28	1.39	34.4	4.9
AES	0	332	47.5	1.3
	28	243	51.0	2.5
BAS	0	634	37.6	1.0
	28	682	37.8	2.4

Hygrothermal Ageing of Phenolic Resin Coatings

With the obtained understanding of the stability of the WAs under hygrothermal conditions, the foundation for subsequent ageing experiment has been laid. Therefore, the extent of ageing of phenolic resin coatings was studied next.

Thermogravimetric measurements of cured PUF-KOH, PUF, and PF resins are shown in Figure 4.5. PUF-KOH and PUF which were cured at 200 °C show a similar degradation profile, which matches with data from literature [29,73]. However, for the PUF powder cured at 150 °C a slightly stronger mass loss up to 350 °C was seen. Because the final mass change at 600 °C is similar independent of the curing temperature (T_c), the initial difference in mass loss is likely the result of post-curing reactions through which for instance formaldehyde and water are liberated.

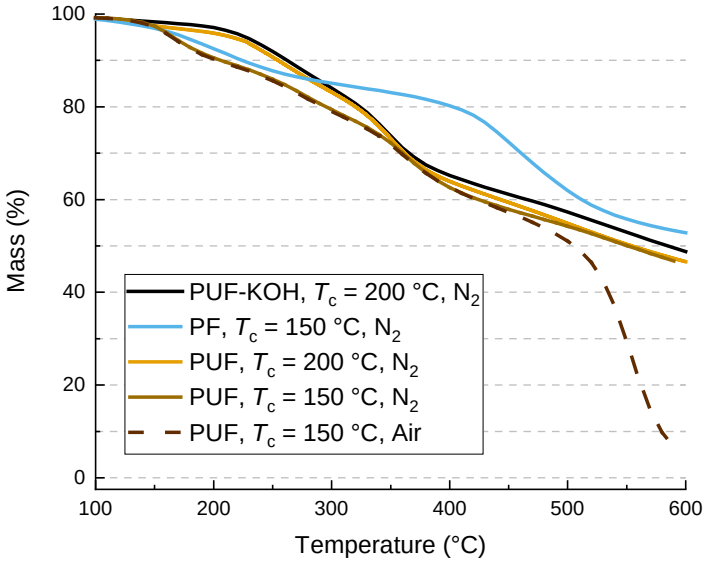


Figure 4.5. Mass change of PUF-KOH, PUF, and PF powders as function of temperature (purge gas is mentioned in legend). Resins were cured at either T_c = 150 °C or T_c = 200 °C.

Although TGA reveals a decent thermal stability of the resins at moderate temperatures, it does not give insight into the stability against ageing per se. Therefore, PUF-KOH coatings with and without WAs were stored at elevated temperature (70 °C) and relative humidity (75% RH) over the course of 28 days, during which their surface wettability was monitored (Figure 4.6). Notably, PUF-KOH coatings became more hydrophobic after 14 days of ageing, indicating a possible post-curing reaction. While it is assumed that after curing the PUF matrix is more or less vitrified, post-curing effects are believed to be facilitated by the elevated relative humidity and the associated plasticisation of the surface layers. The resulting maturing of the network and surface presumably leads to an evolved state of cure where most of the dimethylene ether bridges have been converted to methylene ether linkages, increasing the water contact angle values of these coatings. These phenomena will be addressed in more detail in later sections.

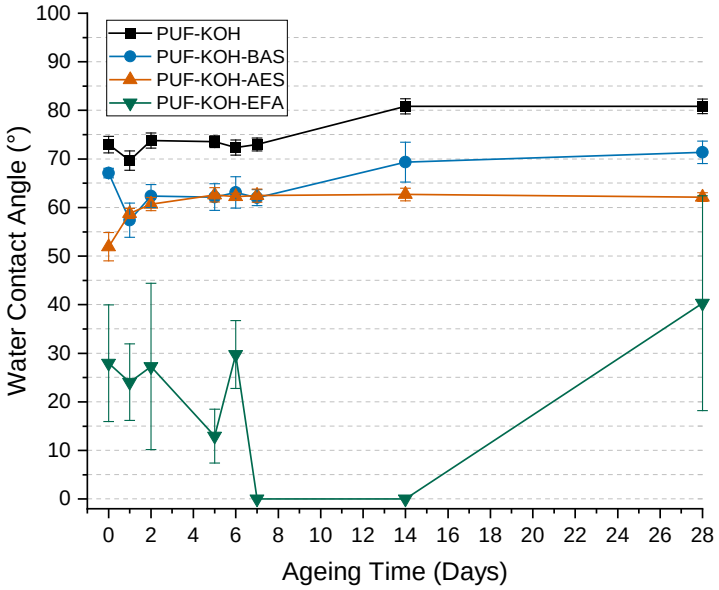


Figure 4.6. Water contact angle values of PUF-KOH(-WA) coatings before and after storage at 70 °C and 75% RH. For PUF-KOH-EFA, coatings measured after 7 and 14 days showed immediate wetting, hence the contact angle value was set to 0. Differently than for Chapter 2, 0.37 wt% of coupling agent 3-aminopropylsilanetriol (APS; 40 wt% in water, kindly provided by Grodan) was added to the binder formulations to avoid delamination.

PUF-KOH-BAS coatings showed a gradual increase in average WCA value for prolonged ageing times, although for samples aged between 1 and 7 days, the average contact angle value was somewhat lower than typically expected. It is likely that this is not because of the ageing procedure, but rather variations from the samples as a result of fluctuations in crystal number density and distribution, in turn affecting also surface

wettability. For PUF-KOH-AES, there appears to be an increase in the hydrophobicity with increasing ageing time, which levelled off after 2 days. Regarding coatings of PUF-KOH-EFA, large variations in wettability were observed already before ageing. Compared with PUF-EFA counterparts (see e.g. Chapter 3), the variations in surface wettability seen here were significantly larger. Most probably, the presence of crystals in PUF-KOH coatings and the immiscibility of EFA with the resin during the cure strongly influences the distribution of EFA on the surface, leading to vastly heterogeneous coatings.

Surface changes of PUF-KOH(-WA) coatings were also monitored with optical microscopy (OM). More specifically, the stability of crystals on the surface and in surface layers was assessed for coatings exposed to elevated temperature and relative humidity for up to 117 days. Salt-doped TEA-containing PUF coatings were also included in this ageing study, on account of a higher affinity of water vapour to PUF compared to PUF-KOH, as measured with dynamic vapour sorption (DVS; see also Figure A4.8). Whilst changes in crystal morphology and wetting agent distribution were observed after direct contact with liquid water and subsequently drying the coating surfaces, changes in crystal morphology and number density due to moisture uptake might also affect surface characteristics of the phenolic resin coatings.

Over the course of 117 days, none of the samples showed signs of physical ageing (Figure 4.7 and Figures A4.9 and A4.10). This is not necessarily surprising given that the deliquescence point of K_2SO_4 is > 95% RH [59,74,75]. However, even in presence of WAs, the K_2SO_4 crystals both on top of the coatings and buried in the surface layers were remarkably stable. While organic compounds such as surfactants can reduce the deliquescence point of salts [76,77], this effect is typically only moderate. Hence, humidity-induced physical ageing will most likely not manifest itself through changes in the K_2SO_4 crystals, even in the long-term.

The next step therefore was to omit these crystals and study the ageing of phenolic resin coatings without crystal-induced roughness and crystal-affected distribution of wetting agents. To this end, PUF(-WA) coatings were prepared and stored at elevated relative humidity of 75%, either at room temperature or at 70 °C. Prior to ageing it was found that the average WCA value of PUF coatings prepared for the ageing experiments was lower than could reasonably expected based on previous results (see Chapter 2 and Chapter 3), with an increased standard deviation. This had been the case for multiple batches within the span of several weeks, where no obvious differences in carrying out the synthesis and coating procedure were made. It is thought that the external conditions during curing, such as relative humidity, play an effect in resulting surface properties. PUF-WA coatings on the other hand were relatively consistent with earlier results (for instance, as described in Chapter 3), indicating that the WAs thoroughly mask the inherent surface wettability of the phenolic resin coating.

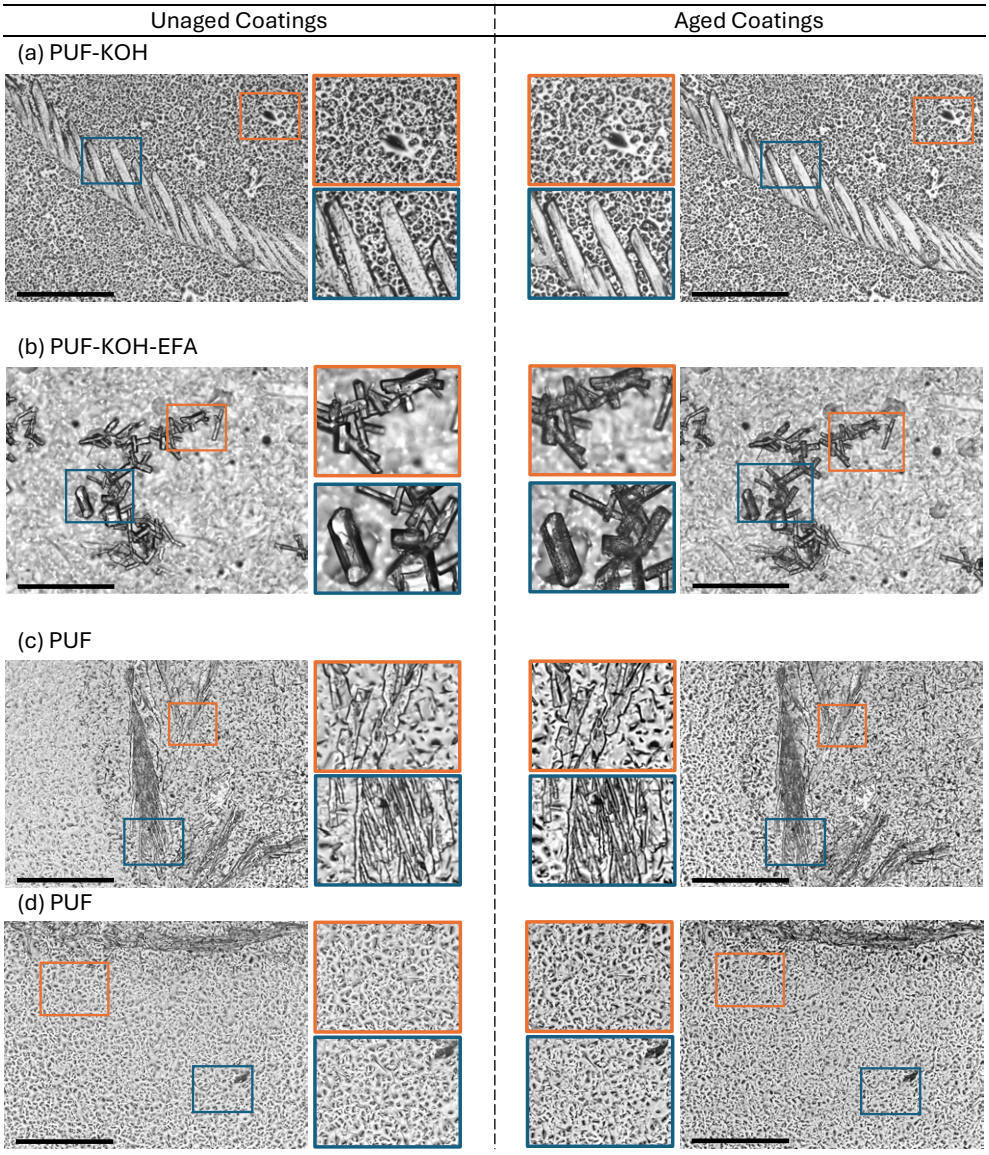


Figure 4.7. Optical micrographs of (a) PUF-KOH, (b) PUF-KOH-EFA, and (c–d) PUF before and after storage at 75% RH and 70 °C for 117 days. Scale bar: 125 µm.

Acknowledging this different surface wettability of PUF coatings at the start of the experiment, it was interesting to see that already after 1 day for both ageing temperatures the WCA values increased (Figure 4.8). Moreover, the standard deviation decreased. In part this is because of an increased amount of datapoints used for the averaging (9 versus 2), however, the overall changes point toward some relaxation or rearrangement effect that occurs in the surface layers. Specifically, the decrease in

hydrophilicity and increase in reproducibility for PUF coatings aged at 20 °C seem to indicate a physical ageing effect rather than a chemical one, enabled by the constant exposure to elevated relative humidity.

For example, it has been reported that absorption of water into films of poly(lactic acid) increases the segmental mobility by disruption of the network (e.g., increasing the free volume) and hence facilitating rearrangements [78]. Water absorption and plasticisation of PUF and PF has been observed both in this work (Chapters 2 and 3) and in literature [79], and could therefore also aid the relaxation of the PUF surface layers.

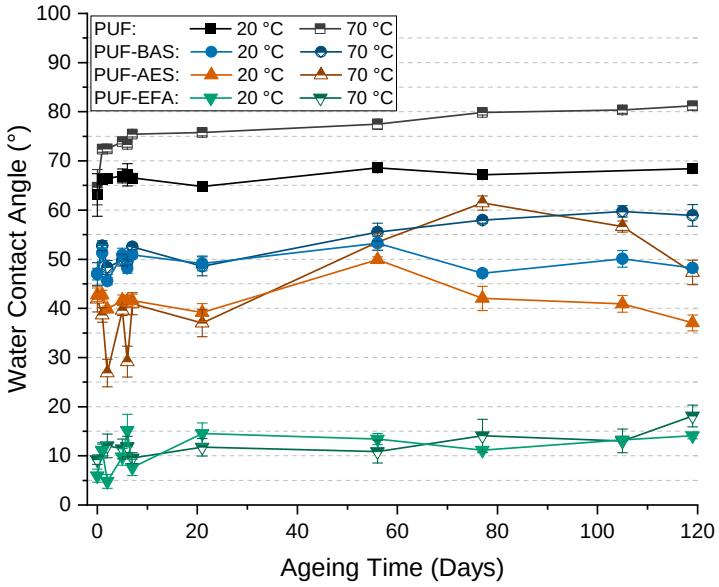


Figure 4.8. Average WCA values of PUF(-WA) coatings before and after storage at 75% RH, either at room temperature (closed symbols) or at 70 °C (semi-closed symbols).

The consequences of plasticisation do not rule out chemical ageing from occurring, however. Table 4.2 shows the surface composition of the PUF coatings after hygrothermal ageing for 1 and 77 days obtained from XPS analyses. The changes in surface chemical composition for coatings held at elevated temperature are reminiscent of the differences seen between coatings cured at 150 °C versus 200°C (Chapter 2). The CO/CC ratio decreases upon ageing at high temperatures and the PUF surfaces become more hydrophobic. Changes in the CO/CC ratio are inherently linked to changes in the N:C and O:C ratios, and as such it follows that these decrease upon ageing, too. A decrease in both N:C and O:C ratios indicates either the degradation of methylolated urea species or their depletion from the surface due to reorientation. The

decrease in O:C ratio is partly due to this, and additionally could also stem from the selective evaporation of formaldehyde from ether linkages in the phenolic resin network [80,81]. No noteworthy changes in surface chemical composition can be discerned for PUF coatings stored at room temperature, in line with the largely unaffected WCA values.

PUF-AES coatings which were stored at 70 °C were always measured first after taking them out of the desiccator. As a result, it can be seen that even at 75% RH a response of AES towards humidity can be observed. This response to humidity has already been discussed in Chapter 3, and is believed to be due to aggregation of the WA at the coating surface. The overall decrease in hydrophilicity seen for PUF-AES coatings exposed to elevated temperatures is observed to varying degrees, and seems to be somewhat inconsistent in part due to the response of AES to the elevated RH.

Table 4.2. Surface composition of PUF and PUF-AES surfaces as determined with XPS after hygrothermal ageing for 1 and 77 days. Standard deviations which were insignificant are omitted.

Coating	*T* (°C)	*t* (days)	N:C	O:C	S:C	CO/CC
PUF	20	1	0.22	0.31	-	0.77 ± 0.01
		77	0.22	0.33	-	0.78
	70	1	0.22 ± 0.01	0.34	-	0.76 ± 0.01
		77	0.18	0.30	-	0.64 ± 0.01
PUF-AES	20	1	0.25 ± 0.03	0.35 ± 0.01	0.01 ± 0.005	1.10 ± 0.30
		77	0.26 ± 0.01	0.34	0.01	0.92 ± 0.03
	70	1	0.23 ± 0.01	0.35 ± 0.01	0.01 ± 0.008	0.92 ± 0.01
		77	0.17	0.30	0.01	0.61 ± 0.03

The surface composition of PUF-AES coatings was also measured with XPS (Table 4.2), however, the detection of wetting agent in the surface layers through the sulphur content was proven to be unreliable to use as a gauge for the actual coating hydrophilicity. As BAS and AES only have one sulphur atom per molecule which chemically distinguishes them from the bulk, the S:C atomic ratio is rather low. Interestingly, a strong difference was again observed for the N:C atomic ratio, indicating that possible rearrangements of urea moieties in the surface layers has a more pronounced effect on the changes in hydrophilicity than the WAs themselves. A similar decrease in CO/CC ratio is seen for PUF-AES and PUF. This substantiates the hypothesis that changes in wettability are not due to chemical ageing of the WAs, but rather a result of chemical and physical ageing processes of the PUF surface.

For PUF-BAS coatings, there appears to be an effect of thermal exposure for a longer period (> 50 days) on the overall wettability of the surface (Figure 4.8). While initially the observed increase might be slightly surprising on account of the thermal stability of BAS, especially compared to EFA and AES, based on the results of previous ageing experiments the observed differences indicate no chemical change from a WA point of view but rather a physical ageing by depletion from the coating–air interface. Such a

depletion could be enabled by the water plasticisation effects of the surface layers of the PUF coating, resulting in the migration of WAs deeper into the surface layers (see also Chapters 2 and 3).

Finally, the wettability of PUF-EFA coatings was relatively unaffected by the ageing procedure. In general, WCA values between 0° (indicating virtually immediate and complete wetting) and 20° were commonly observed for these coatings (Figure 4.8). Overall good hygrothermal stability was already evident from the ageing studies performed on pure EFA, which is also observed here. It is possible that the underlying PUF surface has changed, but that these changes are masked by the demixed nonionic WA.

Calculating the difference in WCA values (Δ*WCA*; see also Equation 4.1) of the aged samples and the same but unaged samples (measured before the start of the experiment) shows in more detail a clear effect of ageing at elevated temperature. Some interesting features can be observed when comparing the Δ*WCA* values of coatings aged at 20 °C (Figure 4.9a,c,e) with those of coatings aged at 70 °C (Figure 4.9b,d,f).

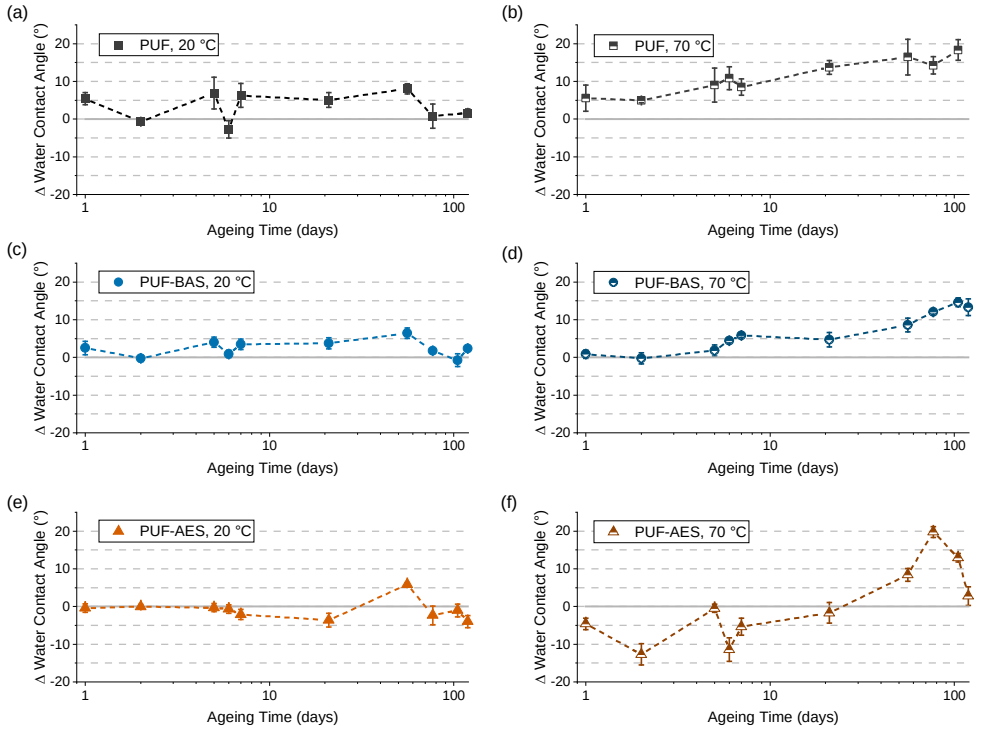


Figure 4.9. The difference (Δ) in WCA values between aged and unaged PUF(-WA) coatings, for coatings exposed to either (a,c,e) 20 °C or (b,d,f) 70 °C and 75% RH. Lines between datapoints have been added to guide the eye.

Although datapoints are connected with a line to guide the eye, it appears that PUF and PUF-BAS coatings change similarly over time. Despite the absolute values still being relatively different, the trend is comparable. This could imply that the change in WCA value observed for BAS is indeed related more to the ageing of the PUF matrix, rather than of the WA itself. In general, all PUF samples kept at 70 °C show an increased WCA value compared to unaged coatings, although it somewhat varies when this increase sets in exactly. This increasing in WCA value is most likely due to a post-curing effect which is facilitated by the plasticisation as a result of the high relative humidity. The difference between unaged coatings and those aged at 20 °C is definitely smaller and can be seen to be slightly more constant than for the coatings aged at 70 °C.

Influence of Substrate on Ageing of Phenol-Urea-Formaldehyde Coatings

The possible influence of the type of substrate on the surface characteristics of PUF(-WA) coatings was monitored first by using two different glasses: fused quartz (QZ) glass and soda lime (SL) glass. Possible changes in the acidity of the coating matrix were monitored using the pH-sensitive methyl red (MR) dye (Figure 4.10a), although this does not directly provide information regarding changes in surface properties. The selection of a suitable dye was based on its availability, solubility in the resin formulation, and its sensitivity or colour range. In accordance with literature [82,83] the absorption spectrum of MR in solution is dependent on the pH, with absorbance peaks visible at 522 nm (acidic media) or 432 nm (basic media). For the transition region between pH 4.4-6.2, contributions from both peaks can be seen.

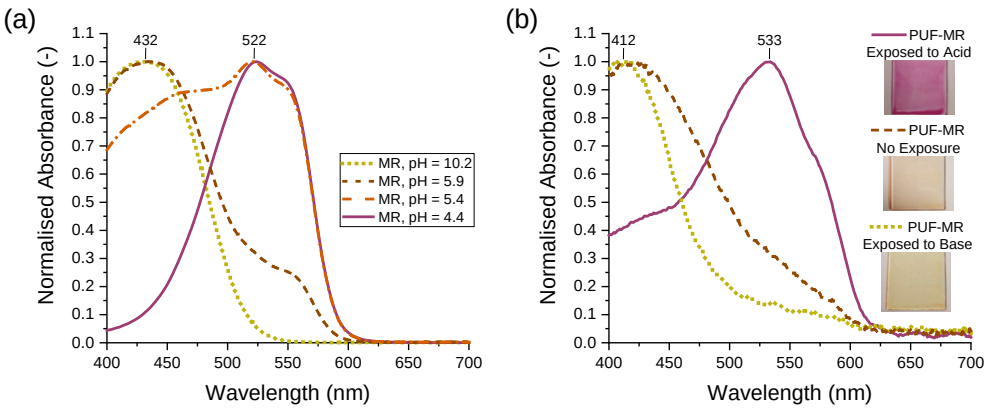


Figure 4.10. Absorption spectra of (a) MR in water at varying pH and (b) PUF-MR coatings exposed to either an acidic or basic medium.

Incorporating MR into the PUF resin yielded coatings which were responsive to their environment, as also reported by Villegas and Pascual [82] for silica coatings doped

with this chromophore. Exposure to a basic or acidic environment yielded a change in coating colour (Figure 4.10b). This responsiveness was seen for both direct immersion in a medium and after exposure to basic or acidic vapour (ammonia and acetic acid, respectively). Additionally, the inclusion of MR also allowed to further corroborate a crucial step during the curing process of PUF resin: acidification. Just after dip coating, applied PUF layers were yellow. Over the course of the hardening process, evaporation of TEA shifted the pH towards acidic values, evidenced by a purple colour of the coatings. After the complete curing time of 20 minutes, slight basification had evidently occurred as the coatings were orange, indicative of a pH value in the transition region.

Although there is some discrepancy between the location of the peak maximum for the given data of methyl red in solution and in coatings, the relationship of peak location with pH still holds true and shows the viability for using the MR dye in PUF coatings. Therefore, coatings of PUF-MR on soda lime and fused quartz glass were prepared next and aged for 45 days at 75% RH, either at 20 °C or at 70 °C. Prior to this, the UV-Vis absorption spectra of coatings was measured, where no obvious differences between coatings on fused quartz and on soda lime glass could be discerned (Figure 4.11). Main features that were seen for coatings on both glasses were the presence of an absorption peak at 420 nm and one at 530 nm, indicating an intermittent pH of the matrix between 4.4 and 6.2. Naturally, because the peak at 420 nm has a larger intensity than the one at 530 nm, the matrix pH is estimated to be more on the basic side of this pH range. The small difference in how pronounced the peak at 530 nm is (also observed when comparing Figure 4.10b with Figure 4.11) is likely due to coating-to-coating variations. Especially in the transition region, slight changes in pH can elicit strong changes in the absorption spectrum (also seen for pH = 5.4 and pH = 5.9 in Figure 4.10a).

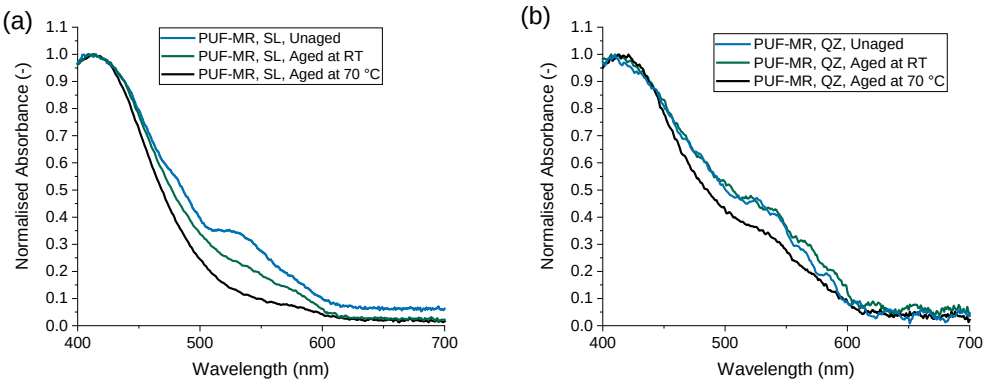


Figure 4.11. Normalised absorption spectra of PUF-MR coatings on (a) soda lime (SL) or (b) fused quartz glass (QZ) before and after ageing at 75% RH at either room temperature or 70 °C for 45 days.

Interestingly, it appears that there is an influence of the substrate on the pH upon ageing. For PUF-MR on soda lime glass, the peak at 530 nm disappears, whilst for PUF-MR on fused quartz glass only a slight decrease in intensity is observed. This modest decrease is likely an effect of post-curing and evaporation of residual TEA, which will be discussed more in the next section.

Comparing PUF-MR held at 75% RH at RT on both substrates, it can also be seen that there is a slight decrease in peak intensity at 530 nm for the coating applied on soda lime glass. Possibly, the coating and curing procedure already induces leaching of Na^+ and OH^- ions, resulting in the eventual alkalinisation. Only at elevated temperatures, however, this continuous leaching and diffusion is sufficient to induce further changes. The leaching and migration of sodium ions from the glass substrate could possibly also be facilitated by water vapour during the ageing process. As such, a note regarding the permeability of PUF coatings to water vapour is implemented in the Appendix.

To test if the observed changes in the pH of the polymer matrix influence the surface properties, coatings of PUF-WA were applied on four different substrates: soda lime glass, fused quartz glass, silicon wafers (Si-Ws) and stone melt wafers (SMWs). By comparing soda lime with fused quartz glass and silicon wafers, the influence of ion leaching on the ageing process of PUF(-WA) coatings can be determined. Soda lime has hitherto been used as a model glass substrate to approximate the chemistry of stone wool fibres. Here, to extend the research, wafers made from a stone melt have been used as substrate which is chemically closer to stone wool substrates. The approximate composition of the different glassy substrates was determined with XPS. Despite cleaning, all samples showed the presence of an adventitious carbon layer (5.4 ± 2.0 at%). This layer, however, did not appear to significantly affect the determination of the ratio of network modifiers and network formers relative to Si (Table 4.3; carbon not shown).

Table 4.3. Average composition of soda lime (SL) glass, stone melt wafers (SMF) and quartz glass (QZ) as determined with XPS. Composition was normalised to Si. Standard deviations which were insignificant are omitted.

Substrate	Atomic Ratio Relative to Si						
	O	**Na**	**K**	**Ca**	**Al**	**Mg**	**Fe**
SL	2.27 ± 0.05	0.092 ± 0.029	0.016 ± 0.001	0.057 ± 0.007	0.022	0.042 ± 0.006	-
SMW	3.66 ± 0.08	0.046 ± 0.003	0.051 ± 0.011	0.28 ± 0.01	0.50	0.073 ± 0.006	0.079 ± 0.010
QZ	1.85 ± 0.02	0.003	-	-	-	-	-

Only a trace amount of sodium was detected for the fused quartz substrates. The composition of soda lime glass and the stone melt wafers was fairly different from one another. Quite distinct is the elevated calcium and aluminium content of the SMWs

compared to soda lime glass, in line with typical stone wool substrates [58,84]. It is well-documented that the composition of a glass affects corrosion and leaching [37,42,85–88]. On that basis, a different ageing behaviour between coatings on SMWs and SL substrates is to be expected.

Reference water contact angle measurements were performed before storing coatings of PUF-WA in a desiccator with a saturated NaCl solution (providing an environment of 75 % RH) at 70 °C. After 45 days, coating surfaces were probed with water droplets again to determine possible changes in the surface wettability.

As shown in Figure 4.12a, all PUF coatings free of WAs on SL, QZ and Si-W show a similar increase in water contact angle value upon ageing. Comparing the surface composition of the unaged and unaged PUF coatings on soda lime, it would seem that a decrease in both the nitrogen and oxygen content contributed to the observed ageing (Table 4.4). Consequentially, the CO/CC ratio is lower than for unaged PUF coatings. In fact, the O:C and CO/CC ratios match well with those reported in Chapter 2 for coatings cured at 200 °C and 150 °C.

Table 4.4. Average composition as determined with XPS of PUF coatings on SL, QZ, and SMW substrates, before and after ageing at 70 °C and 75% RH for 45 days. The full width at half-maximum (FWHM) of the O 1s binding energy spectra has only been determined for PUF coatings without WAs. Standard deviations which were insignificant are omitted.

Coating	Substrate		N : C	O : C	CO/CC	FWHM O 1s (eV)
PUF	SL	Unaged	0.220 ± 0.002	0.331 ± 0.013	0.798 ± 0.014	2.39 ± 0.03
		Aged	0.183 ± 0.008	0.305 ± 0.018	0.698 ± 0.082	2.29 ± 0.10
	QZ	Unaged	0.202 ± 0.001	0.348 ± 0.001	0.789 ± 0.007	2.15 ± 0.01
		Aged	0.172 ± 0.010	0.304 ± 0.019	0.676 ± 0.056	2.27 ± 0.18
	SMW	Unaged	0.197	0.317 ± 0.011	0.676 ± 0.004	2.27 ± 0.02
		Aged	0.168 ± 0.004	0.320 ± 0.013	0.603 ± 0.004	2.23 ± 0.03
PUF-AES	SL	Unaged	0.209 ± 0.004	0.344	0.791 ± 0.033	-
		Aged	0.208 ± 0.005	0.310 ± 0.016	0.750 ± 0.062	-
	QZ[a]	Aged	0.195 ± 0.012	0.317 ± 0.022	0.658 ± 0.048	-
	SMW	Unaged	0.234 ± 0.007	0.334 ± 0.007	0.896 ± 0.037	-
		Aged	0.191 ± 0.010	0.322 ± 0.003	0.697 ± 0.015	-
PUF-BAS	SL	Unaged	0.210 ± 0.009	0.294 ± 0.010	0.606 ± 0.030	-
		Aged	0.195 ± 0.016	0.284 ± 0.020	0.511 ± 0.076	-
	QZ[a]	Aged	0.206 ± 0.012	0.288 ± 0.005	0.566 ± 0.022	-
	SMW	Unaged	0.243 ± 0.002	0.311	0.694 ± 0.006	-
		Aged	0.186 ± 0.004	0.275 ± 0.002	0.567 ± 0.005	-

[a] Based on the initial WCA values of coatings of PUF-AES and PUF-BAS on QZ, it was assumed that the surface chemistry was similar to the same coatings on SL. Hence, no explicit XPS measurement has been performed on unaged PUF-AES and PUF-BAS coatings on QZ.

A notable difference is the average full width at half-maximum (FWHM) of all the O 1s binding energy spectra, which for coatings on SL and QZ were rather inconsistent after ageing. Thus, contributions from oxidation to surface changes cannot be completely

excluded for these coatings. The coatings on the stone melt wafers conversely do not show a drastic change in FWHM upon ageing. However, should oxidation occur for all coatings, there is no obvious explanation for why coatings on SMW would be exempt from oxidation.

Interpretation of the O:C ratio (and thus inherently also the N:C ratio) and CO/CC ratio for PUF-AES and PUF-BAS is challenging, as the changing presence of WAs at the coating–air interface introduces an extra factor affecting these ratios. In part because of this, there does not appear to be a discernible trend regarding the CO/CC ratio and substrates for the PUF-WA coatings.

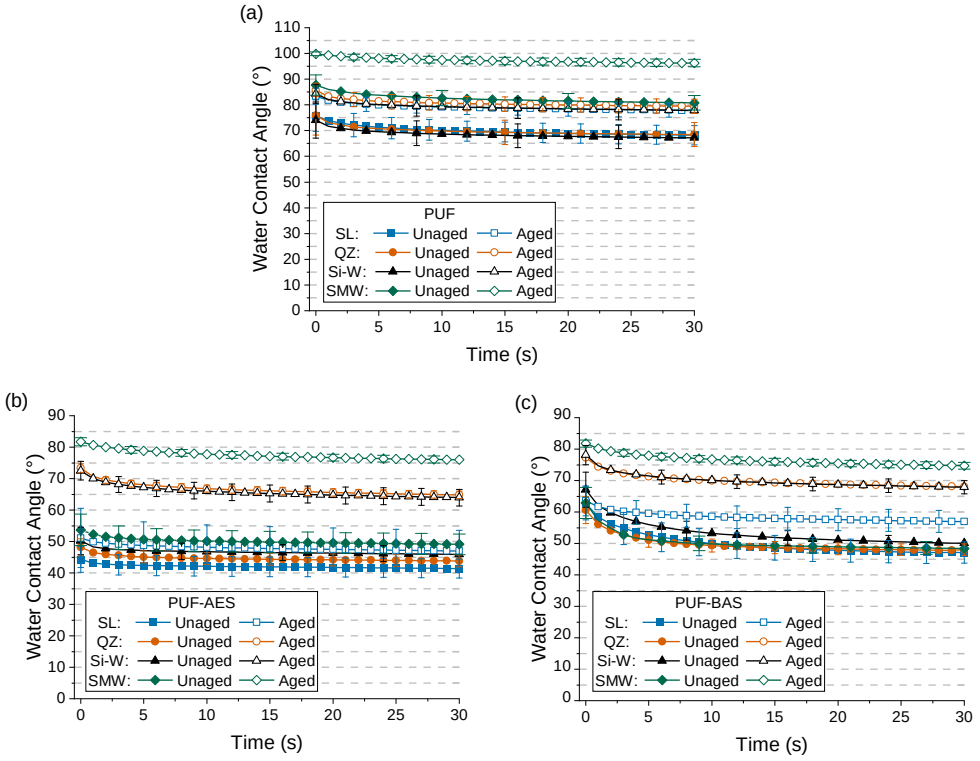


Figure 4.12. Average WCA values before and after ageing of (a) PUF, (b) PUF-AES and (c) PUF-BAS coatings on soda lime glass, fused quartz glass, Si wafers, and stone melt wafers at 75% RH and 70 °C for 45 days.

The difference in surface chemistry between PUF on SL and on SMW was also reflected in the surface wettability. As shown in Figure 4.12a, the unaged PUF-SMW coatings are more hydrophobic than the usual PUF coatings, with an average water contact angle value of 80.8° ± 2.8°. Not only does this yield a vastly different starting point for the ageing of these coatings, but the end point is also significantly different. After 45 days,

coatings appeared to increase even further in their hydrophobicity up to a water contact angle value of 96.3° ± 1.4°. However, it was found that the origin of this large initial WCA value was the size of the substrates (see also Figure A4.12 and corresponding considerations in the Appendix). The smaller substrate size results in a larger edge-to-area ratio of the applied coatings, which in turn is presumed to strongly affect evaporation of TEA, formaldehyde and H_2O, and hence affects curing and the WCA value.

For coatings with AES and BAS, only limited ageing was observed for the coatings applied on soda lime glass (Figure 4.12b,c). For the aged PUF-AES and PUF-BAS coatings on fused quartz and silicon wafers, the average water contact angle value was similar to that of unaged PUF. Although for PUF-AES and PUF-BAS coatings on SMWs the presence of WAs somewhat masked the effects induced by the smaller substrate size, upon ageing the hydrophilicity decreased even more relative to coatings on QZ and Si-W.

In light of the previously established hygrothermal stability of the WAs as well as these results, degradation of the WAs upon ageing again appears unlikely. Although mobility of these anionic WAs was not readily observed (see Chapter 3), the coating surface appears to become significantly less enriched with WAs after ageing on fused quartz glass, silicon wafers, and stone melt wafers. Presumably, the PUF matrix plays an important role in this process, as it is seen to change in surface chemistry and wettability.

One possibility is that the surface plasticisation by water allows for sufficient mobility of the WA through the surface layers, away from the coating-air interface into the bulk. In case of coatings on soda lime glass, however, the leaching of NaOH introduces additional charges into the coating, which fixate the wetting agents below the surface. Another possibility is that the introduction of mobile charges from the soda lime glass leads to enhanced mobility of the wetting agents in the surface layers. Without such charges, wetting agents become fixated in deeper surface layers upon ageing. This fixation occurs through the presence of quaternary ammonium ions (e.g., TEA^+ or hexamethylenetetramine$^+$), which can still be present in the cured matrix (Figure 4.13).

To corroborate these hypotheses, the sodium content of coatings on different substrates was determined. The initial and final WCA value and Na:C ratio of the coatings are presented in Table 4.5, and detailed Na 1s binding energy spectra can be found in Figure A4.13. For coatings on soda lime, the Na content mostly remained similar or increased slightly after ageing. For PUF-AES and PUF-BAS, it was assumed that the initial Na:C ratio of the coatings on QZ substrates was similar to coatings on SL substrates. This is indirectly verified by the fact that initial WCA values of coatings on both types of substrates are similar. Based on this assumption, the decrease in sodium content for coatings on QZ after ageing is striking. Given the absence of sodium ions in PUF layers on fused quartz (Figure A4.13), this implies that there are still some WAs in

the surface layers, although the amount is not sufficient to yield an appreciable decrease in WCA.

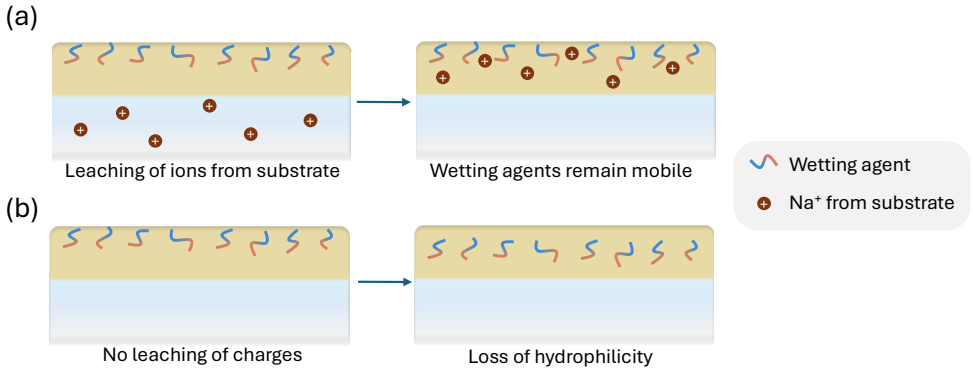


Figure 4.13. Schematic representation of hypotheses of the ageing mechanism on (a) soda lime glass, where ageing is inhibited due to the leaching of mobile charges from the substrate, and (b) fused quartz or silicon wafers, where ageing is observed due to the lack of wetting agent mobility due to the absence of leached, mobile charges from the substrate.

Table 4.5. Average WCA values and sodium content of PUF(-WA) coatings on different substrates before (WCA_0) and after ageing for 45 days at 70 °C and 75% RH (WCA_{45}). Standard deviations which were insignificant are omitted.

Coating	Substrate	WCA_0 (°)	WCA_{45} (°)	ΔWCA (°)	$(Na:C)_0$	$(Na:C)_{45}$	$\Delta(Na:C)$
PUF	SL	68.3 ± 3.7	77.9 ± 2.8	9.8 ± 4.8	0.0008 ± 0.0005	0.0021 ± 0.0012	0.0013 ± 0.0013
	QZ	68.5 ± 4.7	79.5 ± 2.8	11.0 ± 5.4	0.0	0.0	0.0
	Si-W	67.2 ± 4.5	77.9 ± 4.1	10.7 ± 6.1	-[a]	-[a]	-[a]
	SMW	80.8 ± 2.8	96.3 ± 1.4	15.5 ± 3.1	0.0	0.0	0.0
PUF-AES	SL	41.4 ± 3.0	47.0 ± 6.6	5.5 ± 7.2	0.019	0.019 ± 0.002	0.0 ± 0.002
	QZ	43.8 ± 1.9	64.8 ± 1.2	21.0 ± 2.3	-[a]	0.006 ± 0.001	-0.013 ± 0.001
	Si-W	45.9 ± 2.5	64.0 ± 2.6	18.0 ± 3.6	-[a]	-[a]	-[a]
	SMW	49.1 ± 3.3	76.0 ± 1.1	26.9 ± 3.5	0.016	0.007	-0.009
PUF-BAS	SL	47.5 ± 2.5	54.3 ± 2.2	9.8 ± 4.8	0.013 ± 0.002	0.014 ± 0.006	0.001 ± 0.006
	QZ	48.7 ± 1.6	68.5 ± 1.1	20.0 ± 2.1	-[a]	0.009	-0.004 ± 0.002
	Si-W	48.8 ± 1.3	67.2 ± 1.7	17.8 ± 2.7	-[a]	-[a]	-[a]
	SMW	48.4 ± 2.1	74.8 ± 1.1	26.4 ± 2.4	0.014	0.007	-0.007

[a] Not measured.

Although the SMW substrates are rich in network modifiers (Table 4.3), no inhibition of the deterioration of hydrophilicity was observed. With no increase in the sodium content after the ageing procedure for the PUF coatings without WAs, and only a decrease in sodium content for the PUF-WA coatings, it would appear that leaching of ions from the SMW is not prone to happen. One factor contributing to this is likely the

relatively large content of divalent cations in the SMWs such as Ca^{2+}. Smets *et al.* [37] found that the addition of CaO, ZnO, or MgO to a sodium silicate glass increases its corrosion resistance, meaning that this leads to a decreased leaching of Na^{+} ions with increasing divalent cation content. Moreover, significant leaching of the divalent cations was not observed in their research, unless the glass composition yielded a more open glass structure [37].

It can rightfully be argued that the observed increase in Na:C ratio for the PUF coatings on SL glass is minimal, leading to the question whether leaching of sodium ions truly is correlated to the observed inhibited ageing of PUF-WA coatings on soda lime glass. However, combined with the observations made in the previous section with the PUF-MR coatings, it seems reasonable that there is an important contribution of sodium ions to the ageing (or lack thereof) of PUF-WA coatings. Additionally, results of a similar ageing experiment where the relative humidity was not constant at 75% over the course of the ageing period can be found in the Appendix. In general, the same trends were observed but at times in a more exaggerated manner (e.g., larger measured Na concentrations).

Overall, for PUF coatings stored at 75% RH and 70 °C, the following observations were made:

- PUF coatings on soda lime glass become more basic upon ageing compared to PUF coatings on fused quartz glass.
- The basicity increase observed for PUF coatings on soda lime glass are likely a result of leaching of NaOH.
- In all cases, the Na:C ratio of coatings on soda lime glass increases or at the very least remains stable.
- For PUF-WA coatings on fused quartz glass, the sodium content is found to decrease.
- PUF coatings with WAs on soda lime glass age significantly less than similar coatings on fused quartz glass in terms of their hydrophilicity.

Thus, these results would support the hypothesis that mobile charges, like Na^{+}, sufficiently mobilise anionic WAs, thereby allowing them to remain at the coating–air interface to lower the surface energy of the coating.

The effect of relative humidity was also investigated by ageing coatings at 70 °C and 19% RH (Figure 4.14). It should be noted that a saturated LiCl solution was used to control the RH. However, the theoretical value of 11% RH [59] was not attained, but rather an average value of 19.3 ± 0.8 % RH. Of note is that in case of low RH, a strong increase in WCA value is seen for all coatings, regardless of the substrate. This would imply that relative humidity has a strong effect on changes in hydrophilicity. If it is assumed that the content of leached sodium is similar for coatings on SL exposed to 19% and 75% RH, then the requirement for limited ageing would be not only to allow

for mobilisation of anionic WAs through charges, but also through sufficient water in the surface layers. PUF coatings without WAs all show in increased WCA value reminiscent to those in Figure 4.12a, indicating that the lower relative humidity was still sufficient to facilitate post-curing at elevated temperatures. In case of PUF-WA coatings (Figure 4.14b–c), the combination of a denser surface layer and lower relative humidity does not allow for as much mobility of the WAs compared to the cases similar to PUF-WA coatings at 75% RH (Figure 4.12b–c).

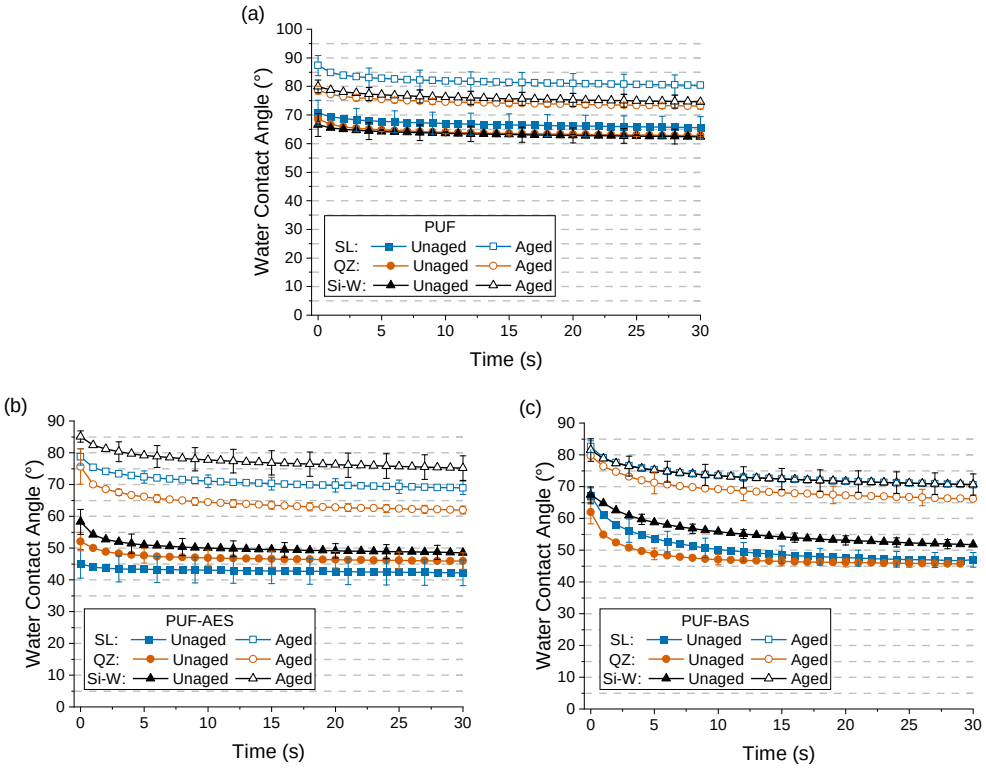


Figure 4.14. Average WCA values before and after ageing of (a) PUF, (b) PUF-AES and (c) PUF-BAS coatings on soda lime (SL) glass, fused quartz (QZ) glass, and Si wafers (Si-W) at 70 °C and 19% RH for 45 days.

To some degree, such a response to varying RH was previously observed in Chapter 3, Figure 3.10a. Exposing PUF-AES coatings to 90% RH for only 1 h already yielded an increase in hydrophilicity, which was largely reversible when subsequently exposing the coatings to 10% RH for 1 h. This points towards a possible reversible humidity-induced mobility of these WAs, resulting in reorientation away from the surface, or vice versa surface enrichment. Similarly, the changes in Figure 4.12b could be due to insufficient mobility as a result of the low humidity conditions.

Investigating Inhibited Ageing of Phenol-Urea-Formaldehyde Coatings on Inert Substrates

Based on the hypothesis that the leached mobile charges facilitate mobilisation of WAs at the coating–air interface, the sodium content in the coating was increased by addition of the sodium salt of methane sulphonate (NaMeS). This should then introduce mobile charges to the coating so that even on inert substrates, such as fused quartz glass, WAs remain mobile and at the coating-air interface (Figure 4.15). An alternative route would be to use a silicate glass with increased Na_2O content, although it is assumed for applications slightly changing the resin formulation is more feasible.

An excess of NaMeS ($n_{NaMeS} = 5 \cdot n_{WA}$) was added to the PUF resin formulations. Increasing the salt concentration even further yielded macroscopically visible crystals after curing, and additionally a drastic decrease in water contact angle value for PUF coatings without any wetting agents. However, even at the used amount of NaMeS, the water contact angle value of PUF coatings was found to be lowered to approximately 57.6° ± 4.8° (Figure 4.16a). Still, as it was thought that this would not interfere with the hydrophilicity of the coatings when WAs were added, this concentration of NaMeS was used for subsequent experiments.

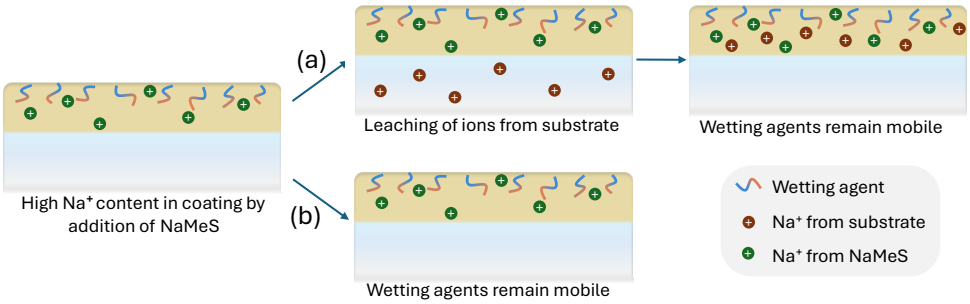


Figure 4.15. Schematic representation of method and hypothesis to immobilise wetting agents in coatings applied on (a) soda lime glass and (b) fused quartz glass and silicon wafers by addition of the sodium salt of methane sulphonate (NaMeS) to the resin.

Interestingly, the presence of NaMeS in fact did interfere with the hydrophilicity of PUF-WA coatings, as seen by a lower average WCA value compared to the salt-free counterparts (Figure 4.16a). Presumably the change in WCA values for the PUF(-WA) coatings with NaMeS can be tuned by decreasing the amount of NaMeS added to the formulations, so that the hydrophilicity of the coatings matches better with the salt-free counterparts. A similar increase in hydrophilicity was also observed for coatings of PUF-AES with varying concentrations of Na_2SO_4 (Figure A4.15). An important distinction

between what is essentially doping the coatings with NaMeS and with Na_2SO_4 is that the latter results in a hazy coating due to formation of crystals upon curing, whereas for the former such crystals are not observed. In both cases, however, the result is that the water-wettability of the PUF-WA coatings is enhanced. Although synergistic phenomena in mixtures of surfactants are reported in literature [89,90], NaMeS would not likely be classified as a surfactant. Therefore, it is more probable that the resulting increase in hydrophilicity is a result of the formation of ion pairs between anionic wetting agents and excess Na^+, thereby screening charges between anionic WAs and lowering the CMC and SFT [91–93]. This would then also affect the distribution of WAs within the coating upon curing, and hence lead to an enhanced hydrophilicity. Additional support for this was found from the non-surface activity of NaMeS in water, for which a water–air interfacial tension of 71.3 ± 0.2 mN/m was measured at a concentration similar to that used in the resin formulation. In case of the decrease in WCA value of PUF-NaMeS coatings, it is proposed that the large salt concentration influences the curing process slightly, leading to an only somewhat different surface chemistry than usual.

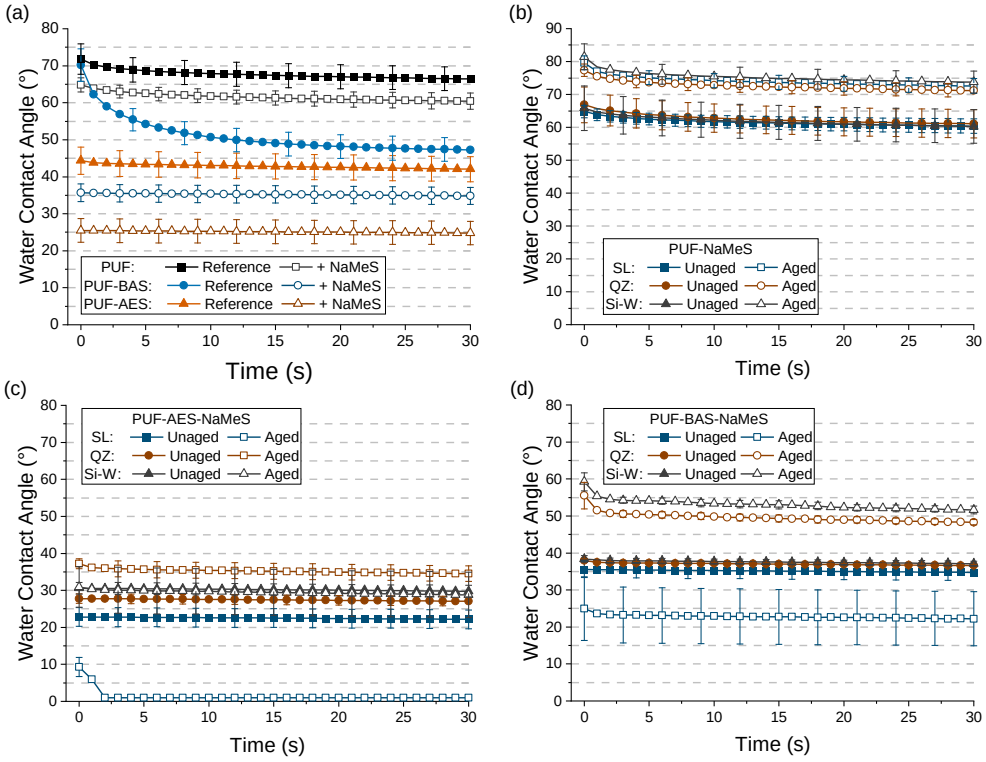


Figure 4.16. Average WCA values of coatings of (a) PUF(-WA)-NaMeS on soda lime (SL) glass, and of (b) PUF-NaMeS, (c) PUF-AES-NaMeS, and (d) PUF-BAS-NaMeS on soda lime (SL) glass, fused quartz (QZ) glass and silicon wafers (Si-W) before and after ageing at 75% RH and 70 °C for 45 days. Datapoints after 2 s for PUF-AES-NaMeS on SL in (c) have been set to 0 to indicate the virtually complete wetting.

The average WCA value of PUF-NaMeS coatings was seen to increase upon ageing the surfaces, regardless of the substrate (Figure 4.16b). Although the added salt can influence the initial hydrophilicity of the PUF coatings, it does not seem to affect any subsequent chemical and/or physical ageing of the PUF surface.

PUF-AES and PUF-BAS surfaces on soda lime glass show a similar response after ageing when doped with NaMeS (Figure 4.16c–d). Interestingly, the hydrophilicity of these coatings increases after the hygrothermal treatment for 45 days. For PUF-AES, addition of NaMeS yields a surface for which virtually immediate wetting occurs, and coatings appeared somewhat hazy, indicative of phase separation and therefore enrichment of AES at the coating–air interface. For PUF-BAS the decrease in WCA value is noticeable, yet less severe. When coated on QZ and Si-W substrates, PUF-AES and PUF-BAS with NaMeS begin to exhibit appreciable differences after ageing. Most distinctly, the average WCA value for PUF-BAS-NaMeS coatings on QZ and Si-W increases by approximately 10–15°. Conversely, for PUF-AES-NaMeS an increase of only 8° is observed, indicating a slower ageing process. In absolute values, the increase in WCA values observed for the PUF-WA-NaMeS coatings is still less than for PUF-WA coatings (Table 4.6), although it should be noted that the initial WCA value was already different. This would imply a difference in concentration of WAs at the coating–air interface. Despite this, it appears that the distribution of BAS in PUF surface layers is still more susceptible to changes in the matrix than AES, even in presence of NaMeS.

Table 4.6. Average CA values and sodium content of PUF(-WA)-NaMeS coatings on different substrates before (WCA_0) and after ageing for 45 days at 70 °C and 75% RH (WCA_{45}). Standard deviations which were insignificant are omitted. Surface chemical composition after ageing could not be measured due to delamination of the coatings from the substrates.

Coating	Substrate	WCA_0 (°)	WCA_{45} (°)	ΔWCA (°)	$(Na : C)_0$
PUF-NaMeS	SL	60.4 ± 2.2	72.5	12.1 ± 3.2	0.010 ± 0.001
	QZ	61.1 ± 4.3	71.1	10 ± 4.6	-[a]
	Si-W	60.3 ± 5.1	73.8	13.5 ± 6.1	-[a]
PUF-AES-NaMeS	SL	22.2 ± 2.5	0[b]	-22.2 ± 2.5	0.035 ± 0.001
	QZ	27.0 ± 13	34.5	7.5 ± 2.5	-[a]
	Si-W	29.7 ± 1.6	28.8	-0.9 ± 6.3	-[a]
PUF-BAS-NaMeS	SL	34.7 ± 2.2	22.2	-12.5 ± 7.6	0.032 ± 0.001
	QZ	36.7 ± 0.3	48.3	11.6 ± 0.7	-[a]
	Si-W	37.1 ± 0.7	51.6	14.5 ± 1.3	-[a]

[a]: not measured

[b]: CA assumed to be 0°.

NaMeS-containing coatings were also aged at 19% RH. However, although there were additional Na^+ ions introduced to the coatings, the mobility of WAs appeared to be insufficient due to the water/moisture content being too low. As a result, the addition of NaMeS in these cases could not prevent the loss of hydrophilicity (Figure 4.17). Together with the results of PUF-WA coatings aged at similar conditions (Figure 4.14),

it is evident that relative humidity has a strong influence on the ageing of surface hydrophilicity of PUF-WA coatings. This is also emphasised by the fact that the final WCA values of PUF-WA-NaMeS coatings are similar to that of their salt-free counterparts, despite the initial WCA values being lower.

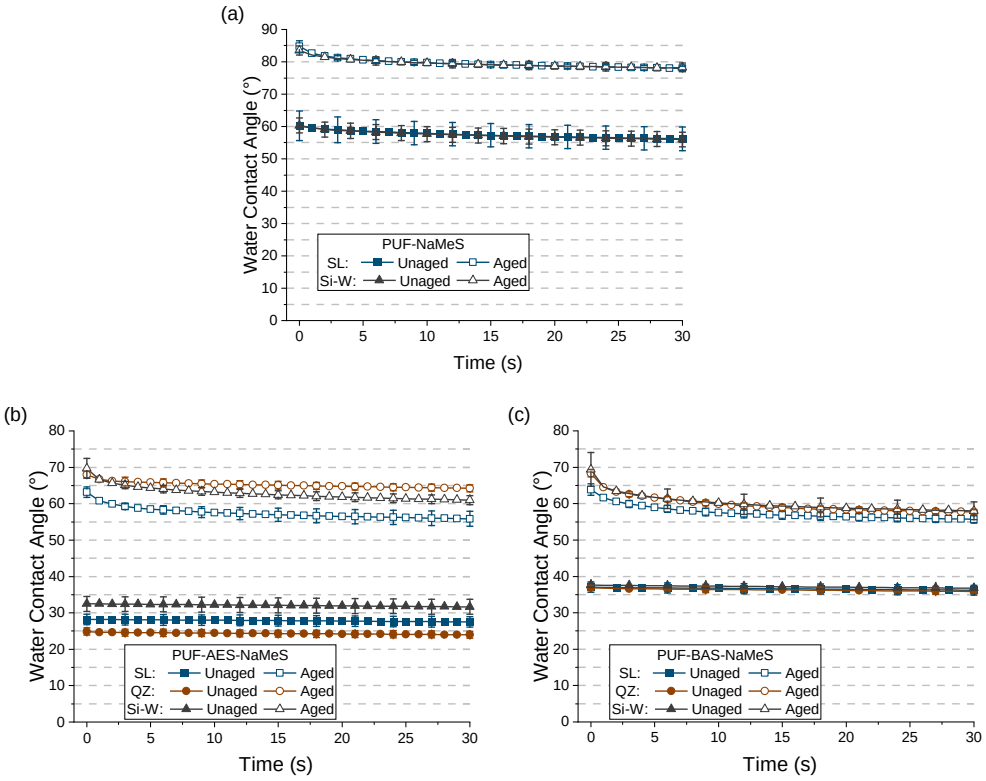


Figure 4.18. Average WCA values of coatings of (a) PUF-NaMeS, (b) PUF-AES-NaMeS, and (c) PUF-BAS-NaMeS on soda lime glass, fused quartz glass and silicon wafers before and after ageing at 19% RH and 70 °C for 45 days.

4.4. Conclusions

The effect of different ageing conditions on the stability and performance of three different WAs and two different types of phenolic resins was studied. Hygrothermal ageing of PUF coatings with and without WAs has shown two interesting phenomena. First, PUF surfaces undergo post-curing reactions, likely facilitated by the combination of elevated relative humidity and temperature. This results in an increase in water contact angle value over time, yielding less hydrophilic coatings. In case of PUF coatings with WAs, only coatings with anionic WAs stored at elevated temperatures

showed a moderate increase in average water contact angle value. Chemical analyses of the coating surfaces show a surface chemistry akin to that of a post-cured, WA-free PUF coating. Some evidence of physical ageing through relaxation facilitated by moisture-induced plasticisation was also observed. In light of the stability of the WAs, it is therefore believed that WAs do not degrade during the accelerated ageing procedure, but rather physically deplete from the coating–air interface due to the chemical and physical changes in the PUF surface layers.

The substrate on which the coatings were applied had a distinct influence on the change in hydrophilicity upon ageing samples at 70 °C and 75% RH. Only coatings of PUF with WA applied on soda lime glass showed a limited decrease in hydrophilicity, whereas the WCA of PUF-WA coatings on fused quartz glass, stone melt wafers, and silicon wafers became reminiscent of that of WA-free PUF surfaces. This was attributed to the leaching of sodium hydroxide, only occurring for the soda lime glass. The influx of positive sodium ions ensures sufficient mobility of the wetting agents upon ageing. However, when coatings are aged at a lower relative humidity of 19%, an increase in WCA was observed regardless of the substrate used, signifying that also water is needed for sufficient mobility.

Addition of NaMeS to PUF-AES resins leads to coatings which either show an increased hydrophilicity after ageing at 70 °C and 75% RH, or a limited decrease of hydrophilicity. PUF-BAS doped with NaMeS under similar conditions does not readily show such inhibition of ageing, possibly due to a stronger affinity with the PUF matrix due to its aromatic content. When PUF-WA-NaMeS coatings were aged at 19% RH and 70 °C, the WCA value of the coatings decreased to a similar value as that of coatings without NaMeS. This again indicates the importance of water plasticisation in addition to the presence of sodium ions.

Ageing of the PUF-WA coatings therefore appeared quite sensitive to the relative humidity in which samples were stored. These insights could provide tools, i.e., addition of a sodium salt or storage at elevated relative humidity, to preserve the hydrophilicity of phenolic resin coatings with wetting agents over time.

References

[1] S. G. Croll and B. R. Hinderliter, “Estimating service lifetimes in weathering: an optimistic view,” *J. Coat. Technol. Res.*, vol. 4, no. 3, pp. 217–230, 2007, doi: 10.1007/s11998-007-9024-1.

[2] S. G. Croll, B. R. Hinderliter, and S. Liu, “Statistical approaches for predicting weathering degradation and service life,” *Prog. Org. Coat.*, vol. 55, no. 2, pp. 75–87, 2006, doi: 10.1016/j.porgcoat.2005.08.006.

[3] M. E. Nichols and C. A. Darr, “Effect of weathering on the stress distribution and mechanical performance of automotive paint systems,” *J. Coat. Technol.*, vol. 70, no. 885, pp. 141–149, 1998, doi: 10.1007/BF02730084.

[4] O. Guseva, S. Brunner, and P. Richner, “Service life prediction for aircraft coatings,” *Polym. Degrad. Stab.*, vol. 82, no. 1, pp. 1–13, 2003, doi: 10.1016/S0141-3910(03)00124-1.

[5] J. Hu, X. Li, J. Gao, and Q. Zhao, “Ageing behavior of acrylic polyurethane varnish coating in artificial weathering environments,” *Prog. Org. Coat.*, vol. 65, no. 4, pp. 504–509, 2009, doi: 10.1016/j.porgcoat.2009.05.002.
[6] D. Y. Perera, “Physical ageing of organic coatings,” *Prog. Org. Coat.*, vol. 47, no. 1, pp. 61–76, 2003, doi: 10.1016/S0300-9440(03)00037-7.
[7] J. M. Hutchinson, “Physical aging of polymers,” *Prog. Polym. Sci.*, vol. 20, no. 4, pp. 703–760, 1995, doi: 10.1016/0079-6700(94)00001-I.
[8] D. Y. Perera, “Effect of thermal and hygroscopic history on physical ageing of organic coatings,” *Prog. Org. Coat.*, vol. 44, no. 1, pp. 55–62, 2002, doi: 10.1016/S0300-9440(01)00241-7.
[9] M. Johlitz, “On the Representation of Ageing Phenomena,” *J. Adhes.*, vol. 88, no. 7, pp. 620–648, 2012, doi: 10.1080/00218464.2012.682905.
[10] L. C. E. Struik, “The mechanical behaviour and physical ageing of semicrystalline polymers: 2,” *Polymer*, vol. 28, no. 9, pp. 1534–1542, 1987, doi: 10.1016/0032-3861(87)90354-5.
[11] J. N. Hay, “The physical ageing of amorphous and crystalline polymers,” *Pure Appl. Chem.*, vol. 67, no. 11, pp. 1855–1858, 1995, doi: 10.1351/pac199567111855.
[12] J. R. White, “Polymer ageing: physics, chemistry or engineering? Time to reflect,” *Comptes Rendus Chim.*, vol. 9, no. 11, pp. 1396–1408, 2006, doi: 10.1016/j.crci.2006.07.008.
[13] S. Etienne and L. David, “Long-term physical ageing of amorphous polymers,” *Philos. Mag.*, vol. 87, no. 3–5, pp. 417–424, 2007, doi: 10.1080/14786430600847107.
[14] P. H. Pfromm and W. J. Koros, “Accelerated physical ageing of thin glassy polymer films: evidence from gas transport measurements,” *Polymer*, vol. 36, no. 12, pp. 2379–2387, 1995, doi: 10.1016/0032-3861(95)97336-E.
[15] R. van der Linde, E. G. Belder, and D. Y. Perera, “Effect of physical aging and thermal stress on the behavior of polyester/TGIC powder coatings,” *Prog. Org. Coat.*, vol. 40, no. 1, pp. 215–224, 2000, doi: 10.1016/S0300-9440(00)00125-9.
[16] Y. Elkebir, S. Mallarino, D. Trinh, and S. Touzain, “Effect of physical ageing onto the water uptake in epoxy coatings,” *Electrochimica Acta*, vol. 337, p. 135766, 2020, doi: 10.1016/j.electacta.2020.135766.
[17] B. Quelennec, Z. Duan, R. Delannoy, N. Gay, M. Briffaut, V. Tognetti, N. Delpouve, L. Delbreilh, L. Bredif, A. Duthoit, *et al.*, “Effect of physical and chemical ageing on barrier properties of epoxy coating,” *Constr. Build. Mater.*, vol. 409, p. 133908, 2023, doi: 10.1016/j.conbuildmat.2023.133908.
[18] S. Bhargava, M. Kubota, R. D. Lewis, S. G. Advani, A. K. Prasad, and J. M. Deitzel, “Ultraviolet, water, and thermal aging studies of a waterborne polyurethane elastomer-based high reflectivity coating,” *Prog. Org. Coat.*, vol. 79, pp. 75–82, 2015, doi: 10.1016/j.porgcoat.2014.11.005.
[19] A. F. Abdelkader and J. R. White, “Influence of relative humidity on the development of internal stresses in epoxy resin based coatings,” *J. Mater. Sci.*, vol. 37, no. 22, pp. 4769–4773, 2002, doi: 10.1023/A:1020838919470.
[20] M. Ogata, N. Kinjo, and T. Kawata, “Effects of crosslinking on physical properties of phenol–formaldehyde novolac cured epoxy resins,” *J. Appl. Polym. Sci.*, vol. 48, no. 4, pp. 583–601, 1993, doi: 10.1002/app.1993.070480403.
[21] P. Mayer-Trzaskowska, M. Robakowska, Ł. Gierz, J. Pach, and E. Mazur, “Observation of the Effect of Aging on the Structural Changes of Polyurethane/Polyurea Coatings,” *Polymers*, vol. 16, no. 1, Art. no. 1, 2024, doi: 10.3390/polym16010023.
[22] V. Pintus, S. Wei, and M. Schreiner, “Accelerated UV ageing studies of acrylic, alkyd, and polyvinyl acetate paints: Influence of inorganic pigments,” *Microchem. J.*, vol. 124, pp. 949–961, 2016, doi: 10.1016/j.microc.2015.07.009.
[23] A. F. Abdelkader and J. R. White, “Comparison of internal stresses in coatings cured on rigid substrates and on unrestrained thin substrates,” *Prog. Org. Coat.*, vol. 44, no. 2, pp. 121–129, 2002, doi: 10.1016/S0300-9440(01)00251-X.
[24] D. O’Connor and F. D. Blum, “Thermal stability of substituted phenol-formaldehyde resins,” *J. Appl. Polym. Sci.*, vol. 33, no. 6, pp. 1933–1941, 1987, doi: 10.1002/app.1987.070330606.
[25] V. Pintus, A. Piccolo, W. Vetter, L. M. Moretto, K. Sterflinger, and M. Schreiner, “What about Phenol Formaldehyde (PF) Foam in Modern-Contemporary Art? Insights into the Unaged and Naturally Aged Material by a Multi-Analytical Approach,” *Polymers*, vol. 13, no. 12, Art. no. 12, 2021, doi: 10.3390/polym13121964.
[26] Y. Yu, P. Xu, M. Chang, and J. Chang, “Aging Properties of Phenol-Formaldehyde Resin Modified by Bio-Oil Using UV Weathering,” *Polymers*, vol. 10, no. 11, Art. no. 11, 2018, doi: 10.3390/polym10111183.

[27] B. Strzemiecka, J. Zięba-Palus, A. Voelkel, T. Lachowicz, and E. Socha, "Examination of the chemical changes in cured phenol-formaldehyde resins during storage," *J. Chromatogr. A*, vol. 1441, pp. 106–115, 2016, doi: 10.1016/j.chroma.2016.02.051.
[28] D.-D. Guo, M.-S. Zhan, and K. Wang, "Microstructure evolution of ammonia-catalyzed phenolic resin during thermooxidative aging," *J. Appl. Polym. Sci.*, vol. 126, no. 6, pp. 2010–2016, 2012, doi: 10.1002/app.36550.
[29] D. V. Okhrimenko, A. B. Thomsen, M. Ceccato, D. B. Johansson, D. Lybye, K. Bechgaard, S. Tougaard, and S. L. S. Stipp, "Impact of curing time on ageing and degradation of phenol-urea-formaldehyde binder," *Polym. Degrad. Stab.*, vol. 152, pp. 86–94, 2018, doi: 10.1016/j.polymdegradstab.2018.04.001.
[30] S. Kowatsch, "Mineral Wool Insulation Binders," in *Phenolic Resins: A Century of Progress*, L. Pilato, Ed., Berlin, Heidelberg: Springer, 2010, pp. 209–242. doi: 10.1007/978-3-642-04714-5_10.
[31] A. Blaakmeer, "Plant growth substrates," WO2001082683A1, 2001 Accessed: 2024. [Online]. Available: https://patents.google.com/patent/WO2001082683A1/en?oq=WO+01%2f82683+
[32] T. A. Thorstenson, J. B. Huang, M. W. Urban, and K. Haubennestel, "Mobility and distribution of silicone additives in coatings; a spectroscopic study," *Prog. Org. Coat.*, vol. 24, no. 1, pp. 341–358, 1994, doi: 10.1016/0033-0655(94)85024-0.
[33] K. W. Evanson and M. W. Urban, "Surface and interfacial FTIR spectroscopic studies of latexes. III. The effects of substrate surface tension and elongation on exudation of surfactants," *J. Appl. Polym. Sci.*, vol. 42, no. 8, pp. 2309–2320, 1991, doi: 10.1002/app.1991.070420822.
[34] E. Kientz and Y. Holl, "Distribution of surfactants in latex films," *Colloids Surf. Physicochem. Eng. Asp.*, vol. 78, pp. 255–270, 1993, doi: 10.1016/0927-7757(93)80331-8.
[35] B. C. Bunker, "Molecular mechanisms for corrosion of silica and silicate glasses," *J. Non-Cryst. Solids*, vol. 179, pp. 300–308, 1994, doi: 10.1016/0022-3093(94)90708-0.
[36] B. M. J. Smets, "On the mechanism of the corrosion of glass by water," *Philips Tech. Rev.*, vol. 42, no. 2, pp. 59–64, 1985.
[37] B. M. J. Smets, M. G. W. Tholen, and T. P. A. Lommen, "The effect of divalent cations on the leaching kinetics of glass," *J. Non-Cryst. Solids*, vol. 65, no. 2, pp. 319–332, 1984, doi: 10.1016/0022-3093(84)90056-5.
[38] L. R. Pederson, D. R. Baer, G. L. McVay, and M. H. Engelhard, "Reaction of soda lime silicate glass in isotopically labelled water," *J. Non-Cryst. Solids*, vol. 86, no. 3, pp. 369–380, 1986, doi: 10.1016/0022-3093(86)90025-6.
[39] N. Sheth, J. Luo, J. Banerjee, C. G. Pantano, and S. H. Kim, "Characterization of surface structures of dealkalized soda lime silica glass using X-ray photoelectron, specular reflection infrared, attenuated total reflection infrared and sum frequency generation spectroscopies," *J. Non-Cryst. Solids*, vol. 474, pp. 24–31, 2017, doi: 10.1016/j.jnoncrysol.2017.08.009.
[40] S. Amma, S. H. Kim, and C. G. Pantano, "Analysis of Water and Hydroxyl Species in Soda Lime Glass Surfaces Using Attenuated Total Reflection (ATR)-IR Spectroscopy," *J. Am. Ceram. Soc.*, vol. 99, no. 1, pp. 128–134, 2016, doi: 10.1111/jace.13856.
[41] T. Akai, K. Kuraoka, D. Chen, Y. Yamamoto, T. Shirakami, K. Urabe, and T. Yazawa, "Leaching Behavior of Sodium from Fine Particles of Soda–Lime–Silicate Glass in Acid Solution," *J. Am. Ceram. Soc.*, vol. 88, no. 10, pp. 2962–2965, 2005, doi: 10.1111/j.1551-2916.2005.00524.x.
[42] S. Gin, P. Jollivet, M. Fournier, F. Angeli, P. Frugier, and T. Charpentier, "Origin and consequences of silicate glass passivation by surface layers," *Nat. Commun.*, vol. 6, no. 1, p. 6360, 2015, doi: 10.1038/ncomms7360.
[43] S. Gin, P. Jollivet, M. Fournier, C. Berthon, Z. Wang, A. Mitroshkov, Z. Zhu, and J. V. Ryan, "The fate of silicon during glass corrosion under alkaline conditions: A mechanistic and kinetic study with the International Simple Glass," *Geochim. Cosmochim. Acta*, vol. 151, pp. 68–85, 2015, doi: 10.1016/j.gca.2014.12.009.
[44] T. A. Abrajano, J. K. Bates, and J. J. Mazer, "Aqueous corrosion of natural and nuclear waste glasses II. Mechanisms of vapor hydration of nuclear waste glasses," *J. Non-Cryst. Solids*, vol. 108, no. 3, pp. 269–288, 1989, doi: 10.1016/0022-3093(89)90297-4.
[45] T. A. Abrajano, J. K. Bates, and C. D. Byers, "Aqueous corrosion of natural and nuclear waste glasses I. Comparative rates of hydration in liquid and vapor environments at elevated temperatures," *J. Non-Cryst. Solids*, vol. 84, no. 1, pp. 251–257, 1986, doi: 10.1016/0022-3093(86)90783-0.
[46] H. V. Walters and P. B. Adams, "Effects of humidity on the weathering of glass," *J. Non-Cryst. Solids*, vol. 19, pp. 183–199, 1975, doi: 10.1016/0022-3093(75)90084-8.

[47] F. Alloteau, O. Majérus, V. Valbi, I. Biron, P. Lehuédé, D. Caurant, T. Charpentier, and A. Seyeux, “Evidence for different behaviors of atmospheric glass alteration as a function of glass composition,” *Npj Mater. Degrad.*, vol. 4, no. 1, pp. 1–11, 2020, doi: 10.1038/s41529-020-00138-1.
[48] R. Zanini, G. Franceschin, E. Cattaruzza, and A. Traviglia, “A review of glass corrosion: the unique contribution of studying ancient glass to validate glass alteration models,” *Npj Mater. Degrad.*, vol. 7, no. 1, pp. 1–17, 2023, doi: 10.1038/s41529-023-00355-4.
[49] O. Majérus, P. Lehuédé, I. Biron, F. Alloteau, S. Narayanasamy, and D. Caurant, “Glass alteration in atmospheric conditions: crossing perspectives from cultural heritage, glass industry, and nuclear waste management,” *Npj Mater. Degrad.*, vol. 4, no. 1, pp. 1–16, 2020, doi: 10.1038/s41529-020-00130-9.
[50] E. Laso, M. Aparicio, and T. Palomar, “Influence of humidity in the alteration of unstable glasses,” *Int. J. Appl. Glass Sci.*, vol. 15, no. 1, pp. 88–103, 2024, doi: 10.1111/ijag.16641.
[51] R. H. Doremus, “Diffusion-controlled reaction of water with glass,” *J. Non-Cryst. Solids*, vol. 55, no. 1, pp. 143–147, 1983, doi: 10.1016/0022-3093(83)90014-5.
[52] B. Smets and T. Lommen, “The leaching of sodium containing glasses: ion exchange or diffusion of molecular water?,” *J. Phys. Colloq.*, vol. 43, no. C9, p. C9, 1982, doi: 10.1051/jphyscol:19829129.
[53] I. S. T. Tsong, C. A. Houser, W. B. White, G. L. Power, and S. S. C. Tong, “Glass leaching studies by sputter-induced photon spectrometry (SIPS),” *J. Non-Cryst. Solids*, vol. 38–39, pp. 649–654, 1980, doi: 10.1016/0022-3093(80)90510-4.
[54] W. A. Lanford, K. Davis, P. Lamarche, T. Laursen, R. Groleau, and R. H. Doremus, “Hydration of soda-lime glass,” *J. Non-Cryst. Solids*, vol. 33, no. 2, pp. 249–266, 1979, doi: 10.1016/0022-3093(79)90053-X.
[55] S. H. Hahn and A. C. T. van Duin, “Surface Reactivity and Leaching of a Sodium Silicate Glass under an Aqueous Environment: A ReaxFF Molecular Dynamics Study,” *J. Phys. Chem. C*, vol. 123, no. 25, pp. 15606–15617, 2019, doi: 10.1021/acs.jpcc.9b02940.
[56] S. H. Hahn, J. Rimsza, L. Criscenti, W. Sun, L. Deng, J. Du, T. Liang, S. B. Sinnott, and A. C. T. van Duin, “Development of a ReaxFF Reactive Force Field for NaSiOx/Water Systems and Its Application to Sodium and Proton Self-Diffusion,” *J. Phys. Chem. C*, vol. 122, no. 34, pp. 19613–19624, 2018, doi: 10.1021/acs.jpcc.8b05852.
[57] E. K. Faulkner, R. K. Whitney, and J. E. Zeman, “Alkali extraction as a determinant in the selection of a glass for displays,” *IEEE Trans. Electron Devices*, vol. 30, no. 5, 1983, doi: 10.1109/T-ED.1983.21164.
[58] E. Jørgensen, “‘Grodan’ stone wool as medium for propagation and culture,” *Acta Hortic.*, no. 54, Art. no. 54, 1975, doi: 10.17660/ActaHortic.1975.54.18.
[59] L. Greenspan, “Humidity Fixed Points of Binary Saturated Aqueous Solutions,” *J. Res. Natl. Bur. Stand. Sect. Phys. Chem.*, vol. 81A, no. 1, pp. 89–96, 1977, doi: 10.6028/jres.081A.011.
[60] J. Crank and G. S. Park, *Diffusion in polymers*, 2nd print. London: Academic Press, 1975.
[61] W. R. Brown, R. B. Jenkins, and G. S. Park, “The sorption and diffusion of small molecules in amorphous and crystalline polybutadienes,” *J. Polym. Sci. Polym. Symp.*, vol. 41, no. 1, pp. 45–67, 1973, doi: 10.1002/polc.5070410107.
[62] G. S. Park, “Transport Principles—Solution, Diffusion and Permeation in Polymer Membranes,” in *Synthetic Membranes: Science, Engineering and Applications*, P. M. Bungay, H. K. Lonsdale, and M. N. de Pinho, Eds., Dordrecht: Springer Netherlands, 1986, pp. 57–107. doi: 10.1007/978-94-009-4712-2_3.
[63] R. L. Hendrikse, A. E. Bayly, and P. K. Jimack, “Studying the Structure of Sodium Lauryl Ether Sulfate Solutions Using Dissipative Particle Dynamics,” *J. Phys. Chem. B*, vol. 126, no. 40, pp. 8058–8071, 2022, doi: 10.1021/acs.jpcb.2c04329.
[64] A. S. Poulos, C. S. Jones, and J. T. Cabral, “Dissolution of anionic surfactant mesophases,” *Soft Matter*, vol. 13, no. 31, pp. 5332–5340, 2017, doi: 10.1039/C7SM01096F.
[65] A. Capaccio, S. Caserta, S. Guido, G. Rusciano, and A. Sasso, “Dissolution of a surfactant-water lamellar phase investigated by combining time-lapse polarized light microscopy and confocal Raman spectroscopy,” *J. Colloid Interface Sci.*, vol. 561, pp. 136–146, 2020, doi: 10.1016/j.jcis.2019.11.092.
[66] A. Sein, J. B. F. N. Engberts, E. van der Linden, and J. C. van de Pas, “Lyotropic Phases of Dodecylbenzenesulfonates with Different Counterions in Water,” *Langmuir*, vol. 12, no. 12, pp. 2913–2923, 1996, doi: 10.1021/la9510745.
[67] R. B. Viana, A. B. F. da Silva, and A. S. Pimentel, “Infrared Spectroscopy of Anionic, Cationic, and Zwitterionic Surfactants,” *Adv. Phys. Chem.*, vol. 2012, p. e903272, 2012, doi: 10.1155/2012/903272.

[68] A. J. Prosser and E. I. Franses, “Infrared Reflection Absorption Spectroscopy (IRRAS) of Aqueous Nonsurfactant Salts, Ionic Surfactants, and Mixed Ionic Surfactants,” *Langmuir*, vol. 18, no. 24, pp. 9234–9242, 2002, doi: 10.1021/la020568g.

[69] S. S. Lin, A. L. Hsieh, D. B. S. Min, and S. S. Chang, “A study of the color stability of commercial oleic acid,” *J. Am. Oil Chem. Soc.*, vol. 53, no. 4, pp. 157–161, 1976, doi: 10.1007/BF02586356.

[70] D. B. S. Min, S. S. Lin, and S. S. Chang, “Study of color stability of tall oil fatty acids through isolation and characterization of minor constituents,” *J. Am. Oil Chem. Soc.*, vol. 52, no. 2, pp. 28–33, 1975, doi: 10.1007/BF02901816.

[71] S. S. Lin, Y. Murase, D. B. S. Min, O. A. L. Hsieh, and S. S. Chang, “Characterization of minor constituents in commercial oleic acid,” *J. Am. Oil Chem. Soc.*, vol. 59, no. 1, pp. 42–46, 1982, doi: 10.1007/BF02670066.

[72] S. S. Lin, Y. Murase, D. B. S. Min, O. A. L. Hsieh, and S. S. Chang, “Qualitative and quantitative comparison of minor constituents in different commercial oleic acids,” *J. Am. Oil Chem. Soc.*, vol. 59, no. 1, pp. 50–51, 1982, doi: 10.1007/BF02670068.

[73] H. W. Lochte, E. L. Strauss, and R. T. Conley, “The thermo-oxidative degradation of phenol–formaldehyde polycondensates: Thermogravimetric and elemental composition studies of char formation,” *J. Appl. Polym. Sci.*, vol. 9, no. 8, pp. 2799–2810, 1965, doi: 10.1002/app.1965.070090814.

[74] H. Zhang, W. Gu, Y. J. Li, and M. Tang, “Hygroscopic properties of sodium and potassium salts as related to saline mineral dusts and sea salt aerosols,” *J. Environ. Sci.*, vol. 95, pp. 65–72, 2020, doi: 10.1016/j.jes.2020.03.046.

[75] C. Peng, L. Chen, and M. Tang, “A database for deliquescence and efflorescence relative humidities of compounds with atmospheric relevance,” *Fundam. Res.*, vol. 2, no. 4, pp. 578–587, 2022, doi: 10.1016/j.fmre.2021.11.021.

[76] B. Jing, C. Peng, Y. Wang, Q. Liu, S. Tong, Y. Zhang, and M. Ge, “Hygroscopic properties of potassium chloride and its internal mixtures with organic compounds relevant to biomass burning aerosol particles,” *Sci. Rep.*, vol. 7, no. 1, p. 43572, 2017, doi: 10.1038/srep43572.

[77] Y.-Y. Chen and W.-M. G. Lee, “The Effect of Surfactants on the Deliquescence of Sodium Chloride,” *J. Environ. Sci. Health Part A*, vol. 36, no. 2, pp. 229–242, 2001, doi: 10.1081/ESE-100102620.

[78] O. Vyavahare, D. Ng, and S. L. Hsu, “Analysis of Structural Rearrangements of Poly(lactic acid) in the Presence of Water,” *J. Phys. Chem. B*, vol. 118, no. 15, pp. 4185–4193, 2014, doi: 10.1021/jp500219j.

[79] W. Zhao, S. L. Hsu, S. Ravichandran, and A. M. Bonner, “Moisture Effects on the Physical Properties of Cross-linked Phenolic Resins,” *Macromolecules*, vol. 52, no. 9, pp. 3367–3375, 2019, doi: 10.1021/acs.macromol.9b00385.

[80] P. W. King, R. H. Mitchell, and A. R. Westwood, “Structural analysis of phenolic resole resins,” *J. Appl. Polym. Sci.*, vol. 18, no. 4, pp. 1117–1130, 1974, doi: 10.1002/app.1974.070180412.

[81] H. Hu, W. Wang, L. Jiang, L. Liu, Y. Zhang, Y. Yang, and J. Wang, “Curing mechanism of resole phenolic resin based on variable temperature FTIR spectra and thermogravimetry-mass spectrometry,” *Polym. Polym. Compos.*, vol. 30, p. 09673911221102114, 2022, doi: 10.1177/09673911221102114.

[82] M. A. Villegas and L. Pascual, “Sol–gel silica coatings doped with a pH-sensitive chromophore,” *Thin Solid Films*, vol. 351, no. 1, pp. 103–108, 1999, doi: 10.1016/S0040-6090(98)01786-6.

[83] Q. Zhang, S. Zhang, S. Liu, X. Ma, L. Lu, and Y. Deng, “Ionic liquid-modified dyes and their sensing performance toward acids in aqueous and non-aqueous solutions,” *Analyst*, vol. 136, no. 7, pp. 1302–1304, 2011, doi: 10.1039/C0AN00885K.

[84] L. M. Jensen, “Production of mineral fibers,” US20100058810A1, 2010 Accessed: 2024. [Online]. Available: https://patents.google.com/patent/US20100058810/en

[85] H. Aréna, D. Rébiscoul, R. Podor, E. Garcès, M. Cabie, J.-P. Mestre, and N. Godon, “Impact of Fe, Mg and Ca elements on glass alteration: Interconnected processes,” *Geochim. Cosmochim. Acta*, vol. 239, pp. 420–445, 2018, doi: 10.1016/j.gca.2018.08.007.

[86] S. Gin, X. Beaudoux, F. Angéli, C. Jégou, and N. Godon, “Effect of composition on the short-term and long-term dissolution rates of ten borosilicate glasses of increasing complexity from 3 to 30 oxides,” *J. Non-Cryst. Solids*, vol. 358, no. 18, pp. 2559–2570, 2012, doi: 10.1016/j.jnoncrysol.2012.05.024.

[87] J. Hopf, S. N. Kerisit, F. Angeli, T. Charpentier, J. P. Icenhower, B. P. McGrail, C. F. Windisch, S. D. Burton, and E. M. Pierce, “Glass–water interaction: Effect of high-valence cations on glass structure and chemical durability,” *Geochim. Cosmochim. Acta*, vol. 181, pp. 54–71, 2016, doi: 10.1016/j.gca.2016.02.023.

[88] D. Wolff-Boenisch, S. R. Gislason, E. H. Oelkers, and C. V. Putnis, "The dissolution rates of natural glasses as a function of their composition at pH 4 and 10.6, and temperatures from 25 to 74°C," *Geochim. Cosmochim. Acta*, vol. 68, no. 23, pp. 4843–4858, 2004, doi: 10.1016/j.gca.2004.05.027.
[89] A. Bera, K. Ojha, and A. Mandal, "Synergistic Effect of Mixed Surfactant Systems on Foam Behavior and Surface Tension," *J. Surfactants Deterg.*, vol. 16, no. 4, pp. 621–630, 2013, doi: 10.1007/s11743-012-1422-4.
[90] V. B. Fainerman, R. Miller, and E. V. Aksenenko, "Simple model for prediction of surface tension of mixed surfactant solutions," *Adv. Colloid Interface Sci.*, vol. 96, no. 1, pp. 339–359, 2002, doi: 10.1016/S0001-8686(01)00088-4.
[91] S. Tiwari, S. Namsani, and J. K. Singh, "Effect of salt on the adsorption of ionic surfactants at the air-water interface," *J. Mol. Liq.*, vol. 360, p. 119498, 2022, doi: 10.1016/j.molliq.2022.119498.
[92] A. S. Rafique, S. Khodaparast, A. S. Poulos, W. N. Sharratt, E. S. J. Robles, and J. T. Cabral, "Micellar structure and transformations in sodium alkylbenzenesulfonate (NaLAS) aqueous solutions: effects of concentration, temperature, and salt," *Soft Matter*, vol. 16, no. 33, pp. 7835–7844, 2020, doi: 10.1039/D0SM00982B.
[93] Y. Lin, W. Tang, P. Xiao, J. Ma, X. Han, X. Xu, J. Luo, and S. Zhao, "Synergistic Effect of Salt and Anionic Surfactants on Interfacial Tension Reduction: Insights from Molecular Dynamics Simulations," *Langmuir*, vol. 39, no. 35, pp. 12392–12401, 2023, doi: 10.1021/acs.langmuir.3c01558.

Appendices

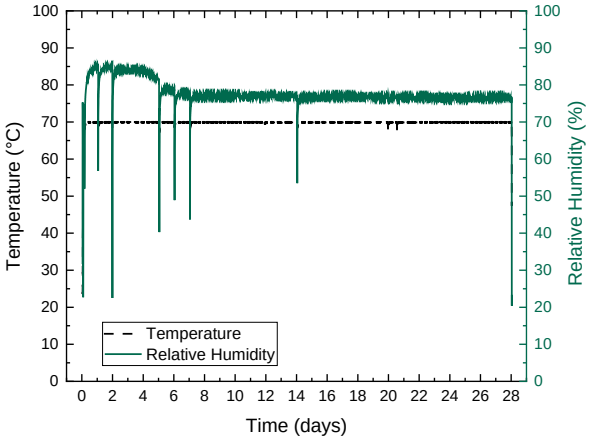


Figure A4.1. Relative humidity and temperature within the desiccator with saturated NaCl solution and samples of EFA, AES and BAS. Sudden drops and subsequent increases in the relative humidity are due to opening and closing of the desiccator to take samples. An increased relative humidity for the first 5 days is likely due to the evaporation of water from BAS and AES.

Thermal Stability of Wetting Agents

The thermal stability of the wetting agents was initially determined at conditions not necessarily close to curing conditions by thermogravimetric measurements (Figure A4.2a). For the anionic WAs, water was evaporated before the temperature ramp by keeping samples at 120 °C for 60 min. The mass at the end of this isothermal step was set to 100%.

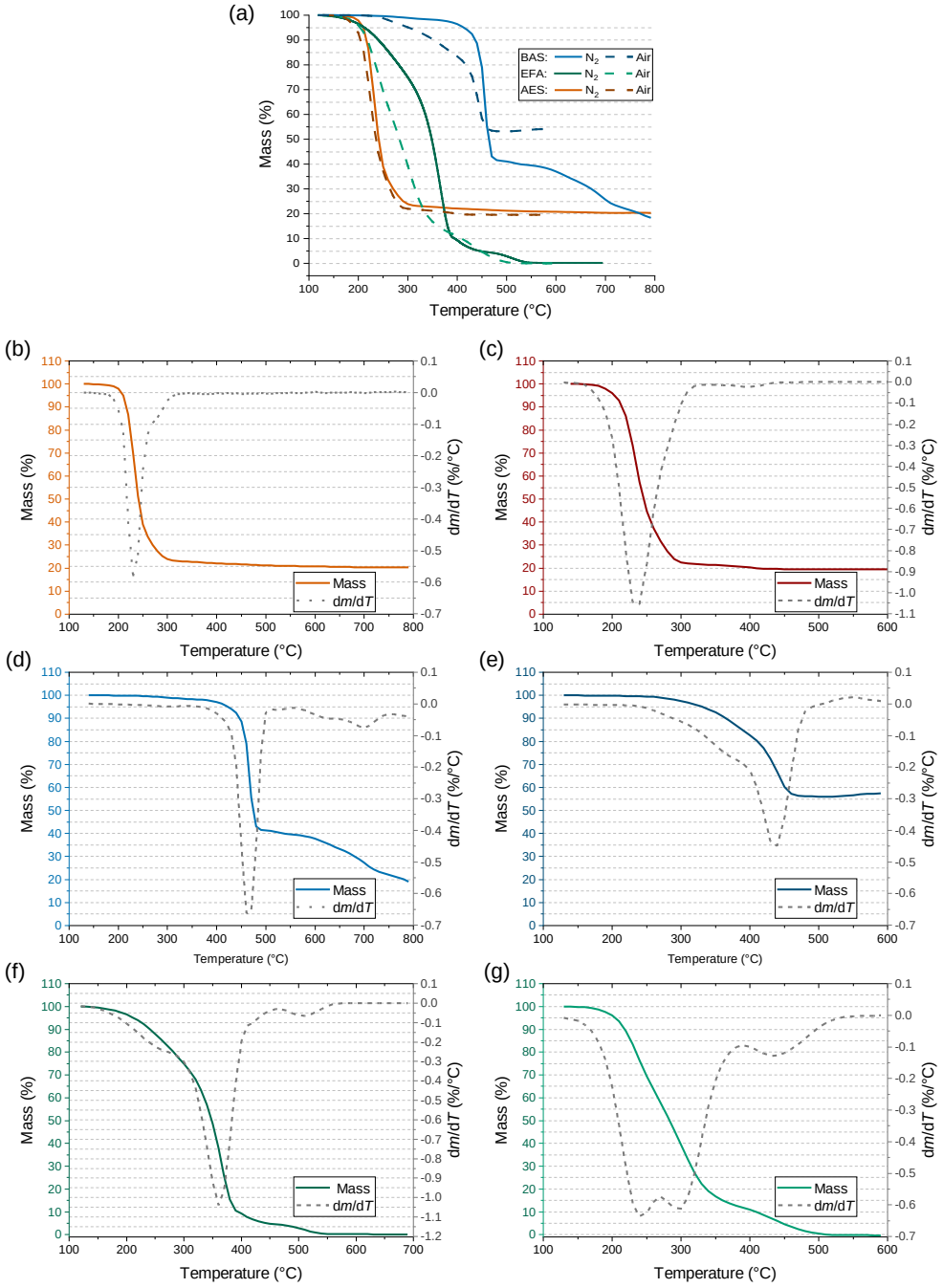


Figure A4.2. (a) Mass change of WAs as function of temperature. Measurements were performed under inert N_2 and air atmosphere. Due to machine limitations, the temperature range was not the same for all samples. Also shown are the same curves together with their corresponding curve of the derivative of mass over temperature (d*m*/d*T*) for (b) AES in N_2, (c) AES in air, (d) BAS in N_2, (e) BAS in air, (f) EFA in N_2, and (g) EFA in air.

While AES and EFA appear to be already slightly starting to degrade just below of 200 °C under inert N_2 atmosphere, BAS remains stable until 400 °C. The degradation profiles for AES are similar to that reported in literature for SDS [A1]. In case of exposure of EFA and AES to air, the onset of degradation is at a lower temperature compared to when the measurements are carried out under N_2 atmosphere (Figure A4.2b–c and A4.2f–g). An oxygen-rich environment accelerates the decomposition of EFA and BAS, although significant degradation still occurs at temperatures higher than for AES.

Chemical changes of the WAs due to thermal exposure are not readily expected based on TGA, but to verify and substantiate these results WAs were subjected to 200 °C, which is a common curing condition for phenolic resins. Typical curing times are approximately 10 minutes, but an extension of this time was chosen whenever possible to test the stability of wetting agents in a more extreme case. For AES, this did not appear to be possible, as longer exposure times resulted in clear degradation of the sample (Figure A4.3). This is corroborated by the results of the TGA, where 200 °C is the onset of a steep mass decrease within a relatively small temperature window. AES was therefore aged for a shorter time period, and additionally at a lower temperature of 150 °C.

Although EFA also shows signs of degradation starting from 200 °C (Figure A4.2), this degradation is more gradual over a broader temperature range. In case of EFA, both an as-received sample was used, and one to which water was added. This was done to study the possibility of hydrolysis occurring under the above-mentioned ageing conditions.

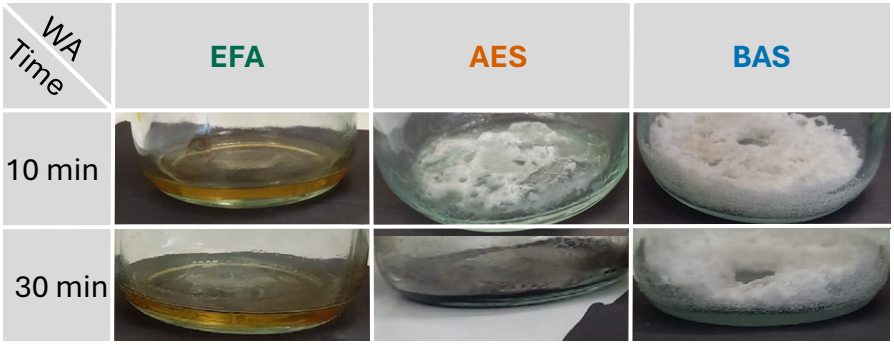


Figure A4.3. Physical changes of WAs after exposure to 200 °C for 10 or 30 minutes in air.

Chemical differences of WAs were monitored after the thermal exposure (Figure A4.4). An overview of the most important signals in the ATR-FTIR spectra are given in Tables A4.1–3. The peak assignment for WA signals in the ^{1}H-NMR spectra can be found in Chapter 3. Both AES samples which were unaged and freeze-dried, and those exposed

to 200 °C for 10 min showed a more detailed ATR-FTIR spectrum than the reference samples. In part, this is due to the absence of water from these samples.

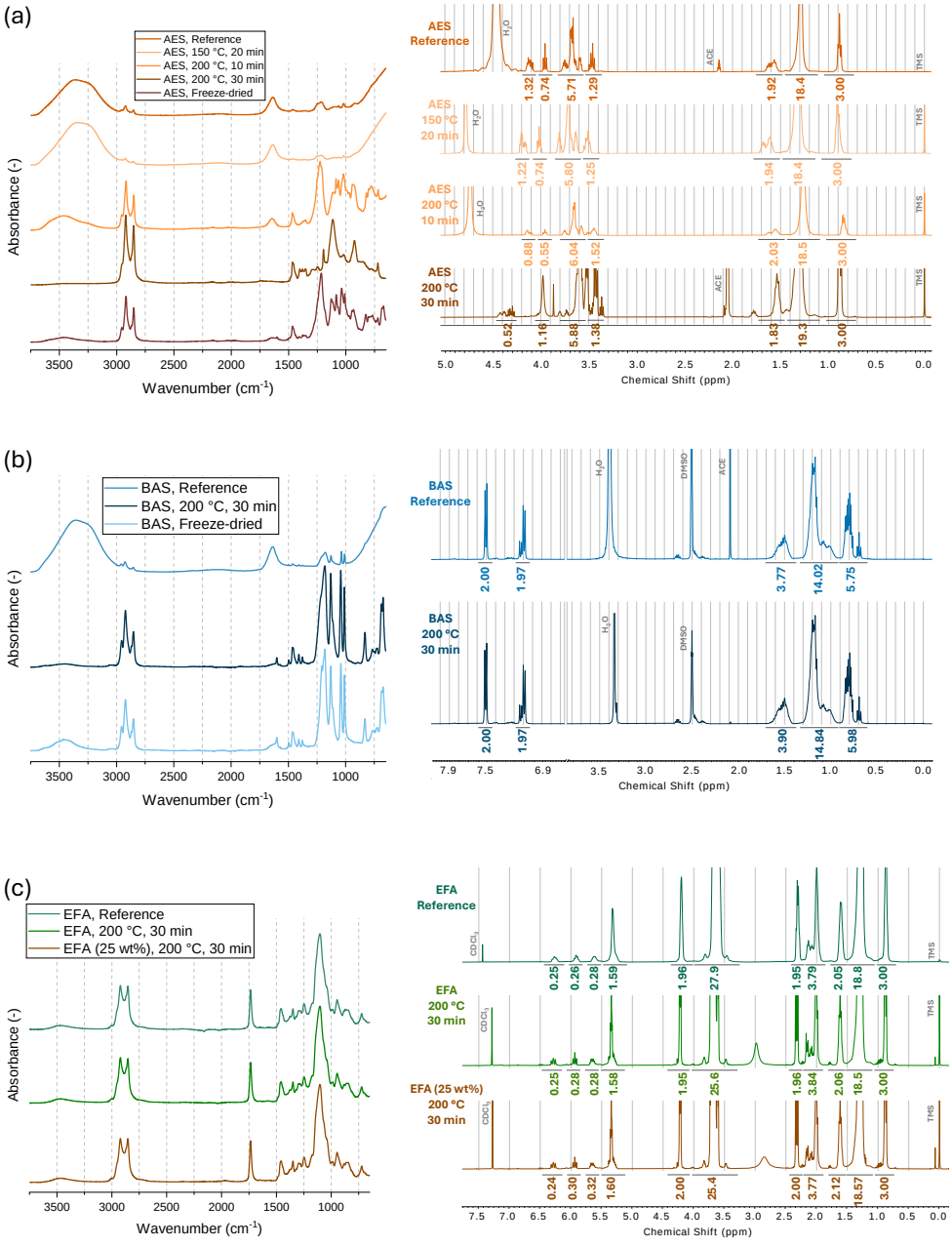


Figure A4.4. ATR-FTIR and ^{1}H-NMR spectra of (a) AES, (b) BAS, and (c) EFA before and after exposure to 200 °C.

Furthermore, for dodecyl sulphate (SDS) in water, which is relatively similar to AES, the concentration and temperature will change the conformation and packing density of SDS, which is seen from differences in FTIR spectra [A2-A4]. The corresponding ^{1}H-NMR spectra show only small differences relative to pristine AES, apart from the two signals between 4.0–4.2 ppm. These signals are attributed to the carbon adjacent to the sulphate headgroup, for which the decrease in integral would imply the occurrence of hydrolysis. Thermal decomposition of SLES and SDS can lead to the formation of dodecane, dodecane ethers, dodecanol, and mixtures thereof [A5,A6]. Based on the FTIR and ^{1}H-NMR spectra of AES held at 200 °C for 10 min, the formation of dodecanol cannot be excluded; the FTIR spectrum shows the presence of hydroxyl moieties and ^{1}H-NMR is not necessarily reliable to detect alcohol functionalities, especially since D_2O was used as a solvent. AES exposed to 200 °C for 30 min, which turned black after the exposure period, shows signs of the presence of hydroxyl groups through the broad and sharp peak at 4 ppm in its ^{1}H-NMR spectrum. On the other hand, the FTIR spectrum does not readily indicate their presence. Yet, the decrease in intensity of the peaks associated with the sulphate headgroup (e.g., 1224 cm^{-1}) would seem to corroborate the decomposition of AES into for instance dodecanol.

Table A4.1. Peak assignment for the ATR-FTIR spectra of EFA, based on [A7].

Wavenumber (cm^{-1})	Vibration	Compound Class
3462	O-H stretch	Alcohol
2922	C-H stretch	Alkane
2854	C-H stretch	Alkane
1735	C=O stretch	Ester
1456	CH_2 scissoring	Alkane
1348	CH_2 wag	Ether
1248	CH_2 wag CH_2 twist	Alkane Ether
1103	CO/CC stretch	Ether
946	C-H bend	Alkene
873	CO/CC stretch	Ether
723	C-H bend	Alkene

Table A4.2. Peak assignment for the ATR-FTIR spectra of AES, based on [A2,A7].

Wavenumber (cm^{-1})	Vibration	Compound Class
3359	O-H stretch	Water
2955	C-H stretch	Alkane
2922	Asymmetric C-H stretch	Alkane
2853	Symmetric C-H stretch	Alkane
1637	H-O-H bend	Water
1466	CH_2 scissoring	Alkane
1215	Asymmetric SO_2 stretch	Primary alkyl sulphate salts
1084	Symmetric SO_2 stretch	Primary alkyl sulphate salts
1037	C-O-C stretch	Aliphatic Ethers
933	C-H stretch	Alkane

Table A4.3. Peak assignment for the ATR-FTIR spectra of BAS, based on [A7-A9].

Wavenumber (cm^{-1})	Vibration	Compound Class
3353	O-H stretch	Water
2956	C-H stretch	Alkane
2923	Asymmetric C-H stretch	Alkane
2853	Symmetric C-H stretch	Alkane
1637	H-O-H bend	Water
1464	CH_2 scissoring	Alkane
1625 – 1430	-C=C- stretch	Benzene
1182	Asymmetric $-SO3^-$ stretch	Sulphonate
1129	C-H bend	Benzene
1042	Symmetric $-SO3^-$ stretch	Sulphonate
1010	C-H bend	Benzene
832	$SO3^-$ stretch	(*para* substituted) benzenesulphonate

BAS and EFA remained unchanged after being exposed to 200 °C for 10 min (Figure A4.4 b–c). The appearance of a broader signal between 2.5–3.5 ppm is attributed to water presence in the $CDCl_3$ solvent, and therefore not indicative of possible hydrolysis having occurred during the thermal exposure. Although the appearance of EFA appears to be slightly darker in colour, chemical consequences of such a darkening (e.g., oxidation; see also the discussion in the main text) were not observed.

In most cases, no convincing effect of the thermal stability study on the chemistry of WAs was observed, despite the discoloration.

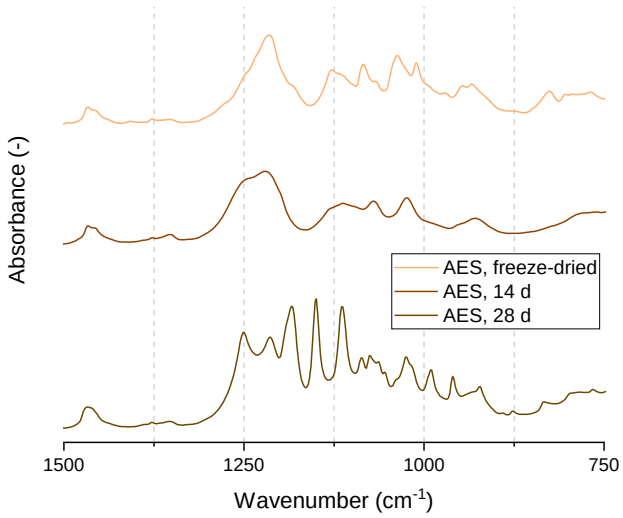


Figure A4.6. ATR-FTIR spectra of freeze-dried and aged AES. Ageing conditions were 75% RH and 70 °C.

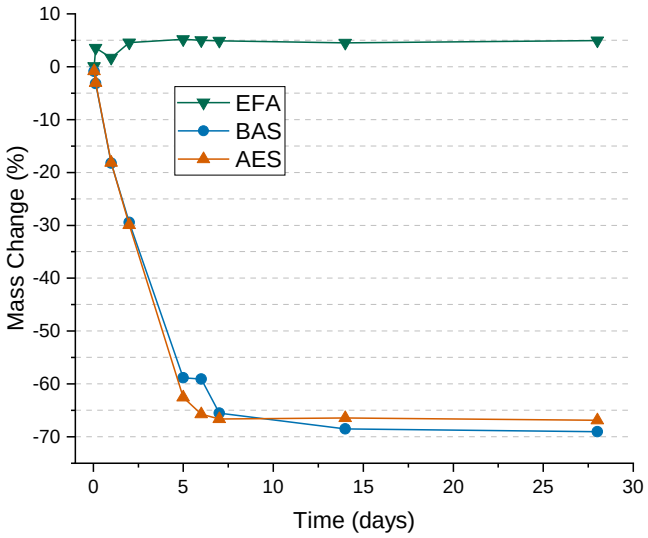


Figure A4.7. Mass change of wetting agents upon ageing by exposure to 70 °C and 75% RH for up to 28 days. BAS and AES decrease in mass on account of the evaporation of water. Only EFA absorbs water vapour.

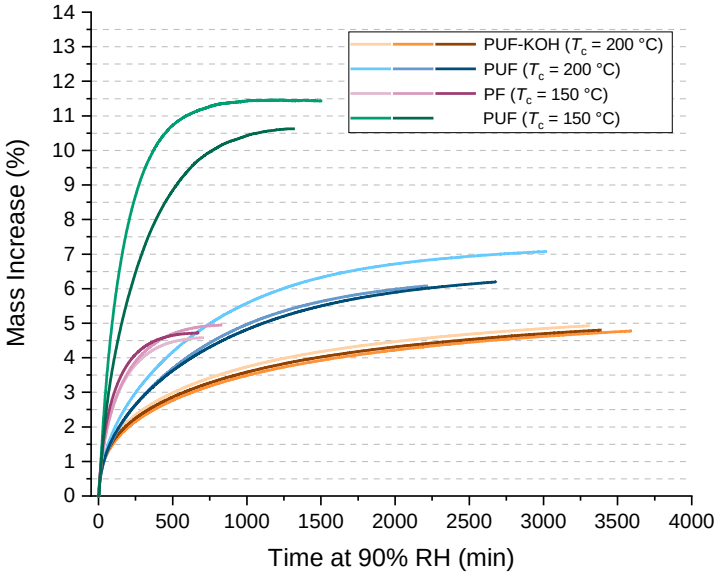


Figure A4.8. Mass increase of cured PUF-KOH, PF, and PUF powders (cured at either T_c = 200 °C for 10 min or T_c = 150 °C for 20 min) when exposed to 90% RH, as measured with DVS.

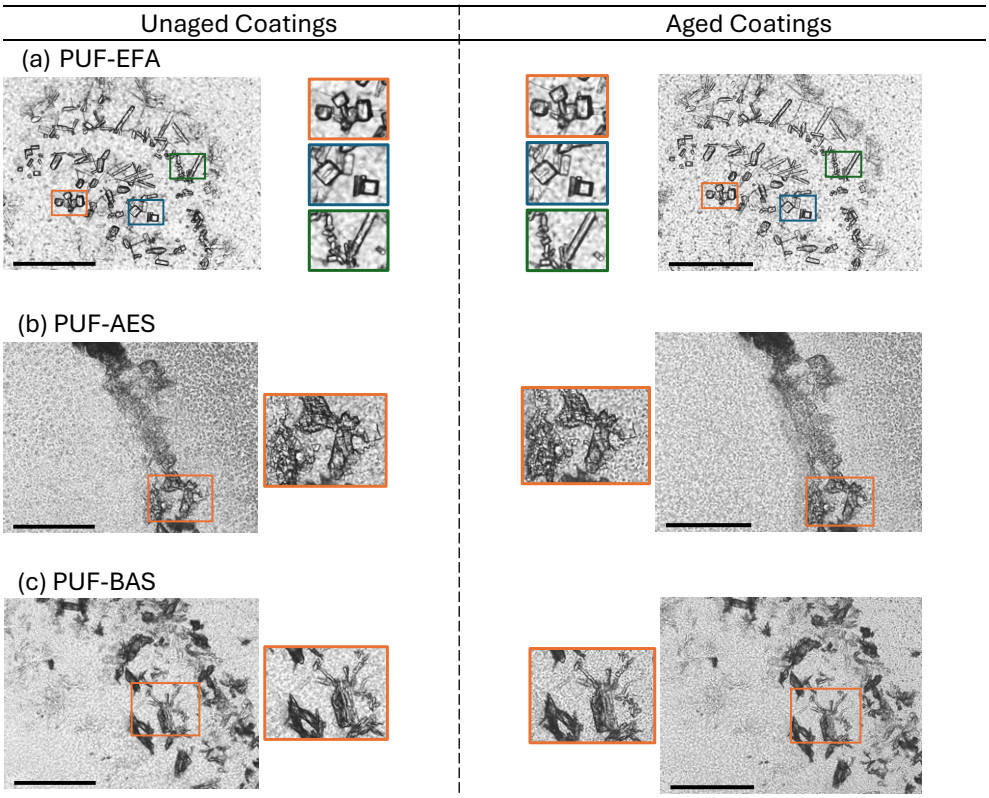


Figure A4.9. Optical micrographs of (a) PUF-EFA, (b) PUF-AES, and (c) PUF-BAS before and after storage at 75% RH and 70 °C for 117 days. Scale bar: 125 µm.

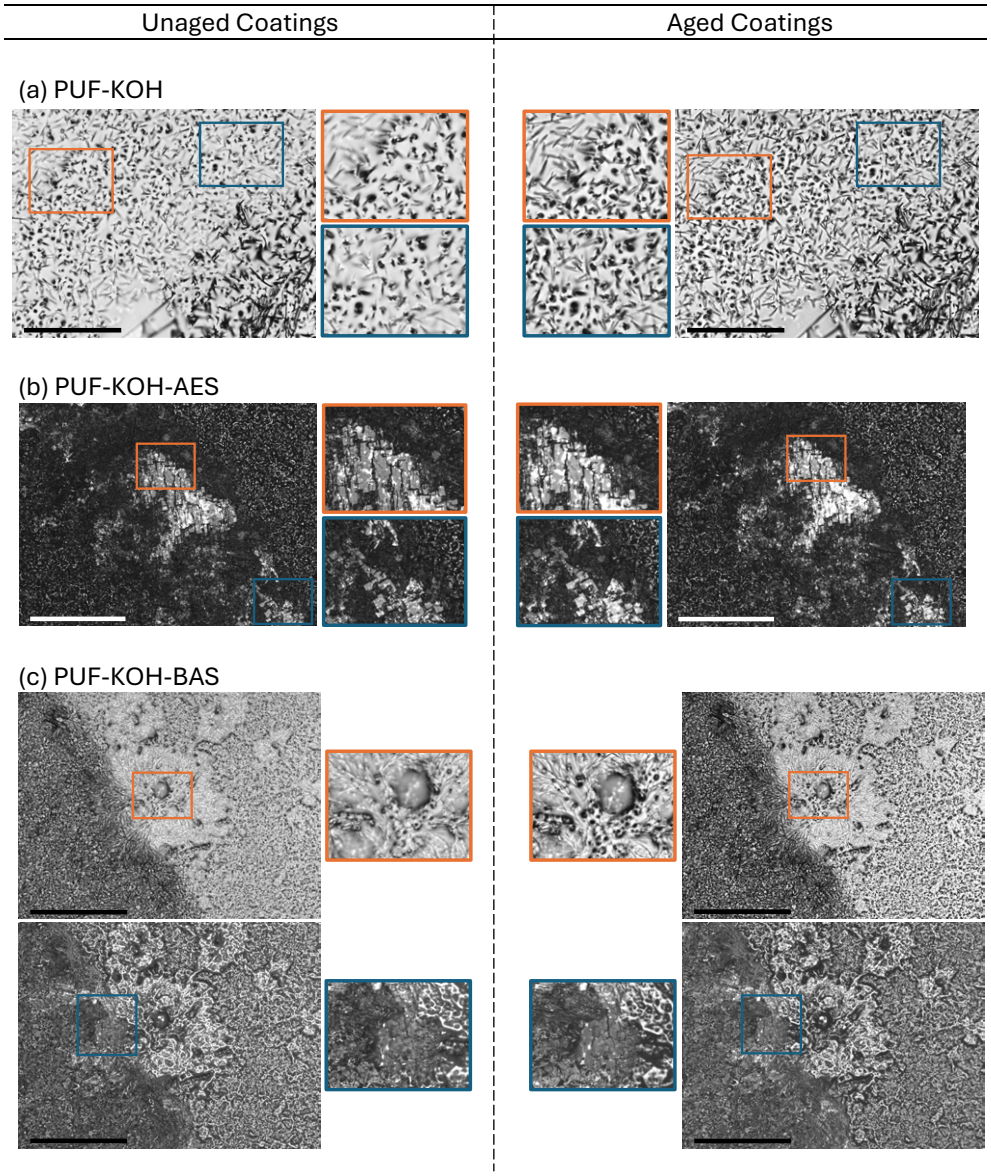


Figure 4.10. Optical micrographs of (a) PUF-KOH, (b) PUF-KOH-AES, and (c) PUF-KOH-BAS before and after storage at 75% RH and 70 °C for 117 days. Scale bar for (a): 50 µm. Scale bar for (b–c): 125 µm.

A Note on the Possibility of Leaching During Ageing

As mentioned in the main text, it could not be determined if the typical increase in sodium content for coatings on soda lime glass is a result of initial ion exchange and migration during dip-coating and curing, or also the result of continuous leaching due to the elevated relative humidity conditions. The former is to be reasonably expected on account of the relatively high water content of the resin (approximately 66 wt%) and the rapid acidification of the resin upon curing. The latter is dependent on the water-barrier properties of the applied PUF layer and the corrosion resistance of the glass substrate.

The diffusion of water vapour can be measured using dynamic vapour sorption (DVS), employing a Payne cell. Here, a free-standing film is clamped in between a headspace filled with drying agent and a lid with a hole in the middle. Exposing the outside of the cell and film to elevated relative humidity, and tracking the resulting mass changes, allows for the calculation of the diffusion coefficient.

Mass changes of PF and PUF powders and films were measured at 75% RH by dynamic vapour sorption (DVS; Figure A4.11). For PUF powders, the average mass change recorded was found to be 8.4% ± 0.8% and for PF the average mass change amounted to 4.2% ± 0.1% (Table A4.5). Especially PUF appeared to show a stronger affinity towards water vapour, likely on account of the more polar matrix due to the presence of urea moieties. Although the mass change for the PF and PUF films is similar, it is interesting to observe a quite low diffusion coefficient and permeability of PUF films compared to the PF films. This can be attributed to the polar nature of the bulk of the PUF film, which increases the interaction of water vapour with the film. The increased interactions with the material relative to PF films then would lead to an overall slower diffusion process. It should be noted that the determined permeability values for both PUF and PF are larger than what has been reported for Bakelite (0.6 $\frac{mg \cdot m}{bar \cdot m^2 \cdot min}$) in literature [A10]. However, processing and synthesis parameters influence the material properties of the final cured phenolic resin (see also Chapter 2), so a direct comparison is challenging to make.

Table A4.5. Mass change of PUF and PF powders and films upon exposure to 75% RH, and determined diffusion coefficient D, permeability P, and solubility S of water vapour through a P(U)F film.

Sample	Form	Δm_{75} (%)	D (cm^2/s)	P ($\frac{mg \cdot m}{bar \cdot m^2 \cdot min}$)	S ($\frac{mg}{bar \cdot m^3}$)
PUF	Film	1.2	$3.3 \cdot 10^{-10} \pm 1.0 \cdot 10^{-10}$	13.6 ± 1.0	$6.9 \cdot 10^{12} \pm 2.2 \cdot 10^{12}$
	Powder	8.4 ± 0.8	-	-	-
PF	Film	1.1	$4.1 \cdot 10^{-8} \pm 1.6 \cdot 10^{-8}$	107 ± 12	$4.4 \cdot 10^{11} \pm 1.8 \cdot 10^{11}$
	Powder	4.2 ± 0.1	-	-	-

As a final note, the silica gel with dye which was used in the headspace of the Payne cell was in all cases colourless, a direct result of the absorption of moisture. On the whole, there are indications of the possibility of moisture playing a role in the ion exchange and migration at the coating-substrate interface.

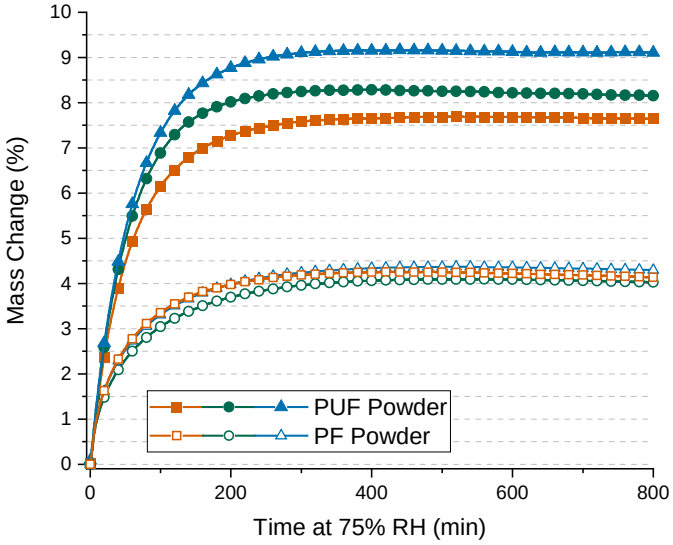


Figure 4.11. Mass change of PUF and PF powders when exposed to 75% relative humidity, as measured with DVS. Measurements were carried out at 25 °C.

Effect of substrate size on wettability

The most notable difference between the substrates is the size: stone melt wafers are pre-cut into 1 x 1 cm^2 pieces, whilst the total coated area of soda lime substrates is typically 2 x 5–6 cm^2.

When curing coatings on soda lime substrates of reduced size, often an increased average contact angle value was found compared to the normal-sized soda lime (Figure A5.12). Hence, it appears that the substrate size has a profound influence on the curing process and on the resulting surface chemistry of the coating. It is thought there are two possible factors contributing to this decreasing wettability with decreasing substrate size. First, smaller substrates have a lower total dipping time and as such experience draining forces for a smaller time relative to larger substrates. This way, coatings with a different thickness gradient are produced (5.2 µm ± 0.6 µm for coatings on stone melt wafers; 4.9 µm ± 1.5 µm for coatings on normal-sized soda lime). Second, the edge-to-area ratio is significantly different for the two samples. For coatings on SMWs, edge effects such as enhanced evaporation of solvent and TEA

could be more dominant, leading to a more advanced state of cure than could be seen for coatings on SL.

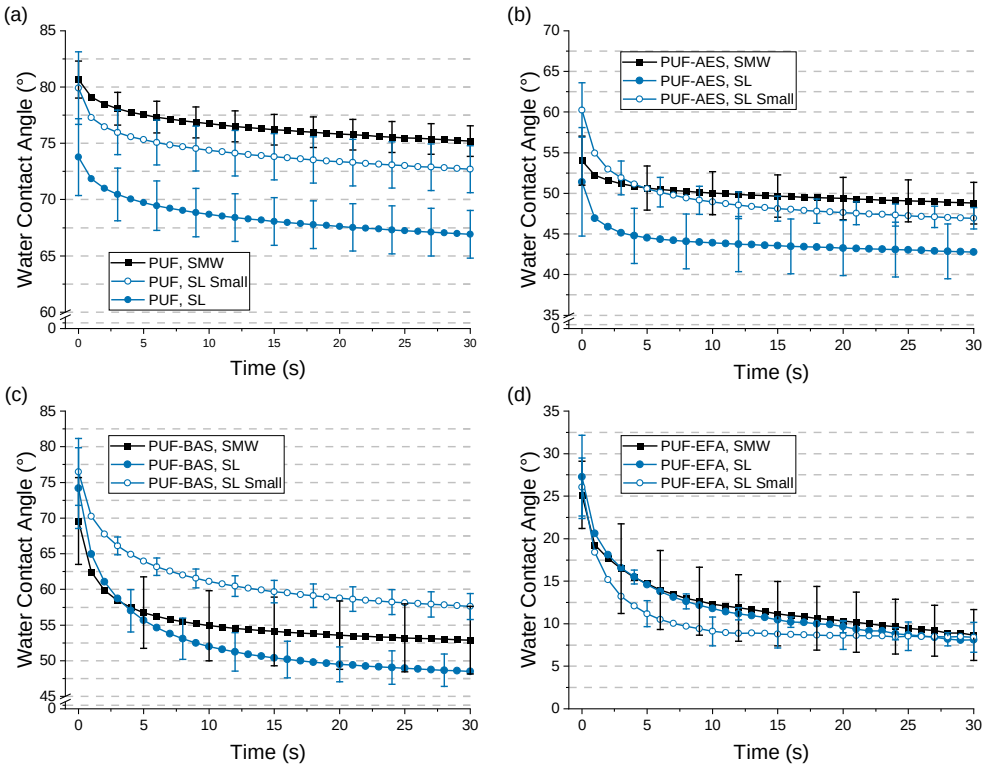


Figure A4.12. Average water contact angle value over time of (a) PUF, (b) PUF-AES, (c) PUF-BAS and (d) PUF-EFA coatings on stone melt wafers (SMW; 1 x 1 cm), soda lime (SL; 2.5 x 5 cm) and cut soda lime (SL Small; 1 x 1 cm) substrates.

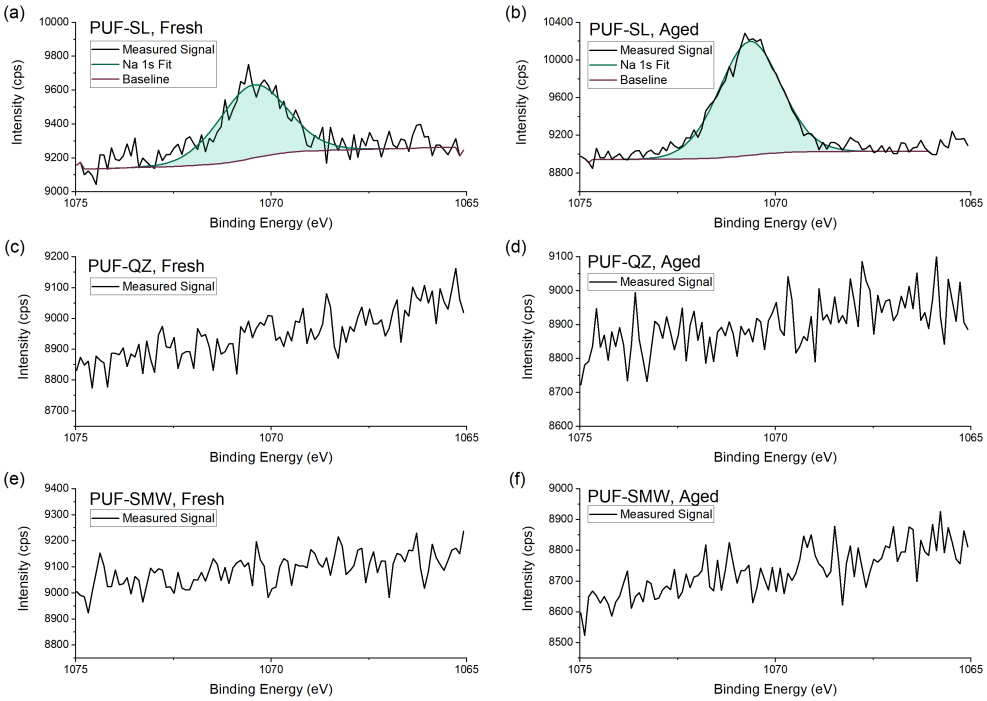


Figure A4.13. Na 1s binding energy spectra of PUF coatings on (a) SL, (b) QZ, and (c) SMW before and after ageing for 45 days at 70 °C and 75% RH.

Ageing of PUF coatings on different substrates with uncontrolled RH

As described in the main text, an initial ageing experiment of PUF(-WA) coatings was performed where the relative humidity was not consistently 75%. Unfortunately, the humidity and temperature logger inside the desiccator was also not recording, so the exact relative humidity profile over time is unknown. Yet rather than dismissing this experiment, it is worthwhile to examine the results of this ageing procedure still.

Figure A4.14 shows the initial and final average water contact angle values of PUF(-WA) coatings on soda lime, quartz and Si wafers. In general, the results are in line with those discussed in the main text: WA-free coatings all show an increase in WCA value, and only coatings of PUF-WA show a lesser increase in WCA value when applied on soda lime substrates. There are also some key differences, however. First, the increase in WCA value seen for PUF coatings is drastically larger compared to that presented in the main text. The same holds true for PUF-AES and PUF-BAS coatings on soda lime. Additionally, the sodium content is also quite different before and after ageing (Table A4.6).

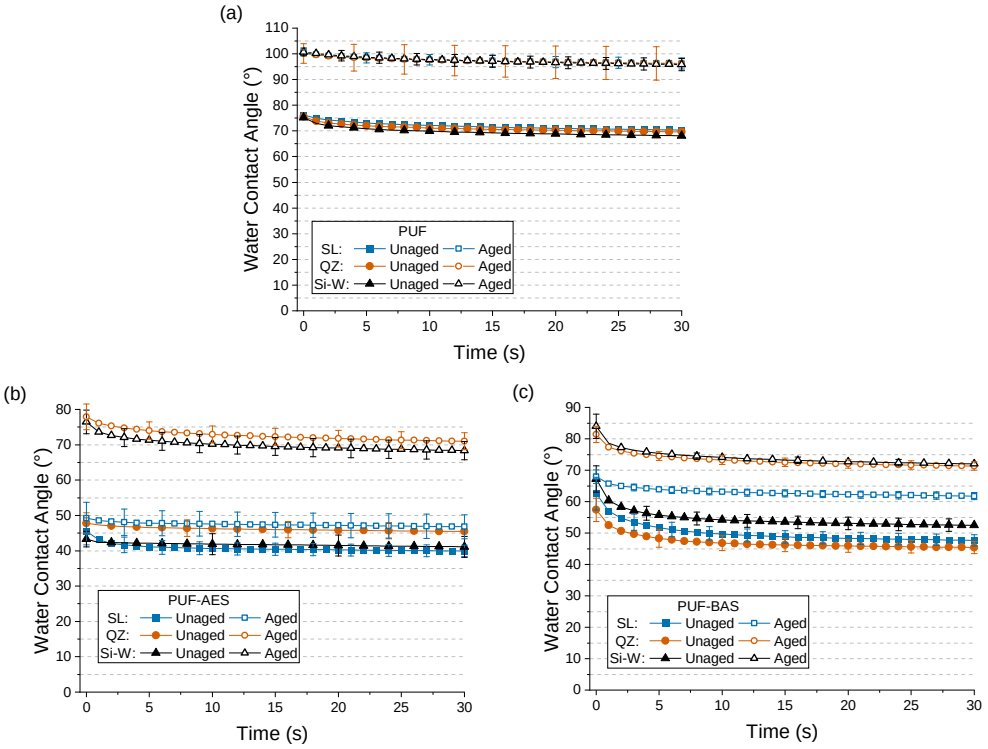


Figure A4.14. Average WCA values of PUF(-WA) coatings before and after ageing for 45 days at 70 °C. Starting relative humidity was 75%, and 28% at the end.

Table A4.6. Average WCA values and Na : C ratios of PUF(-WA) coatings on different substrates before and after ageing for 45 days at 70 °C. Starting relative humidity was 75%, and 28% at the end.

Coating	Substrate	CA_0 (°)	CA_{45}(°)	ΔCA (°)	$(Na:C)_0$	$(Na:C)_{45}$
PUF	SL	70.4 ± 2.5	96.2 ± 2.2	25.8 ± 3.3	0.0011	0.018
	QZ	69.7 ± 3.2	96.1 ± 6.5	26.4 ± 7.2	-	0
	Si-W	68.1 ± 3.2	95.8 ± 2.3	27.7 ± 3.9	-	-
PUF-AES	SL	39.9 ± 1.7	46.8 ± 3.4	6.9 ± 3.8	0.019	0.046 ± 0.008
	QZ	45.5 ± 2.3	71.0 ± 2.4	25.5 ± 3.3	-	0.025 ± 0.01
	Si-W	41.1 ± 3.0	68.3 ± 2.6	27.2 ± 4.0	-	-
PUF-BAS	SL	47.7 ± 1.8	61.8 ± 1.2	14.1 ± 2.2	0.013 ± 0.002	0.037 ± 0.002
	QZ	45.4 ± 2.0	71.3 ± 1.3	25.9 ± 2.4	-	0.020
	Si-W	52.4 ± 2.0	72.0 ± 1.0	19.6 ± 2.2	-	-

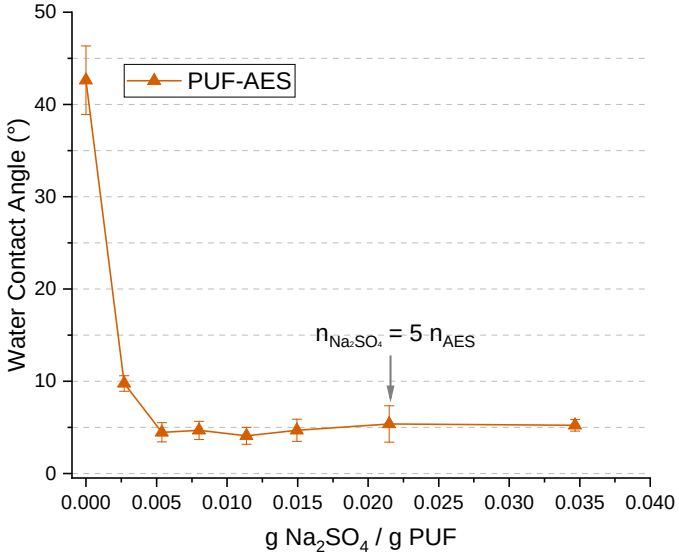


Figure A4.15. Average WCA values of PUF-AES coatings doped with Na_2SO_4. The arrow indicates the concentration at which there is approximately a 5 x molar excess of Na_2SO_4 relative to AES.

References

[A1] S. Willai, M. Bacquet, and M. Morcellet, "Organosilica Mesoporous Materials with Double Functionality: Amino Groups and β-Cyclodextrin Synthesis and Properties," in *Silicon Based Polymers*, F. Ganachaud, S. Boileau, and B. Boury, Eds., Dordrecht: Springer Netherlands, 2008, pp. 213–221. doi: 10.1007/978-1-4020-8528-4_15.

[A2] R. B. Viana, A. B. F. da Silva, and A. S. Pimentel, "Infrared Spectroscopy of Anionic, Cationic, and Zwitterionic Surfactants," *Advances in Physical Chemistry*, vol. 2012, p. e903272, 2012, doi: 10.1155/2012/903272.

[A3] R. P. Sperline, "Infrared Spectroscopic Study of the Crystalline Phases of Sodium Dodecyl Sulfate," *Langmuir*, vol. 13, no. 14, pp. 3715–3726, 1997, doi: 10.1021/la9702087.

[A4] R. P. Sperline, Y. Song, and H. Freiser, "Temperature Dependent Structure of Adsorbed Sodium Dodecyl Sulfate at the Al2O3/Water Interface," *Langmuir*, vol. 13, no. 14, pp. 3727–3732, 1997, doi: 10.1021/la970209z.

[A5] Y.-H. Kim and K. Lee, "Characterization of aerosols produced during shampoo use and harmful chemicals in shampoo aerosols," *Environmental Research*, vol. 204, p. 111957, 2022, doi: 10.1016/j.envres.2021.111957.

[A6] J. M. Patterson, Z. Kortylewicz, and W. T. Jr. Smith, "Thermal degradation of sodium dodecyl sulfate," *J. Agric. Food Chem.*, vol. 32, no. 4, pp. 782–784, 1984, doi: 10.1021/jf00124a020.

[A7] G. Socrates, *Infrared and Raman Characteristic Group Frequencies: Tables and Charts*. John Wiley & Sons, 2004.

[A8] A. Farshchi, A. Sadeghpour, M. Rappolt, H. Tantawy, J. Caragay, E. S. J. Robles, A. Hassanpour, and A. Bayly, "Liquid crystalline phases of linear alkylbenzene sulphonate in spray-dried detergent powders studied by small-angle X-ray scattering, TEM, and ATR-IR spectroscopy," *Colloids and Surfaces A: Physicochemical and Engineering Aspects*, vol. 614, p. 126130, 2021, doi: 10.1016/j.colsurfa.2020.126130.

[A9] T. Ramcharan and A. Bissessur, "Analysis of Linear Alkylbenzene Sulfonate in Laundry Wastewater by HPLC–UV and UV–Vis Spectrophotometry," *Journal of Surfactants and Detergents*, vol. 19, no. 1, pp. 209–218, 2016, doi: https://doi.org/10.1007/s11743-015-1763-x.

[A10] J. Crank and G. S. Park, *Diffusion in polymers*, 2nd print. London: Academic Press, 1975.

5

Stability of Phenolic Resin–Wetting Agent Mixtures upon Curing



Abstract

Wetting agents (WAs) are most efficient if they are distributed well throughout coatings, leading to an improved water-wetting or hydrophilicity of the coating surface. This distribution depends on a delicate balance between miscibility and surface segregation. The compatibility of various types of WAs with phenol-urea-formaldehyde (PUF) and phenol-formaldehyde (PF) resins was examined by evaluating their miscibility upon curing at elevated temperature. Demixing induced by added nonionic WAs was typically observed in PUF coatings, whereas for the same WAs in PF coatings neither instability nor improvement in the coating hydrophilicity was observed. The most important selection criteria for effective WAs for phenolic resin coatings are the length of alkyl and ethylene oxide groups. Additionally, an anionic headgroup is required to achieve both sufficient miscibility with PUF and PF during the cure process and an increase in hydrophilicity of the resulting coatings. These insights provide a framework for the selection or design of new WAs for improved wetting performance of phenolic resin coatings.

5.1. Introduction

Multiple considerations need to be accounted for to select a specific wetting agent (WA) with the right functionalities for hydrophilic phenolic resin coating applications. Some criteria can be related to dynamic properties (e.g., viscosity of the resulting formulation) which influence processing, or can be based on regulatory restrictions [1]. Other criteria can be related to the interactions between WA and resin, where the chemical and structural properties of the WA are relevant [1]. In turn, this ultimately dictates the hydrophilicity of the hardened resin. As discussed in Chapter 3, incompatibility between resin and WA can lead to demixing, which not only strongly affects the efficiency and effectiveness but also the persistence of the WA. For instance, demixing of a WA from a PF resin upon curing yields hydrophilic surfaces, but the resulting coatings are prone to loss of functionality. A framework to select or design a WA to be compatible with a given resin is therefore of utmost value.

For polymer blends and additives in resins, surface segregation and demixing has already been thoroughly investigated [2–14]. For phenolic resins (PRs) without WAs, demixing has been observed upon curing due to the formation of network species with different molecular structure and weight, increasing incompatibility with the solvent [15,16]. From a surface-enrichment point of view at the coating–air interface, both entropic and enthalpic arguments can be given to explain why a particular component enriches this interface [4,5].

Studies of mixtures of nonionic surfactants with hydrophobic and hydrophilic hydroxyethyl cellulose-based polymers have shown the effect of the chemical nature of surfactant and resin on their phase stability [17]. Using 4-octylphenol polyethoxylate (Triton X-100) and alkyl ethoxylates (C_nEO_m), Robb *et al*. [17] found that demixing occurs at a lower concentration when the hydrophilic resin was used, and that the surfactant concentration needed to induce this instability decreased with increasing alkyl chain length of the polymer. Conversely, the concentration of surfactant required to induce a phase separation from the more hydrophobic resin was consistently larger due to the more favourable interactions between the polymer resin and the surfactants.

The addition of surfactants to phenolic resins is common practice for making foams and mesoporous structures [18–20]. Although in some cases incompatibility of surfactants and the resin is observed prior to the hardening of the PR [21], demixing as a result of the curing process has not been reported. A study by DSouza *et al*. [22] addressed the location and distribution of sodium dodecyl sulphate (SDS) and sodium dodecyl sulphonate WAs in PF foams. Foams prepared from PF resins with these WAs added showed a significantly larger water uptake than foams onto which the WAs were sprayed. This highlights the importance of the distribution of WAs on the hydrophilic properties of the foam, and suggests that the distribution and degree of surface

enrichment of WAs in PR coatings therefore also strongly impacts the surface properties.

While the initial stability of the PR formulation is important, it is crucial to realise that a typical PR is comprised of relatively low molar mass species [23,24]. The thermal curing facilitates the rapid formation of an extensive network and concentrates the resin by evaporation of water, which will have an impact on the miscibility of WAs with the (forming) phenolic resin network. Wetting agents can be classified as nonionic or ionic, and the absence or presence of a charge will inevitably affect their compatibility with the resin and the forming polymer network as well. Even for a WA with the same headgroup, different counterions can affect its compatibility with a polymer resin and overall stability against demixing, as it is known that different counterions influence, for instance, their critical micelle concentration (CMC) and cloud point in a specific resin formulation [25,26].

Incompatibility between additives such as block-copolymers and a forming polymer network can also advantageously be used when one part of the additive can be incorporated in the polymer network. This leads to a distribution of dangling chains throughout the coating, creating a reservoir in the bulk which can later provide a source to self-replenish hydrophobic [27–30] and hydrophilic [31,32] surfaces. In view of the need to preserve WAs in phenolic resin coatings, such an incorporation could be desirable to prevent or limit the loss of functionality over time. This requires a deeper understanding of some of the factors which influence the miscibility of WAs with phenolic resins, so that the interactions eventually can be effectively tuned. Therefore, this Chapter focusses not on functionalised WAs to be chemically bonded with the resin, which would enable the creation of the bulk-reservoir, but rather aims to lay the foundation to make such a step possible. To this end, various nonionic and ionic WAs have been mixed with PUF and PF resins, and the coating quality in terms of haziness and wettability was assessed.

5.2. Experimental Procedures

Materials

Ethoxylated fatty acid (EFA), alkyl ethoxylated sulphate (AES-2; 27 wt% in water, and AES-6; 30 wt% in water), branched alkylbenzene sulphonate (BAS; 25 wt% in water), and alkyl ethoxylated alcohols (AEA) were kindly provided by ROCKWOOL A/S. Poly(ethylene glycol) (PEG; average M_n = 600, 4000 and 10000 g/mol), BRIJ® L4 (henceforth termed AEA-4), and BRIJ® L23 (30 wt% in water; henceforth called AEA-23), diethylene glycol monobutyl ether (AEA-2, ≥ 98%), cetyltrimethylammonium bromide (CTAB) tretraethylammonium bromide (TEAB; ≥ 99%), and nonyl phenyl ether (NPE; IGEPAL™ CO-520) were obtained from Merck. Triethylamine (TEA; > 99.5%), urea (U; ≥

99%), phenol (P; > 99%), sodium dodecyl sulphate (SDS), decyltrimethylammonium bromide (DTAB), tretraethylammonium bromide (TEAB; ≥ 98%), and tetraoctylammonium bromide (TOAB; > 98%) were received from Sigma-Aldrich. Formaldehyde (F; 37 wt% in water, includes 10–15% methanol as stabiliser) was bought from ThermoScientific. Sodium hexadecyl sulphate (SHS; > 95%, contains 40% sodium stearyl sulphate) was purchased from TCI Chemicals. Before use, phenol, SHS, and DTAB were stored in an exicator with P_2O_5. All other chemicals were used as received.

Procedures

PUF-TEA and PF-TEA resin was synthesised as described in Chapters 2 and 3. Henceforth in this Chapter, the -TEA suffix will be omitted for brevity. WA concentration was initially held at 0.33–0.34 mg a.s. / g S.C. for both PUF-WA and PF-WA resins.

Coating application and curing was done as described in Chapter 3. Characterisation of the coatings by ^{1}H-NMR spectroscopy and water contact angle (WCA) goniometry was done as described in Chapters 2 and 3. For contact angle measurements, results are the average of the individual left and right contact angle values for three measurements per coating, on a total of 6–8 coatings.

HLB Calculation

The hydrophilic-lipophilic balance (HLB) is a quantitative measure of the tendency of a surfactant to partition between water and oil. The HLB value indicates the ability of a surfactant to stabilise emulsions. For that reason, it has been of value in areas such as cosmetics [33], medicine and pharmaceutics [34], and in the petroleum and construction industry [35,36] as a parameter to select surfactants for the desired application. Below two commonly used approaches to estimate HLB numbers are presented.

Davies [37] used group contributions to define an additive relationship for the HLB:

$$HLB_{\mathrm{D}} = 7 + \sum_{k=0}^{n} G_k \cdot N_k \ , \tag{5.1}$$

where, k refers to the individual group (hydrophilic or lipophilic) with corresponding group number G_k which is multiplied by the number of groups N_k.

In part due to the possible large deviations between experimentally determined HLB values and those calculated by the Davies method, Guo *et al*. [38] defined the HLB value by taking into account the effective chain length (ECL) of ethylene oxide and alkyl blocks:

$$HLB_{ECL} = 7 + G_{CH_2} \cdot N_{CH_2}^{eff} + G_{EO} \cdot N_{EO}^{eff} + \sum_{k=0}^{n} G_k \cdot N_k \ , \quad (5.2)$$

where G_{CH_2} and G_{EO} refer to the alkyl and ethylene oxide group number, and $N_{CH_2}^{eff}$ and N_{EO}^{eff} refer to the corresponding effective lengths as defined in [38].

Group numbers (G_k) were re-calculated by Guo *et al.* [38] and as a result the disparity between the Davies method and ECL calculation can be relatively large. Unfortunately, HLB group values for cationic surfactants are scarcely available in literature, with one of the few sources listing group contributions being the research of Ho [39]. All group numbers used in this Chapter are listed in Table 5.1. Comparing some of the group contributions as originally published by Davies [37] to those of Ho, some large deviations can be found for the sulfonate group contribution. Hence, for fair comparison, both Eq. 5.1 and Eq. 5.2 were used to assess and compare the HLB of WAs.

Table 5.1. Group numbers as proposed by Davies [37], Guo *et al.* [38], and Ho [39].

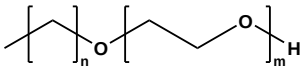
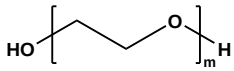
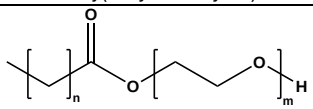
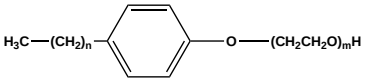
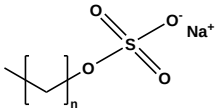
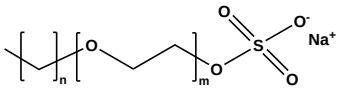
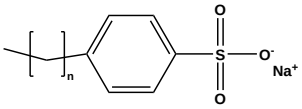
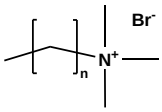
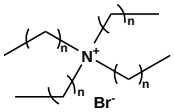
Group	Group Numbers		
	Davies	ECL	Ho
$-SO_4Na$	38.7	38.4	-
$-SO_3Na$	11	10.7	-
$-CH_2-O-CH_2-$	2.4	2.316	-
-OH	1.9	2.255	-
$-CH_2CH_2O-$	0.33	0.33	-
$-CH_2$ / $-CH_3$	-0.475	-0.475	-
$-C_6H_5$	-1.662	-1.601	-
R_4N^+	-	-	22

5.3. Results & Discussion

Wetting Agents Selection and Characterisation

An overview of the WAs used in this Chapter is given in Table 5.2. WAs were chosen with different chemical groups (ethylene oxide units, alkyl chain, and ionic head group) which could be systematically varied to discern the influence of each respective group on the WA compatibility with the PUF and PF resins. Where applicable, ^{1}H-NMR was used to determine the average number of repeating units and average molar mass of the WAs.

Table 5.2. Overview of WAs used in this research, including the number average repeating units, average molecular weight and HLB values determined with the Davies (HLB_D) and the ECL (HLB_{ECL}) method. The number average of repeating units $\bar{n}$ and $\bar{m}$ were determined as an average from two ^{1}H-NMR spectra, unless otherwise specified.

Chemical Structure	Name	Repeat Units		$\bar{M}_n$ (g/mol)	HLB_D	HLB_{ECL}
		$\bar{n}$	$\bar{m}$			
 Alkyl Ethoxylated Alcohol	AEA-2	3.0	2.1	166	7.7	11.1
	AEA-3	9.4	2.8	285	4.9	9.4
	AEA-4	11.5	4.1	371	4.3	10.1
	AEA-7	11.3	7.0	498	5.4	12.4
	AEA-10	11.3	10.7	662	6.6	14.1
	AEA-23	11.1	23.6	1225	11.0	16.9
	AEA-O9	16.2	8.8	645	3.6	11.0
 Poly(Ethylene Glycol)	PEG-600	-	13.4	608	-	-
	PEG-4000	-	90[a]	4000[a]	-	-
	PEG-10000	-	226[a]	10000[a]	-	-
 Ethoxylated Fatty Acid	EFA[b]	15.1	7.3	590	6.1	13.1
 Nonyl Phenol Ether	NPE	8.3	5.5	443	4.7	10.9
 Sodium Alkyl Sulphate	SDS	10.9	-	287	40.0	40.0
	SHS	15	-	344	38.2	38.2
 Alkyl Ethoxylated Sulphate	AES-2	11	1.8	371	40.6	42.8
	AES-6	10.8	6.2	549	42.2	48.3
 Branched Alkylbenzene Sulphonate	BAS[b]	10.5	-	341	10.9	10.9
 Alkyl Trimethyl Ammonium Bromide	CTAB	15[a]	-	364[a]	21.4	-
	DTAB	9[a]	-	280[a]	25.3	-
 Tetra Alkyl Ammonium Bromide	TEAB	1[a]	-	210[a]	25.2	-
	TOAB	7[a]	-	547[a]	13.8	-

[a] Theoretical value.

[b] Technically, the repeating unit of EFA is displayed incorrectly as there is an alkene bond in the chain (see Chapter 3), and BAS is branched instead of linear, which was omitted here for simplicity.

One fixed WA concentration was tested. When WAs would induce demixing in the PRs upon curing, a lower concentration could alleviate this problem at the cost of there being less WA overall in the coating (see also Chapter 3). Furthermore, the use of some of the WAs in this Chapter in applications such as horticultural substrates is not necessarily recommended based on the possible hazardous effects to the environment when they would leach from the coating. Finally, only two different resins, TEA-catalysed PUF and PF, have been used to exclude the influence of inorganic crystals on the distribution of WAs (discussed in Chapter 3).

Effect of Alkyl and Ethylene Oxide Content of Wetting Agents on Miscibility with Phenolic Resins

Several characteristics were used to establish whether demixing of the wetting agents from the phenolic resin had occurred. First, demixing upon curing typically yields a macroscopically visible hazy coating, and for most of the coatings their visual appearance is shown in Figure A5.1. Additionally, as a result of the demixing, the wettability of coating surfaces was usually found to be rather inconsistent, i.e. large variations in the WCA values were found.

As a benchmark, the stability of mixtures of poly(ethylene glycol) (PEG) of varying molar mass mixed with PUF and PF resin were studied. There were no visible indications of unmixing for PUF-PEG and PF-PEG coatings (Figure 5.1). This is in line with previous research for PEG-PF blends [40,41], although demixing of higher molar mass PEG (>2000 g/mol) is known to occur when using the commercial PUF-KOH resin [42]. As shown in Figure 5.1, the average WCA for P(U)F-PEG coatings decreased with increasing PEG molar mass from 600 g/mol to 4000 g/mol, and hence with increasing EO content (using the same concentration).

For PUF-PEG10000, the coating surfaces showed an irreproducible hydrophilicity, indicating a large chemical heterogeneity. The data in Figure 5.1c for PUF-PEG10000 (named ‘Average High’ and ‘Average Low’) is shown as two separate curves for better illustration of this heterogeneity, but in fact is from coatings made from the same resin batch. Either immediate or moderate spreading of water droplets on the surface occurred, which indicates that distinct domains of PEG had formed upon curing. Interestingly, spontaneous wetting for several of the PUF-PEG10000 coatings was observed (Figure 5.1c; named ‘Spot 1’ and ‘Spot 2’). Occasionally, a water droplet on the coating surface suddenly began to spread after some delay time in contact with the surface. As PEG is known to change its conformation in water depending on its concentration [43–45], this abrupt change in wettability may be due to reorientations of PEG at the coating–water interface. Alternatively, the dissolution of the more crystalline PEG domains into the water droplet can also play a role. The time at which this wetting started and the kinetics of this wetting varied. As a result, this spreading was not consistently observed for all samples measured. The example shown in Figure 5.1c (‘Spot 1’ and ‘Spot 2’) is from two separate measurements, showing the difference in wetting procedure.

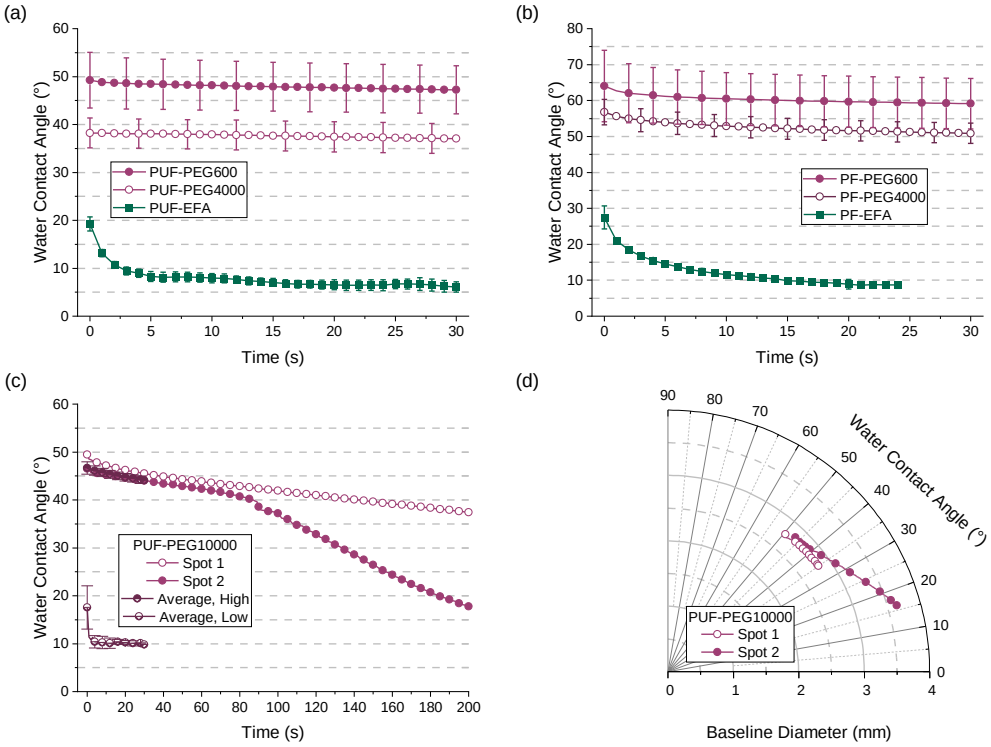


Figure 5.1. Average WCA values of (a) PUF-PEG and (b) PF-PEG coatings. For comparison with the P(U)F-PEG600 coatings, the wettability of P(U)F-EFA is also shown. Varying WCA values for PUF-PEG10000 coatings are shown in (c) by the evolution of water contact angle over time for two single measurements. Additionally, the average of all WCA values on PUF-PEG10000 coatings is shown as two split curves. For the two individual measurements, (d) shows the change of baseline diameter and water contact angle.

Proof that the sudden decrease in WCA value was due to spreading rather than evaporation is shown in both Figure 5.1c–d. First, the kink in the data for PUF-PEG10000 'Spot 2' in Figure 5.1c, indicating a change in slope, suggests an additional mechanism for the sudden decrease in water contact angle, as before this inflection point both curves have similar slopes. Last, plotting the baseline diameter of the water droplet on the coating surface for both measurements in a polar plot together with the water contact angle shows an increase in droplet size for one sample, whereas in case of solely evaporation a constant contact diameter would be observed (Figure 5.1d) [46].

Comparison of the water characteristics of PUF and PF coatings with EFA and PEG600 can provide insights into what drives demixing upon curing, as EFA and PEG600 are of similar molar mass but chemically dissimilar. There is a difference of approximately 40° between the WCA value of PUF-EFA and PUF-PEG600 coatings. Additionally, EFA was seen to demix from PUF during curing (see also Figure A5.1). Chemically, PEG600 is more polar, whereas EFA has both a polar group and contains an apolar alkyl chain. The miscibility between the resin and WA is therefore impacted strongly by the presence and length of the alkyl chain of the WA.

To study the role of the alkyl tail in the demixing induced by nonionic WAs in phenolic resin coatings, different alkyl ethoxylated alcohols (AEAs) were used. Interesting contrasts were found between PUF-AEA and PF-AEA coatings (Figure 5.2). In case of PUF-AEA coatings, only AEA-2 and AEA-3 did not lower the WCA value significantly compared to PUF coatings without WAs. Furthermore, visual inspection of the coatings also showed no signs of instability (Figure A5.1). Increasing the length of both the alkyl block and the EO block of AEA-3, however, drastically changes both the surface hydrophilicity and appearance of the coatings. The large increase in hydrophilicity observed for the hazy coatings is likely related to the strong surface enrichment as a result of the demixing of WAs. Even when extending the length of the EO block to 24 repeating units by using AEA-23, coatings appeared hazy and again showed improved hydrophilicity. Therefore, the EO content seemingly cannot compensate for the incompatibility between WA and resin brought forth by the apolar alkyl block.

In view of the results obtained for PUF-PEG and PUF-EFA coatings as discussed above, it follows that the incompatibility between AEA and PUF stems from the unfavourable interactions between the apolar tail of AEA and the more polar PUF bulk matrix. Although the demixing tendency increased the WCA value of PUF-AEA coatings by at least 20°, this increase was not particularly consistent nor exceptional compared to the performance of anionic WAs (see Chapter 3 and the next section). It is therefore important to not only consider efficiency and compatibility of WAs in and with phenolic resin (coatings), but also their effectiveness when selecting new compounds for hydrophilic phenolic resin coating applications.

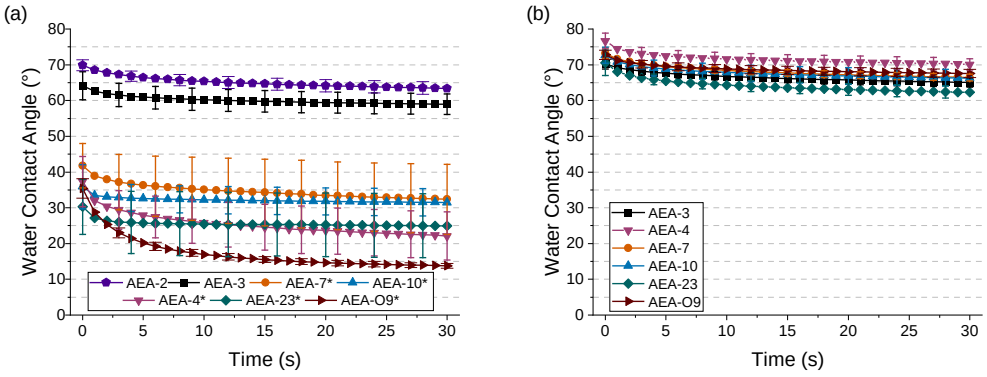


Figure 5.2. Average WCA values of (a) PUF-AEA and (b) PF-AEA coatings. Coatings which were visibly hazy, suggesting the WAs induced demixing, are indicated with an asterisk (*) in the legend.

In case of PF-AEA coatings, no visible demixing upon curing was detected for the selected WA concentration, indicating a better match between the polarity of the bulk and the various tested AEA WAs (Figure 5.2b). This is likely a result of the lack of the more polar urea moieties in PF compared to PUF. Unfortunately, none of the tested AEA WAs were found to increase the hydrophilicity of the PF coatings and hence there was

no discernible surface enrichment by the WAs. Rather unexpectedly, AEA-O9 did not induce unmixing upon curing when added to the PF resin. This WA is structurally close to EFA, for which such demixing was observed before (see also Chapter 3). The only key differences between them are a slight variation in alkyl and EO content (differing only 1 repeating unit each), and most notably the carbonyl group present in EFA. Although unlikely on account of AEA-O9 not showing any surface activity in the PF coating (as there is no decrease in WCA value compared to WA-free PF coatings), it could be that the carbonyl group in EFA provides enough incompatibility with the forming PF matrix to facilitate demixing.

Considering the AEA WAs which demixed and those that did not in the PUF coatings, the HLB values as calculated and presented in Table 5.2 do not seem to provide a useful guide to predict the (im)miscibility of the WAs. For instance, AEA-2 mixed with PUF did not demix upon curing. AEA-2 has an HLB_{ECL} value of 11.1 whereas AEA-4 and AEA-7 both did induce demixing and have HLB_{ECL} values of 10.1 and 12.4, respectively. When evaluating the HLB_{D} values, similar observations can be made for different combinations of AEA WAs which are miscible and immiscible with PUF.

To a large degree, the observations made for PUF-AEA and PF-AEA coatings in terms of surface hydrophilicity and compatibility with the resin also hold for nonylphenol ether (NPE). The instability when mixed with PUF was more modest based on the haziness, but nonetheless visible (Figure A5.1). This was surprising, as the aromatic content of the NPE WA in principle is expected to provide for an increased compatibility with phenolic species. PUF-NPE coatings show an increased hydrophilicity compared to both WA-free PUF coatings and to PF-NPE coatings (Figure 5.3a), which is likely a consequence of NPE demixing from PUF upon curing.

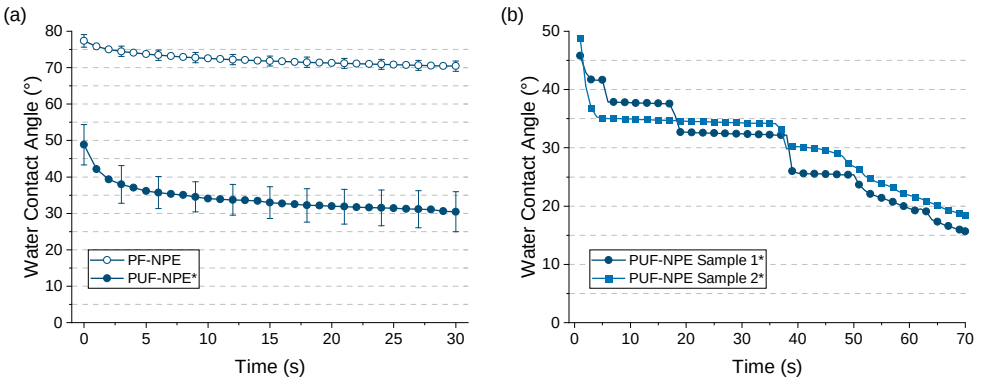


Figure 5.3. Wetting behaviour of PUF-NPE and PF-NPE coatings shown from the (a) average WCA values and (b) water contact angle of two distinct measurements on PUF-NPE surfaces. Demixed WAs are indicated with an asterisk (*) in the legend.

A peculiar behaviour of water droplets on surfaces of PUF-NPE coatings was also observed (Figure 5.3b). Rapid wetting of these coatings was readily observed, but at times this wetting was found to proceed in a sudden, step-wise manner for measurement times longer than 30 s. This intermittent wetting behaviour could be the result of dissolution of NPE into the water droplet, or reorientation of NPE in the surface layers of the coating.

The (in)stability mediated by various WAs as described above are intriguing. Unfortunately, based on the insights provided by varying the alkyl chain length and ethylene oxide content, a parameter based on their ratio, expressed as $\bar{n}/\bar{m}$, seemingly does not give insight into the tendency of a WA to induce demixing in PUF and PF upon curing (Table 5.3; additional results for the persistence of some WAs as determined with wiping tests are implemented in Table A5.1). This implies that consideration of only the alkyl chain length would suffice.

Table 5.3. Overview of the measured average WCA values of PUF and PF coatings with nonionic WAs, as well as the ratio of alkyl content over EO content, literature values of the CMC of nonionic WAs in water at 20–25 °C, and concentration C_{WA} of WAs in the resin formulations. Haziness was determined from the visual observation of the coatings after curing and used as an indicator of demixing (see also Figure A.5.1).

WA	PUF		PF		$\bar{n}/\bar{m}$	CMC (M)	C_{WA} (M)	C_{WA} – CMC (M)
	Hazy?	WCA (°)	Hazy?	WCA (°)				
AEA-2	N	63.4 ± 1.8	-	-	1.4	-	$2.3 \cdot 10^{-3}$	-
AEA-3	N	60.0 ± 2.9	N	65.1 ± 1.3	3.4	$6.6 \cdot 10^{-4}$ [47]	$1.3 \cdot 10^{-3}$	$6.7 \cdot 10^{-4}$
AEA-4	Y	22.1 ± 6.7	N	70.1 ± 1.6	2.8	$6.4 \cdot 10^{-5}$ [48]	$1.0 \cdot 10^{-3}$	$9.6 \cdot 10^{-4}$
AEA-7	Y	32.4 ± 9.8	N	66.4 ± 1.0	1.6	$7.3 \cdot 10^{-5}$ [49]	$7.6 \cdot 10^{-4}$	$6.9 \cdot 10^{-4}$
AEA-11	Y	31.5 ± 3.8	N	66.2 ± 2.3	1.1	$6.2 \cdot 10^{-5}$ [50]	$5.7 \cdot 10^{-4}$	$5.1 \cdot 10^{-4}$
AEA-23	Y	24.9 ± 8.9	N	62.5 ± 1.7	0.5	$2.5 \cdot 10^{-5}$ [51]	$3.1 \cdot 10^{-4}$	$2.8 \cdot 10^{-4}$
AEA-O9	Y	13.8 ± 0.7	N	67.6 ± 1.2	1.9	$1.3 \cdot 10^{-5}$ [52]	$5.9 \cdot 10^{-4}$	$5.7 \cdot 10^{-4}$
EFA	Y	10.8 ± 1.2	Y	8.7 ± 0.7	2.1	$1.9 \cdot 10^{-6}$	$6.4 \cdot 10^{-4}$	$6.4 \cdot 10^{-4}$
NPE	Y	30.4 ± 5.5	N	70.4 ± 1.4	1.5	$4.7 \cdot 10^{-1}$ [53]	$8.5 \cdot 10^{-4}$	$-4.7 \cdot 10^{-1}$

Another factor which can be taken into consideration for this discussion is the CMC of the WAs. Although for most of the WAs the CMC was not measured in this work, values were available from literature. Notwithstanding NPE, for PUF a cutoff CMC can be defined between $6.4 \cdot 10^{-5}$ and $6.6 \cdot 10^{-4}$ M. For CMC values below $6.4 \cdot 10^{-5}$, demixing of WAs in PUF readily occurs. For PF, this cutoff is lower as only for EFA in PF demixing was observed. It should be noted that the concentration of WA in the resin formulation exceeds the CMC for every WA apart from NPE. For a fair comparison between the CMC and the actual concentration of WA that was used, CMC values of WAs in resin formulations should ideally be used, however.

The concentration of WAs in excess of the CMC, defined as C_{WA}-*CMC*, varies between 9.6–$2.8 \cdot 10^{-4}$ M. For EFA, this excess is similar to that of AEA-3 and AEA-7. However, EFA induces demixing in PF, while AEA-3 and AEA-7 do not. Therefore, although the CMC is

affected by the length of polar and apolar groups [54], it seems unlikely that it can be used as a parameter to accurately predict the compatibility of nonionic WAs with phenolic resin formulations.

Effect of the Ionic Headgroup of Wetting Agents on Miscibility with Phenolic Resins

Based on the haziness and wettability of PUF-AEA and PF-AEA coatings, the next step was to use anionic surfactants to study the effect of a charged headgroup on the compatibility with the phenolic resins and associated resulting surface wettability of the coatings. All relevant properties are summarised in Table 5.4, and additional results for persistence tests of some WAs by wiping tests are shown in Table A5.1. Because of the above-mentioned behaviour of NPE in PUF coatings and difficulties in acquiring branched alkylbenzene sulphonate structures with varying total branch lengths, only sulphates were considered for this study.

Despite SDS having a similar alkyl chain length as most of the AEA WAs which induce demixing in PUF, the charged headgroup seemingly provides enough compatibility with the matrix of PUF coatings for it to remain miscible (Figure A5.1). As the WCA values of PUF-SDS were found to be quite reproducible, the balance between compatibility with and demixing in PUF was sufficient (Figure 5.4a). Interestingly, a small effect of EO content on the compatibility was observed for PUF. When using SLES (i.e., AES-2 and AES-6) instead of SDS, a slight increase in average WCA was seen when increasing the EO content from 2 repeating units to 6. This could indicate a larger compatibility with the bulk and hence a lower surface enrichment by the WA. Before curing, SHS did not fully dissolve in the PUF resin at the normal concentration (approximately 0.33–0.34 mg a.s. / g S.C.), nor at a 5 times lower concentration. The SHS that was used also contains a large fraction of sodium stearyl sulphate (approximately 40wt% according to the supplier; not observed from the ^{1}H-NMR spectrum), which could limit the solubility of the WA in the resin.

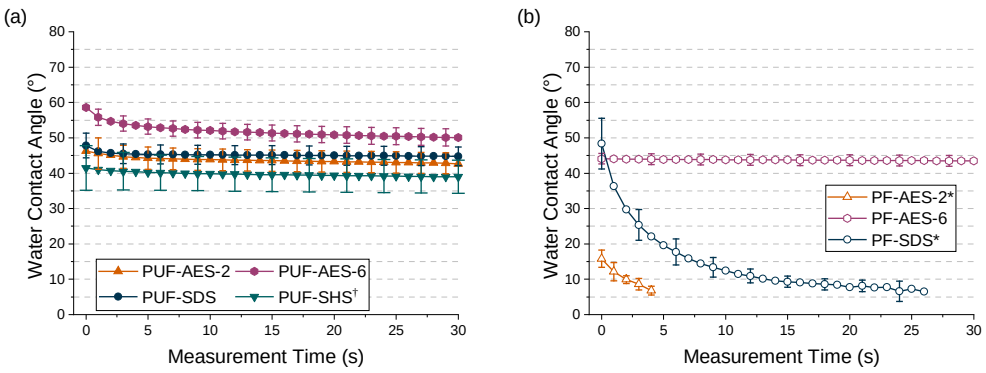


Figure 5.4. Average water contact angle of (a) PUF and (b) PF coatings with anionic sulphate-based WAs. WA-resin mixtures which demixed upon curing are indicated with an asterisk (*) in the legend. WAs which did not completely dissolve are indicated with an obelus (†) in the legend.

Anionic WAs are generally incompatible with PF matrices (as seen in Chapter 3), leading to demixing upon curing. While this was indeed the case for AES-2 and SDS in PF, addition of AES-6 to PF did not yield hazy coatings. On account of SDS, which already demixed from PF during the hardening at elevated temperatures, SHS in PF was not tested. A particularly interesting behaviour of water droplets on PF-SDS surfaces was consistently seen in the form of oscillations of the sessile drop. The origins of this phenomenon are unknown and beyond the scope of this research, but an example of such an occurrence can be found in the Appendix. For PF-AES-6, the wetting profile was significantly more stable over time compared to the PF coatings with SDS and AES-2, indicating a limited amount of spreading (Figure 5.4b). As structurally the only difference between AES-2 and AES-6 is the EO content, it would appear that in this case the hydrophilic EO groups provide an increased compatibility with the PF matrix, allowing for surface enrichment of these coatings without complete demixing. This indicates that the selection or design of an anionic WA that does not induce demixing in PF resins is in fact possible.

Although it does not provide insights into possible selection criteria for future WAs, the responsiveness of SDS and AES-6 in PUF and PF coatings towards elevated relative humidity was also studied (Figure A5.2). A more detailed discussion can be found in the Appendix of this Chapter, but similar to AES-2 as reported in Chapter 3, a reversible responsiveness was observed when exposing coatings to 90% RH.

The cationic WAs that were tested either formed a gel when the resin formulation was left standing for too long, or caused dewetting of the resin from the glass substrate during curing (Figure A5.3). Increasing the cleanliness and surface energy of the glass by treating the substrates with UV-ozone before coating application did not prevent this dewetting. It could be the case that the unfavourable interaction between the cationic WA and residual positive charges in the P(U)F matrix (e.g., TEA^+ or hexamethylenetetramine$^+$, see Chapter 1) results in the observed severe dewetting. Changing the counterion is known to affect the binding interactions between ionic micelles and the counterion and therefore affects the CMC [26,55–60]. The influence of counterions and added electrolytes on the performance and miscibility of ionic WAs has not been tested in this research, but could provide a strategy to prevent complete resin dewetting.

The one exception for dewetting during curing was found for PUF-TEAB, which yielded coatings with a slightly decreased WCA value of approximately 58° relative to PUF coatings without WAs. Presumably, the positive charge of the WA is shielded more due to the steric hindrance provided by the four short alkyl chains. On the whole, it still appears that cationic WAs are not to be favoured over anionic WAs when it comes to their use in phenolic resin formulations.

An overview of coating and ionic WA properties of PUF and PF surfaces is given in Table 5.4. Considering only PUF, a possibly strained correlation between CMC and demixing

can be made, as demixing based on this data occurs below a CMC of $2.2 \cdot 10^{-4}$. However, as the sample space is limited and as this does not seem to hold for PF, it is likely that the direct interactions between anionic WA and forming phenolic matrix are more important factors. A purely concentration-based argument for the compatibility between AES-6 and PF could be made, as its concentration relative to the other anionic WAs is lower. This is also in line with what has been shown for e.g. AES-2 in PF coatings in Chapter 3 (see also Figure A3.7), where a decrease in concentration from $1.1 \cdot 10^{-3}$ to $4.0 \cdot 10^{-4}$ M could prevent demixing. However, at that concentration the average WCA was still lower than currently measured for PF-AES-6 coatings, indicating a possible compatibilising effect of the increased EO content of AES-6 with the PF matrix.

Table 5.4. Overview of the measured average WCA values of PUF and PF coatings with anionic WAs, as well as the ratio of alkyl content over EO content, literature values of the *CMC* of ionic WAs in water at 20–25 °C, and concentration C_{WA} of WAs in the resin formulations. Haziness was determined from the visual observation of the coatings after curing and used as an indicator of demixing (see also Figure A.5.1).

WA	PUF		PF		$\overline{n}/\overline{m}$	CMC (M)	C_{WA} (M)	C_{WA} – CMC (M)
	Hazy?	WCA (°)	Hazy?	WCA (°)				
SDS	N	44.8 ± 2.7	Y	7.8 ± 1.9	-	$8.2 \cdot 10^{-3}$ [61]	$1.3 \cdot 10^{-3}$	-6.810^{-4}
SHS	N[a]	35.0 ± 8.7	-	-	-	$2.2 \cdot 10^{-4}$ [62]	$1.1 \cdot 10^{-3}$	$1.1 \cdot 10^{-3}$
AES-2	N	42.6 ± 2.9	Y	6.8 ± 1.2	6.3	$9.0 \cdot 10^{-4}$	$1.0 \cdot 10^{-3}$	$1.2 \cdot 10^{-4}$
AES-6	N	50.0 ± 2.5	N	43.5 ± 1.5	1.7	$1.7 \cdot 10^{-3}$ [b]	$6.9 \cdot 10^{-4}$	$6.9 \cdot 10^{-4}$
BAS	N	47.9 ± 2.4	Y	8.1 ± 1.4	-	$1.9 \cdot 10^{-3}$	$1.1 \cdot 10^{-3}$	$-7.9 \cdot 10^{-4}$
DTAB	-	-	-		-	$6.8 \cdot 10^{-2}$ [63]	$1.4 \cdot 10^{-3}$	$1.8 \cdot 10^{-3}$
CTAB	-	-	-		-	$1.0 \cdot 10^{-3}$ [64]	$1.0 \cdot 10^{-3}$	$-6.7 \cdot 10^{-2}$
TEAB	N	58.5 ± 2.7	-		-	0.26 [65]	$1.8 \cdot 10^{-3}$	$-2.6 \cdot 10^{-1}$

[a] PUF-SHS coatings were not hazy but rather there was often an undissolved fraction in the formulation which led to deposits on the coating, yielding an inhomogeneous surface.

[b] Value based on data for AES-1, -2, -5, and -10 from [66], through which an asymptotic function was fitted to approximate the CMC of AES-6.

5.4. Conclusions

Several wetting agents (WAs) have been used in phenol-urea-formaldehyde (PUF) and phenol-formaldehyde (PF) resins in order to establish parameters that influence the miscibility of WAs with the resin during the curing process. Nonionic WAs were found to be effective in increasing the hydrophilicity of the phenolic resin coatings only when demixing from the polymer matrix. However, this can lead to easy loss of surface functionality due to the easy removal from the coating surface as a consequence. In cases were the nonionic WAs did not demix, there did not seem to be an influence on the surface energy of the coatings as there was no discernible increase in hydrophilicity.

Anionic WAs were found to be more promising, in that the balance between surface segregation and miscibility is more easily struck compared to nonionic WAs. For PUF resins, such WAs were readily miscible until the linear alkyl chain became too large

(total of > 16 methylene groups). Promisingly, anionic WAs are not per definition immiscible with PF resins, provided that the relative ethylene oxide content is sufficiently large. Addition of cationic WAs to the phenolic resins led to either complete dewetting during curing, or no significant improvement in hydrophilicity.

A concrete criterion for the selection or design of new WAs was not found in the form of commonly used parameters such as the HLB value. However, some guidelines were identified for future studies into miscible and effective WAs. For both PUF and PF resins, the anionic headgroup seems to be preferred in order to achieve appreciable decreases in WCA values. For PF, a further stipulation is that the anionic WA should have a sufficient ethylene oxide content to provide the necessary compatibility with the forming polymer matrix during the cure process.

References

[1] D. Myers, *Surfactant Science and Technology*. John Wiley & Sons, 2005.

[2] M. Khayet, M. Vázquez Álvarez, K. C. Khulbe, and T. Matsuura, "Preferential surface segregation of homopolymer and copolymer blend films," *Surf. Sci.*, vol. 601, no. 4, pp. 885–895, 2007, doi: 10.1016/j.susc.2006.11.024.

[3] D. R. Iyengar, S. M. Perutz, C.-A. Dai, C. K. Ober, and E. J. Kramer, "Surface Segregation Studies of Fluorine-Containing Diblock Copolymers," *Macromolecules*, vol. 29, no. 4, pp. 1229–1234, 1996, doi: 10.1021/ma950544z.

[4] H. Lee and L. A. Archer, "Functionalizing Polymer Surfaces by Field-Induced Migration of Copolymer Additives. 1. Role of Surface Energy Gradients," *Macromolecules*, vol. 34, no. 13, pp. 4572–4579, 2001, doi: 10.1021/ma001278e.

[5] H. Lee and L. A. Archer, "Functionalizing polymer surfaces by surface migration of copolymer additives: role of additive molecular weight," *Polymer*, vol. 43, no. 9, pp. 2721–2728, 2002, doi: 10.1016/S0032-3861(02)00041-1.

[6] J. Chen, S. Das, M. Shao, G. Li, H. Lian, J. Qin, J. F. Browning, J. K. Keum, D. Uhrig, G. Gu, *et al.*, "Phase segregation mechanisms of small molecule-polymer blends unraveled by varying polymer chain architecture," *SmartMat*, vol. 2, no. 3, pp. 367–377, 2021, doi: 10.1002/smm2.1036.

[7] H. Wang, J. F. Douglas, S. K. Satija, R. J. Composto, and C. C. Han, "Early-stage compositional segregation in polymer-blend films," *Phys. Rev. E*, vol. 67, no. 6, p. 061801, 2003, doi: 10.1103/PhysRevE.67.061801.

[8] C. Huang, M. O. De La Cruz, and B. W. Swift, "Phase Separation of Ternary Mixtures: Symmetric Polymer Blends," *Macromolecules*, vol. 28, no. 24, pp. 7996–8005, 1995, doi: 10.1021/ma00128a005.

[9] S. Kang, W.-G. Koh, and Y. K. Joung, "Enhancing surface segregation with cyclic polymer additives: A facile approach to surface modification," *Eur. Polym. J.*, vol. 205, p. 112759, 2024, doi: 10.1016/j.eurpolymj.2024.112759.

[10] L. Piculell and B. Lindman, "Association and segregation in aqueous polymer/polymer, polymer/surfactant, and surfactant/surfactant mixtures: similarities and differences," *Adv. Colloid Interface Sci.*, vol. 41, pp. 149–178, 1992, doi: 10.1016/0001-8686(92)80011-L.

[11] J. Mansouri, V. K. Truong, S. MacLaughlin, D. E. Mainwaring, G. Moad, I. J. Dagley, E. P. Ivanova, R. J. Crawford, and V. Chen, "Polymerization-Induced Phase Segregation and Self-Assembly of Siloxane Additives to Provide Thermoset Coatings with a Defined Surface Topology and Biocidal and Self-Cleaning Properties," *Nanomaterials*, vol. 9, no. 11, Art. no. 11, 2019, doi: 10.3390/nano9111610.

[12] S. L. Giles, N. W. M. Heller, C. R. Clayton, M. E. Walker, M. J. Wytiaz, and J. H. Wynne, "Novel Methods of Producing Low-Reflectance Coatings Utilizing Synergistic Effects of Polymer Phase Separation," *ACS Appl. Mater. Interfaces*, vol. 8, no. 39, pp. 26251–26257, 2016, doi: 10.1021/acsami.6b06037.

[13] J. T. Koberstein, "Molecular design of functional polymer surfaces," *J. Polym. Sci. Part B Polym. Phys.*, vol. 42, no. 16, pp. 2942–2956, 2004, doi: 10.1002/polb.20157.

[14] P. Zhao, Q. Zhou, X. Liu, R. Zhu, Q. Ran, and Y. Gu, “Phase separation in benzoxazine/epoxy resin blending systems,” *Polym. J.*, vol. 45, no. 6, pp. 637–644, 2013, doi: 10.1038/pj.2012.179.
[15] T.-A. Yamagishi, M. Ozawa, Y. Nakamoto, and S. Ishida, “Phase separation of phenolic resins2. The fractionation of phenol-formaldehyde resin based on molecular weight and structure,” *Polym. Bull.*, vol. 40, no. 1, pp. 69–74, 1998, doi: 10.1007/s002890050225.
[16] X. Yi, L. Kong, X. Dong, X. Zuo, X. Kuang, Z. Feng, and D. Wang, “Polymerization induced viscoelastic phase separation of porous phenolic resin from solution,” *Polym. Int.*, vol. 65, no. 9, pp. 1031–1038, 2016, doi: 10.1002/pi.5147.
[17] I. D. Robb, P. A. Williams, P. Warren, and R. Tanaka, “Phase separation in concentrated mixtures of polymers and surfactants,” *J. Chem. Soc. Faraday Trans.*, vol. 91, no. 21, pp. 3901–3906, 1995, doi: 10.1039/FT9959103901.
[18] K. R. Denslow and G. K. Rickle, “Surfactant Effects in Phenolic Foam Resins,” *J. Cell. Plast.*, vol. 25, no. 1, pp. 31–42, 1989, doi: 10.1177/0021955X8902500102.
[19] X. Hu, W. Cheng, C. Li, G. Wang, X. Lin, and Z. Liu, “Effects of surfactants on the mechanical properties, microstructure, and flame resistance of phenol–urea–formaldehyde foam,” *Polym. Bull.*, vol. 73, no. 1, pp. 1–20, 2016, doi: 10.1007/s00289-015-1470-9.
[20] I. Muylaert, A. Verberckmoes, J. De Decker, and P. Van Der Voort, “Ordered mesoporous phenolic resins: Highly versatile and ultra stable support materials,” *Adv. Colloid Interface Sci.*, vol. 175, pp. 39–51, 2012, doi: 10.1016/j.cis.2012.03.007.
[21] S. Minu, R. Ramani, R. Indu Shekar, T. Math Kotresh, and N. Vijay Padaki, “Influence of dodecyl surfactants on the cross-linking, plasticization and damping behavior of epoxy novolac resins,” *Soft Matter*, vol. 18, no. 38, pp. 7380–7393, 2022, doi: 10.1039/D2SM01126C.
[22] G. C. DSouza, H. Li, Z. Yuan, C. C. Xu, M. B. Ray, and A. Prakash, “Investigating the hydrophilicity of phenol formaldehyde foams: Effects of synthesis parameters,” *J. Appl. Polym. Sci.*, vol. 141, no. 5, p. e54877, 2024, doi: 10.1002/app.54877.
[23] A. Pizzi, Ed., “Phenolic Resin Adhesives,” in *Handbook of Adhesive Technology*, 3rd ed., CRC Press, 2017.
[24] S. Kowatsch, “Mineral Wool Insulation Binders,” in *Phenolic Resins: A Century of Progress*, L. Pilato, Ed., Berlin, Heidelberg: Springer, 2010, pp. 209–242. doi: 10.1007/978-3-642-04714-5_10.
[25] S. Kumar, H. Patel, and S. R. Patil, “Test of Hofmeister-like series of anionic headgroups: clouding and micellar growth,” *Colloid Polym. Sci.*, vol. 291, no. 9, pp. 2069–2077, 2013, doi: 10.1007/s00396-013-2942-9.
[26] J. Łuczak, M. Markiewicz, J. Thöming, J. Hupka, and C. Jungnickel, “Influence of the Hofmeister anions on self-organization of 1-decyl-3-methylimidazolium chloride in aqueous solutions,” *J. Colloid Interface Sci.*, vol. 362, no. 2, pp. 415–422, 2011, doi: 10.1016/j.jcis.2011.06.058.
[27] A. C. C. Esteves, I. D. Günbas, J. M. van Riel, B. A. J. Noordover, G. de With, and R. A. T. M. van Benthem, “Time-resolved surface rearrangements of polymer films monitored by dynamic recovery contact angle (DRCA),” *RSC Adv.*, vol. 4, no. 39, pp. 20094–20101, 2014, doi: 10.1039/C4RA01329H.
[28] A. C. C. Esteves, K. Lyakhova, L. G. J. van der Ven, R. A. T. M. van Benthem, and G. de With, “Surface Segregation of Low Surface Energy Polymeric Dangling Chains in a Cross-Linked Polymer Network Investigated by a Combined Experimental–Simulation Approach,” *Macromolecules*, vol. 46, no. 5, pp. 1993–2002, 2013, doi: 10.1021/ma302236w.
[29] Y. Zhang, F. Karasu, C. Rocco, L. G. J. van der Ven, R. A. T. M. van Benthem, X. Allonas, C. Croutxé-Barghorn, A. C. C. Esteves, and G. de With, “PDMS-based self-replenishing coatings,” *Polymer*, vol. 107, pp. 249–262, 2016, doi: 10.1016/j.polymer.2016.11.026.
[30] M. Wouters, J. van Zanten, F. Huijs, and T. Vereijken, “Surface rearrangement of tailored polyurethane-based coatings,” *J. Coat. Technol. Res.*, vol. 2, no. 6, pp. 435–443, 2005, doi: 10.1007/BF02733886.
[31] I. Jiménez-Pardo, L. G. J. Van der Ven, R. A. T. M. Van Benthem, G. De With, and A. C. C. Esteves, “Hydrophilic Self-Replenishing Coatings with Long-Term Water Stability for Anti-Fouling Applications,” *Coatings*, vol. 8, no. 5, Art. no. 5, 2018, doi: 10.3390/coatings8050184.
[32] A. Golmohammadian Tehrani, H. Makki, S. R. Ghaffarian Anbaran, H. Vakili, H. Ghermezcheshme, and N. Zandi, “Superior anti-biofouling properties of mPEG-modified polyurethane networks via incorporation of a hydrophobic dangling chain,” *Prog. Org. Coat.*, vol. 158, p. 106358, 2021, doi: 10.1016/j.porgcoat.2021.106358.
[33] C. P. Fernandes, M. P. Mascarenhas, F. M. Zibetti, B. G. Lima, R. P. R. F. Oliveira, L. Rocha, and D. Q. Falcão, “HLB value, an important parameter for the development of essential oil

phytopharmaceuticals," *Rev. Bras. Farmacogn.*, vol. 23, no. 1, pp. 108–114, 2013, doi: 10.1590/S0102-695X2012005000127.

[34] L. O. Orafidiya and F. A. Oladimeji, "Determination of the required HLB values of some essential oils," *Int. J. Pharm.*, vol. 237, no. 1, pp. 241–249, 2002, doi: 10.1016/S0378-5173(02)00051-0.

[35] A. M. Al-Sabagh, "The relevance HLB of surfactants on the stability of asphalt emulsion," *Colloids Surf. Physicochem. Eng. Asp.*, vol. 204, no. 1, pp. 73–83, 2002, doi: 10.1016/S0927-7757(01)01115-3.

[36] A. Lange, T. Hirata, and J. Plank, "Influence of the HLB value of polycarboxylate superplasticizers on the flow behavior of mortar and concrete," *Cem. Concr. Res.*, vol. 60, pp. 45–50, 2014, doi: 10.1016/j.cemconres.2014.02.011.

[37] J. T. Davies, "A quantatitive kinetic theory of emulsion type. I. Physical chemistry of the emulsifying agent," in *Proc. Intern. Congr. Surface Active Substances*, London, 1957, p. 426.

[38] X. Guo, Z. Rong, and X. Ying, "Calculation of hydrophile–lipophile balance for polyethoxylated surfactants by group contribution method," *J. Colloid Interface Sci.*, vol. 298, no. 1, pp. 441–450, 2006, doi: 10.1016/j.jcis.2005.12.009.

[39] O. B. Ho, "Electrokinetic Studies on Emulsions Stabilized by Ionic Surfactants: The Electroacoustophoretic Behavior and Estimation of Davies' HLB Increments," *J. Colloid Interface Sci.*, vol. 198, no. 2, pp. 249–260, 1998, doi: 10.1006/jcis.1997.5316.

[40] F.-Y. Wang, C.-C. M. Ma, and W.-J. Wu, "Kinetic parameters of thermal degradation of polyethylene glycol-toughened novolac-type phenolic resin," *J. Appl. Polym. Sci.*, vol. 80, no. 2, pp. 188–196, 2001, doi: 10.1002/1097-4628(20010411)80:2<188::AID-APP1086>3.0.CO;2-B.

[41] P. P. Chu, H.-D. Wu, and C.-T. Lee, "Thermodynamic properties of novolac-type phenolic resin blended with poly(ethylene oxide)," *J. Polym. Sci. Part B Polym. Phys.*, vol. 36, no. 10, pp. 1647–1655, 1998, doi: 10.1002/(SICI)1099-0488(19980730)36:10<1647::AID-POLB6>3.0.CO;2-M.

[42] E. Médus, "Influence of the molecular architecture of the wetting agent on the water characteristics of stone wool growing media," Confidential Master Thesis, Vrije Universiteit Brussel, Brussel, 2023.

[43] K.-J. Liu and J. L. Parsons, "Solvent Effects on the Preferred Conformation of Poly(ethylene glycols)," *Macromolecules*, vol. 2, no. 5, pp. 529–533, 1969, doi: 10.1021/ma60011a015.

[44] K. Tasaki, "Poly(oxyethylene)–Water Interactions: A Molecular Dynamics Study," *J. Am. Chem. Soc.*, vol. 118, no. 35, pp. 8459–8469, 1996, doi: 10.1021/ja951005c.

[45] F. E. Bailey Jr. and R. W. Callard, "Some properties of poly(ethylene oxide)1 in aqueous solution," *J. Appl. Polym. Sci.*, vol. 1, no. 1, pp. 56–62, 1959, doi: 10.1002/app.1959.070010110.

[46] A. J. D. Shaikeea, S. Basu, A. Tyagi, S. Sharma, R. Hans, and L. Bansal, "Universal representations of evaporation modes in sessile droplets," *PLOS ONE*, vol. 12, no. 9, p. e0184997, 2017, doi: 10.1371/journal.pone.0184997.

[47] J. F. Rincón-Romero, F. Ríos, A. Reyes-Requena, G. Luzón-González, and A. I. García-López, "Surface and thermodynamics properties of commercial fatty-alcohol ethoxylate surfactants," *J. Mol. Liq.*, vol. 376, p. 121396, 2023, doi: 10.1016/j.molliq.2023.121396.

[48] M. J. Rosen, "The relationship of structure to properties in surfactants. IV. Effectiveness in surface or interfacial tension reduction," *J. Colloid Interface Sci.*, vol. 56, no. 2, pp. 320–327, 1976, doi: 10.1016/0021-9797(76)90257-5.

[49] R. P. Frankewich and W. L. Hinze, "Evaluation and Optimization of the Factors Affecting Nonionic Surfactant-Mediated Phase Separations," *Anal. Chem.*, vol. 66, no. 7, pp. 944–954, 1994, doi: 10.1021/ac00079a005.

[50] A. Berthod, S. Tomer, and J. G. Dorsey, "Polyoxyethylene alkyl ether nonionic surfactants: physicochemical properties and use for cholesterol determination in food," *Talanta*, vol. 55, no. 1, pp. 69–83, 2001, doi: 10.1016/S0039-9140(01)00395-2.

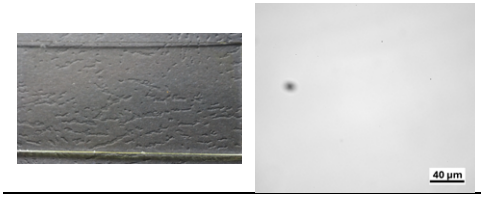
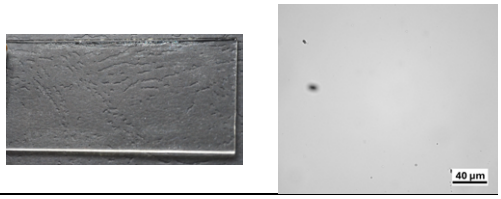
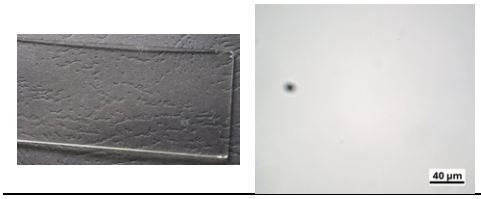
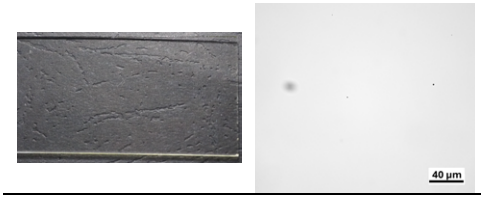
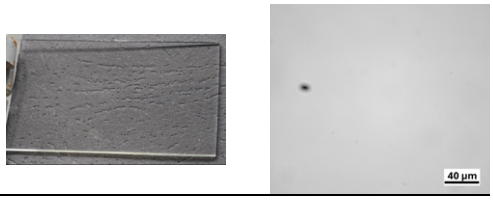
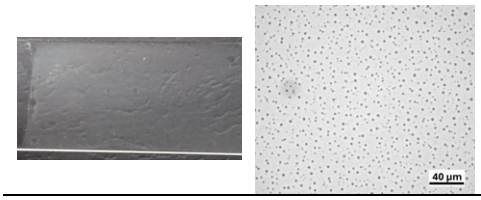
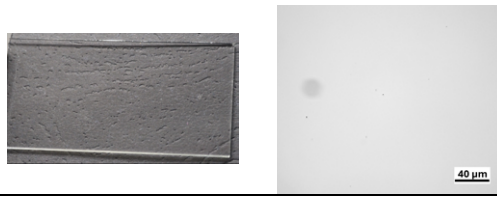
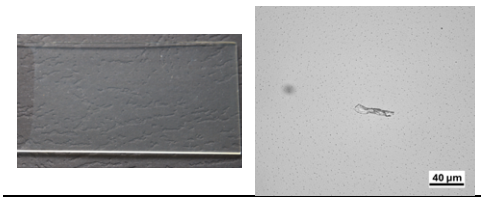
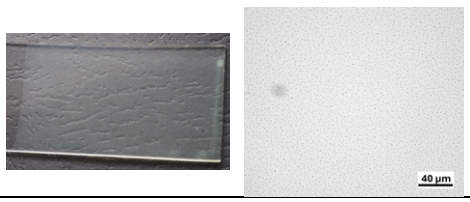
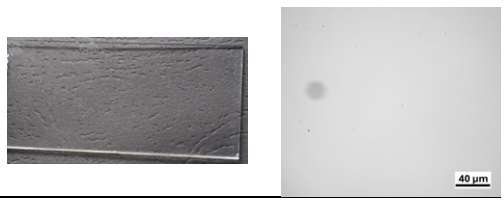
[51] V. Shah, B. Bharatiya, A. D. Shukla, T. Mukherjee, and D. O. Shah, "Adsorption of nonionic Brij and Tween surfactants at PTFE-water and air-water interfaces: Investigations on wetting, dispersion stability, foaming and drug solubilization," *Colloids Surf. Physicochem. Eng. Asp.*, vol. 508, pp. 159–166, 2016, doi: 10.1016/j.colsurfa.2016.08.057.

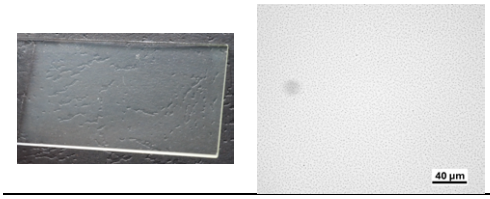
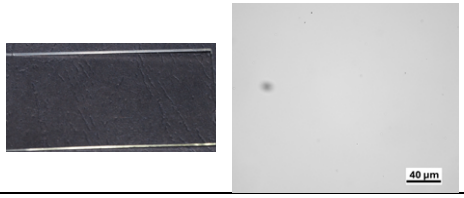
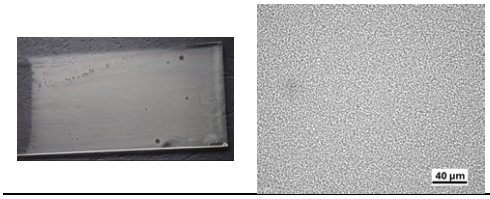
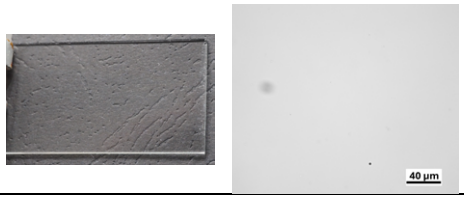
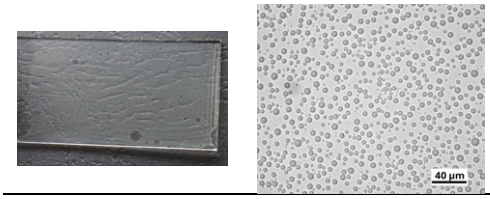
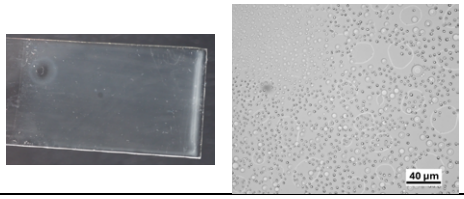
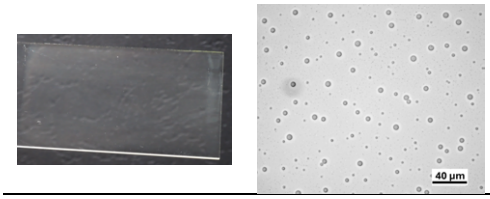
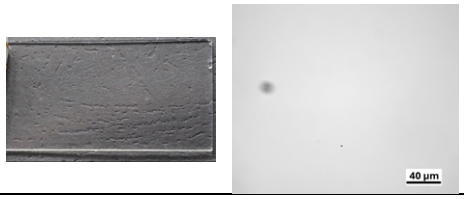
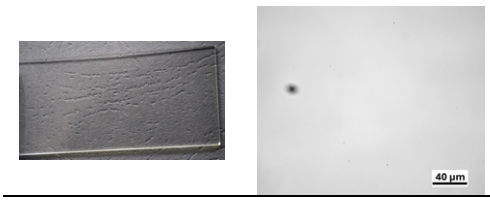
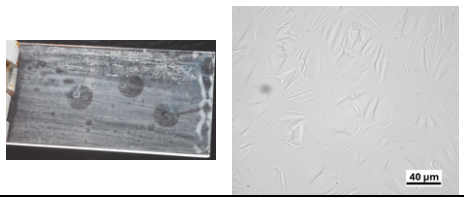
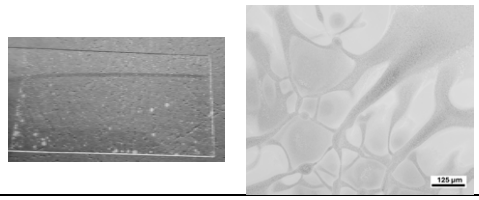
[52] S. Obradović and M. Poša, "The influence of the structure of selected Brij and Tween homologues on the thermodynamic stability of their binary mixed micelles," *J. Chem. Thermodyn.*, vol. 110, pp. 41–50, 2017, doi: 10.1016/j.jct.2017.01.020.

[53] S. K. Ghosh, P. K. Khatua, and S. C. Bhattacharya, "Aggregation of Non Ionic Surfactant Igepal in Aqueous Solution: Fluorescence and Light Scattering Studies," *Int. J. Mol. Sci.*, vol. 4, no. 11, Art. no. 11, 2003, doi: 10.3390/i4110562.

[54] T. Cosgrove, *Colloid science: principles, methods and applications*, 2nd ed. Chichester, United Kingdom: Wiley, 2010.
[55] K. K. Sharker, Md. Nazrul Islam, and S. Das, "Interactions of Some Hofmeister Cations with Sodium Dodecyl Sulfate in Aqueous Solution," *J. Surfactants Deterg.*, vol. 22, no. 2, pp. 249–258, 2019, doi: 10.1002/jsde.12227.
[56] P. K. Weissenborn and R. J. Pugh, "Surface Tension and Bubble Coalescence Phenomena of Aqueous Solutions of Electrolytes," *Langmuir*, vol. 11, no. 5, pp. 1422–1426, 1995, doi: 10.1021/la00005a002.
[57] G. Para, E. Jarek, and P. Warszynski, "The Hofmeister series effect in adsorption of cationic surfactants—theoretical description and experimental results," *Adv. Colloid Interface Sci.*, vol. 122, no. 1, pp. 39–55, 2006, doi: 10.1016/j.cis.2006.06.017.
[58] L. M. Pegram and M. T. Record, "Hofmeister Salt Effects on Surface Tension Arise from Partitioning of Anions and Cations between Bulk Water and the Air−Water Interface," *J. Phys. Chem. B*, vol. 111, no. 19, pp. 5411–5417, 2007, doi: 10.1021/jp070245z.
[59] M. Benrraou, B. L. Bales, and R. Zana, "Effect of the Nature of the Counterion on the Properties of Anionic Surfactants. 1. Cmc, Ionization Degree at the Cmc and Aggregation Number of Micelles of Sodium, Cesium, Tetramethylammonium, Tetraethylammonium, Tetrapropylammonium, and Tetrabutylammonium Dodecyl Sulfates," *J. Phys. Chem. B*, vol. 107, no. 48, pp. 13432–13440, 2003, doi: 10.1021/jp021714u.
[60] W. Kunz, P. Lo Nostro, and B. W. Ninham, "The present state of affairs with Hofmeister effects," *Curr. Opin. Colloid Interface Sci.*, vol. 9, no. 1, pp. 1–18, 2004, doi: 10.1016/j.cocis.2004.05.004.
[61] J. R. Lu, A. Marrocco, T. J. Su, R. K. Thomas, and J. Penfold, "Adsorption of Dodecyl Sulfate Surfactants with Monovalent Metal Counterions at the Air-Water Interface Studied by Neutron Reflection and Surface Tension," *J. Colloid Interface Sci.*, vol. 158, no. 2, pp. 303–316, 1993, doi: 10.1006/jcis.1993.1261.
[62] H. Kumar and G. Kaur, "Effect of changing alkyl chain in imidazolium based ionic liquid on the micellization behavior of anionic surfactant sodium hexadecyl sulfate in aqueous media," *J. Dispers. Sci. Technol.*, vol. 42, no. 7, pp. 970–983, 2021, doi: 10.1080/01932691.2020.1724796.
[63] R. Zieliński, S. Ikeda, H. Nomura, and S. Kato, "Effect of temperature on micelle formation in aqueous solutions of alkyltrimethylammonium bromides," *J. Colloid Interface Sci.*, vol. 129, no. 1, pp. 175–184, 1989, doi: 10.1016/0021-9797(89)90428-1.
[64] A. Zdziennicka, K. Szymczyk, J. Krawczyk, and B. Jańczuk, "Critical micelle concentration of some surfactants and thermodynamic parameters of their micellization," *Fluid Phase Equilibria*, vol. 322–323, pp. 126–134, 2012, doi: 10.1016/j.fluid.2012.03.018.
[65] R. D. Singh and R. Garg, "Study of Micellar Behavior of Crown Ether and Tetraethylammonium Bromide in Aqueous Media," *J. Chem.*, vol. 7, no. 2, p. 927642, 2010, doi: 10.1155/2010/927642.
[66] F. Tokiwa, "Solubilization behavior of sodium dodecylpolyoxyethylene sulfates in relation to their polyoxyethylene chain lengths," *J. Phys. Chem.*, vol. 72, no. 4, pp. 1214–1217, 1968, doi: 10.1021/j100850a024.

Appendices

PUF	PF
No WA	No WA
	
AEA-2	
	n/a
AEA-3	AEA-3
	
AEA-4*	AEA-4
	
AEA-7*	AEA-7
	
AEA-10*	AEA-10
	

PUF	PF
AEA-23* 	AEA-23 
AEA-O9* 	AEA-O9 
EFA* 	EFA* 
NPE* 	NPE 
SDS 	SDS* 
SHS 	n/a

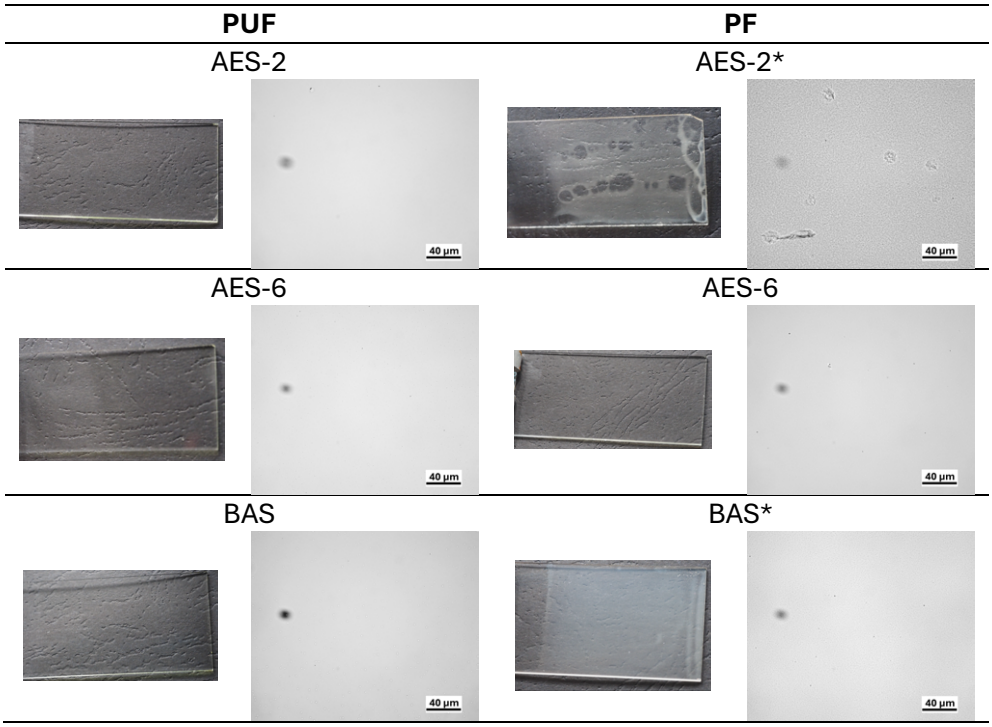


Figure A5.1. Visual appearance of coatings of PUF and PF with and without WAs. Coatings for which WAs induced demixing was observed are indicated with an asterisk (*).

Wiping Experiments

The wiping procedure as described in Chapter 3 was also followed for a selection of coatings in this Chapter, for which the results are shown in Table A5.1. Broadly, the same trends are observed: the wiping procedure either removes WA from the surface (in case of demixed WAs), or the water induces physical changes of the matrix which yields surfaces depleted of WAs.

Table A5.1. Average water contact angle values of phenolic resin coatings with WAs before and after they were consecutively wiped with a wet and dry tissue, as well as after 4 days following this procedure. Coatings for which WAs induced demixing from the resin upon curing are indicated with an asterisk (*).

Coating	WCA Before Wiping (°)	WCA After Wiping (°)	WCA 4 Days After Wiping (°)
PUF-AEA-7*	45.5 ± 4.8	63.0 ± 1.6	67.9 ± 2.3
PUF-AEA-23*	29.7 ± 4.1	63.1 ± 1.1	67.6 ± 1.3
PUF-AEA-O9*	13.2 ± 0.7	71.3 ± 2.5	72.4 ± 3.9
PUF-PEG4000	46.5 ± 1.3	57.2 ± 2.1	67.2 ± 4.1
PUF-SDS	45.9 ± 1.3	55.3 ± 2.4	68.4 ± 3.8
PUF-AES-6	52.4 ± 2.8	59.7 ± 1.6	71.5 ± 1.5
PF-AES-6	43.5 ± 1.6	62.4 ± 1.2	69.3 ± 2.2

Responsiveness of P(U)F Coatings With Anionic WAs to Relative Humidity

The wettability of phenolic resin coatings with anionic WAs of similar structure, i.e., SDS-like WAs, was monitored after exposing these coatings to 90 and 10% RH for 1 h (Figure A5.2). Although the magnitude of change varies, for all coatings a reversible response was observed. Clearly, the common structure (sulphate headgroup) shared by these WAs influences this responsiveness. The subtlest changes were seen for PUF-AES-6, which is likely a result of the lower surface enrichment for these coatings by the WA.

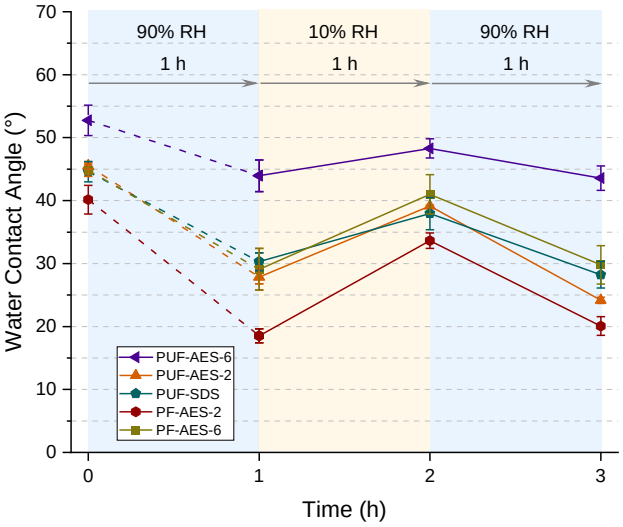


Figure A5.2. Effect of relative humidity on the WCA value of PUF and PF coatings with anionic WAs. Measurements were performed after equilibration for 1 h in a semi-closed chamber at 90% or 10% relative humidity. The first datapoints correspond to values of the coatings determined outside of the chamber, under ambient conditions and relative room humidity. Reported values are the average of six measurements total, each time on a different spot, on two different coatings.

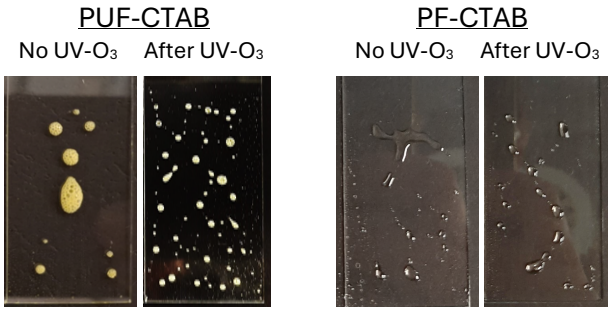


Figure A5.3. Coatings of PUF- and PF-CTAB after curing, leading to dewetting regardless of an extra surface treatment of the glass substrate prior to curing.

Oscillating droplet on PF-SDS surface

A peculiar behaviour was seen for droplets on PF-SDS coatings. After the initial normal wetting, droplets were found to seemingly oscillate. An example can be found by scanning the QR code below; the oscillating behaviour starts at approximately 35 seconds. Although a slight decrease in the apex height of the droplet can be observed from the onset of this oscillation, it is thought that this is a result of evaporation rather than imbibition into surface layers. This is mainly believed on account of the contact line, despite the fluctuations, not consistently decreasing.

Scan to see video



6

Epilogue



6.1. Conclusions

Surface properties of hydrophilic phenolic resin (PR) coatings for applications such as stone wool growing substrates have been studied. The results and interpretation are reported in this thesis. The focus was on understanding the interactions between the polymer resin and wetting agents (WAs) and the resulting PR-WA coatings for efficient use and re-design of such hydrophilic coatings.

First, hydrophilicity and surface chemistry of phenolic resin coatings without wetting agents were investigated. Coatings made with two different resin chemistries, i.e., phenol-formaldehyde (PF) and phenol-urea-formaldehyde (PUF), and two different catalysts (triethylamine (TEA) and potassium hydroxide (KOH)) were studied. Using a combination of contact angle goniometry and X-ray photoelectron spectroscopy, it was found that the hydrophilicity of the coatings is strongly affected by the curing conditions. This is the result of a combination of the network structure being dependent on curing conditions, as well as the occurrence of oxidation reactions which alter the surface chemistry (Chapter 2).

Next, the distribution, performance, and persistence of WAs in PF and PUF coatings were studied using three chemically distinct WAs. Variations in the compatibility of WAs with the PF and PUF resins were observed, where demixing readily occurred in PF. Lowering the WA concentration mitigates this instability, at the cost of there being less WA in the coating. Insights into the response of PUF and PF surfaces, in absence and presence of WA, were obtained using successive advancing contact angle measurements. A partially reversible water plasticisation effect of the PUF and PF matrices was detected, of which the absolute value was affected by the presence of WAs (Chapter 3).

The thermal and hygrothermal stability of wetting agents and phenolic resin coatings were studied at various temperatures and relative humidity values. WAs were found to be remarkably stable, whereas phenolic resin coatings underwent post-cure reactions over the ageing period. Gradual loss of hydrophilicity for PUF-WA coatings is therefore attributed to changes in the surface layers of the PUF coating and subsequent physical ageing of WAs as a result of reorientation or migration, rather than due to their thermal degradation. The effect of relative humidity and the substrate type on the changes in coating surface properties was also studied. Coatings with anionic WAs on soda lime glass showed a limited decrease in hydrophilicity after exposure to elevated temperature and relative humidity compared to the same coatings on quartz glass, silicon wafers and stone melt wafers. This difference in ageing kinetics was found to be affected by the relative humidity, as at lower values the hydrophilicity of all coatings (regardless of the substrate) decreased in a similar manner. Both the substrate and relative humidity therefore have a profound effect on ageing of the coating surfaces

(containing anionic wetting agents). Addition of sodium methanesulphonate can slow down the ageing process, but only for coatings exposed to high relative humidity as this most likely enables the mobility of the introduced charges in the coating. The results highlight the importance of storage conditions for PR coatings, and provides fundamental tools to limit or prevent deterioration of hydrophilic properties from occurring (Chapter 4).

Revisiting some observations made in Chapter 3, the miscibility and surface activity of ionic WAs in phenolic resin coatings was researched in detail. This was done by varying the length of alkyl and ethylene oxide blocks for both nonionic and anionic WAs. Different behaviours were found depending on whether PF or PUF resin was used. In general, nonionic WAs are immiscible with PUF resins upon curing when the alkyl chain length is longer than, say, 12 atoms. In such a case, PUF-WA mixtures become unstable upon curing. Below this critical chain length, however, no significant enhancement of hydrophilicity of the coating surface was observed. For the same WAs in PF coatings, neither demixing nor improvement of surface hydrophilicity was observed. Anionic WAs were found to be most suitable for both PUF and PF coatings, as these typically enable hydrophilic coating surfaces without demixing from the resin during curing (Chapter 5).

6.2. Outlook

In its broadest sense, the focus of this thesis was on hydrophilic coatings. Several further steps can be made in this field, specifically regarding the choice of catalyst, wetting agents, and even resin itself.

The organic catalyst TEA is industrially (and arguably generally) unfavourable due to its toxicity and volatility, which adds to the volatile organic compounds being emitted during the curing process (the other components being formaldehyde and ammonia). A possible alternative for tertiary amine catalysts would be to use tertiary alkanolamines, for instance 2-dimethylamino-2-methyl-1-propanol (DMAMP) or 2-dimethylamino-2-hydroxymethyl-1,3-propanediol (DMAHMP; Figure 6.1a–b), which are reported to lead to lower emissions due to their possible incorporation into the forming phenolic network upon curing [1]. Additionally, this still allows the omission of inorganic catalysts, which are traditionally used in industrial applications of (hydrophilic) PRs, thereby preventing crystal formation during curing.

Chapter 5 discussed preliminary studies regarding what makes for an effective WA for PUF resins. Further insights into the interactions between WAs and PRs can also be obtained with theoretical approaches. For instance, self-consistent field theory (SCF) can be used to study the phase behaviour and distribution of WAs in the resin and their

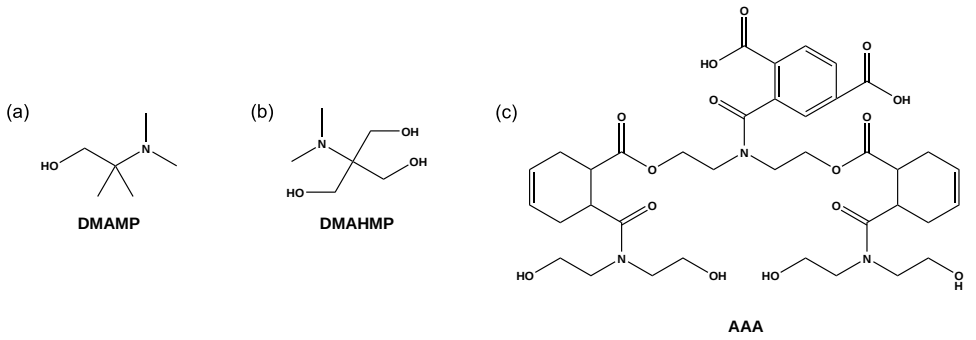


Figure 6.1. Chemical structures of organic catalysts (a) DMAMP and (b) DMAHMP. The hypothesised chemical structure of (c) AAA seems consistent confirmed with ^{1}H-NMR (not shown) and based on [2].

self-assembly [3,4], as mediated by the resin. This requires a thorough analysis of the interaction parameters between the different chemical groups in PRs and WAs. In turn, the obtained insights from theory help with designing and testing different WA architectures to enable hydrophilic coatings with the desired properties.

As was experimentally observed, demixing of WAs can typically only be prevented when anionic WAs are used. Still, the incompatibility observed for nonionic WAs which have a sufficiently long alkyl chain can possibly be advantageously used to produce coatings where WAs are chemically bound to the polymer network. Because of this, a loss of hydrophilicity over time can be minimised. A proof of concept for this could be to use a acid-functionalised poly(ethylene glycol) WA [5]. The acid group facilitates the incorporation of the poly(ethylene glycol) into the PR network, either through reactions before curing, or during the curing step. Methods and experiments employed in this thesis, e.g., the successive advancing contact angle measurements and the ageing procedure at high and low RH, can then be used to assess if initial hydrophilic properties of the coatings can be retained over time.

A somewhat unconventional approach is to not make use of phenolic resins, but rather opt for more sustainable and environmentally friendly alternatives. This departure from PRs does not mean that observations made in this work are irrelevant, as the research in Chapters 2–4 highlights important more general considerations which are valid for any resin. It can therefore provide a framework to use for the research and development of new resins. Some preliminary experiments have been carried out with resins based on an alkanol amine–acid anhydride (AAA; Figure 6.1c), which is formaldehyde-free [2,6–10]. Additionally, reducing sugars can be added as a co-binder to accelerate the cure, and cut back on the amount and cost of alkanol amine and acid anhydride components [7,8]. From an ageing point of view, coatings made with an AAA resin are also a promising alternative for PR coatings. For instance, it has been reported that over

the course of 7 days at 70 °C and 95% RH, no significant changes in its composition was seen, as opposed to PUF coatings [2].

This thermal stability does not imply that surface characteristics such as hydrophilicity are unaffected by the ageing procedure. This is illustrated with preliminary WCA measurements on fresh and aged AAA(-WA) coatings (Figure 6.2). The initial surface of AAA and AAA-BAS coatings appears to be more hydrophilic than their PUF counterparts. Additionally, dynamic vapour sorption (DVS) measurements indicate a significant mass increase when hardened AAA is exposed to relative humidity values >40 % (not shown), which could facilitate plasticisation effects. Similar studies done for PUF(-WA) coatings are therefore interesting to also do for AAA(-WA) coatings, such as performing successive ACA measurements.

The effect of relative humidity on the WCA value of these coatings was noticeable over the course of an ageing experiment (Figure 6.2b). After 14 days of ageing coatings at 70 °C and 75% RH inside a desiccator, causing a decrease in the average WCA value, the desiccator was serendipitously not properly closed. Over the course of the remainder of the ageing experiment, the relative humidity dropped to 10%, showing an interesting increase in average WCA.

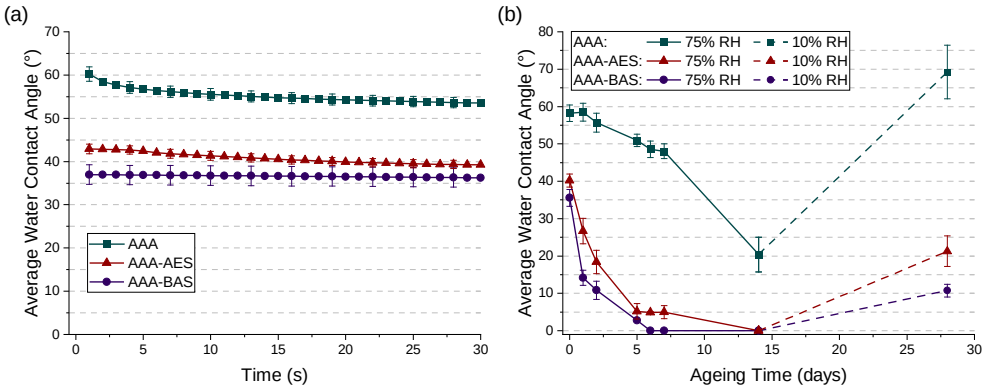


Figure 6.2. Average WCA of coatings of AAA(-WA) (a) before and (b) after ageing at 70 °C and 75% RH. After 14 days of ageing, the coatings were exposed to 10% RH for the remainder of 14 days.

This underscores the importance of ageing studies. Considering the use of hydrophilic resins, be it P(U)F-WA or AAA-WA, in stone wool substrates for horticultural applications, ageing studies should focus not only on elevated relative humidity conditions, but also low (e.g., 20% RH) and preferably intermittent (e.g., 40% RH) to fully understand the response of the coatings to changes in RH. It should be noted that the average relative humidity in greenhouses typically varies between 40–100 % [11–

13], so exposure to low RH during use for extended periods of time are not likely in use conditions. However, RH can fluctuate and storage conditions might be uncontrolled. Additionally, by using both low and high RH conditions, a possible method to regenerate hydrophilic properties of the coatings can be devised.

Finally, an interesting expansion of the research would be to close the gap between the model systems used in this thesis and industrially produced hydrophilic stone wool substrates. Capillary rise techniques, such as the one developed by Washburn [14], allow for the measurement of an advancing contact angle of a porous material and can thus provide additional information next to commonly-used sinking times [15,16]. The advantage is that this method allows for the use of stone wool substrates, and as such no model systems are required. However, difficulties in drying the sample in a similar manner as for wetted coatings can provide a challenge, and it would therefore be impossible to determine the degree and influence of plasticisation on such samples. Nevertheless, direct measurements on hydrophilic stone wool samples exposed to different relative humidity values over time can give insights into how results of the model systems employed in this work relate to the performance of actual products.

References

[1] G. Wu, "Strongly basic tertiary amino alcohols as catalyst," WO1997000900A1, 1997 Accessed: 2022. [Online]. Available: https://patents.google.com/patent/WO1997000900A1/en?oq=WO+1997%2f000900

[2] A. Zafar, J. Schjødt-Thomsen, R. Sodhi, R. Goacher, and D. de Kubber, "Investigation of the ageing effects on phenol-urea-formaldehyde binder and alkanol amine-acid anhydride binder coated mineral fibres," *Polym. Degrad. Stab.*, vol. 98, no. 1, pp. 339–347, 2013, doi: 10.1016/j.polymdegradstab.2012.09.007.

[3] F. A. M. Leermakers and J. Lyklema, "On the self-consistent field theory of surfactant micelles," *Colloids Surf.*, vol. 67, pp. 239–255, 1992, doi: 10.1016/0166-6622(92)80302-I.

[4] J. Opdam, S. P. W. Govers, J. Melio, L. G. J. van der Ven, G. de With, R. Tuinier, and A. C. C. Esteves, "Distribution of block copolymers in drying polymer films," *J. Colloid Interface Sci.*, vol. 612, pp. 617–627, 2022, doi: 10.1016/j.jcis.2021.12.130.

[5] J. Li and W. J. Kao, "Synthesis of Polyethylene Glycol (PEG) Derivatives and PEGylated−Peptide Biopolymer Conjugates," *Biomacromolecules*, vol. 4, no. 4, pp. 1055–1067, 2003, doi: 10.1021/bm034069l.

[6] D. A. W. Stanssens, T. Husemoen, and E. L. Hansen, "Compound for use as a mineral fibre binder and process for providing such," US6706853B1, 2004 Accessed: 2022. [Online]. Available: https://patents.google.com/patent/US6706853B1/en?oq=US+patent+6706853+B1

[7] L. Naerum, P. Nissen, E. L. Hansen, J. M. W. Cuypers, E. G. Hempenius, and F. H. P. Janssen, "A method of growing plants," NL2007312C2, 2012 Accessed: 2025. [Online]. Available: https://patents.google.com/patent/NL2007312C2/en

[8] E. L. Hansen, "Aqueous binder composition for mineral fibres," EP2230222A1, 2010 Accessed: 2025. [Online]. Available: https://patents.google.com/patent/EP2230222A1/en

[9] R. A. T. M. van Benthem, "Novel hyperbranched resins for coating applications," *Prog. Org. Coat.*, vol. 40, no. 1, pp. 203–214, 2000, doi: 10.1016/S0300-9440(00)00122-3.

[10] R. A. T. M. van Benthem, N. Meijerink, Geladé Erik, C. G. de Koster, D. Muscat, P. E. Froehling, P. H. M. Hendriks, C. J. A. A. Vermeulen, and T. J. G. Zwartkruis, "Synthesis and Characterization of Bis(2-hydroxypropyl)amide-Based Hyperbranched Polyesteramides," *Macromolecules*, vol. 34, no. 11, pp. 3559–3566, 2001, doi: 10.1021/ma001267l.

[11] L. M. Mortensen, “Effect of relative humidity on growth and flowering of some greenhouse plants,” *Sci. Hortic.*, vol. 29, no. 4, pp. 301–307, 1986, doi: 10.1016/0304-4238(86)90013-0.
[12] H. A. Ahmed, Y. Tong, Q. Yang, A. A. Al-Faraj, and A. M. Abdel-Ghany, “Spatial distribution of air temperature and relative humidity in the greenhouse as affected by external shading in arid climates,” *J. Integr. Agric.*, vol. 18, no. 12, pp. 2869–2882, 2019, doi: 10.1016/S2095-3119(19)62598-0.
[13] X. Wei, B. Li, H. Lu, J. Guo, Z. Dong, F. Yang, E. Lü, and Y. Liu, “Distribution Characteristics and Prediction of Temperature and Relative Humidity in a South China Greenhouse,” *Agronomy*, vol. 14, no. 7, Art. no. 7, 2024, doi: 10.3390/agronomy14071580.
[14] E. W. Washburn, “The Dynamics of Capillary Flow,” *Phys. Rev.*, vol. 17, no. 3, pp. 273–283, 1921, doi: 10.1103/PhysRev.17.273.
[15] M. Emborg, “Drainage structure,” EP3670743B1, 2023 Accessed: 2025. [Online]. Available: https://patents.google.com/patent/EP3670743B1/en
[16] E. L. Hansen and J. F. D. Groot, “Process for the manufacture of a mineral wool plant growth substrate,” US6562267B1, 2003 Accessed: 2025. [Online]. Available: https://patents.google.com/patent/US6562267B1/en

Summary

Phenolic resins (PRs) are widely used as adhesives for wood, as ablative and abrasive materials for air- and spacecraft, in laminates, and as binders for fibrous materials. While the field of PRs is quite mature, the area of hydrophilic phenolic resins and coatings has not yet been thoroughly explored. Such resins are for instance used in stone wool substrates, which enable a soilless method to germinate, propagate and cultivate fruits and vegetables. Desired water characteristics of hydrophilic stone wool is attained by addition of wetting agents (WAs) to the resin formulation. Knowledge of how processing conditions of PR coatings, the interaction between WAs and the PR, and the behaviour of the PRs and WAs when exposed to water (vapour) affects surface characteristics of PR coatings provides valuable insights. These insights can be crucial for the optimisation and selection of the appropriate WAs for applications where phenolic resin coatings with hydrophilic surfaces are required. This thesis aims to cultivate more understanding of surface properties of hydrophilic phenolic resin coatings and how these change over time by using techniques such as contact angle goniometry, X-ray photoelectron spectroscopy, and scanning electron microscopy.

First, the influence of resin composition and curing conditions on surface characteristics such as morphology, chemistry and wettability was studied. This was done by using different resin compositions (Phenol-Formaldehyde; PF, and Phenol-Urea-Formaldehyde; PUF) and different catalysts for their synthesis and curing (triethylamine (organic catalyst) and potassium hydroxide (inorganic catalysts)). Although the catalyst choice affects the surface roughness of the coatings, the curing temperature was found to have the strongest influence on surface properties. Curing at an industrially common temperature of 200 °C yields surfaces with varying degrees of oxidation, differences in linkages between phenolic and urea species, and a lower overall nitrogen content for the urea-containing coatings compared to coatings cured at 150 °C. In turn, this results in stronger fluctuations in water-wettability for coatings hardened at elevated temperatures compared to those cured at lower temperatures.

Hydrophilic PR coatings were prepared by addition of wetting agents to the formulation. Three chemically distinct WAs were used: a nonionic ethoxylated fatty acid (EFA), an anionic alkyl ethoxylated sulphate (AES), and an anionic branched alkylbenzene sulphonate (BAS). The interaction between these WAs and a PUF and PF resin was then studied by successive advancing contact angle measurements. This way, not only the WA persistence in the surface layers but also the response of the PR coating to the presence of water could be studied. Successive wetting of the PR coating surfaces was seen to yield a plasticising effect, evidenced by a partially reversible reduced water

contact angle value with increasing exposure time to water. This water plasticisation was observed even when anionic WAs were present in the coatings. A fundamental difference in the compatibility between WAs and PUF and PF was observed, as anionic WAs demixed in PF upon curing. Conversely, the presence of urea moieties in PUF provides a better compatibility of anionic WAs with the forming polymer network and as such no demixing of anionic WAs was observed.

WAs are efficient when they are well-distributed throughout the PR coatings, resulting in an improved hydrophilicity of the coating surface. The distribution of WAs depends on the balance between miscibility with the PR resin and forming polymer network upon curing, as well as the surface segregation. The research of compatibility between PR and WA was therefore extended by systematically changing the length of the alkyl block or ethylene oxide block of nonionic and anionic WAs. Demixing induced by nonionic WAs was generally observed in PUF coatings, where the length of the alkyl chain was a dominant factor for this instability. Conversely, for the same nonionic WAs in PF coatings, neither demixing nor an improvement in hydrophilicity was observed. Overall, anionic WAs were found to be most suited to use to enable hydrophilic PF and PUF coatings. The anionic headgroup provides both sufficient miscibility with PUF during the cure process and an increase in hydrophilicity of the resulting coatings. For PF, anionic WAs do not induce demixing provided that the ethylene oxide content of the WA is sufficiently large.

The life- and service-time of hydrophilic PUF coatings was studied by monitoring the hygrothermal stability of WAs and PUF(-WA) coatings. Additionally, the role of the glass substrate in ageing phenomena of the PUF(-WA) coatings was taken into account. Samples were exposed to accelerated ageing conditions of 75% RH at 70 °C for a prolonged time. WAs were found to be remarkably stable, with no appreciable changes in their structure nor in their surface activity. PUF(-WA) coatings became more hydrophobic over the course of 120 days of ageing, partly due to post-curing reactions. The coating substrate also played an important role in the ageing process. Using a pH-sensitive dye, PUF coatings applied on soda lime glass were seen to alkalinise upon ageing, contrary to coatings applied on quartz glass. Only coatings applied on soda lime glass showed inhibited ageing as gauged from limited changes in hydrophilicity. This was attributed to WAs remaining more mobile at the coating-air interface due the leaching of mobile charges from the soda lime glass substrate. By addition of an organic sodium salt to the PUF(-WA) resin, ageing was found to be inhibited even for inert substrates. However, all ageing processes were also seen to be strongly affected by the relative humidity, indicating that storage and use conditions of such coatings is crucial for the retention of hydrophilicity. These results can provide a tool to improve the stability of hydrophilic PRs.

Glossary

Abbreviation	Meaning
a.s.	active substance
AAA	Alkanol amine–acid anhydride
ACA	Advancing water contact angle
ACE	Acetone
AEA	Alkyl ethoxylated alcohols
AES	Alkyl ethoxylated sulphate
APS	(3-aminopropyl)silanetriol
ATR-FTIR	Attenuated total reflection infra-red spectroscopy
BAS	Branched alkylbenzene sulphonate
CAG	Contact angle goniometry
CMC	Critical micelle concentration
CTAB	Cetyltrimethylammonium bromide
DCA	Dynamic contact angle
DMAHMP	2-dimethylamino-2-hydroxymehtyl-1,3-propanediol
DMAMP	2-dimethylamino-2-methyl-1-propanol
DMEb	Dimethylene ether bridge
DMSO	Dimethylsulfoxide
DSA	Drop shape analysis
DTAB	Decyltrimethylammonium bromide
DVS	Dynamic vapour sorption
E_b	Binding energy
ECL	Effective chain length
EDX	Energy-dispersive X-ray spectroscopy
EFA	Ethoxylated fatty acid
EO	Ethylene oxide
F	Formaldehyde
FWHM	Full-width at half maximum
γ_{LV}	Liquid–vapour surface tension
γ_{SL}	Solid–liquid surface tension
γ_{SV}	Solid–vapour surface tension
HLB	Hydrophilic–lipophilic balance
HMTA	Hexamethylenetetramine
IFT	Interfacial tension
iGC	Inverse gas chromatography
KOH	Potassium hydroxide
Mb	Methylene bridge
M_n	Molar mass
MR	Methyl red
NaMeS	Sodium methanesulphonate
NaOH	Sodium hydroxide

NMR	Nuclear magnetic resonance spectroscopy
NPE	Nonylphenol ether
OM	Optical microscopy
P	Phenol
PDMS	Poly(dimethylsiloxane)
PEG	Poly(ethylene glycol)
PF	Phenol-formaldehyde
PR	Phenolic resin
PTFE	Poly(tetrafluoroethylene)
PUF	Phenol-urea-formaldehyde
QZ	Quartz
RH	Relative humidity
RSF	Relative sensitivity factor
RT	Room temperature
S.C.	Solids content
SCF	Self-consistent field theory
SDS	Sodium dodecyl sulphate
SEM	Scanning electron microscopy
SFT	Surface tension
SHS	Sodium hexadecyl sulphate
Si-W	Silicon wafers
SL	Soda lime
SLES	Sodium lauryl ether sulphate
SLS	Sodium lauryl sulphate
SMF	Stone melt wafer
T_c	Curing temperature
t_e	Air exposure time
TEA	Triethylamine
TEAB	Tetraethylammonium bromide
T_g	Glass transition temperature
TGA	Thermogravimetric analysis
TMS	Tetramethylsilane
TOAB	Tetraoctylammonium bromide
U	Urea
UF	Urea-formaldehyde
UV-Vis	Ultra violet visible light
WA	Wetting agent
WCA	Water contact angle
XPS	X-ray photoelectron spectroscopy

Curriculum Vitae



Luuk Moone was born on the 5th of April 1997 in Eindhoven, The Netherlands. After graduating from the Van Maerlant lyceum in Eindhoven in 2015, he studied Chemical Engineering and Chemistry at Eindhoven University of Technology. In 2018, he obtained his BSc degree after finishing his thesis on the fabrication of infra-red reflecting broadband coatings in the Stimuli-Responsive Functional Materials and Devices group in Eindhoven. He continued his education with a master study at Eindhoven University of Technology, specialising in Molecular Systems and Materials Chemistry. He did his thesis work at the Laboratory of Physical Chemistry under the supervision of dr. Catarina Esteves and prof. Remco Tuinier on the topic of functional coating surfaces via block-copolymer dangling chains. After an internship at Fujifilm in Tilburg, working on oleophobic coatings, he started his PhD project in 2020 under supervision of dr. Catarina Esteves, prof. Remco Tuinier and prof. Rolf van Benthem. The project was a collaboration with Grodan (ROCKWOOL B.V.; Roermond, The Netherlands) and ROCKWOOL A/S (Hedehusene, Denmark) and involved cultivating understanding of phenolic resin coatings for hydrophilic applications. During his PhD, he was involved with guiding and supervision of students, and helping organising practical skills sessions within the group.

Publications List

Publications related to this thesis:

L. Moone, M.P.J. Donners, K. van Durme, D.V. Okhrimenko, R.A.T.M. van Benthem, R. Tuinier, and A.C.C. Esteves, "Surface characteristics of phenolic resin coatings," *Surf. Interfaces*, vol. 45, p. 103840, 2024, doi: 10.1016/j.surfin.2023.103840.

L. Moone, I. A. C. van de Ven, M. P. J. Donners, K. van Durme, D. V. Okhrimenko, R. A. T. M. van Benthem, R. Tuinier, and A. C. C. Esteves, "Tunable wettability of phenolic resin coatings," *Prog. Org. Coat.*, vol. 198, p. 108883, 2025, doi: 10.1016/j.porgcoat.2024.108883.

L. Moone, I.A.C. van de Ven, M. Robben, M.P.J. Donners, K. van Durme, D.V. Okhrimenko, R.A.T.M. van Benthem, R. Tuinier, and A.C.C. Esteves, "Ageing phenomena in hydrophilic phenolic resin coatings," expected in 2025, *in preparation*.

L. Moone, M.P.J. Donners, K. van Durme, D.V. Okhrimenko, R.A.T.M. van Benthem, R. Tuinier, and A.C.C. Esteves, "Selection criteria for miscible wetting agents in phenolic resins," *in preparation*.

Acknowledgements

In more ways than one, this thesis would not have been lying in front of you without the help of many marvellous people.

First and foremost, I would like to thank my three amazing supervisors together: **Catarina, Remco and Rolf**. You are a *dream team* to work with, both in terms of expertise and gezelligheid during our meetings.

Catarina, you are tremendously kind, understanding, involved, cheerful, positive, and open, as well as a brilliant coatings, surfaces, and interfaces expert! Thank you so, so much for your encouragement and faith throughout these years. You were always there for me when I needed it, for both science-related challenges and personal struggles. I am super glad and honoured that I have been able to make this journey with you as my first promoter. Throughout the years, we have had plenty of laughs and victories, which I will never forget!

Rolf, besides being a coating-guru, you are a fount of knowledge and have the wonderful gift of phrasing things in an exceptionally poetic way. I recall when you told me that a certain argument had 'more holes than cheese', which I really like. Also, you often noticed I saw some potential issues with certain experiments. Indeed, I often saw bears on the road. Eventually, you said that it probably would only be just a teddy bear, and that I should just slap the teddy bear to get rid of it. Thank you for that motivator, amongst many, and for all the pleasant discussions we had! (N.B.: no teddy bears were hurt in the making of this thesis!).

Remco, thank you for your insights and jokes throughout the project, striking a nice balance between seriousness and fun during project and group meetings. This makes for a great atmosphere! I still vividly remember an example of you effortlessly combining science with comedy: one grey morning you came into my office, dripping wet from the rain, and said with a huge smile that you just did a wetting experiment. Things like that really do brighten the (rainy) day!

I would also like to express gratitude to my committee members, Prof. **Søren Kill**, Prof. **Robin Ras**, Prof. **Željko Tomović**, and Dr. **Santiago Garcia** for their time and effort to read and assess this thesis. Also, thanks to Prof. **Albert Schenning** for chairing the defence ceremony.

Furthermore, a big thank you to **Maurice**, **Kurt, Denis**, **Peter, Dorte** and **Rasmus** for the pleasant and fruitful quarterly meetings we had over the past years. **Maurice,** thank you for your guidance and involvement since the start of the project and the many times you dropped by to drop off commercial resins or other samples. Your curiosity and drive to want to find pieces of the puzzle were motivating! **Denis**, you too were involved from

the start, and provided many inputs from the substrate point of view. Thank you for that, and for measuring several samples with ICP-OES. Although the results are not included in the thesis, they were very helpful in figuring out what those micron-sized features on the binder were. **Kurt,** I thoroughly enjoyed your critical questions during meetings ever (and on paper) ever since you joined. Oftentimes, that stimulated me to think about results in a different way, and over time taught me how to think in a different way, too. It was great working with you all, so thank you!

Then there are my phenomenal paranymphs, **Lisette** and **Patrick**. **Lisette**… I could not have wished for a better lab neighbour and (almost) office neighbour. You are an amazing friend with whom I can complain, cry, laugh, share, and happy dance. Be it about science, about life in general, books, or just any other silly thing. I still remember that one day we were both in the lab and basically could hear each other being frustrated with science in general, which was a great bonding moment. I know that the road ahead might sometimes look daunting or long, but I also know you will do amazingly throughout the last stretch of your PhD journey, just like you have done before. Believe me, you will not need any pewter for what is to come, because you are already so strong by yourself! **Patrick**, I think it is fair to say we can drive each other slightly crazy at times (although I think you would like me to explicitly say that probably I annoy you significantly more than you me). We have known each other for 10 years already, and I am grateful for all the fun adventures we have had, from fishing trips and the interrail holiday to our during/after-dinner puzzling. Whatever the situation and day brings, you always manage to enjoy the most of it and are a very cheerful person. You are insanely smart and optimistic, and when I needed it most I could always count and rely on you. Thank you so much for being amazing! I know you will keep on doing amazing things, as the clevergoat you are.

On to **SPC**, which is a wonderful group, comprised of extraordinary people. One such person is **Ingeborg**. Ingeborg, you are amazing, and without you we would all be lost! You have the great ability to make hilarious comments in a very matter-of-fact way. It is admirable how many tasks you are juggling, and it is always both pleasant and fun talking to and working with you. **Ton**, thank you for your patience and your diligent and precise work. It was always properly enjoyable talking to you, and I have come to learn that you can be quite the jokester and trickster! **Pleunie**, thank you for arranging so many things for everyone! Additionally, thank you for always being so high-spirited and going through your day with a smile, whatever life throws at you. It brightens the day of everyone else! **Eleonora**, I hope you will continue to believe in your trust regions. Thank you for being an amazing office mate and providing multiple great pieces of wisdom for the wall of Ele-quotes. You can do it! Don't forget to be awesome, and see you later, Ele-gator. **Eva**, I think we can admit that we were all *un poco loco* in our office. You are kind and strong, and often gave me plenty of advice on how to navigate the tumultuous sea of life. Let's meet for coffee at the bookstore again soon! **Ryno**, ek vertrou dat jy sal voortgaan om jou primêre taak uit te voer, net soos die lychee. Dankie vir die

besprekings by die laboratorium en al jou ewekansige stellings uit die bloute. **Roman**, it was very nice to be able to work and discuss with you. Also, together with Ryno we occasionally undertook some nice activities such as that day trip to Leiden and cycling to the Achelse Kluis. **Mallika**, you experience the world in an interesting way, and I mean that in the most sincere and positive way (or would you deem this to be a 'shallow-nice' comment?). Thank you for all the banter, laughs, and working on the 'bunny-board/rabboard' with me. It is always great fun hanging out with you! **Dasol**, you are tremendously funny and sassy! I like how you sometimes use offices of other people as a waiting room or a spot to just briefly decompress (I will not disclose the location of the Dasol-chairs, so that you can keep on using them in secret). Thank you for the laughs and incredible food you prepared for us, and for joining Mallika and me on a lot of nice (forest) walks. **Gautam,** thank you for the laughs in the lab and also for the invitations to have an excellent dinner at your place. Also, your wisdom and contemplations on life provided me with some new insights on how to look at some things. **Tommaso**, thank you for showing and sharing your scientific curiosity whenever you are in Helix! **Alba**, you bring a nice energy to the group and your doodles are really solid work. Keep on doodling and hiding those beans! **Laura**, your energy and enthusiasm about science, the world, and others is really unparallelled! It is amazingly inspiring how much you undertake and accomplish. Thank you for inviting me to the ESRF in Grenoble, and for always being so open, caring, and honest. **Bert**, although you were not directly involved with my project and only occasionally in Helix, it was always a tremendous pleasure talking with you. Be it about iGC, the history of science, or whatever is happening in the world at the moment. **Heiner**, I have always enjoyed your questions during the FAM and chatting during borrels with some nice IPAs. **Mark**, your puns, jokes, and the speed at which you think of them are impressive and enjoyable. **Max**, your knowledge and curiosity have always been admirable and inspiring to me. **Dixit**, many thanks for arranging the excellent trip to Gent with Pleunie! **Volodymyr**, thank you for the chats we had when we met each other in the mornings when starting the day. **Anne-Floor,** thank you for almost always being so lively and uplifting and bringing a nice vibe to the group. **Francesco**, thank you for being so light-hearted and trying to argue whether Nutella could be considered a fruit. **Nitin**, thank you for teaching us how to draw a figure in the most confusing way possible, reminding us how your name is a palindrome, and for always being cheerful. **Maarten**, thank you for sharing your opinion on the grating size of mini-stroopwafels compared with the grating size of normal stroopwafels. **Rick**, you were a real 'smaakmaker' during breaks and drinks, and as such conversations were never dull when you were around. **Anne**, you are caring, kind and interested in people, and it is always lovely talking with you. Keep being amazing! **Pauline**, thank you for your care, the laughs we shared, and microscopy expertise as well! **Bernette**, although we did not share an office for that long, it was nice to get to know you better in that time. Thank you for the deerspotting attempts and geocaching we did! **Siyu**, thank you for always being able to lighten the mood in the room, in part due to your quite infectious laugh! **Sai,** we only shared the office for a brief amount of time, but you made me feel welcome from day one and it was clear how

passionate you were about science. **Jeroen**, breaks were never boring with you around! **Stefan**, thank you for the guidance and support when I just started my project, and for the subsequent laughs during the occasional catching-ups. **Jiankang,** you often shared a lot of your wisdom and expertise with everyone, and were always in for a discussion, which was great and much appreciated! **Stijn**, thank you for arranging and joining plenty of activities! **Mohammad**, thank you for your words and the conversations we had at the start of my PhD. I will never forget your kindness! **Machi and Joeri**, it was always so much fun talking to you! **Ferid,** unfortunately we did not have that much time to interact (at the time of writing, that is), but I feel you will do great! Also a special thanks to our colleagues from **PTG/e**: **Maurice**, **Timo**, **Thomas**, **Jordan**, **Alex**. You often brought plenty of liveliness to the breaks and drinks, making sure it was gezellig. To each and everyone: thank you for all the support and terrific times!

I also want to thank the three (four?) wonderful students I got to supervise. **Britte**, you were the first student I had to privilege to supervise, and taught me what it actually meant to guide someone in a project. Your work provided a good basis for both Inge and me to continue with. **Maudy**, you tackled an entirely different beast of a resin and did so with optimism and enthusiasm. The AAA binder still is an interesting alternative to PUF, and I hope someone will continue your nice work on that some day. I really appreciate that we could also give each other honest feedback, making your project a chance for us both to grow. Thank you for the pleasant and open collaboration! **Inge**, you were quite the independent hard worker from the beginning! I enjoyed your drive to try and understand as much as you could about the wetting agent, resin and crystals. I still remember you going out of your way (without telling me!) to measure the surface roughness of samples at a time when you should have already stopped with experiments and been busy wrapping up your report. Your work ethics and dedication was great to see, as well as the growth you went through. A big thanks to all three of you! **Wilko**, although I was not involved in your project at all, we interacted plenty on the lab and quickly became friends. I thoroughly enjoyed all the sports and games we have played over the years, from playing squash for so long that walking was nearly impossible for a week, to collecting sigils, to running from creatures of the mythos…Here's to more adventures!

Next up, **Bliep van Blop: Zançat**, **Danny**, **Julio, Richard, Patrick.** Collectively, thank you for making the past 10 years at TU/e memorable, bearable (referring mostly to the study times!), and fun. **Zançat,** since we started our PhDs we did not really see each other that often in Helix on account of you being all over the place (not sure because of holidays or because of Modelta ;P), but still it was always a pleasure to see you in those rare instances when the stars happened to be aligned. **Danny,** we did not really see each other that often in Helix as well, but the rare occasions we did meet up were brilliant as always. Also, thank you for enduring playing 30 Seconds with us nearly every time we had a boardgame night. **Julio**! We also did not really see each other that often in Helix, on account of you not doing your PhD in Eindhoven but rather in Leiden. So that

makes sense. Thank you for sharing your great sense of humour and all the times you joined for boardgame nights! Though playing Everdell at 4 in the morning was quite intense haha. **Mike**, it was always great to see you switch from serious Mike to bantering Mike (especially when it was directed at Patrick), and I am sure you will continue to do great things now that you are dr. Mike! **Richard**, thanks for being unapologetically yourself (as it should be!) and that way teaching me to be myself as well. We should really play squash again soon, although I fear I am quite rusty…

Now then, on to the **Chinchillas**: **Tim Persoon**, **Christiaan** and **Bram**. It is amazing that we have known each other for such a long time, and are still going strong. I like that whenever we do something, we very much do them *our* way (to be fair, sometimes much to our own exhaustion). I am glad to have you as friends, and look forward to determining who will be the next 'Wumbo' champion. **Tim,** thank you for your support, humour, and (biology-)enthusiasm. We have had great adventures, such as climbing 'death mountain' in Tromsø, or trying some birdspotting in Valkenswaard only to be interrupted by a forest worker using a chainsaw 5 minutes in… I am looking forward to all that is to come! **Christiaan**, you have a wonderful ability to phrase things in a particularly nice manner, using a carefully curated selection of words. I hope you will always remember that the bear is not the villain in the story (although the bear did cost you several euros more than it should, which is a crime…), and that cardboard wizard tokens should *not* be kept in fruit juice ;P. **Bram**, you are at times amazingly unpredictable in both your physical location and your next move, but the fun we all have when you are around is a constant. Thank you for your enthusiasm to try and meet up whenever possible. Let's meet up in Japan one day… or try and go to the last Inca bridge!

Also thanks to the **Aight Gees**: **Stan**, **Roel**, **Stijn**, **Laurens**, **Lex**, **Tim Paulusse, Wouter, Zançat, Tim Persoon, Christiaan,** and **Bram**. I am glad we still celebrate 3^{e} kerstdag together and do other slightly more crazy activities (you know, something to do with an unreasonable amount of poffertjes…). The entire group is not always present for every activity, but it is great that we are still in contact.

De afgelopen jaren is er veel gebeurd en veranderd qua familie. Zonder iedereen die ik nu ga bedanken had ik deze reis zeker niet aan gekund. **Peter en Anne-Marie**, bedankt voor jullie steun en hulp in de afgelopen jaren. Mede dankzij jullie heb ik een aantal jaar geleden een stap gezet die de eerste was in een lange weg naar weer kleur in mijn leven kunnen zien. Ook al zien we elkaar misschien niet zo vaak, het voelt wel altijd goed, gezellig, bekend en als familie aan als we bij elkaar zijn. Dus nogmaals, super bedankt! **Ine**, ik kan eigenlijk amper mijn dankbaarheid uitdrukken voor alle tijd, ruimte, zorgzaamheid en liefde die je Dennis en mij hebt gegeven in de afgelopen jaren. Ik heb mezelf zo ontzettend vaak verloren in mijn eigen gedachten en gevoelens, maar bij jou kon ik altijd terecht om erover te praten. Ik hoop dat je beseft hoe geweldig, open, en sterk je bent. En zo niet, dan ga ik je daar zeker aan blijven herinneren! Uiteraard ook dank aan **Jacob, Maike, Tim, Niek, Nikki,** en **(slag)Romy** voor jullie steun, warmte, en pret. **Wally**, ik weet dat je niet kunt lezen omdat je een hond bent, maar dank je voor het

vies maken van mijn kleren door tegen me aan te springen en me te tackelen in je enthousiasme. Elke. Keer. Weer. **Dennis**, je bent een geweldige broer. We zijn zeker hechter geworden de afgelopen jaren. Beiden hebben we gestoeid met alles wat er is gebeurd, en ik spreek in ieder geval voor mezelf als ik zeg dat ik (nog steeds) geen kei ben in het delen van gevoelens en gedachten. Maar we zijn er voor elkaar, en dat is zeker gebleken. Niet alleen mogen we trost zijn op onszelf en elkaar, maar ik kan je zeggen dat ik dat ook echt bent. We komen er wel, en we blijven er voor elkaar. **Mama**, ik geloof er in dat je mee kan kijken via dingen die met jou te maken hebben, of van jouw zijn geweest. Dus ik geloof er in dat deze woorden, die qua gevoel wat ik heb niet eens een beetje toereikend zijn, jouw bereiken. Bedankt dat je er altijd voor Dennis en mij was. Bedankt dat je ongeremd jezelf was, met je quotes, kreten, al je verzamelingen, je groene vingers, je bemoeienis als iemand ook maar ergens een laatje open deed, je eigenschap te kunnen genieten van de kleine dingetjes (zoals rommelen in zo'n laatje), je warmte, zorgzaamheid, liefde, steun, en soms lichte gestoordheid (met een knipoog gezegd). We missen je allemaal nog steeds verdomd veel, en dat is een goed teken. Bedankt dat je niet alleen een geweldige moeder voor ons was, maar ook onze beste vriend (toch nog een soort van Toy Story erin weten te verwerken, speciaal voor jou).

